UNIVERSITY OF CALIFORNIA, SAN DIEGO

Extending the Physicochemical Characterization of Aerosol Particles in California

A dissertation submitted in partial satisfaction of the

requirements for the degree

Doctor of Philosophy

in

Engineering Sciences (Mechanical Engineering)

by

Melanie Dorothy Zauscher

Committee in charge:

Professor Kimberly A. Prather, Chair

Professor Jan P. Kleissl, Co-Chair

Professor Carlos F. Coimbra

Professor Richard K. Herz

Professor Daniel M. Tartakovsky

2012

The dissertation of Melanie Dorothy Zauscher is approved, and it is acceptable in quality and form for publication on microfilm and electronically:

Co-Chair

Chair

University of California, San Diego

2012

DEDICATION

To all the victims of predicted natural disasters,
including the 22,400 unnecessary lives lost during
the 1985 Nevado del Ruíz lahar

"What's the use of having developed a science
well enough to make predictions if,
in the end, all we're willing to do is stand around
and wait for them to come true?"
- Sherwood Rowland

.

EPIGRAPH

“ We cannot solve our problems with the same thinking when we created them.”

Albert Einstein

TABLE OF CONTENTS

LIST OF ABBREVIATIONS AND SYMBOLS

APS	Aerodynamic particle sizer
ART-2a	Adaptive resonance theory 2a
ATOFMS	Aerosol time-of-flight mass spectrometer
BBA	Biomass burning aerosol
BC	Black carbon
CCN	Cloud condensation nuclei
CCNc	Cloud condensation nuclei counter
CN	Condensation nuclei
CPC	Condensation particle counter
Da	Aerodynamic diameter
D_{act}	Activation diameter
DMA	Differential mobility analyzer
f_{CCN}	Fraction of cloud condensation nuclei
GMD	Geometric mean diameter
GT	Growth tube
HDDV	Heavy duty diesel vehicle
HFO	Heavy fuel oil
κ	Hygroscopicity parameter
LDI	Laser desorption/ionization
m/z	mass-to-charge
N_{CCN}	Number concentration of cloud condensation nuclei
N_{CN}	Number concentration of condensation nuclei
NOP	Number of particles
OC	Organic carbon

PILS-IC	Particle-into-liquid sampler ion chromatography
$PM_{0.4}$	Mass of particulate matter of diameters < 0.4 μm
$PM_{1.0}$	Mass of particulate matter of diameters < 1.0 μm
PM_{10}	Mass of particulate matter of diameters < 10 μm
$PM_{2.5}$	Mass of particulate matter of diameters < 2.5 μm
PMF	Positive matrix factorization
PSL	Polystyrene latex sphere
RH	Relative humidity
RPA	Relative peak area
SMPS	Scanning mobility particle sizer
SS	Supersaturation
UF-ATOFMS	Ultrafine aerosol time-of-flight mass spectrometer

LIST OF FIGURES

LIST OF TABLES

ACKNOWLEDGEMENTS

None of this would be possible without the support from my advisor Professor Kim Prather. I am especially grateful to her for taking a chance by letting me join her lab after my previous advisor left the university. I am thankful for the opportunity she gave me to work on such interesting and applied research. I appreciate Kim's excitement and enthusiasm for science, in addition to her ability to see the big picture. I would also like to acknowledge my co-advisor, Professor Jan Kleissl for his steady support. Dr. Steve Buckley, my first advisor, also deserves recognition for the guidance he gave me during my first two years of graduate school.

Also, I want to acknowledge the other members of my Ph.D. committee for their thoughtful comments and advice regarding my research: Professor Carlos Coimbra, Professor Richard Herz, and Professor Daniel Tartakovsky. I am grateful to various professors for their patience as I embarked into the mechanical engineering field: Professors Linden, Llewellyn-Smith, Sarkar, Rottman and Herz. I would also like to acknowledge Professor Linden for his overall support during my transition into MAE and between laboratories. I am also thankful to Dr. Craig Wildman for his friendship and patience and to Dr. Diogo Bolster for his time and willingness to help me prepare for the departmental exam.

I am deeply grateful for the opportunities I had to work with such wonderful collaborators. To Dr. Susanne Hering, Dr. Greg Lewis, and everyone at Aerosol Dynamics, Inc. for their willingness to try the growth tube with the ATOFMS and for continuously improving the growth tube-ATOFMS interface. To Dr. Greg Roberts at Scripps Institution of Oceanography for collaborating with the Prather Lab and letting us borrow his prized cloud condensation nuclei counters. To Professor Mike Tauber for teaching us how to and letting us use his analytical instruments. I am thankful to Professor Oberdoerster and everyone in his lab at the University of Rochester for the collaboration on particle health effects.

These past five years have gone by really fast because of the positive outlook and energy of all past and current members of the Prather Research Group. I am thankful for EVERYONE's help preparing for field studies, troubleshooting instruments, analyzing data, proof-reading, discussing ideas, and making science enjoyable! However, I am particularly indebted to Dr. Meagan Moore and Dr. Ryan Sullivan for welcoming me into the group with their wisdom and friendship. In addition, Meagan's unwavering support, even after her graduation, of my laboratory and field work and writing was central to my many accomplishments. Meagan's good-nature and dedication to making a difference in her community and in the world continue to inspire me. Ryan's deep intellect and humbleness truly astonishes me. Many, many, many thanks also go to Jack Cahill, Lindsay Hatch, and Kaitlyn Suski who provided continuous moral support, friendship, insights, and crucial feedback. In particular, Jack's curiosity has enabled him to become a prolific learner in fields outside of his specialty and an excellent teacher. I am inspired by his work ethic, humor, and ability to combine scientific knowledge with his artistic creativity. Lindsay contributes significantly to the whole group's success by providing critical feedback during group meetings and informal discussions and by making sure newer students stay on the right track; not because she's the senior student in lab, but because she wants everyone to succeed. I admire Lindsay's analytical ability, dedication to science and the excellence of all her work, despite multiple laboratory setbacks. I am grateful that I have been able to observe Kaitlyn maintaining work-life balance while still being extremely productive because it gives me hope that one day I too will be able to achieve this. I am amazed by Kaitlyn's love of life and the natural-world, including all the critters, and her ability to distill the essence of complex concepts and articulate them clearly. I am also thankful to Dr. Bob Moision for answering never ending questions about electronics and computer programming and for sharing his humor with the lab. I have always been amazed at Liz Fitzgerald's critical thinking, perseverance, and her ability to mix work with play successfully. Jessie Creamean is always willing to help out, is not afraid of getting dirty, and has managed to become an expert analyzing satellite data. Doug Collins has a positive attitude and is a dedicated team player able to work on multiple projects at

once. Dr. Cassandra Gaston is an extremely committed scientist that is very passionate about her research. Dr. Luis Cuadra-Rodriguez, who has impressive analytical skills allowing him to learn rapidly and apply his knowledge to a variety of problems, is extremely friendly and positive. Matt Ruppel has contributed to a great work environment by creating the list and being its keeper. I also want to acknowledge the technical and moral support from Joe Mayer on countless, but crucial "small" things. In addition to those aforementioned, I'm also appreciative of the influence Dr. Yongxuan Su, Dr. Sergio Guazzotti, Dr. Sharon Qin, Dr. Steve Toner, Dr. Laura Shields, Dr. Kerri Pratt, Dr. Andy Ault, Dr. Ying Wang, Dr. Defeng Zhao, Dr. Alberto Cazorla, Dr. Tim Guasco, Chris Lee, Camille Sultana, and Katherine Nadler have had on my science and personal development. Last but not least, I am also very grateful for the opportunity I had to work with such bright undergraduates, so I could be re-inspired with their energy: Maggie Yandell, Brandon Heilman, Tom Bytnerowicz, and Mallory Pickett from the Prather Group, and Dr. Michael Gollner, Jason Harp, Jim Kerins, and Halden Oxenbol from the Buckley Group.

I would like to acknowledge the California Energy Commission for funding for the Calwater 2010 Mariposa field study, everyone at Dr. Marty Ralph's lab at National Oceanic and Atmospheric Administration and at the Mariposa Airport for the logistical support setting up the field site. I am thankful to the "Butterfly Crew" during the Mariposa field study including Kaitlyn Suski, Jack Cahill, Jake Lipmann, Dr. Craig Corrigan, Dr. Scott Noblitt, Dr. Greg Roberts, Dr. Amy Sullivan, Professor Jeff Collette, Dr. Susanne Hering, and Dr. Greg Lewis for the productive conversations, good science, and fun times.

The Los Angeles Port Study of 2011 was funded by the U.S. Environmental Protection Administration PM Center Grant. I would also like to acknowledge all the staff at the Southern California Marine Institute for letting us use their space for sampling. I'm thankful to our collaborators present at the field site, including Dr. Susanne Hering, Dr. Greg Lewis, Dr. Steven Spielman, and especially to Dr. Arantza Eiguren-Fernandez. In addition, I acknowledge the help from Dr. Luis Cuadra-

Rodriguez, Dr. Defeng Zhao, Jack Cahill, and Liz Fitzgerald during sampling set-up and instrument transport.

I am also thankful for the experiences I gained in other field studies. Dr. Sharon Qin taught me how to tune the ATOFMS once I joined the lab, so I could participate in my first field study a couple of weeks later. During the Los Angeles Air Basin I and II studies I learned a lot from Dr. Ying Wang, Maggie Yandell, Dr. Andy Ault, Dr. Cassandra Gaston, and Dr. Bob Moision. I also appreciate the opportunity to be part of the Puerto Rican African Dust and Clouds Study. Liz Fitzgerald is acknowledged for sharing the responsibility and fun of this field study campaign. In addition, I am thankful to everyone at Professor Olga Mayol-Bracero's lab, but especially Felix Zurcher, for helping to make this study as successful as possible given the harsh conditions (such high and sustained relative humidity the scientific equipment is not used to, constant pot holes and flat tires, leaky roof, moldy crates, and other random things).

I am also extremely grateful to all staff that keep the university running smoothly. The support staff in the chemistry business office was instrumental in the success of my lab and field studies, especially Myra Kosak, Carmen Alfarro, Ben Rodriguez, and Shanley Miller.

I am very grateful of the U.S. Environmental Protection Administration PM Center Grant where the majority of my funding came from. I am also thankful for UCSD's Interdisciplinary Collaboratories Fellowship and the National Science Foundation Bridge to the Doctorate fellowship I received my first two years at UCSD through the AEP and CAMP programs. All the current and previous staff at AEP and CAMP have provided me with support and motivation since I was an undergraduate. I would especially like to thank Dr. Jacquie Azize-Brewer, Dr. Norienne Saign, Dr. David Artis, Elizabeth Blocker, and Marjorie DeMartino.

I also want to acknowledge previous research mentors that have helped me become who I am today. My first research experience was in the lab of Professor Martin

Wahlen at Scripps Institution of Oceanography (SIO) and I am grateful for his patience. I received a lot of mentorship and opportunities from working at Professor Jeff Bada's lab, also at SIO, dating whales. I am very thankful I had the chance to work with Dr. Frank Flocke at the National Center for Atmospheric Research through the SOARS program. Last but not least, I am extremely grateful of the opportunity I had to work in Professor James White's Stable Isotope Lab at the Institute of Arctic and Alpine Research at the University of Colorado Boulder and greatly appreciate his guidance on following my own passions. I also appreciate the support of Bruce Vaughn and Valerie Claymore while working there.

I am also extremely thankful for the opportunities I had to venture outside of lab to discover and develop new interests and passions. I would like to acknowledge everyone involved with the Greenline Biodiesel Shuttle and the Biofuels Awareness and Action Network, but especially Fleet Manager Jim Ruby, Vice Chancellor Gary Matthews, and Professor Skip Pomeroy. Jim Ruby's dedication to his work and commitment to greening the fleet are truly inspiring, but his friendliness and humor are even more amazing. I am also thankful for the opportunity I had to participate in the UCSD Graduate Student Association and am appreciative of all whom have worked and continue to work to improve the graduate student experience. Also, I am grateful to the University Corporation of Atmospheric Research/National Center for Atmospheric Research, and particularly to Dr. Rajul Pandya, for their continued support since my participation in the SOARS program a decade ago, including the funding to participate in the American Meteorological Society's Summer Policy Colloquium last summer.

Last but not least, I would like to acknowledge the support I have received from my family and friends. Manuel Ruidíaz is the best husband by far, and I appreciate his daily support, encouragement, patience, and love. His support has been really important, particularly when I was away during extensive field campaigns. I acknowledge my parents, Diane and Fernando, my siblings, Blanca, Nancy, and William, and their significant others, for their continuous support. I am most grateful to my Aunt Nita for opening up her home and family to me when I first moved to the U.S. My friends Lara,

Fabi, Didi, Chris, Lois, Shivani, and Seren have always been there for me, even when I wasn't there for them because of grad school. Finally, I am also grateful to all the friends and colleagues I've met at UCSD for their regular support and friendship.

The text and figures of Chapter 2 are a reprint of a published paper, Zauscher M.D., Moore M.J.K., Lewis G.S., Hering S.V., and Prather K.A., "Approach for measuring the chemistry of individual particles in the size range critical for cloud formation." *Analytical Chemistry* Feb. 2011. DOI: 10.1021/ac103152g. Copyright 2011, American Chemical Society. The dissertation author was the primary researcher and author of this work.

The contents of Chapter 3 are part of a manuscript in preparation, Zauscher, M.D., Cahill, J.F., Suski, K.J., Hatch, L.E., Sullivan, A.P., Collett, J.L., and Prather, K.A. "Quantitative comparison and aerosol mixing state in the western California Sierra Nevada foothills during pollution transport events in winter 2010." The dissertation author was the primary researcher and author of this work.

The contents of Chapter 4 are part of a manuscript in preparation, Zauscher, M.D., Cahill, J.F., Suski, K.J., Moore, M.J.K., Sullivan, A.P., Collett, J.L., Prather, K.A., and Roberts, G.C. "Cloud condensation nuclei properties and aerosol composition in the foothills of California's Sierra Nevada." The dissertation author was the primary researcher and author of this work.

The contents of Chapter 5 are part of a manuscript in preparation, Zauscher, M.D., Wang, Y., Moore, M.J.K., Gaston C.J., Prather, K.A. "Mixing state and aging of individual biomass burning aerosols during the 2007 San Diego Wildfires." The dissertation author was the primary researcher and author of this work.

The contents of Chapter 6 are part of a manuscript in preparation, Zauscher, M.D., and Prather, K.A. "Impact of Central Valley emissions on local aerosols sampled at San Pedro Bay Ports." The dissertation author was the primary researcher and author of this work.

VITA

Mar 2003	B.S. in Environmental Chemistry, University of California, San Diego
2000-2003	Research Assistant, Scripps Institution of Oceanography
2002-2003	Teaching Assistant, University of California, San Diego
2003-2004	Professional Scientist, Institute of Arctic and Alpine Research
2005-2012	Graduate Student Researcher, University of California, San Diego
2008	Teaching Assistant, University of California, San Diego
2012	Ph.D. in Engineering Sciences (Mechanical Engineering), University of California, San Diego

PUBLICATIONS

Zauscher MD, Moore MJK, Lewis GS, Hering SV, Prather, KA; "Approach for Measuring the Chemistry of Individual Particles in the Size Range Critical for Cloud Formation." *Analytical Chemistry*. Feb. 2011. DOI: 10.1021/ac103152g

C Rosa, J Zeh, C George, O Botta, MD Zauscher, J Bada, and TM O' Hara "Age estimates based on aspartic acid racemization for bowhead whales (Balaena mysticetus) harvested in 1998-2000" accepted in *Marine Mammals Science*

ABSTRACT OF THE DISSERATION

Extending the Physicochemical Characterization of Aerosol Particles in California

by

Melanie Dorothy Zauscher

Doctor of Philosophy in Engineering Sciences (Mechanical Engineering)

University of California, San Diego, 2012

Professor Kimberly A. Prather, Chair

Professor Jan P. Kleissl, Co-Chair

Aerosols affect the radiative balance of earth, alter cloud formation, and adversely impact human health. Knowledge of the physicochemical properties of particles, which can rapidly change, is essential to predict and mitigate their negative impacts. Hence, in-situ measurements of single-particle composition and physical properties are needed. Aerosol time-of-flight mass spectrometry (ATOFMS), which measures the size-resolved chemical mixing state of individual particles, was used to study aerosols at different locations in California.

Soot particles internally mixed with soluble ammonium, nitrate, and sulfate transported from the Central Valley were found to be a major source of cloud condensation nuclei in the Sierra Nevada during winter 2010, never identified before.

These aged soot particles may be affecting regional cloud microphysics and potentially precipitation.

Rapid aging of biomass burning aerosols during intense urban fires were analyzed for the first time via single-particle mass spectrometry throughout the 2007 San Diego Wildfires. Furthermore, estimated size-resolved mass concentrations of particulate matter during the wildfires showed for the first time that particles < 400 nm contributed significantly to mass, with maximum $PM_{0.4}$=148 μg/m^3. These observations are essential for predicting climate and health impacts of biomass burning aerosols.

Measurements during May, 2011 at the Port of Los Angeles coupled to air mass back-trajectories indicate that transport from the Central Valley brings amines to the Los Angeles air basin, which has not been documented previously. Unexpectedly, nearly 60% of all ambient particles sampled contained amines. These results are important because amines cause adverse health problems.

In addition to these ambient studies, work was done to improve the ATOFMS technique. Due to concern over health and climate impacts, a novel method was developed to study ultrafine (<100 nm) particles by coupling condensational growth to the ATOFMS. In a separate study, ion peak areas were successfully scaled into mass concentrations for the first time by comparison with data obtained from the particle-into-liquid sampler coupled to ion chromatography (PILS-IC) allowing the quantification of chemical data from the ATOFMS. By being able to probe smaller particles and quantify ATOFMS data, further insights into the variability of aerosol chemistry and sources can be gained.

Chapter 1. Introduction

1.1 Atmospheric aerosol particles

An aerosol is a liquid or solid particle suspended in a gaseous medium. Herein, the gaseous medium is the atmosphere. Aerosols are directly emitted as primary particles or formed and modified in the atmosphere through secondary processes. Aerosols are ubiquitous in the troposphere, even in remote environments (Heintzenberg, 1982; Patterson et al., 1980; Weber et al., 1999), but are present in higher number and mass concentrations in urban environments than in rural and clean regions (Laakso et al., 2003; Wiedensohler et al., 2002). Aerosols are key players in the atmosphere affecting climate and human health, which are further discussed in sections 1.2.1 and 1.2.2.

Aerosols are composed of complex mixtures of inorganic and organic species, which depend mainly on their source but are also affected by transport and atmopsheric conditions. Many naturally-occuring particles can be emitted directly into the atmosphere through mechanical processes, such as wind and abrasion which resuspend mineral dust and soil into the atmosphere (Morales, 1986), or through wave breaking which aerosolize sea salt particles (de Leeuw et al., 2000; Fitzgerald, 1991). Dust and sea salt particles are mostly comprised of different mixtures of inorganic species. Combustion generated aerosols, including emissions from diesel and gasoline engines, biomass and coal burning, are a dominant source of ambient particles, specially in urban regions (Lighty et al., 2000; Ning and Sioutas, 2010); these particles are composed of mostly carbonaceous material. Additionally, particles are formed in the atmosphere through secondary gas-to-particle conversions (Fitzgerald, 1991; Kulmala et al., 2004); gases that can nucleate new particles include biogenic emissions and combustion by-products, such as various organic carbon species and sulfur dioxide (SO_2). Therefore, these new particles can be composed of inorganic and/or organic species mixed to various degrees. All of these sources of aerosols are highly variable in space and time.

Aerosol particles are typically divided by size range into supermicron, submicron, and ultrafine with diameters (D) > 1, < 1, and < 0.1 μm, respectively. Dust and sea salt particles are predominantly supermicron. Typically, freshly emitted combustion particles occur in the ultrafine and accumulation (0.1-1 micron) size modes, while newly formed particles occur between 1-10 nm. Larger particles have significantly more mass compared to smaller particles, as mass is proportional to D^3. Thus, particles above 1 micron make up most of the mass, whereas ultrafine particles are typically the most abundant by number.

Aerosols are continuously undergoing physical and chemical changes in the atmosphere. As aerosols age, they can grow rapidly in size by coagulating with each other (Ning and Sioutas, 2010) and by the condensation of semi-volatile compounds, which may result from oxidation of larger organic species, onto pre-existing particles (Kerminen, 1999; Li et al., 2011; Ning and Sioutas, 2010). Under some conditions, combustion-generated and newly formed particles can grow to be 10-100 times their original size. In addition, gas phase species, like nitric and sulfuric acids (HNO_3 and H_2SO_4), can react with compounds on the particle, like sodium chloride (NaCl), calcium carbonate ($CaCO_3$), or potassium chloride (KCl), via heterogenous reactions to form secondary particulate sulfate (SO_4^{2-}) and nitrate (NO_3^-) (Gard et al., 1998; Gaudichet et al., 1995; Usher et al., 2003). These reactions depend on the availability of gaseous precursors and on particle composition (Sullivan et al., 2007).

Meteorology also influences particle composition. Semi-volatile species, such as ammonium nitrate (NH_4NO_3), volatilize during periods of high temperatures and low humidity and condense onto particles during periods of low temperature and high humidity (Stelson and Seinfeld, 1982). In humid environments, particles may contain more water, thus influence which reactions occur (Mozurkewich and Calvert, 1988). During intense solar radition, compounds are aged through photooxidation (Hennigan et al., 2011; Miracolo et al., 2010; Presto et al., 2010; Presto et al., 2009; Robinson et al., 2007). In addition, meteorological parameters that drive wind play a role in the

transport of air masses from one region to another, across continents, and even globally (Husar et al., 2001; Liu et al., 2009b; Morales, 1986). Meteorology can sometimes produce temperature inversions, which trap pollution near the boundary layer, thus allowing particles more time to further age and concentrate (Lu and Turco, 1995; Watson and Chow, 2002). Overall, the diversity of chemical reactions that occur, the concentrations of gas-phase precursors, meteorology, and the transport of particles and trace gases across continents, all contribute to the large temporal and spatial variability in the composition of aerosols.

1.2 Environmental impacts of aerosols

Governements, including the United States, regulate ambient particles in order to mitigate their impacts. For example, the U.S. National Ambient Air Quality Standards (NAAQS) limits the mass of particulate matter of diameters < 10 and 2.5 μm (PM_{10} and $PM_{2.5}$, respectively). The 24-hour average $PM_{2.5}$ (fine) and PM_{10} (coarse) NAAQS limits are 35 and 150 $\mu g/m^3$, respectively. These mass metrics are relatively easy and inexpensive to measure compared to speciated size-resolved mass and number concentrations. A critism of these NAAQS standards is that they treat all particulate matter similarly by not differentiating particles of different compositions and sizes (Green et al., 2002). Furthermore, the number concentrations of ultrafine particles do not correlate with $PM_{2.5}$ mass concentrations (de Hartog et al., 2005; Ruuskanen et al., 2001). As elaborated upon in the remainder of this section, particle size, number concentrations, and mixing state, or the associations between chemical species in individual particles, also influences how the aerosols will impact climate and health. An internal aerosol mixture is defined by all particles having the same composition, while external mixtures are comprised of particles with distinct combinations of chemical species. Thus, knowing the composition of individual size-resolved particles is key for predicting their environmental impacts.

1.2.1 Climate effects of aerosols

Aerosols have a large, albeit highly uncertain, impact on the climate system. Particles directly absorb and scatter solar and terrestrial radiation, known as the aerosol direct effect, which alters the radiative balance of the atmosphere (Solomon et al., 2007). After carbon dioxide, black carbon (or soot) emissions are the second strongest contributor to global warming (Ramanathan and Carmichael, 2008). The composition of each particle helps determine the strength of its radiative forcing, therefore knowing particle composition is essential for predicting the effects that particles will have on Earth's radiative balance. As mentioned previously, black carbon is a strong absorber and its absorption can be made stronger by mixing with secondary species, like sulfate (Moffet and Prather, 2009). Modeling and in-situ studies have shown that soot particles coated with secondary species, such as sulfate, have a stronger radiative forcing than fresh soot particles that have not been atmospherically processed (Chung et al., 2012; Jacobson, 2001; Moffet and Prather, 2009). Although relatively well understood, the aerosol direct effect is not well constrained over land, on regional scales, or with a temporal resolution less than one day because of the lack of detailed spatial characterizations of aerosols including their distribution with altitude and in time (Yu et al., 2006).

In addition to impacting Earth's radiation budget directly, a subset of particles serve as cloud condensation nuclei (CCN) upon which water will spontaneously condense and form cloud droplets (Solomon et al., 2007). The CCN number concentrations help determine cloud droplet size, which may in turn affect cloud lifetime, cloud albedo, and regional precipitation patterns, thus affecting the climate system (Albrecht, 1989; Lohmann, 2006; McFiggans et al., 2006; Tao et al., 2012; Twomey, 1977). These aerosol indirect effects are currently the largest uncertainty in climate change (Solomon et al., 2007), which is due to not being able to accurately predict the spatial and temporal distribution of CCN concentrations and sources (Andreae and Rosenfeld, 2008; Pierce and Adams, 2009) and from lack of understanding of cloud formation and microphysics (Khain et al., 2000).

The ability of an aerosol to serve as a CCN can be predicted based on its size and chemical composition at a given supersaturation (SS) using Kohler theory (Seinfeld and Pandis, 1998). Kohler theory balances the Raoult effect, which defines how the equilibrium vapor pressure above a surface is lowered by the presence of a solute, and the Kelvin effect, which states that the vapor pressure over a curved surface is always larger than that of a flat surface. At higher supersaturations, particles activate more easily. Therefore, ambient CCN number concentrations depend on particle size, amount of soluble mass, and ambient supersaturation. Given two particles of equal size, the one with a greater mass of soluble species, such as NaCl, will preferentially activate because soluble species reduce the vapor pressure above the surface. Given two particles with the same mass of soluble species, the larger one will preferentially activate because increased curvatures in smaller particles lead to higher vapor pressures. While particles with diameter < 50 nm are rarely CCN-active because of their large curvatures, particles > 200 nm are typically always CCN-active. Therefore, 50-200 nm particles usually represent the CCN activation size range where particle composition is a key factor determining cloud droplet activation. However, it is analytically challenging to determine the soluble mass and size of individual particles in this size range because of the small amount of material in particles in this size range.

1.2.2 Health effects of aerosols

Even though the exact biological mechanisms are not fully understood, human exposure to aerosols has been associated with adverse health impacts, such as increased morbidity and mortality due to respiratory and cardiovascular diseases and cancer (Pope et al., 2002; Pope and Dockery, 2006; Schwartz et al., 2002). Previous epidemiological studies have found a linear correlation between $PM_{2.5}$ mass concentrations, even at low concentrations, and premature deaths (Pope, 2004; Schwartz et al., 2002); reduced $PM_{2.5}$ mass concentrations are associated with decreased mortality rates (Laden et al., 2006). Exposure to aerosol pollution is an international problem because particles are transported to regions outside of where they were emitted (Liu et al., 2009b).

Approximately 380,000 premature deaths worldwide are associated with exposure to foreign $PM_{2.5}$ each year (Liu et al., 2009a).

In addition to total particle mass, particle size also influences the health impacts of aerosols. Compared to larger particles, ultrafine particles can penetrate more deeply into the lungs and be translocated to other organs including the brain (Oberdorster, 2001; Oberdorster et al., 2004; Oberdorster et al., 2002). Laboratory studies have shown that ultrafine particles cause pulmonary inflammation and more oxidative stress than fine and coarse particles (Li et al., 2003; Oberdorster, 2001). When rats were exposed to titanium oxide particles, the ultrafine dose had a greater inflammatory response than the fine dose of equal mass (Oberdorster, 2000). Furthermore, epidemiological studies have also confirmed that increased exposure to ultrafine and fine particles are correlated to adverse health effects in humans compared to larger particles (Delfino et al., 2005; Peters et al., 1997; Ramgolam et al., 2009).

In some studies, chemical composition determined the health outcomes of particulate matter exposure. For example, human subjects exposed to fine and ultrafine magnesium oxide particles had no detectable inflammatory pulmonary response in contrast to those exposed to zinc oxide particles (Kuschner et al., 1995; Kuschner et al., 1997). Also, previous studies have shown that polystyrene latex particles coated with amines may induce clotting (McGuinnes et al., 2011; Nemmar et al., 2002). Additionally, particle toxicity may be exacerbated due to synergy between different chemical compounds on the same particle. A study which exposed rats to soot particles internally mixed with iron oxide generated measurable oxidative stress, whereas exposure to only soot or iron particles did not (Zhou et al., 2003). Similarly, rats exposed to aerosolized particles containing both vanadium and nickel resulted in higher biological responses than exposure to particles with just one of these species (Campen et al., 2001). In order to advance the epidemiological field of how aerosol particles affect human health, it is important to know the number concentrations and size-resolved composition of individual particles across all size ranges that humans are exposed to in our daily lives.

1.3 Air quality in California

In 2012, the American Lung Association ranked five California regions as having the worst particulate matter pollution in the U.S. based on $PM_{2.5}$ mass concentrations (Nolen 2011); these areas are located in the Central Valley and the Los Angeles (L.A.) metropolitan area. One of the most agriculturally productive regions in the world, the Central Valley is surrounded by mountains, including the Sierra Nevada on east, the Coastal Range on the west, and the Tehachapi Mountains on the south. Emissions from agriculture, traffic, and biomass burning become trapped in the valley when temperature inversions are present resulting from topologically driven air flow, typically in the winter (Chow et al., 2006; MacDonald et al., 2006; Watson and Chow, 2002). These meteorological phenomena result in high concentrations of particulate matter that are difficult to control. During high particulate matter events, pollution from the Central Valley can be transported to the Sierra Nevada foothills, as investigated in Chapter 3 & 4, and may affect regional cloud properties.

Although pollution levels have improved over time, the Los Angeles area has had a long history with high particulate pollution (Magill, 1949). The Los Angeles basin is a large metropolitan region, surrounded by mountains and the Pacific Ocean to the southwest. Most primary pollution is generated on the western side of the basin by traffic, including gasoline passenger cars, heavy-duty diesel trucks, and sea-faring ships. Specifically, the Ports of Los Angeles and Long Beach have a significant number of trucks and ships that emit high concentrations of aerosols (Agrawal et al., 2009; Arhami et al., 2009; Bishop et al., 2012; Kozawa et al., 2008; Moore et al., 2009). Chapter 6 will address particle composition in this port complex. The pollution is then trapped in the basin by the mountains. The typical regional airflow at the port complex during the daytime, when most of the pollution is generated, is onshore which transports the primary pollution inland (Lu and Turco 1995; Blumenthal et al. 1978). Transport time enables the pollution to photochemically age and acquire secondary species (Seinfeld and Pankow 2003; Turpin et al. 1991). The topography surrounding the L.A. basin and the temperature difference over the ocean and land help create temperature inversion

layers that trap this pollution, allowing it to further age and concentrate (Lu and Turco 1995; Blumenthal et al. 1978). Therefore, the poor air quality is a regional problem that cannot be solved by only addressing emissions inland where higher concentrations of particles are found.

Another major source of particulate matter pollution in California is wildfires. Wildfires represent a significant yet highly variable source of aerosols in California, and therefore pose a significant problem for air quality (Park et al., 2007; Westerling and Bryant, 2008). For example, the 2003 Southern California Wildfires, which lasted less than one week, contributed ~28% of annual anthropogenic $PM_{2.5}$ that year (Muhle et al., 2007). Although unpredictable, the frequency of wildfires and amount of area burned has increased since the 1970s in the western U.S. due to regional warming, earlier spring arrival, and increased droughts (Westerling et al., 2006). Biomass burning aerosols have been associated with increased respiratory and cardiovascular problems (Delfino et al., 2009; Kunzli et al., 2006; Viswanathan et al., 2006) and can also serve as CCN (Petters et al., 2009). Chapter 5 investigates the air quality impact of the 2007 wildfires in San Diego's air basin.

1.4 Aerosol time-of-flight mass spectrometer (ATOFMS)

As previously explained, knowledge of the size-resolved mixing state of particles is crucial for predicting aerosol impacts on climate and human health. However, most aerosol sampling methods can only measure the chemical bulk properties with low size resolution. The aerosol time-of-flight mass spectrometer (ATOFMS), the main sampling technique used in all of the work presented in this thesis, acquires the size-resolved chemical composition of individual particles (Gard et al., 1997; Su et al., 2004). Particles enter the instrument into a vacuum undergoing a supersonic expansion, accelerating them to their size-dependent terminal velocity. Next, particles traverse the beam of two continuous 532-nm wavelength lasers, which are spaced 6-cm apart. As the particle passes through each laser beam, the light is scattered and focused onto photomultiplier tubes (PMTs), which send pulses to an electronic timing circuit that measures the time it takes each particle to cross both laser beams.

From this measured time, particle velocity is calculated and converted to aerodynamic vacuum diameter (D_a) through a calibration with polystyrene latex spheres (PSLs) of known sizes. The timing circuit calculates when the particle will enter the mass spectrometer source region and sends a signal to a Q-switched 266-nm Nd:YAG laser for desorption/ionization (LDI) to fire. This laser pulse rapidly desorbs the constituents of the particle into the gas phase and ionizes them simultaneously. These resulting ions are then accelerated by voltage differences sending the positive and negative ions into separate ion flight tubes. At the end of each flight tube is a reflectron which is used to increase the mass resolution. The micro-channel plate detector then intercepts the ions as they exit the reflectron, thus acquiring a dual polarity mass spectrum based on the time-of-flight of each ion. A mass calibration is also performed with particles of known composition to ensure that the mass-to-charge (*m/z*) assignments are correct.

There are two different inlet systems for the ATOFMS, which determine the size range of particles that can be sampled. The standard ATOFMS instrument, whose inlet consists of a converging nozzle, can analyze 0.2-3.0 μm particles with a maximum transmission efficiency at D_a~1.7 μm. (Gard et al., 1997). Instead of the converging nozzle, the ultrafine (UF)-ATOFMS has an aerodynamic focusing lens (AFL) (Liu et al., 1995), which is more efficient in collimating the particle beam (Su et al., 2004). Because of the AFL and improved optics, the UF-ATOFMS can detect particles with D_a=100-1500 nm with maximum transmission efficiency at D_a~300 nm. The standard ATOFMS was utilized for data collection in Chapters 3-4, while the UF-ATOFMS was used for Chapters 2, 4, and 6. Specifically, Chapter 2 describes a technique that extends the size range of particles sampled with the UF-ATOFMS to particles with D_a as small as 39 nm.

The ATOFMS technique can analyze and identify a variety of aerosol types including soot, organic carbon (OC), soot mixed with OC (soot-OC), biomass burning, dust, and sea salt and determine their chemical composition and mixing states with secondary species. Although quantification of specific chemical components has been achieved (Bhave et al., 2002; Jeong et al., 2011), overall quantification remains

challenging because each resulting ion peak area in the mass spectra not only depends on how well each component absorbs the LDI pulse and its ionization potential but also on what other species are found in the same particle (Reilly et al., 2000). This last effect is known as the matrix effect. For example, although the main component in biomass burning aerosol is OC, the biomass burning aerosol ATOFMS mass spectra are characterized by an intense $^{39}K^{+}$ ion peak, due to the low ionization potential of potassium, which suppresses the carbonaceous peaks (Reid et al., 2005; Silva et al., 1999). The beam intensity of the LDI is also highly variable and may have "hot-spots" or regions with higher laser power which also influence the resulting mass spectra (Wenzel and Prather, 2004). Despite these challenges, the ATOFMS ammonium, nitrate, and sulfate ion peak areas were successfully quantified for different particle types and compared to independent measurements from a collocated instrument, as discussed in Chapter 3.

1.5 Objectives thesis

The overall goal of the work described herein is to extend our knowledge of the physicochemical properties of aerosols. This was accomplished by two overlapping approaches:

1) Improve analytical techniques that sample aerosol particles

    a. Extend the ATOFMS to sample ultrafine particles to improve understanding of health effects and impacts of CCN composition (Chapter 2)

    b. Develop method to quantify ATOFMS data to increase use of data obtained (Chapter 3)

2) Sample ambient particles in various regions within California

    a. Determine mixing state and source of aerosols and CCN active particles in the Sierra Nevada foothills and relate with decreased orographic precipitation (Chapter 3 & 4)

b. Analyze aging and mixing state of biomass burning aerosols during the 2007 San Diego Wildfires and their overall impact on local air quality (Chapter 5)

c. Explore the mixing state and source of particles observed at the Port of Los Angeles, which may impact human health (Chapter 6)

1.6 Synopsis of thesis

Chapter 2 describes a novel method that expands the lower size limit of the ATOFMS to allow chemical analysis of individual ultrafine particles, while Chapter 3 illustrates a new quantitative procedure that transforms ion peak areas into mass concentrations by using data obtained from a collocated particle-into-liquid sampler ion chromatography (PILS-IC) system. The Calwater 2010 field campaign took place on the western foothills of California Sierra Nevada during winter and was the first study to identify the composition and sources of aerosols and CCN-active particles, described in Chapter 3 & 4, that may be altering regional precipitation. Rapid aging of biomass burning aerosols throughout the 2007 San Diego Wildfires were analyzed for the first time on a single-particle level during intense coastal urban fires in Chapter 5. Furthermore, the impact of the 2007 San Diego Wildfires on local air quality was also explored in Chapter 5. Finally, as part of a health effects study, Chapter 6 investigates the composition of particles at the Port of Los Angeles and attempt to identify their source. Unexpectedly, amines were found on 59% of all particles sampled and were observed to be transported from the Central Valley.

In addition to Chapter 2, ambient ultrafine data obtained with novel technique developed is shown in Appendix 2 & 3. Chapter 3 applies the method to scale ATOFMS peak areas into mass concentrations from data obtained in the Sierra Nevada foothills. Appendix 1 also contains data showing ATOFMS quantitation using a chemical standard in laboratory work.

1.7 Acknowledgments

Jessie Creamean and Elizabeth Fitzgerald are acknowledged for their thoughtful comments that greatly improved this chapter.

1.8 References

Agrawal, H., Eden, R., Zhang, X., Fine, P. M., Katzenstein, A., Miller, J. W., Ospital, J., Teffera, S., and Cocker, D. R. (2009).Primary Particulate Matter from Ocean-Going Engines in the Southern California Air Basin, *Environmental Science & Technology*, *43* (14), 5398-5402.

Albrecht, B. A. (1989).Aerosols, Cloud Microphysics, and Fractional Cloudiness, *Science*, *245* (4923), 1227-1230.

Arhami, M., Sillanpaa, M., Hu, S. H., Olson, M. R., Schauer, J. J., and Sioutas, C. (2009).Size-Segregated Inorganic and Organic Components of Pm in the Communities of the Los Angeles Harbor, *Aerosol Science and Technology*, *43* (2), 145-160.

Bhave, P. V., Allen, J. O., Morrical, B. D., Fergenson, D. P., Cass, G. R., and Prather, K. A. (2002).A Field-Based Approach for Determining Atofms Instrument Sensitivities to Ammonium and Nitrate, *Environmental Science & Technology*, *36* (22), 4868-4879.

Bishop, G. A., Schuchmann, B. G., and Stedman, D. H. (2012).Emission Changes Resulting from the San Pedro Bay, California Ports Truck Retirement Program, *Environmental Science & Technology*, *46* (1), 551-558.

Campen, M. J., Nolan, J. P., Schladweiler, M. C. J., Kodavanti, U. P., Evansky, P. A., Costa, D. L., and Watkinson, W. P. (2001).Cardiovascular and Thermoregulatory Effects of Inhaled Pm-Associated Transition Metals: A Potential Interaction between Nickel and Vanadium Sulfate, *Toxicological Sciences*, *64* (2), 243-252.

Chow, J. C., Chen, L. W. A., Watson, J. G., Lowenthal, D. H., Magliano, K. A., Turkiewicz, K., and Lehrman, D. E. (2006).Pm2.5 Chemical Composition and Spatiotemporal Variability During the California Regional Pm10/Pm2.5 Air Quality Study (Crpaqs), *Journal of Geophysical Research-Atmospheres*, *111* (D10), 17.

Chung, C. E., Lee, K., and Muller, D. (2012).Effect of Internal Mixture on Black Carbon Radiative Forcing, *Tellus Series B-Chemical and Physical Meteorology*, *64*, 1-13.

de Hartog, J. J., Hoek, G., Mirme, A., Tuch, T., Kos, G. P. A., ten Brink, H. M., Brunekreef, B., Cyrys, J., Heinrich, J., Pitz, M., Lanki, T., Vallius, M., Pekkanen, J., and Kreyling, W. G. (2005).Relationship between Different Size Classes of Particulate Matter and Meteorology in Three European Cities, *Journal of Environmental Monitoring*, *7* (4), 302-310.

de Leeuw, G., Neele, F. P., Hill, M., Smith, M. H., and Vignali, E. (2000).Production of Sea Spray Aerosol in the Surf Zone, *Journal of Geophysical Research-Atmospheres*, *105* (D24), 29397-29409.

Delfino, R. J., Brummel, S., Wu, J., Stern, H., Ostro, B., Lipsett, M., Winer, A., Street, D. H., Zhang, L., Tjoa, T., and Gillen, D. L. (2009).The Relationship of Respiratory and Cardiovascular Hospital Admissions to the Southern California Wildfires of 2003, *Occupational and Environmental Medicine*, *66* (3), 189-197.

Delfino, R. J., Sioutas, C., and Malik, S. (2005).Potential Role of Ultrafine Particles in Associations between Airborne Particle Mass and Cardiovascular Health, *Environmental Health Perspectives*, *113* (8), 934-946.

Fitzgerald, J. W. (1991).Marine Aerosols - a Review, *Atmospheric Environment Part a-General Topics*, *25* (3-4), 533-545.

Gard, E., Mayer, J. E., Morrical, B. D., Dienes, T., Fergenson, D. P., and Prather, K. A. (1997).Real-Time Analysis of Individual Atmospheric Aerosol Particles: Design and Performance of a Portable Atofms, *Analytical Chemistry*, *69* (20), 4083-4091.

Gard, E. E., Kleeman, M. J., Gross, D. S., Hughes, L. S., Allen, J. O., Morrical, B. D., Fergenson, D. P., Dienes, T., Gaelli, M. E., Johnson, R. J., Cass, G. R., and Prather, K. A. (1998).Direct Observation of Heterogeneous Chemistry in the Atmosphere, *Science*, *279*, 1184-1187.

Gaudichet, A., Echalar, F., Chatenet, B., Quisefit, J. P., Malingre, G., Cachier, H., Buatmenard, P., Artaxo, P., and Maenhaut, W. (1995).Trace-Elements in Tropical African Savanna Biomass Burning Aerosols, *Journal of Atmospheric Chemistry*, *22* (1-2), 19-39.

Green, L. C., Crouch, E. A. C., Ames, M. R., and Lash, T. L. (2002).What's Wrong with the National Ambient Air Quality Standard (Naaqs) for Fine Particulate Matter (Pm2.5)?, *Regulatory Toxicology and Pharmacology*, *35* (3), 327-337.

Heintzenberg, J. (1982).Size Segregated Measurements of Particulate Elemental Carbon and Aerosol Light-Absorption at Remote Arctic Locations, *Atmospheric Environment*, *16* (10), 2461-2469.

Hennigan, C. J., Miracolo, M. A., Engelhart, G. J., May, A. A., Presto, A. A., Lee, T., Sullivan, A. P., McMeeking, G. R., Coe, H., Wold, C. E., Hao, W. M., Gilman, J. B., Kuster, W. C., de Gouw, J., Schichtel, B. A., Collett, J. L., Jr.,

Kreidenweis, S. M., and Robinson, A. L. (2011).Chemical and Physical Transformations of Organic Aerosol from the Photo-Oxidation of Open Biomass Burning Emissions in an Environmental Chamber, *Atmospheric Chemistry and Physics*, *11* (15), 7669-7686.

Husar, R. B., Tratt, D. M., Schichtel, B. A., Falke, S. R., Li, F., Jaffe, D., Gasso, S., Gill, T., Laulainen, N. S., Lu, F., Reheis, M. C., Chun, Y., Westphal, D., Holben, B. N., Gueymard, C., McKendry, I., Kuring, N., Feldman, G. C., McClain, C., Frouin, R. J., Merrill, J., DuBois, D., Vignola, F., Murayama, T., Nickovic, S., Wilson, W. E., Sassen, K., Sugimoto, N., and Malm, W. C. (2001).Asian Dust Events of April 1998, *Journal of Geophysical Research-Atmospheres*, *106* (D16), 18317-18330.

Jacobson, M. Z. (2001).Strong Radiative Heating Due to the Mixing State of Black Carbon in Atmospheric Aerosols, *Nature*, *409* (6821), 695-697.

Jeong, C. H., McGuire, M. L., Godri, K. J., Slowik, J. G., Rehbein, P. J. G., and Evans, G. J. (2011).Quantification of Aerosol Chemical Composition Using Continuous Single Particle Measurements, *Atmospheric Chemistry and Physics*, *11* (14), 7027-7044.

Kerminen, V. M. (1999).Roles of So(2) and Secondary Organics in the Growth of Nanometer Particles in the Lower Atmosphere, *Journal of Aerosol Science*, *30* (8), 1069-1078.

Khain, A., Ovtchinnikov, M., Pinsky, M., Pokrovsky, A., and Krugliak, H. (2000).Notes on the State-of-the-Art Numerical Modeling of Cloud Microphysics, *Atmospheric Research*, *55* (3-4), 159-224.

Kozawa, K. H., Fruin, S. A., and Winer, A. M. (2008).Using a Mobile Monitoring Platform to Characterize Pollution Concentrations on and near Heavily-Traveled Roadways in Communities Adjacent to the Ports of Los Angeles and Long Beach, *Epidemiology*, *19* (6), S224-S225.

Kulmala, M., Vehkamaki, H., Petaja, T., Dal Maso, M., Lauri, A., Kerminen, V. M., Birmili, W., and McMurry, P. H. (2004).Formation and Growth Rates of Ultrafine Atmospheric Particles: A Review of Observations, *Journal of Aerosol Science*, *35* (2), 143-176.

Kunzli, N., Avol, E., Wu, J., Gauderman, W. J., Rappaport, E., Millstein, J., Bennion, J., McConnell, R., Gilliland, F. D., Berhane, K., Lurmann, F., Winer, A., and Peters, J. M. (2006).Health Effects of the 2003 Southern California Wildfires on Children, *American Journal of Respiratory and Critical Care Medicine*, *174* (11), 1221-1228.

Kuschner, W. G., Dalessandro, A., Wintermeyer, S. F., Wong, H., Boushey, H. A., and Blanc, P. D. (1995).Pulmonary Responses to Purified Zinc-Oxide Fume, *Journal of Investigative Medicine*, *43* (4), 371-378.

Kuschner, W. G., Wong, H. F., D'Alessandro, A., Quinlan, P., and Blanc, P. D. (1997).Human Pulmonary Responses to Experimental Inhalation of High Concentration Fine and Ultrafine Magnesium Oxide Particles, *Environmental Health Perspectives*, *105* (11), 1234-1237.

Laakso, L., Hussein, T., Aarnio, P., Komppula, M., Hiltunen, V., Viisanen, Y., and Kulmala, M. (2003).Diurnal and Annual Characteristics of Particle Mass and Number Concentrations in Urban, Rural and Arctic Environments in Finland, *Atmospheric Environment*, *37* (19), 2629-2641.

Laden, F., Schwartz, J., Speizer, F. E., and Dockery, D. W. (2006).Reduction in Fine Particulate Air Pollution and Mortality - Extended Follow-up of the Harvard Six Cities Study, *American Journal of Respiratory and Critical Care Medicine*, *173* (6), 667-672.

Li, N., Sioutas, C., Cho, A., Schmitz, D., Misra, C., Sempf, J., Wang, M. Y., Oberley, T., Froines, J., and Nel, A. (2003).Ultrafine Particulate Pollutants Induce Oxidative Stress and Mitochondrial Damage, *Environmental Health Perspectives*, *111* (4), 455-460.

Li, S. M., Liggio, J., Graham, L., Lu, G., Brook, J., Stroud, C., Zhang, J., Makar, P., and Moran, M. D. (2011).Condensational Uptake of Semivolatile Organic Compounds in Gasoline Engine Exhaust onto Pre-Existing Inorganic Particles, *Atmospheric Chemistry and Physics*, *11* (19), 10157-10171.

Lighty, J. S., Veranth, J. M., and Sarofim, A. F. (2000).Combustion Aerosols: Factors Governing Their Size and Composition and Implications to Human Health, *Journal of the Air & Waste Management Association*, *50* (9), 1565-1618.

Liu, J. F., Mauzerall, D. L., and Horowitz, L. W. (2009a).Evaluating Inter-Continental Transport of Fine Aerosols:(2) Global Health Impact, *Atmospheric Environment*, *43* (28), 4339-4347.

Liu, J. F., Mauzerall, D. L., Horowitz, L. W., Ginoux, P., and Fiore, A. M. (2009b).Evaluating Inter-Continental Transport of Fine Aerosols: (1) Methodology, Global Aerosol Distribution and Optical Depth, *Atmospheric Environment*, *43* (28), 4327-4338.

Liu, P., Ziemann, P. J., Kittelson, D. B., and McMurry, P. H. (1995).Generating Particle Beams of Controlled Dimensions and Divergence .1. Theory of Particle Motion in Aerodynamic Lenses and Nozzle Expansions, *Aerosol Science and Technology*, *22* (3), 293-313.

Lohmann, U. (2006).Aerosol Effects on Clouds and Climate, *Space Science Reviews*, *125* (1-4), 129-137.

Lu, R., and Turco, R. P. (1995).Air Pollutant Transport in a Coastal Environment 2: 3-Dimensional Simulations over Los-Angeles Basin, *Atmospheric Environment*, *29* (13), 1499-1518.

MacDonald, C. P., McCarthy, M. C., Dye, T. S., Wheeler, N. J. M., Hafner, H. R., and Roberts, P. T. (2006).Transport and Dispersion During Wintertime Particulate Matter Episodes in the San Joaquin Valley, California, *Journal of the Air & Waste Management Association*, *56* (7), 961-976.

Magill, P. L. (1949).The Los Angeles Smog Problem, *Industrial and Engineering Chemistry*, *41* (11), 2476-2486.

McFiggans, G., Artaxo, P., Baltensperger, U., Coe, H., Facchini, M. C., Feingold, G., Fuzzi, S., Gysel, M., Laaksonen, A., Lohmann, U., Mentel, T. F., Murphy, D. M., O'Dowd, C. D., Snider, J. R., and Weingartner, E. (2006).The Effect of Physical and Chemical Aerosol Properties on Warm Cloud Droplet Activation, *Atmospheric Chemistry and Physics*, *6*, 2593-2649.

McGuinnes, C., Duffin, R., Brown, S., Mills, N. L., Megson, I. L., MacNee, W., Johnston, S., Lu, S. L., Tran, L., Li, R. F., Wang, X., Newby, D. E., and Donaldson, K. (2011).Surface Derivatization State of Polystyrene Latex Nanoparticles Determines Both Their Potency and Their Mechanism of Causing Human Platelet Aggregation in Vitro, *Toxicological Sciences*, *119* (2), 359-368.

Miracolo, M. A., Presto, A. A., Lambe, A. T., Hennigan, C. J., Donahue, N. M., Kroll, J. H., Worsnop, D. R., and Robinson, A. L. (2010).Photo-Oxidation of Low-Volatility Organics Found in Motor Vehicle Emissions: Production and Chemical Evolution of Organic Aerosol Mass, *Environmental Science & Technology*, *44* (5), 1638-1643.

Moffet, R. C., and Prather, K. A. (2009).In-Situ Measurements of the Mixing State and Optical Properties of Soot with Implications for Radiative Forcing Estimates, *Proceedings of the National Academy of Sciences of the United States of America*, *106* (29), 11872-11877.

Moore, K., Krudysz, M., Pakbin, P., Hudda, N., and Sioutas, C. (2009).Intra-Community Variability in Total Particle Number Concentrations in the San Pedro Harbor Area (Los Angeles, California), *Aerosol Science and Technology*, *43* (6), 587-603.

Morales, C. (1986).The Airborne Transport of Saharan Dust - a Review, *Climatic Change*, *9* (1-2), 219-241.

Mozurkewich, M., and Calvert, J. G. (1988).Reaction Probability of N2o5 on Aqueous Aerosols, *Journal of Geophysical Research-Atmospheres*, *93* (D12), 15889-15896.

Muhle, J., Lueker, T. J., Su, Y., Miller, B. R., Prather, K. A., and Weiss, R. F. (2007).Trace Gas and Particulate Emissions from the 2003 Southern California Wildfires, *Journal of Geophysical Research-Atmospheres*, *112* (D3).

Nemmar, A., Hoylaerts, M. F., Hoet, P. H. M., Dinsdale, D., Smith, T., Xu, H. Y., Vermylen, J., and Nemery, B. (2002).Ultrafine Particles Affect Experimental Thrombosis in an in Vivo Hamster Model, *American Journal of Respiratory and Critical Care Medicine*, *166* (7), 998-1004.

Ning, Z., and Sioutas, C. (2010).Atmospheric Processes Influencing Aerosols Generated by Combustion and the Inference of Their Impact on Public Exposure: A Review, *Aerosol and Air Quality Research*, *10* (1), 43-58.

Oberdorster, G. (2000).Toxicology of Ultrafine Particles: In Vivo Studies, *Philosophical Transactions of the Royal Society of London Series a-Mathematical Physical and Engineering Sciences*, *358* (1775), 2719-2739.

Oberdorster, G. (2001).Pulmonary Effects of Inhaled Ultrafine Particles, *International Archives of Occupational and Environmental Health*, *74* (1), 1-8.

Oberdorster, G., Sharp, Z., Atudorei, V., Elder, A., Gelein, R., Kreyling, W., and Cox, C. (2004).Translocation of Inhaled Ultrafine Particles to the Brain, *Inhalation Toxicology*, *16* (6-7), 437-445.

Oberdorster, G., Sharp, Z., Atudorei, V., Elder, A., Gelein, R., Lunts, A., Kreyling, W., and Cox, C. (2002).Extrapulmonary Translocation of Ultrafine Carbon Particles Following Whole-Body Inhalation Exposure of Rats, *Journal of Toxicology and Environmental Health-Part A*, *65* (20), 1531-1543.

Park, R. J., Jacob, D. J., and Logan, J. A. (2007).Fire and Biofuel Contributions to Annual Mean Aerosol Mass Concentrations in the United States, *Atmospheric Environment*, *41* (35), 7389-7400.

Patterson, E. M., Kiang, C. S., Delany, A. C., Wartburg, A. F., Leslie, A. C. D., and Huebert, B. J. (1980).Global Measurements of Aerosols in Remote Continental and Marine Regions - Concentrations, Size Distributions, and Optical Properties, *Journal of Geophysical Research-Oceans and Atmospheres*, *85* (NC12), 7361-7376.

Peters, A., Wichmann, H. E., Tuch, T., Heinrich, J., and Heyder, J. (1997).Respiratory Effects Are Associated with the Number of Ultrafine Particles, *American Journal of Respiratory and Critical Care Medicine*, *155* (4), 1376-1383.

Petters, M. D., Carrico, C. M., Kreidenweis, S. M., Prenni, A. J., DeMott, P. J., Collett, J. L., and Moosmuller, H. (2009).Cloud Condensation Nucleation Activity of Biomass Burning Aerosol, *Journal of Geophysical Research-Atmospheres*, *114*, 16.

Pope, C. A. (2004).Air Pollution and Health - Good News and Bad, *New England Journal of Medicine*, *351* (11), 1132-1134.

Pope, C. A., Burnett, R. T., Thun, M. J., Calle, E. E., Krewski, D., Ito, K., and Thurston, G. D. (2002).Lung Cancer, Cardiopulmonary Mortality, and Long-Term Exposure to Fine Particulate Air Pollution, *Jama-Journal of the American Medical Association*, *287* (9), 1132-1141.

Pope, C. A., and Dockery, D. W. (2006).Health Effects of Fine Particulate Air Pollution: Lines That Connect, *Journal of the Air & Waste Management Association*, *56* (6), 709-742.

Presto, A. A., Miracolo, M. A., Donahue, N. M., and Robinson, A. L. (2010).Secondary Organic Aerosol Formation from High-Nox Photo-Oxidation of Low Volatility Precursors: N-Alkanes, *Environmental Science & Technology*, *44* (6), 2029-2034.

Presto, A. A., Miracolo, M. A., Kroll, J. H., Worsnop, D. R., Robinson, A. L., and Donahue, N. M. (2009).Intermediate-Volatility Organic Compounds: A Potential Source of Ambient Oxidized Organic Aerosol, *Environmental Science & Technology*, *43* (13), 4744-4749.

Ramanathan, V., and Carmichael, G. (2008).Global and Regional Climate Changes Due to Black Carbon, *Nature Geoscience*, *1* (4), 221-227.

Ramgolam, K., Favez, O., Cachier, H., Gaudichet, A., Marano, F., Martinon, L., and Baeza-Squiban, A. (2009).Size-Partitioning of an Urban Aerosol to Identify Particle Determinants Involved in the Proinflammatory Response Induced in Airway Epithelial Cells, *Particle and Fibre Toxicology*, *6*, 12.

Reid, J. S., Koppmann, R., Eck, T. F., and Eleuterio, D. P. (2005).A Review of Biomass Burning Emissions Part Ii: Intensive Physical Properties of Biomass Burning Particles, *Atmospheric Chemistry and Physics*, *5*, 799-825.

Reilly, P. T. A., Lazar, A. C., Gieray, R. A., Whitten, W. B., and Ramsey, J. M. (2000).The Elucidation of Charge-Transfer-Induced Matrix Effects in Environmental Aerosols Via Real-Time Aerosol Mass Spectral Analysis of Individual Airborne Particles, *Aerosol Science and Technology*, *33* (1-2), 135-152.

Robinson, A. L., Donahue, N. M., Shrivastava, M. K., Weitkamp, E. A., Sage, A. M., Grieshop, A. P., Lane, T. E., Pierce, J. R., and Pandis, S. N. (2007).Rethinking Organic Aerosols: Semivolatile Emissions and Photochemical Aging, *Science*, *315* (5816), 1259-1262.

Ruuskanen, J., Tuch, T., Ten Brink, H., Peters, A., Khlystov, A., Mirme, A., Kos, G. P. A., Brunekreef, B., Wichmann, H. E., Buzorius, G., Vallius, M., Kreyling, W. G., and Pekkanen, J. (2001).Concentrations of Ultrafine, Fine and Pm2.5

Particles in Three European Cities, *Atmospheric Environment*, *35* (21), 3729-3738.

Schwartz, J., Laden, F., and Zanobetti, A. (2002).The Concentration-Response Relation between Pm2.5 and Daily Deaths, *Environmental Health Perspectives*, *110* (10), 1025-1029.

Seinfeld, J. H., and Pandis, S. N. (1998). **Atmospheric Chemistry and Physics**, John Wiley & Sons, New York.

Silva, P. J., Liu, D., Noble, C. A., and Prather, K. A. (1999).Size and Chemical Characterization of Individual Particles Resulting from Biomass Burning of Local Southern California Species, *Environmental Science & Technology*, *33* (18), 3068-3076.

Solomon, S., Qin, D., Manning, M., Chen, Z., Marquis, M., Averyt, K. B., Tignor, M., and Miller, H. L. (2007). Climate Change 2007: The Physical Science Basis. Contribution of Working Group I to the Fourth Assessment Report of the Intergovernmental Panel on Climate Change, Cambridge, United Kingdom and New York, USA.

Stelson, A. W., and Seinfeld, J. H. (1982).Relative-Humidity and Ph-Dependence of the Vapor-Pressure of Ammonium-Nitrate Nitric Acid-Solutions at 25-Degrees-C, *Atmospheric Environment*, *16* (5), 993-1000.

Su, Y. X., Sipin, M. F., Furutani, H. F., and Prather, K. A. (2004).Development and Characterization of an Aerosol Time-of-Flight Mass Spectrometer with Increased Detection Efficiency, *Analytical Chemistry*, *76*, 712-719.

Sullivan, R. C., Guazzotti, S. A., Sodeman, D. A., and Prather, K. A. (2007).Direct Observations of the Atmospheric Processing of Asian Mineral Dust, *Atmospheric Chemistry and Physics*, *7* (5), 1213-1236.

Tao, W. K., Chen, J. P., Li, Z. Q., Wang, C., and Zhang, C. D. (2012).Impact of Aerosols on Convection Clouds and Precipitation, *Reviews of Geophysics*, *50*, 62.

Twomey, S. (1977).Influence of Pollution on Shortwave Albedo of Clouds, *Journal of the Atmospheric Sciences*, *34* (7), 1149-1152.

Usher, C. R., Michel, A. E., and Grassian, V. H. (2003).Reactions on Mineral Dust, *Chemical Reviews*, *103* (12), 4883-4939.

Viswanathan, S., Eria, L., Diunugala, N., Johnson, J., and McClean, C. (2006).An Analysis of Effects of San Diego Wildfire on Ambient Air Quality, *Journal of the Air & Waste Management Association*, *56* (1), 56-67.

Watson, J. G., and Chow, J. C. (2002).A Wintertime Pm2.5 Episode at the Fresno, Ca, Supersite, *Atmospheric Environment*, *36* (3), 465-475.

Weber, R. J., McMurry, P. H., Mauldin, R. L., Tanner, D. J., Eisele, F. L., Clarke, A. D., and Kapustin, V. N. (1999).New Particle Formation in the Remote Troposphere: A Comparison of Observations at Various Sites, *Geophysical Research Letters*, *26* (3), 307-310.

Wenzel, R. J., and Prather, K. A. (2004).Improvements in Ion Signal Reproducibility Obtained Using a Homogeneous Laser Beam for on-Line Laser Desorption/Ionization of Single Particles, *Rapid Communications in Mass Spectrometry*, *18* (13), 1525-1533.

Westerling, A. L., and Bryant, B. P. (2008).Climate Change and Wildfire in California, *Climatic Change*, *87*, S231-S249.

Westerling, A. L., Hidalgo, H. G., Cayan, D. R., and Swetnam, T. W. (2006).Warming and Earlier Spring Increase Western Us Forest Wildfire Activity, *Science*, *313* (5789), 940-943.

Wiedensohler, A., Wehner, B., and Birmili, W. (2002).Aerosol Number Concentrations and Size Distributions at Mountain-Rural, Urban-Influenced Rural, and Urban-Background Sites in Germany, *Journal of Aerosol Medicine-Deposition Clearance and Effects in the Lung*, *15* (2), 237-243.

Yu, H., Kaufman, Y. J., Chin, M., Feingold, G., Remer, L. A., Anderson, T. L., Balkanski, Y., Bellouin, N., Boucher, O., Christopher, S., DeCola, P., Kahn, R., Koch, D., Loeb, N., Reddy, M. S., Schulz, M., Takemura, T., and Zhou, M. (2006).A Review of Measurement-Based Assessments of the Aerosol Direct Radiative Effect and Forcing, *Atmospheric Chemistry and Physics*, *6*, 613-666.

Zhou, Y. M., Zhong, C. Y., Kennedy, I. M., Leppert, V. J., and Pinkerton, K. E. (2003).Oxidative Stress and Nf Kappa B Activation in the Lungs of Rats: A Synergistic Interaction between Soot and Iron Particles, *Toxicology and Applied Pharmacology*, *190* (2), 157-169.

Chapter 2. Approach for measuring the chemistry of individual particles in the size range critical for cloud formation

Aerosol particles, especially those ranging from 50-200 nm, strongly impact climate by serving as nuclei upon which water condenses and cloud droplets form. However, the small number of analytical methods capable of measuring the composition of particles in this size range, particularly at the individual particle level, has limited our knowledge of cloud condensation nuclei (CCN) composition and hence our understanding of aerosols effect on climate. To obtain more insight into particles in this size range, we developed a method which couples a growth tube (GT) to an ultrafine aerosol time of flight mass spectrometer (UF-ATOFMS); a combination that allows in-situ measurements of the composition of individual particles as small as 38 nm. The growth tube uses water to grow particles to larger sizes so they can be optically detected by the UF-ATOFMS, extending the size range to below 100 nm with no discernible changes in particle composition. To gain further insight into the temporal variability of aerosol chemistry and sources, the GT-UF-ATOFMS was used for on-line continuous measurements over a period of 3 days.

2.1 Introduction

Aerosol particles play a central role in impacting climate by cooling or warming the atmosphere by scattering and absorbing incoming solar radiation. Particles also impact climate by serving as cloud condensation nuclei (CCN) upon which water condenses and cloud droplets ultimately form. When the CCN concentrations increase, the same amount of water is spread over more nuclei, thus yielding a larger number of smaller droplets. These smaller droplets make longer lived more reflective clouds that

do not grow large enough to precipitate (McFiggans et al., 2006; Solomon et al., 2007). These processes, referred to as the indirect effects, represent the single largest uncertainty in our understanding of climate change, which limits our ability to predict future temperatures (McFiggans et al., 2006; Solomon et al., 2007). In order to reduce the uncertainties associated with aerosol effects on clouds and climate, we must improve our understanding of the global CCN sources, size-resolved chemical composition, and concentrations (Andreae and Rosenfeld, 2008; McFiggans et al., 2006; Pierce and Adams, 2009; Solomon et al., 2007). CCN concentrations are readily measured using a CCN counter (CCNc), which exposes particles to known supersaturations of water vapor (McFiggans et al., 2006; Roberts and Nenes, 2005). Particles of suitable size and chemical composition are activated and grow large enough (> 1 μm) to be detected by an optical particle counter and counted as CCN (Roberts and Nenes, 2005). Particles in the 50-200 nm size range are the most interesting from an atmospheric chemistry perspective because this is the size range where: 1) the peak in the size distribution occurs in regions not dominated by fresh emission sources or nucleation processes, and 2) the threshold for ambient particle activation to CCN takes place based on their chemical composition (McFiggans et al., 2006)

Kohler theory can be used to predict which particles will activate to form clouds based on size and chemical composition (Lohmann and Feichter, 2005; Seinfeld and Pandis, 1998). Particles containing a larger fraction of soluble material, which reduces the vapor pressure above the surface as described by Raoult's law, will activate more readily at a given size. Curvature effects limit the size of particles that can activate because species on the surface of smaller particles with greater curvature have higher vapor pressures. Cloud supersaturation values typically extend up to 2% with a median value of around 0.1% (Pruppacher and Klett, 1997). In regions of clouds with higher supersaturations (>0.2%), very soluble particles such as ammonium sulfate and sodium chloride as small 50 nm can activate and serve as CCN. Size and composition are critical for particle activation, but particle composition is especially important in clouds with lower supersaturations (McFiggans et al., 2006). Given two particles of the same

size, the one with a larger fraction of more soluble species will activate at lower supersaturations than the one containing less soluble species.

Particle number concentrations, composition, and size vary considerably in time and space even in remote regions and will therefore greatly impact CCN concentrations (Furutani et al., 2008). Capturing this variability and being able to use the knowledge of size-resolved particle chemistry and sources of CCN represents a major area of need in climate change research (Clarke et al., 2006; McFiggans et al., 2006; Merikanto et al., 2009; Pierce and Adams, 2006; Pierce and Adams, 2007; Pierce and Adams, 2009; Smith et al., 2010). Measuring the composition of individual CCN active particles poses a major analytical challenge due to the small amount of material in each particle (Johnston et al., 2006; McFiggans et al., 2006). For example, single component particles in the 50-200 nm size range contain 10^{-18} to 10^{-21} g of material. An added challenge is that the composition of these small particles changes via rapid dynamic and chemical processes and thus capturing the variability with real-time measurements has been an elusive goal for some time. Hence, a technique capable of measuring the chemical mixing state of these small particles with high temporal resolution is critical for advancing our understanding of the impacts of aerosols on clouds.

Most measurements of aerosol chemistry in the 50-200 nm size range are bulk measurements, which provide the average composition of the internal mixture of all particles sampled, and often do not represent the actual composition of any individual particle. Atmospheric aerosols frequently are comprised of external mixtures of complex chemical species with varying degrees of solubility with respect to hygroscopicity (Furutani et al., 2008; McFiggans et al., 2006; Tiitta et al., 2010; Wex et al., 2010). Therefore, predictions based on bulk measurements of the number of CCN in a cloud where the particles are externally mixed will be inaccurate (Cubison et al., 2008; Wex et al., 2010). In order to accurately predict CCN concentrations under a variety of conditions, knowledge of particle mixing state is needed, especially at low supersaturations or in urban environments with high numbers of small externally mixed particles (Bougiatioti et al., 2009; Cubison et al., 2008; Gysel et al., 2007; Lance et al.,

2009; McFiggans et al., 2006; Rose et al., 2010; Wex et al., 2010). However, CCN and hygroscopicity closure studies are frequently forced to assume complete internal mixing of particles, which is a particularly poor assumption in the 50-100 nm size range where particles are fresher and thus more often externally mixed (Stroud et al., 2007; VanReken et al., 2003). Thus, it is critical to obtain single particle measurements in order to establish closure between measured hygroscopicity, CCN concentrations and aerosol chemistry (McFiggans et al., 2006; Wex et al., 2010)

Due to their low mass, particle collection onto filters with subsequent analysis with a wide range of techniques is the traditional way to determine the chemical composition of bulk ultrafine particles (UFP), those with aerodynamic diameters (D_a) less than 100 nm (Chen et al., 2010; Hughes and Cass, 1998; Sardar et al., 2005). These techniques can provide quantitative information on aerosol chemistry, yet they have limited temporal capabilities as collection times are long and no information is acquired on single-particle chemical mixing state. There are several analytical instruments based on the collection of particles with improved time resolutions. The thermal desorption chemical ionization mass spectrometer (TDCIMS) analyzes 6-20 nm particles collected with a time resolution of 5-30 minutes (Held et al., 2009; Smith et al., 2004). Similarly, the aerosol mass spectrometer (AMS) thermally desorbs the volatile and semi-volatile species of 30-1000 nm particles collected, and ionizes the resulting gas via electron impaction for bulk analysis with a quadrupole or time of flight mass spectrometer, resulting in rapid and quantitative measurements (Jayne et al., 2000). The AMS can collect enough particles for analysis in as few as 5 minutes (Sun et al., 2010). Another example is the newly developed ultrafine two-step aerosol time-of-flight mass spectrometer, which collects ultrafine particles as small as 22 nm mobility diameter (D_m) for 20-30 minutes on a metal substrate before performing desorption and ionization in two separate steps via lasers (Laitinen et al., 2009). Although these instruments based on particle collection do have higher temporal capabilities and the ability to be quantitative, they still only provide the bulk composition of particles. Previous studies have shown that sulfate mass concentration changes do not correlate with changes in the number of cloud nuclei (Garrett and Hobbs, 1995; Hudson and Li,

1995; Panel on Aerosol Radiative Forcing and Climate Change, 1996). In order to address impacts of aerosols on cloud properties, correlations between chemistry and the number of particles activating as CCN rather than mass are the most relevant. Ultimately, understanding the variations in chemistry at the single particle level will yield insights into how composition plays a role in determining the overall fraction of activated particles within a cloud.

Few methods have the potential to determine the number and corresponding composition of individual ambient particles in the ultrafine size range with high time and size resolution. The most commonly used method for measuring particle chemistry of individual cloud residues is electron microscopy (Kojima et al., 2005; Matsuki et al., 2010; Petzolda et al., 1998; Twohy et al., 2005; Twohy and Gandrud, 1998). However, electron microscopy does not provide spatial information so limited information exists, as yet, on the chemical variability of cloud nuclei within a cloud due to the low time resolution inherent to off-line sampling techniques (Maynard, 1995; Twohy and Anderson, 2008; Utsunomiya et al., 2004).

Single particle mass spectrometers (SPMS) can be used to study real-time individual ultrafine particle composition and thus CCN chemistry (Carson et al., 1997; Cubison et al., 2006; Johnston et al., 2006; Phares et al., 2002; Pratt et al., 2009b; Su et al., 2004; Wang et al., 2006; Zelenyuk et al., 2010). Since the measurements are in real-time, changes in aerosol chemistry can be linked with other microphysical properties within the cloud. Previous studies with an ultrafine aerosol time-of-flight mass spectrometer (UF-ATOFMS) and another single particle time of flight mass spectrometer (SPLAT II) have been able to obtain real-time chemical information on individual particles as small as 50 nm D_a (Cubison et al., 2008; Pratt et al., 2009b; Shields et al., 2008; Su et al., 2004; Su et al., 2005; Su et al., 2006; Toner et al., 2008; Zelenyuk et al., 2009). Both of these instruments rely on optical detection. However, particles with sizes below 100 nm D_a detected optically are typically fractal and thus have small aerodynamic diameters but larger optical or geometric diameters. Therefore,

the lower size limit of single particle mass spectrometers that rely on optical detection of the particles is ~100 nm D_a.

One way to overcome the optical sizing limitation inherent to most single particle techniques is to use an alternative sizing approach. For example, the real-time single particle mass spectrometer (RSMS) samples particles from D_a = 50-1250 nm using rotating critical orifices that restrict the size of the entering particles (Johnston et al., 2006; Lake et al., 2003). However, the rate of obtaining mass spectra is very slow even in a very polluted environment with particle concentrations > 10^4 cm^{-3} (Lake et al., 2003). The nanoaerosol mass spectrometer (NAMS) samples single particles from D_a = 7-30 nm using an aerodynamic focusing lens to guide particles into a ion trap for on-line mass spectrometry analysis (Johnston et al., 2006; Wang et al., 2006). Once trapped, each particle encounters a laser-induced plasma creating atomic ions, yielding elemental information on particle chemistry with limited insight relevant for understanding the hygroscopicity of aerosols. Both the RSMS and NAMS detect the composition of UFP, but have not been used in CCN studies.

Another way to circumvent the optical sizing limitation involves growing UFP through condensation of water vapor in a region of high supersaturation. This principle is utilized in several aerosol measurement techniques such as the previously mentioned CCNc and the water based condensation particle counter (WCPC), which measures particle number concentrations (Hering et al., 2005; Roberts and Nenes, 2005). Combined with various analytical techniques, condensational growth has already been used for chemical measurements of particles such as the particle into liquid sampler coupled to ion chromatography (PILS-IC) that quantifies ionic species (Weber et al.) and the Condensation-Growth and Impaction System (C-GIS) that quantifies organic carbon species (Sierau and Stratmann, 2003). Both of these techniques are rapid, but require particle collection for 4-20 minutes to acquire enough mass for analysis. A new aerosol chip electrophoresis (ACE) system combines laminar flow with the water condensation growth tube from the water-based CPC and couples it to a microchip capillary electrophoresis system in order to quantify a limited subset of soluble

components, including nitrate, sulfate, and oxalate, in particles with temporal resolution down to 1 minute (Noblitt et al., 2009). Further details on the different methods of characterizing the composition of UFP have been discussed in recent review articles (Burleson et al., 2004; Morawska et al., 2009).

In this study, results are shown for the combined water-based growth tube(Hering and Stolzenburg, 2005) single particle mass spectrometry(Su et al., 2004) approach for measuring individual ultrafine particles down to 38 nm. A discussion describes the optimized parameters used to most effectively detect UFP without inducing artifacts. The goal is to develop a robust method that will provide insight into the spatial and temporal variability of the mixing state and composition of ultrafine particles that most strongly influence cloud properties and precipitation processes.

2.2 Experimental

2.2.1 Growth Tube

As described by Hering and Stolzenburg (2005), the growth tube creates a region of water vapor supersaturation in a laminar flow, thereby activating the condensational growth of particles as small as 5 nm (Hering and Stolzenburg, 2005). It is comprised of a wet-walled tube, the first half of which is cooled and the second half of which is heated. Within the warmed section, water vapor diffuses from the walls into the flow. Due to the high diffusivity of water vapor, the transport of water vapor mass into the flow is faster than the transport of sensible heat, creating a region of supersaturation within the center core of the laminar flow. This growth tube concept is the same as that utilized in the water-based condensation particle counters, which measure particle number concentrations by optical detection of the condensationally enlarged particles (Hering et al., 2005). In contrast to the older butanol-based laminar flow condensation particle counters, which enlarge particles by alcohol condensation in a cold-walled tube, the growth tube concept explicitly accounts for the high diffusivity of water vapor to enable its use as the condensing vapor (Iida et al., 2008).

This study uses a miniature growth tube measuring 4 mm ID by 110 mm length. The walls are wetted passively using a rolled paper filter in contact with a small water reservoir. A thermoelectric device, which acts as a heat pump, is sandwiched between the cooled and warmed halves of the growth tube. The warm side is equipped with cooling fans to dissipate excess heat from the thermoelectric device. Typical operating temperatures are 13° and 30°C for the cooled (T_{cold}) and warmed (T_{hot}) sides, respectively. This produces a supersaturation of 20% along the centerline, corresponding to an activation size of 12 nm for an insoluble, wettable particle. Particle growth is rapid and uniform at the high supersaturations produced in the GT such that all particles, even hydrophobic ones, grow to the same size. The design flow rate range is 0.1 – 0.4 lpm. At the 0.1 lpm flow utilized in this study the residence time in the condensation region is 400 ms.

2.2.2 UF-ATOFMS

Briefly, the UF-ATOFMS measures the size and dual polarity mass spectra of individual particles in real time (Su et al., 2004). To increase the size range of particles detected, the UF-ATOFMS was used without the MOUDI pre-cut, extending the upper size limit to 1200 nm D_a, although the optimum size range transmitted by the aerodynamic focusing lens is ~200-400 nm D_a. Two 532 nm continuous wave lasers, separated a known distance, scatter light from each individual particle in order to set the timing for a third pulsed laser operating at 266 nm, which desorbs and ionizes chemical species from each particle producing positive and negative ion mass spectra for each particle.

ATOFMS data were analyzed using the YAADA (http://www.yaada.org) toolkit in Matlab with the neural network algorithm ART-2a, which separates the main particle types into clusters based on their unique ion patterns (Song et al., 1999). Parameters used in this study were: vigilance factor of 0.85, learning rate of 0.05 and iteration number of 20. Clusters with very similar ion patterns of varying intensities were manually combined, resulting in a total of 8 major classes. The standard error of the fraction of each particle type was calculated assuming Poisson statistics and is included

below in the discussion regarding ambient particle comparison with and without the growth tube as well as the size segregated chemical comparison.

2.2.3 Coupled GT-UF-ATOFMS

A coupled GT-UF-ATOFMS system was formed by securing the growth tube directly above the critical orifice in the aerodynamic lens in the UF-ATOFMS. One concern was to control the condensational growth of the UFP to size ranges that coincide with the size range of particles detected with the UF-ATOFMS. The temperature difference of the GT must be large enough to create a large enough supersaturation to activate and grow all particles, but small enough to not grow them larger than the upper limit of the UF-ATOFMS. We attempted to control the size of the grown particles by drying them with humidified dry nitrogen as they exited the GT before entering the UF-ATOFMS. However, this approach was not successful because all the particles dried out to their original ultrafine size, precluding their optical detection. In the future, it may be possible to set up an RH control system that allows one to more carefully remove the water from the particles and reduce their sizes to the required size range. A differential mobility analyzer (DMA) is utilized upstream of the GT-UF-ATOFMS in order to know the original size of the particles before condensational growth and the parameters used are described in the supplementary material.

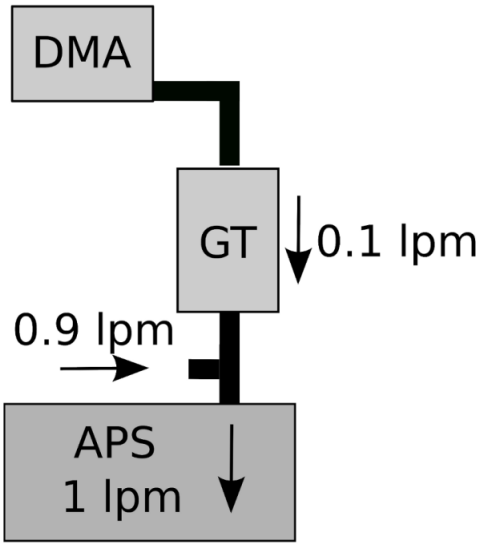

Figure 2.1: Experimental configuration of GT coupled to APS with differential mobility analyzer upstream. When the GT is coupled to APS only the size distribution of the grown particles is obtained.

2.2.4 Sizing Studies

Size selected grown ambient particles were measured with an Aerodynamic Particle Sizer (APS) (3321, TSI) to determine the sizes of the condensationally enlarged particles (Figure 2.1). The GT-UF-ATOFMS system was tested with polystyrene latex spheres (PSLs) (Interfacial Dynamics Microsphere & Nanosphere, Oregon and Invitrogen Molecular Probes, Oregon) of known size. For details see supplementary material.

2.2.5 Chemical Composition and Ambient UFP Studies

To evaluate whether the condensational growth within the GT affected measurement of particle composition, 175 ± 10 nm ambient particles were sampled on 5/26/09 with the UF-ATOFMS under three conditions as shown in Figure 2.2: a) no GT, b) GT with drying, and c) GT. The no GT sampling condition consists of just a DMA upstream of the UF-ATOFMS. The GT with drying sampling condition consists of an inline mixer (1/4” diameter, Koflo, Koflo Corporation, Illinois) that mixes the GT

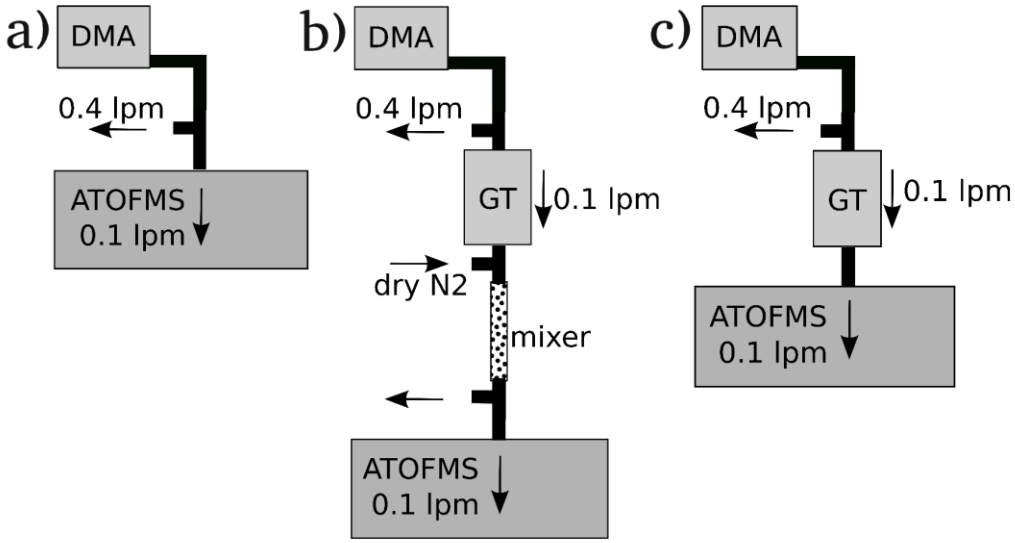

Figure 2.2: Experimental configurations: (a) UF-ATOFMS with no GT, (b) GT coupled to UF-ATOFMS with drying (an inline mixer with dry nitrogen gas) in between, and (c) GT coupled to UF-ATOFMS. All experimental set-ups have a differential mobility analyzer upstream. Both chemical composition and particle size are obtained when the GT is coupled to the UF-ATOFMS.

output with dry filtered nitrogen prior to sampling with the UF-ATOFMS, thereby evaporating the condensed water and returning the particles to their original size. Sampling with the GT followed by drying allows one to determine if particle chemistry changes after growth with water followed by evaporation to its original size. The GT sampling condition has the GT between the DMA and UF-ATOFMS. For the no GT and GT with drying conditions, 2000 mass spectra were obtained, while only 1000 were acquired for the GT sampling arrangement.

In order to study differences in the chemical composition of ambient particles across a range of sizes, ambient particles of 150, 100, 80 and 60 ± 10 nm were sampled over the course of the morning on 12/12/08 with the GT-UF-ATOFMS. Over 100 mass spectra were obtained at each of these sizes. To determine the long-term sampling capabilities of the GT approach, ambient particles with sizes of 80 ± 10 nm were sampled continuously from 6/12/09 thru 6/16/09 with the GT-UF-ATOFMS. Parallel to these measurements, ambient particle size distributions were obtained with a scanning

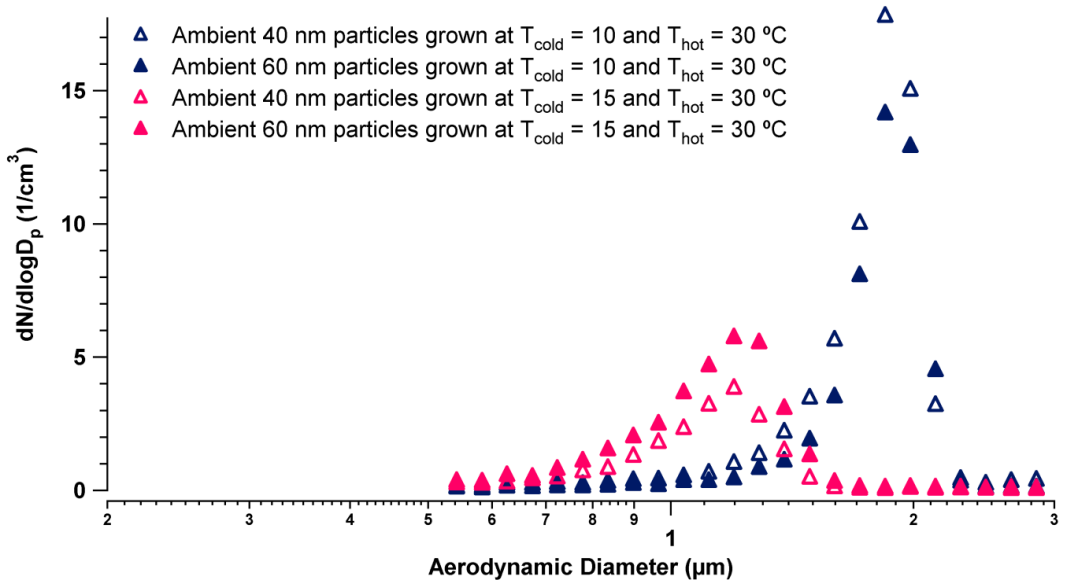

Figure 2.3: Size distribution of grown 40 and 60 nm ambient particles (open and solid triangle symbols, respectively) measured with APS when GT is set at T_{cold} = 10°C and T_{hot} = 30°C (dark blue) and T_{cold} = 15°C and T_{hot} = 30°C (red).

mobility particle sizer (SMPS), using a second 3081 DMA coupled to a TSI 3010 CPC with 4.0 and 0.4 lpm sheath and aerosol flows, respectively. All of the ambient experiments were performed at the campus of the University of California, San Diego.

2.3 Results and Discussion

2.3.1 Sizing Studies

Results from the APS size distribution measurements of ambient grown particles are shown in Figure 2.3. The 40 and 60 nm size selected ambient particles grew to ~1.2-1.8 µm as discussed in the supplementary material. The smallest PSL size sampled with the GT-UF-ATOFMS system for which mass spectra were obtained was 38 nm.

2.3.2 Chemical Composition of Ambient UFP

Example mass spectra of the different types of ambient particles measured by the UF-ATOFMS in this study are shown in Figure 2.4. As particles age, they grow in size and, depending on ambient conditions, will become coated with secondary species

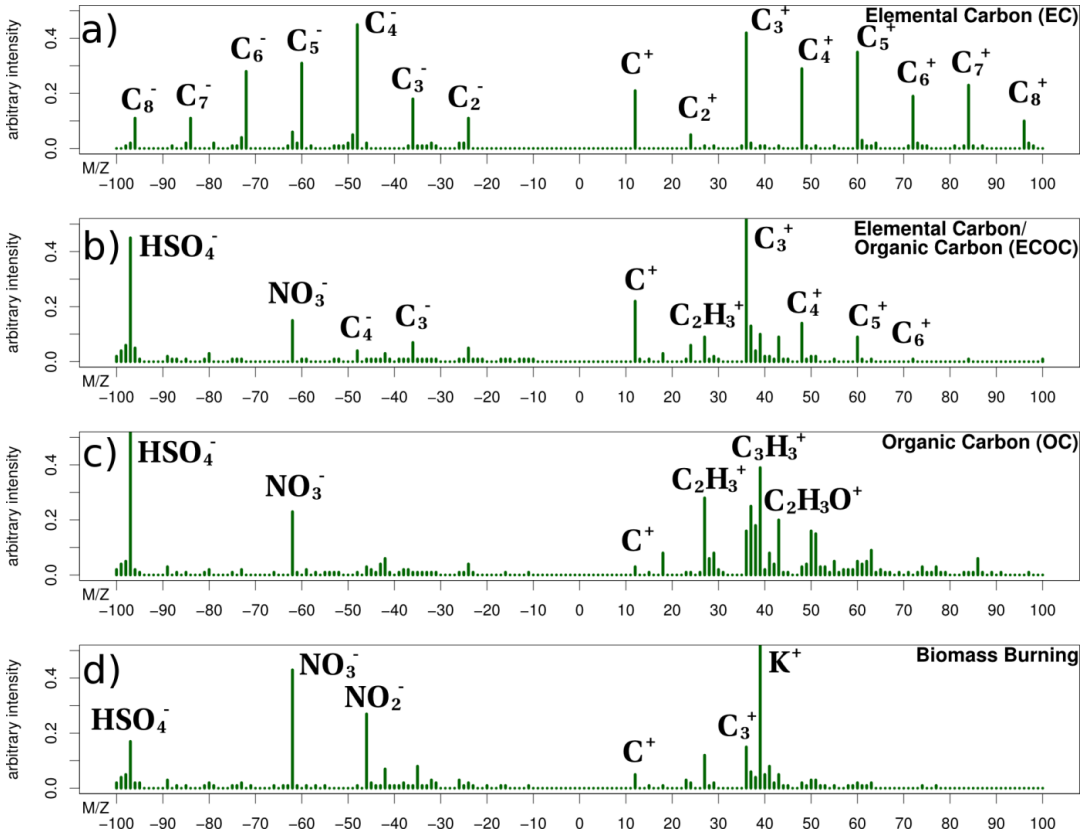

Figure 2.4: Example ambient particle types sampled with just the UF-ATOFMS without the GT: a) elemental carbon (EC), b) elemental/organic carbon (EC/OC), c) organic carbon (OC), and d) biomass burning.

such as organics, including oxidized OC at m/z +43, amines (m/z + 86), ammonium (m/z +18), and nitrate (m/z +30) (Angelino et al., 2001; Bhave et al., 2002; Dekenberger et al., 2007; Liu et al., 2000; Pratt et al., 2009a; Sullivan et al., 2007). The amines marker at m/z +86 is due to the alkylamine fragment $(C_2H_5)_2N{=}CH_2^+$ (Angelino et al., 2001). These types of secondary markers are important for CCN studies because ammonium, amine and nitrate salts have been linked with increased particle hygroscopicity (Petters and Kreidenweis, 2007; Smith et al., 2010). In addition, it has been shown that more chemically aged particles have higher CCN activities, although particle mixing state is key for determining hygroscopicity (Asmi et al., 2010; Choularton et al., 2008; Furutani et al., 2008; Shilling et al., 2007; Sullivan et al., 2009).

2.3.3 Ambient Sampling Comparison With and Without Growth Tube

One question that arises is how much does the GT alter the chemical composition of the ambient particles sampled by the UF-ATOFMS. Prior work with a different condensational system, one designed to enrich the concentrations of ambient ultrafine particles for health effects studies, has shown that particle chemistry can change upon the addition of water followed by evaporation (Su et al., 2006). By measuring particles at the output of the concentrator and comparing them to the composition of UFP upstream, an UF-ATOFMS was used to show that the chemistry of the concentrated UFP had undergone substantial changes. Specifically, organic species and markers indicative of aqueous phase processing appeared in the mass spectra of the single ultrafine particles exiting the concentrator, as compared to that observed upstream of the concentrator. Recently, it has also been shown that soluble gases are enriched in the condensed water of these concentrators possibly affecting the particulate composition (Jung et al., 2010). Thus, a question exists as to whether the growth tube particles undergo similar types of processes and chemical reactions.

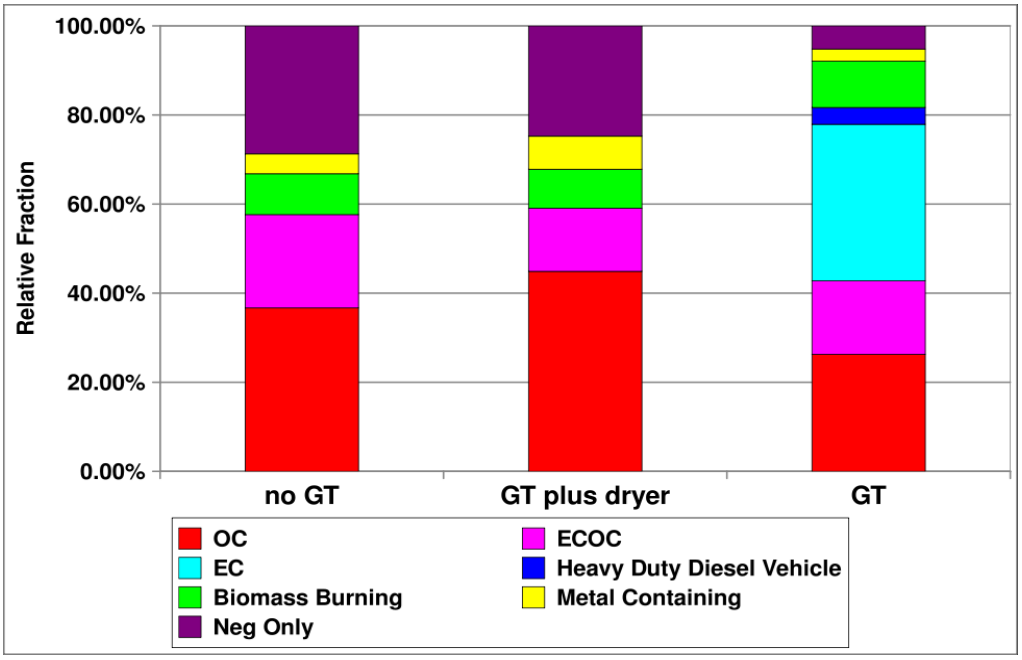

Figure 2.5: Particle types of 175 ± 10 nm ambient particles sampled on May 26, 2009, at the University of California, San Diego with no GT, GTwith drying, and GT conditions.

Results from UF-ATOFMS measurements for the GT are shown in Figure 2.5, displaying the chemical composition of 175 ± 10 nm D_m ambient particles measured under each of the three conditions: no growth tube, growth tube with drying and growth tube. The standard error of the fraction of each particle type in all three conditions was less than 2% based on Poisson statistics. Clearly, Figure 2.5 shows a similar distribution of particle types obtained with the no GT and GT with drying conditions, where the main dual ion particle types sampled were organic carbon (OC), elemental carbon and organic carbon (ECOC), and biomass burning. Some particles produced spectra with negative ions only, consisting of nitrate and/or sulfate ions. Based on the similar fraction of particle types detected with no GT and GT with drying conditions, the growth tube does not appear to irreversibly induce significant changes in particle chemistry, at least to any detectable extent. Although some peaks would sometimes appear in the mass spectra, such as ammonium and nitrate markers, the overall particle types were very similar under the different conditions of our experiments. For example, the difference mass spectra of ECOC particles sampled with and without the growth tube, shown in Figure 2.6, highlights the similarity between these two mass spectra. Similar observations were obtained by comparing mass spectra from other particle types, including biomass burning and OC, sampled under different sampling configurations.

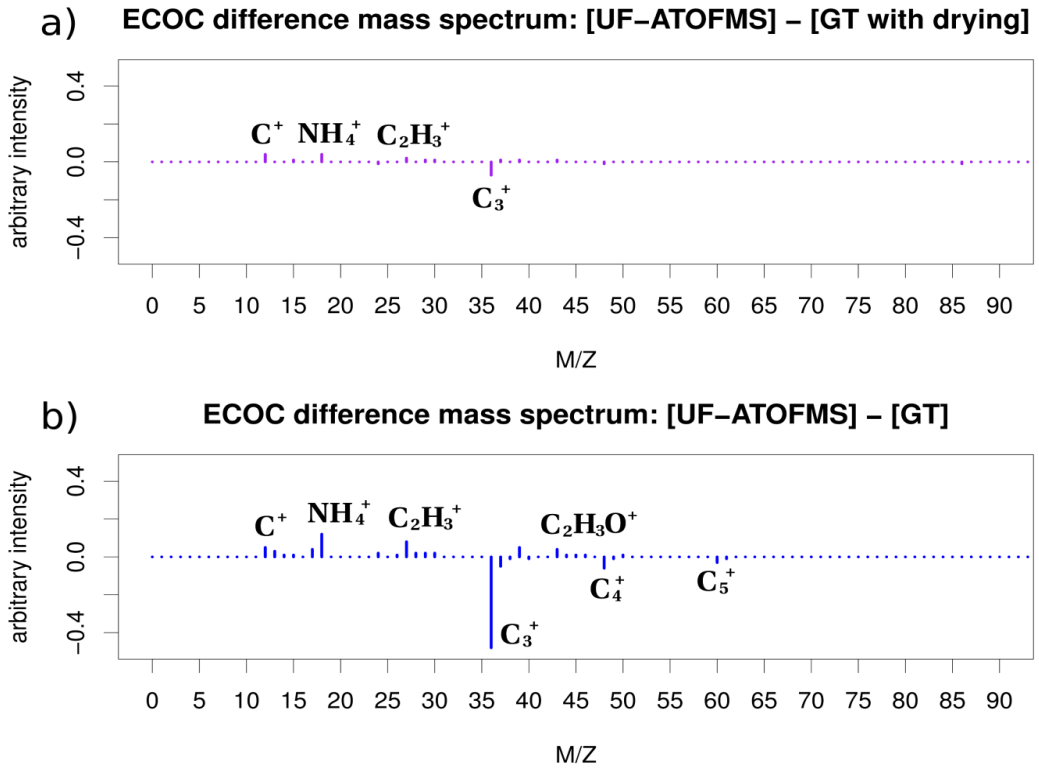

Figure 2.6: Difference spectra for ECOC particles measured on 5/26/09 at 175 ± 10 nm (a) mass spectrum from direct sampling with the UF-ATOFMS without a GT minus spectrum from sampling through the Growth Tube with drying, and b) direct UF-ATOFMS mass spectrum minus GT-UF-ATOFMS mass spectrum.

The distribution of ambient particle types sampled with the GT-UF-ATOFMS clearly differs from the fraction of types sampled with the GT followed by drying. As shown in Figure 2.5, when sampling with the growth tube the largest fraction (35%) observed were the elemental carbon (EC) and heavy duty diesel vehicle (HDDV) particle types. It is worth noting that there were no EC particles observed using the other non-growth tube sampling configurations. These results differ from those obtained in the previous concentrator study, where EC particles were present before entering the concentrator but became ECOC and OC particle types after exiting the concentrator, an effect attributed to condensation of semivolatile organic gas phase species that underwent aqueous phase oxidation and remained on the particles after drying (Su et al., 2006). The fact that with the growth tube, we observe a high fraction

of EC particles offers further support that the technique is not chemically modifying the particles by adding large amounts of organic carbon.

The EC particles were more recently introduced to the atmosphere than the ECOC and OC particles. As the EC particles age, more oxidized organic species are added and appear in the mass spectra. Over time, sulfate, nitrate, and ammonium also condense on these particles, making them more hygroscopic (Weingartner et al., 1997). In the current configuration, negative ions are not typically detected in the GT mass spectra due to the increased water content of the particles from the condensational growth (Neubauer et al., 1998). As shown previously, particle humidity affects the ability to obtain negative mass spectra (Neubauer et al., 1998). This issue is addressed in more detail in the supplementary material, but plans are underway to adapt the ATOFMS to a two-step desorption/ionization system in order to remove the chemical species from the water content in order to minimize this issue (Morrical et al., 1998). Because of the difficulty in obtaining negative mass spectra, we are unable to compare sulfate peak areas with the same particle types found with the no growth tube and growth tube with drying. However, it is clear there are relatively less OC particles as well as less ammonium, which is presumed to be the nitrate and sulfate counter ion, measured with just the growth tube than without, and thus it is likely less secondary sulfate is present on these smaller particles as well.

We hypothesize that the freshly produced combustion particles sampled with the GT are more fractal and thus their mobility diameters are significantly larger from their aerodynamic diameters. In a previous UF-ATOFMS study, Spencer et al. showed that EC particles with mobility diameters of 400 nm possessed aerodynamic diameters as measured in the ATOFMS as small as 100 nm (Spencer et al., 2007). This difference in diameters results from differences in the shape and density of the particles. Thus it is highly likely that particles with mobility diameters of 175 nm produced by combustion processes have aerodynamic diameters much smaller than can be optically detected by the UF-ATOFMS (< 143 nm) in its current configuration. Therefore, these ultrafine

particles, which are known to be present in the highest number concentrations in the atmosphere, cannot be detected without first being grown to a larger detectable size.

If the GT were changing the chemical composition of particles, as reported for the concentrator, it would lead to addition of species not their removal (Su et al., 2006). The difference ECOC GT mass spectrum in Figure 2.6, which shows a decrease in secondary species in the ECOC GT mass spectrum compared to that obtained without GT, contributes to the idea that the GT is not chemically biasing particles with addition of these species. At the same time, the difference mass spectrum supports the hypothesis that the particles sampled with the GT are less chemically aged because the GT allows the sampling of particles of smaller aerodynamic diameters (and hence fresher) than without the GT. The observations of similar chemical fractions of particles between the no GT and GT with drying conditions and more fresh particles sampled with the GT only are encouraging and suggest that under the conditions of these experiments, the GT did not chemically modify the particles to a significant extent. It should be noted that further more detailed studies are needed to probe the gas phase species concentrations and ascertain that when higher concentrations exist, the same results hold.

2.3.4 Size Segregated Chemical Comparisons

Figure 2.7 shows the different particle types segregated by mobility size sampled with the GT-UF-ATOFMS on the morning of 12/12/08. The standard error of the fraction of each particle types for all four sizes was less than 5% as calculated using Poisson statistics. Two trends are readily apparent. As size increases, a decrease in the fraction of particles containing metals and an increase in particles containing ECOC and OC occurs. Overall, particles are externally mixed and show distinct chemical signatures at these small sizes. The 60 nm D_m particles consist of an external mixture of HDDV, metals, and biomass burning particles and there are no OC particles internally or externally mixed. As stated in the supplementary material, pure OC particles are different than the OC-rich biomass burning particles, which the ATOFMS mainly detects as K ECOC due to matrix effects. The 80 nm D_m particles are similarly

composed of externally mixed HDDV, metals, and biomass as well as small amounts EC, ECOC, and pure OC. The 80 nm D_m OC particles are internally mixed with amines, ammonium, and nitrate, as has been previously shown for ultrafine organic particles (Pratt et al., 2009a; Pratt et al., 2009b; Shields et al., 2008). The 100 nm D_m particle type distribution is similar to the 80 nm D_m particles, except there are no EC particles. In addition to OC, 100 nm D_m ECOC and some of the biomass burning particles are internally mixed with amines, ammonium, and nitrate. The 150 nm D_m particle types show EC, biomass burning, ECOC, HDDV, metals and OC. All the 150 nm D_m particle types, except HDDV, are internally mixed with amines, ammonium, and nitrate. Throughout all sizes, the ECOC particle type contains EC and OC species internally mixed on the same particles. These size-selected growth tube studies show that, at these different discrete sizes, a large and distinct difference occurs in the fraction of major particle types, indicative of changes in particle sources as well as the chemistry due to atmospheric aging processes.

The metal particle spectra contain just iron for particles less than 150 nm, whereas the 150 nm metal particles included both iron and vanadium. These two metal particle types come from different sources. Vanadium has been associated with bunker fuel used in ships; regional air transport studies have shown the ubiquity of these particles which can travel long distances from major port regions (Ault et al., 2010; Ault et al., 2009; Healy et al., 2009). A possible source of the iron rich particles could be from welding at the campus machine shop which is located in close proximity to the UCSD lab where sampling was being conducted. This is consistent with the time of the sampling, Friday morning, when the machine shop is regularly active as well as a previous ATOFMS welding study which yielded similar mass spectra (Su et al., 2005).

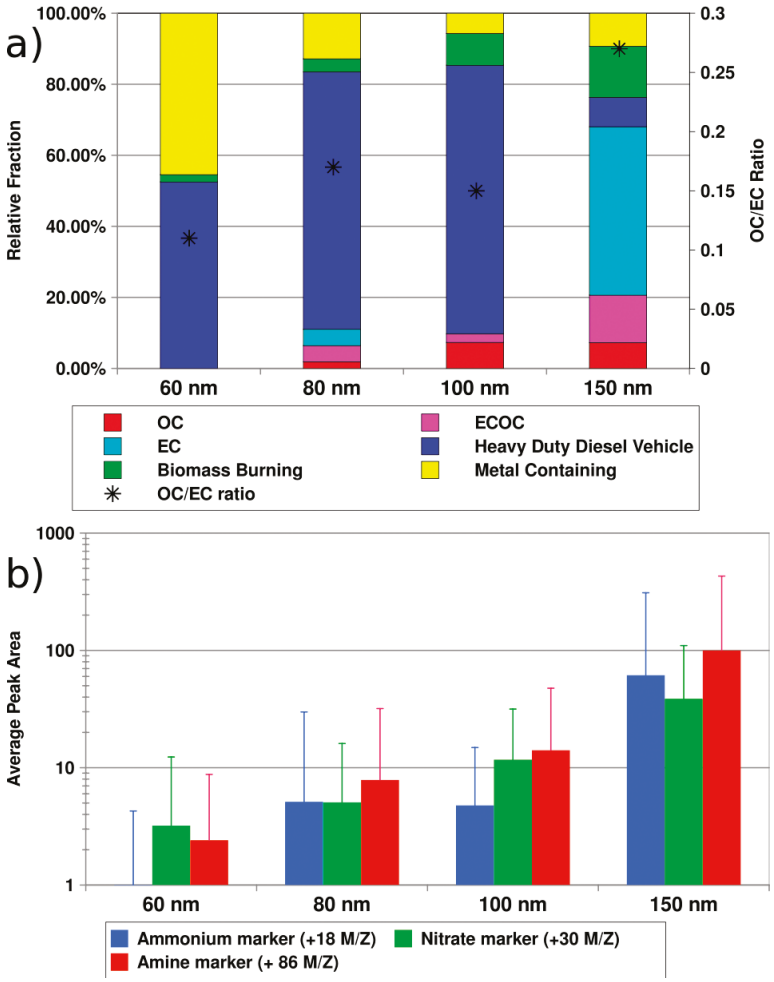

Figure 2.7: Particle chemical composition as a function of size determined with the GT-UF-ATOFMS system measured on December 12, 2008, at the University of California, San Diego: (a) relative particle type distribution and OC/EC ratio, and (b) average intensity of ammonium, nitrate, and amine markers as a function of particle size.

Figure 2.7a also shows the OC/EC ratio determined for all particles in each size bin, as was done in the concentrator study referenced above, but using the verified OC/EC peaks from Spencer (Spencer and Prather, 2006; Su et al., 2006). The low OC/EC ratio calculated for the smaller particle sizes in this study is opposite of that observed after the particles passed through the concentrator, which showed an increase in OC content with decreasing particle size (Su et al., 2006). On the contrary, the OC/EC ratio of the smaller particles sampled with the growth tube (0.15 for 80 nm D_m) is similar to those sampled in the concentrator study before entering the concentrator

(0.26 for 75 nm D_a). This result supports the other observations described above that the growth tube does not alter the chemistry of the grown particles. We note that with the GT-UF-ATOMFS system the residence time of droplets prior to entering the vacuum of the UF-ATOFMS is of the order of 400 ms, which is short compared to the calculated transport time for vapor phase organics at typical ambient concentrations, and thus the uptake of these vapors should be kinetically limited.

Another way to contrast chemical differences between smaller ultrafine and larger particles involves comparing the ion intensities of the secondary species ammonium, nitrate, and amines (+18, +30, and 86 m/z, respectively). Figure 2.7b shows that as particle size increases, so does the intensity of secondary marker ions as would be expected. For example, the ammonium, amines, and nitrate markers were over 70, 40, and 10, times more intense in the 150 nm particles than in the 60 nm ones, respectively. The 150 nm particles have four times the fraction of OC particles and an increase of over 1.5 times in the OC/EC ratio compared to the 80 nm particles. As stated above, OC is expected in larger particles as the condensation of oxidized semi-volatile species occurs as they undergo atmospheric aging processes. The observation of increasing amounts of amines, ammonium, nitrate and OC markers is evidence that condensation occurred on the smaller sized ultrafine particles sampled, originated from primary sources: welding, fossil fuel and biomass burning. These observations support our understanding that as smaller particles age and grow, they may become more CCN active through the addition of soluble secondary species.

2.3.5 Real-time ambient UFP measurements.

Chemical composition results of the GT-UF-ATOFMS measurements of 80 ± 10 D_m particles over a 3 day period in San Diego, CA are shown in the bottom panel of Figure 2.8. The top panel in Figure 2.8 shows the ambient particle size distribution measured with the SMPS. Overall, the number of particles sampled with the GT-UF-ATOFMS correlates with SMPS measurements of particle size. When the SMPS detected a higher fraction of 80 nm particles, the GT-ATOFMS system also analyzed more particles. The spike in particles seen after midnight on 6/12/09 corresponds with

biomass burning and ECOC particles. The next big spike in particles can be attributed to morning rush hour traffic emissions on a Monday, as the majority of particles detected during this time period were EC with calcium, indicative of HDDV (Toner et al., 2008). During this longer sampling period, we encountered two periods, as noted in Figure 2.8, where no data were acquired when the GT clogged the critical orifice in the UF-ATOFMS with water. We are working to minimize this problem by adding a heated region to the critical orifice where the GT is connected to the ATOFMS. This modification will allow for longer term unattended studies of CCN chemistry with high time resolution. In addition, we are preparing to couple a syringe pump to the GT's water reservoir to avoid having to manually add water every 5-7 hours.

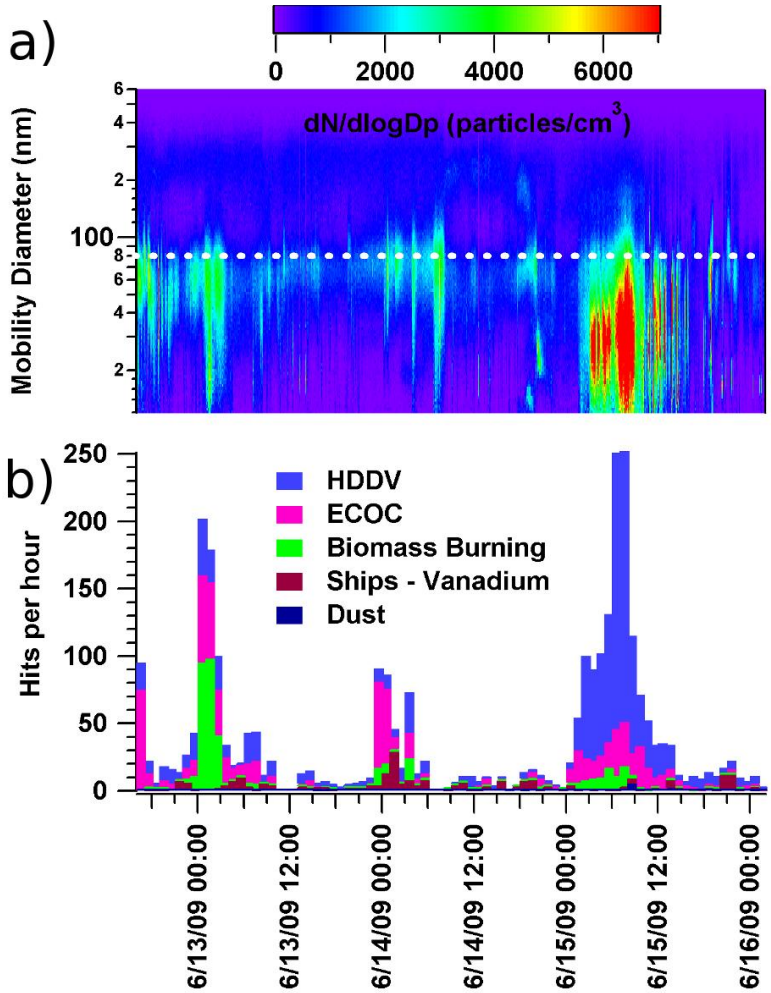

Figure 2.8: Long-term study between June 12, 2009, to June 16, 2009, sampled at the University of California, San Diego: (a) temporal size distribution of ambient particles and (b) temporal particle type distribution of ambient 80 ± 10 nm sampled with GT-UF-ATOFMS technique. White dashed line indicates the 80 nm particles in the size distribution. There were no GT-ATOFMS data was obtained due to water from the GT clogging the UF-ATOFMS inlet: June 13, 2009 10:00-13:00 and June 14, 2009 6:00-8:00.

Recent measurements of ambient CCN concentrations alongside the mixing state of ultrafine particles with the GT-UF-ATOFMS system will continue to help improve the insight into the chemistry of particles in the CCN active size range. This will increase our understanding of the spatial and temporal variability of the sources and composition of CCN, thereby decreasing the uncertainties associated with the indirect effect of aerosols on climate.

2.4 Conclusions

A new approach for studying the composition of UFP by coupling a water-based condensation growth tube with an UF-ATOFMS has been demonstrated and can now be used to detect the chemistry of particles as small as 38 nm. The GT-UF-ATOFMS technique, when coupled with a DMA, will provide insight into changes in particle chemistry in the critical 50-200 nm size range in cloud and regional climate studies. Ambient particles down to 60 nm showed significantly less secondary species, such as ammonium, nitrate, and amines, and a higher fraction of fresh EC and HDDV particles compared to larger particles. In addition, many of the same particle types are detected using the growth tube as those encountered in the larger size range, however, as expected, the smaller ultrafine particles are not as chemically aged. There is no evidence of particles undergoing chemical changes due to the GT, a result that may be attributed to the short droplet residence time in the GT-UF-ATOFMS system. However, future testing will include different concentrations of precursor gases to examine the potential for gas/particle partitioning in greater detail. The GT-UF-ATOFMS system was capable of long term operation, successfully sampling particles at 80 ± 10 nm D_m over a 3 day period. Further studies will quantify the types of particles in this size range in a wider range of environments (i.e. remote, coastal, mountain). The GT-UF-ATOFMS will be used to probe how changes in meteorological conditions, which can vary minute to minute, change particle chemistry. Correlated studies of the chemistry of the particles in the size range critical for cloud formation and fast cloud condensation nuclei concentration measurements, which can now be measured in seconds (Moore and Nenes, 2009), will be performed to better understand particle sources contributing to increased CCN concentrations. Optimization of this technique will include major improvements to increase the detection of negative ions, minimize water blockage, and automate water delivery. Ultimately, the use of the growth tube for studies of particle chemistry in this smaller size range will impact health effects studies, industrial applications, semi-conductor processing and clean rooms, and nanoparticle characterization.

2.5 Acknowledgements

This work was supported by the U.S. Environmental Protection Agency PM Center Grant (No. R832415) and the National Institute of Health (grants # R44ES014997 and R44ES014997-S1).

Chapter 2 in full, is a reprint of the material as it appears in Approach for measuring the chemistry of individual particles in the size range critical for cloud formation in *Analytical Chemistry* 2011. Melanie D. Zauscher, Meagan J.K. Moore, Gregory S. Lewis, Susanne V. Hering, Kimberly A. Prather; Copyright 2011, American Chemical Society.

2.6 Supplemental Materials

2.6.1 Sizing Studies

The GT-UF-ATOFMS system was evaluated using UFP of known diameter obtained by size selection with a differential mobility analyzer (DMA) (Model 3081, TSI). Notably, the DMA size selection is based on mobility diameter (D_m) which depends on particle shape, but is independent of particle density, and thus is different than aerodynamic sizing of the ATOFMS which depends on both shape and density (D_a). Although the DMA is typically used with an aerosol to sheath flow ratio of 1:10, in order to increase the number of particles detected, the DMA was "de-tuned" in order to admit a broader size distribution with a higher particle concentration into the UF-ATOFMS (Flagan, 1999). This was accomplished by adjusting the sheath and aerosol flows to 2 and 0.5 lpm, respectively. In order for the aerosol flow going through the DMA to be 0.5 lpm, and to reduce the residence time of particles in the tubing, a tee was set-up with a vacuum line pulling at 0.4 lpm because the UF-ATOFMS only pulls ~0.1 lpm. In order to ensure there were no leaks in the system, at least once a day, the voltage on the DMA was set to 0 V for ~5 minutes to ensure no particles were being transmitted through the DMA or GT into the UF-ATOFMS.

DMA size selected grown ambient particles were measured with an Aerodynamic Particle Sizer (APS) (3321, TSI) to determine the sizes of the activated particles. The set-up, shown in Figure 2.1, has a tee connected between the growth tube and APS directly on the aerosol inlet. The growth tube settings were flow of 0.1 lpm and T_{cold} = 10 or 15^{o}C and T_{hot} = 30^{o}C. Because the APS aerosol inlet pulls 1 lpm, a make-up flow of 94% humidified, filtered nitrogen was pushed at 0.9 lpm through the tee into the APS.

Lab studies probed how much the growth tube increases the particle size under different conditions. Figure 2.3 shows the size distribution of 40 and 60 nm ambient particles activated using the growth tube and sampled with the APS using two different cold inlet temperatures, 10 and 15 ^{o}C respectively and a hot wall temperature of 30 ^{o}C. These particles grew to ~1.2-1.8 μm, as shown here for the APS. As expected, the particles exposed to a smaller temperature difference and hence supersaturation grew less than those exposed to a larger supersaturation. Also, fewer particles activated at the lower supersaturation values. The GT-UF-ATOFMS has a higher detection efficiency at lower supersaturation when there is less water on the particles. Thus, in order to optimize the number of particles that activate at higher supersaturations that can be detected, the GT temperatures were adjusted to T_{cold} = 13 and T_{hot}= 30^{o}C for the remainder of the experiments. When measuring the size distribution of grown particles with the UF-ATOFMS, there is a slight size difference from the APS measurements likely due to particles evaporating in the aerodynamic focusing lens of the UF-ATOFMS as well as the upper size limit of the UF-ATOFMS (~1 μm) compared to the larger upper size limit of the APS (~ 20μm) (Zelenyuk et al., 2006). It is also worth noting that although the make-up flow was humidified to 94% RH, it is very likely that the grown particles may have slightly reduced in sized while exposed to this non-saturated air as they traveled into the instruments from the GT. With our current set-up, we were not able to quantify the size decrease of the grown droplets.

The GT-UF-ATOFMS system was tested with polystyrene latex spheres (PSLs) (Interfacial Dynamics Microsphere & Nanosphere, Oregon and Invitrogen Molecular

Probes, Oregon) of known size. Varying sizes down to 38 nm were introduced in order to test the lower size limit of particles detected with the GT-UF-ATOFMS. PSLs were atomized, sized selected with DMA (4 and 0.4 lpm sheath flow and aerosol flow, respectively) and sampled with the GT-UF-ATOFMS system. PSLs have identical mobility and aerodynamic diameters, therefore the size selected with the DMA is identical to the aerodynamic size measured in the UF-ATOFMS. The smallest PSL size sampled with the GT-UF-ATOFMS system for which mass spectra were obtained was 38 nm.

2.6.2 Example of Typical Ambient Mass Spectra

Example mass spectra of the different types of ambient particles measured by the UF-ATOFMS in this study are shown in Figure 2.4. These types are quite similar to those observed in previous field studies (Shields et al., 2007; Silva et al., 1999; Silva and Prather, 2000; Toner et al., 2008; Toner et al., 2006). In particular, the elemental carbon (EC) particle type (Figure 2.4) is characterized by peaks appearing at carbon clusters such as at m/z = 12, 24, 36. Many EC particles also include organic carbon (OC) markers with C_nH_m clusters with peaks at +27, +39, +43 m/z and are hence named ECOC (Figure 2.4). OC particles are comprised of primarily intense organic carbon peaks (Figure 2.4) with less intense EC markers ions at 12, 24, and 36 (Silva and Prather, 2000). Particles from heavy duty diesel vehicles (HDDV) have a calcium peak at m/z + 40 on an otherwise EC or ECOC particle type (Shields et al., 2007; Toner et al., 2008; Toner et al., 2006). Although biomass burning particles are OC rich, the mass spectra obtained with ATOFMS is a combination of ECOC markers and potassium with an intense peak at m/z +39 (Figure 2.4) (Silva et al., 1999). The calcium and potassium peaks indicate the importance of using combinations of peaks in the mass spectra for source apportionment. One way to compare the amount of specific species on the particles is to compare the peak areas in each spectrum. This comparison can be done for particles of the same chemical matrix (ie dust, organic carbon, soot, sea salt). Typically we characterize ambient studies using the fractions of particle types, which

changes depending on the temporal distribution of sources and chemical evolution of the particles.

2.6.3 ECOC Ambient Sampling Comparison With and Without Growth Tube

It is informative to compare the average mass spectra for the same particle type sampled using the different sampling configurations. As an example, we have shown the difference mass spectra of ECOC sampled with the GT with drying and GT conditions subtracted from the no GT condition in Figure 2.6 (for a representative ECOC mass spectra, see Figure 2.4). The difference ECOC mass spectrum of the growth tube with drying has very few small peaks, showing the no GT and GT with drying conditions produce mass spectra that appear almost indistinguishable from each other with the same peaks and similar ion intensities. The dot product between the ECOC no GT and ECOC GT with drying spectra confirms the similarity in their spectra with a value of 0.98, very close to 1 which represents identical spectra, further supporting the observations that the growth tube does not cause any detectable changes in particle composition. Similar observations were obtained by comparing mass spectra from other particle types, such as biomass burning and OC, sampled under different sampling configurations.

The dot product of ECOC no GT and GT mass spectra is 0.64. If the GT were changing the chemical composition of particles, as reported for the concentrator, it would lead to addition of species not their removal (Su et al., 2006). The difference ECOC GT mass spectrum in Figure 2.6 shows a decrease in the OC markers +27 and 43 m/z indicating that the ECOC particles sampled with the GT have less oxidized OC species than particles sampled without the GT. Also, the ammonium peak is smaller in the ECOC GT mass spectrum compared to the no GT mass spectrum. The decrease in secondary species in the ECOC GT mass spectrum compared to that obtained without GT contribute to the idea that the GT is not chemically biasing particles with addition of these species. At the same time, the difference mass spectrum supports the hypothesis that the particles sampled with the GT are less chemically aged because the GT allows

the sampling of particles of smaller aerodynamic diameters (and hence fresher) than without the GT.

2.6.4 Challenges of Increased Water Content

One major challenge in interpreting the data with the growth tube is the increased fraction of particles with positive only spectra. The decrease in the negative ion spectra observed with the GT-UF-ATOFMS can be explained by the increased water content of the particles grown by water condensation (Neubauer et al., 1998). Because water tends to suppress the negative ion signal, typical ambient aerosol measurements are usually done with a dried inlet flow (Cubison et al., 2008; Johnston et al., 2006; Rhoads et al., 2003). Negative ions provide critical information on the inorganic components of aerosols such as sulfate, which in small amounts can greatly impact the CCN activity of particles and drive water uptake (Bilde and Svenningsson, 2004). Since it is crucial for cloud studies that this GT-UF-ATOFMS technique be able to detect negative ions, we are working on increasing the number of negative spectra obtained with the GT-UF-ATOFMS. Controlling particle growth, such that some excess water can be removed, should allow the detection of more negative mass spectra. One approach to improve control of particle growth is by sampling the particles into a nozzle ATOFMS, which optically detects particles up to 3 μm, and heating the nozzle to carefully remove some of the water. Another possibility to better controlling the size of the activated particles is by using a relative humidity controlled flow tube to shrink the particles down. Another approach is to modify an ATOFMS to use two lasers to perform two step laser desorption/ionization, as previously shown by Morrical et al (Morrical et al., 1998). One laser desorbs the chemical components into the gas phase as neutral species while a second laser ionizes these desorbed species. Because the chemical species are removed from the water matrix, suppression of the negative ions by water would no longer be an issue. Being able to obtain dual polarity mass spectra will greatly improve the chemical analysis ability of the GT-UF-ATOFMS technique and its applicability to cloud studies. However even with single polarity only, a great deal can still be learned about *individual* particles and their effects on

clouds in this previously blind region of the aerosol size spectrum with real-time measurement capabilities.

2.7 References

Andreae, M. O., and Rosenfeld, D. (2008).Aerosol-Cloud-Precipitation Interactions. Part 1. The Nature and Sources of Cloud-Active Aerosols, *Earth Science Reviews*, *89*, 13-41.

Angelino, S., Suess, D. T., and Prather, K. A. (2001).Formation of Aerosol Particles from Reactions of Secondary and Tertiary Alkylamines: Characterization by Aerosol Time-of-Flight Mass Spectrometry, *Environmental Science & Technology*, *35* (15), 3130-3138.

Asmi, E., Frey, A., Virkkula, A., Ehn, M., Manninen, H. E., Timonen, H., Tolonen-Kivimaki, O., Aurela, M., Hillamo, R., and Kulmala, M. (2010).Hygroscopicity and Chemical Composition of Antarctic Sub-Micrometre Aerosol Particles and Observations of New Particle Formation, *Atmospheric Chemistry and Physics*, *10*, 4253-4271.

Ault, A. P., Gaston, C., Wang, Y., Dominguez, G., Thiemens, M. H., and Prather, K. A. (2010).Characterization of the Single Particle Mixing State of Individual Ship Plume Events Measured at the Port of Los Angeles, *Environmental Science & Technology*, *44* (6), 1954-1961.

Ault, A. P., Moore, M. J. K., Furutani, H. F., and Prather, K. A. (2009).Impact of Emissions from the Los Angeles Port Region on San Diego Air Quality During Regional Transport Events, *Environmental Science & Technology*, *43* (10), 3500-3506.

Bhave, P. V., Allen, J. O., Morrical, B. D., Fergenson, D. P., Cass, G. R., and Prather, K. A. (2002).A Field-Based Approach for Determining Atofms Instrument Sensitivities to Ammonium and Nitrate, *Environmental Science & Technology*, *36* (22), 4868-4879.

Bilde, M., and Svenningsson, B. (2004).Ccn Activation of Slightly Soluble Organics: The Importance of Small Amounts of Inorganic Salt and Particle Phase, *Tellus*, *56B*, 128-134.

Bougiatioti, A., Fountoukis, C., Kalivitis, N., Pandis, S. N., Nenes, A., and Mihalopoulos, N. (2009).Cloud Condensation Nuclei Measurements in the Marine Boundary Layer of the Eastern Mediterranean: Ccn Closure and Droplet Growth Kinetics, *Atmospheric Chemistry and Physics*, *9* (18), 7053-7066.

Burleson, D. J., Driessen, M. D., and Penn, R. L. (2004).On the Characterization of Environmental Nanoparticles, *Journal of Environmental Science and Health*

Part a- Toxic/Hazardous Substances & Environmental Engineering, *39* (10), 2707-2753.

Carson, P. G., Johnston, M. V., and Wexler, A. S. (1997).Laser Desorption/Ionization of Ultrafine Aerosol Particles, *Rapid Communications in Mass Spectrometry*, *11* (9), 993-996.

Chen, S. C., Tsai, C. J., Chou, C. C. K., Roam, G. D., Cheng, S. S., and Wang, Y. N. (2010).Ultrafine Particles at Three Different Sampling Locations in Taiwan *Atmospheric Environment*, *44* (4), 533-540.

Choularton, T. W., Bower, K. N., Weingartner, E., Crawford, I., Coe, H., Gallagher, M. W., Flynn, M., Crosier, J., Connolly, P., Targino, A., Alfarra, M. R., Baltensperger, U., Sjogren, S., Verheggen, B., Cozic, J., and Gysel, M. (2008).The Influence of Small Aerosol Particles on the Properties of Water and Ice Clouds, *Faraday Discussions*, *137*, 205-222.

Clarke, A. D., Owens, S. R., and Zhou, J. (2006).An Ultrafine Sea-Salt Flux from Breaking Waves: Implications for Cloud Condensation Nuclei in the Remote Marine Atmosphere, *Journal of Geophysical Research*, *111* (D6), 10.1029/2005jd006565.

Cubison, M. J., Alfarra, M. R., Allan, J., Bower, K. N., Coe, H., McFiggans, G. B., Whitehead, J. D., Williams, P. I., Zhang, Q., Jimenez, J. L., Hopkins, J., and Lee, J. (2006).The Characterisation of Pollution Aerosol in a Changing Photochemical Environment, *Atmospheric Chemistry and Physics*, *6*, 5573-5588.

Cubison, M. J., Ervens, B., Feingold, G., Docherty, K. S., Ulbrich, I. M., Shields, L., K., P., Hering, S., and Jimenenez, J. L. (2008).The Influence of Chemical Composition and Mixing State of Los Angeles Urban Aerosol on Ccn Number and Cloud Properties, *Atmospheric Chemistry and Physics*, *8*, 5649-5667.

Dekenberger, K. A., Moffet, R. C., Holecek, J. C., Rebotier, T. P., and Prather, K. A. (2007).Real-Time, Single-Particle Measurements of Oligomers in Aged Ambient Aerosol Particles, *Environmental Science & Technology*, *41* (15), 5439-5446.

Flagan, R. C. (1999).On Differential Mobility Analyzer Resolution, *Aerosol Science and Technology*, *30* (6), 556-570.

Furutani, H. F., Dall'osto, M., Roberts, G. C., and Prather, K. A. (2008).Assessment of the Relative Importance of Atmospheric Aging on Ccn Activity Derived from Field Observations, *Atmospheric Environment*, *42*, 3130-3142.

Garrett, T. J., and Hobbs, P. V. (1995).Long-Range Transport of Continental Aerosols over the Atlantic Ocean and Their Effects on Cloud Structures, *Journal of Atmospheric Science*, *52*, 2977-2984.

Gysel, M., Crosier, J., Topping, D. O., Whitehead, J. D., Bower, K. N., Cubison, M. J., Williams, P. I., Flynn, M. J., McFiggans, G. B., and Coe, H. (2007).Closure Study between Chemical Composition and Hygroscopic Growth of Aerosol Particles During Torch2, *Atmospheric Chemistry and Physics*, *7* (24), 6131-6144.

Healy, R. M., O'Connor, I. P., Hellebust, S., Allanic, A., Sodeau, J. R., and Wenger, J. C. (2009).Characterisation of Single Particles from in-Port Ship Emissions, *Atmospheric Environment*, *43* (40), 6408-6414.

Held, A., Rathbone, G. J., and Smith, J. N. (2009).A Thermal Desorption Chemical Ionization Ion Trap Mass Spectrometer for the Chemical Characterization of Ultrafine Aerosol Particles, *Aerosol Science and Technology*, *43* (3), 264-272.

Hering, S. V., and Stolzenburg, M. R. (2005).A Method for Particle Size Amplification by Water Condensation in a Laminar, Thermally Diffusive Flow, *Aerosol Science and Technology*, *39* (5), 428-436.

Hering, S. V., Stolzenburg, M. R., Quant, F. R., Oberreit, D. R., and Keady, P. B. (2005).A Laminar-Flow, Water-Based Condensation Particle Counter (Wcpc), *Aerosol Science and Technology*, *39* (7), 659-672.

Hudson, J. G., and Li, H. (1995).Microphysical Contrasts in Atlantic Stratus, *Journal of Atmospheric Science*, *52*, 3031-3040.

Hughes, L. S., and Cass, G. R. (1998).Physical and Chemical Characterization of Atmospheric Ultrafine Particles in the Los Angeles Area, *Environmental Science & Technology*, *32* (9), 1153-1161.

Iida, K., Stolzenburg, M. R., McMurry, P. H., Smith, J. N., Quant, F. R., Oberreit, D. R., Keady, P. B., Eiguren-Fernandez, A., Lewis, G. S., Kreisberg, N. M., and Hering, S. V. (2008).An Ultrafine, Water-Based Condensation Particle Counter and Its Evaluation under Field Conditions, *Aerosol Science and Technology*, *42* (10), 862-871.

Jayne, J. T., Leard, D. C., Zhang, X., Davidovits, P., Smith, K. A., Kolb, C. E., and Worsnop, D. R. (2000).Development of an Aerosol Mass Spectrometer for Size and Composition Analysis of Submicron Particles, *Aerosol Science and Technology*, *33* (1), 49-70.

Johnston, M. V., Wang, S. Y., and Reinard, M. S. (2006).Nanoparticle Mass Spectrometry: Pushing the Limit of Single Particle Analysis, *Applied Spectroscopy*, *60* (10), 264A-272A.

Jung, H., Arellanes, C., Zhao, Y., Paulson, S., Anastasio, C., and Wexler, A. (2010).Impact of the Versatile Aerosol Concentration Enrichment System (Vaces) on Gas Phase Species *Aerosol Science and Technology*, *44* (12), 1113-1121.

Kojima, T., Buseck, P. R., and Reeves, J. M. (2005).Aerosol Particles from Tropical Convective Systems: 2. Cloud Bases, *Journal of Geophysical Research*, *110*, D09203.

Laitinen, T., Hartonen, K., Kulmala, M., and Riekkola, M. L. (2009).Aerosol Time-of-Flight Mass Spectrometer for Measuring Ultrafine Aerosol Particles, *Boreal Environmental Research*, *14* (4), 539-549.

Lake, D. A., Tolocka, M. P., Johnston, M. V., and Wexler, A. S. (2003).Mass Spectrometry of Individual Particles between 50 and 750 Nm in Diameter at the Baltimore Supersite, *Environmental Science & Technology*, *37* (15), 3268-3274.

Lance, S., Nenes, A., Mazzoleni, C., Dubey, M. K., Gates, H., Varutbangkul, V., Rissman, T. A., Murphy, S. M., Sorooshian, A., Flagan, R. C., Seinfeld, J. H., Feingold, G., and Jonsson, H. H. (2009).Cloud Condensation Nuclei Activity, Closure, and Droplet Growth Kinetics of Houston Aerosol During the Gulf of Mexico Atmospheric Composition and Climate Study (Gomaccs), *Journal of Geophysical Research*, *114*, D00F15.

Liu, D. Y., Prather, K. A., and Hering, S. V. (2000).Variations in the Size and Chemical Composition of Nitrate-Containing Particles in Riverside, Ca, *Aerosol Science and Technology*, *33* (1), 71-86.

Lohmann, U., and Feichter, J. (2005).Global Indirect Aerosol Effects: A Review, *Atmospheric Chemistry and Physics*, *5*, 715-737.

Matsuki, A., Schwarzenboeck, A., Venzac, H., Laj, P., Crumeyrolle, S., and Gomes, L. (2010).Cloud Processing of Mineral Dust: Direct Comparison of Cloud Residual and Clear Sky Particles During Amma Aircraft Campaign in Summer 2006, *Atmospheric Chemistry and Physics*, *10* (3), 1057-1069.

Maynard, A. D. (1995).The Application of Electron-Energy-Loss Spectroscopy to the Analysis of Ultrafine Aerosol-Particles, *Journal of Aerosol Science*, *26* (5), 757-777.

McFiggans, G., Artaxo, P., Baltensperger, U., Coe, H., Facchini, M. C., Feingold, G., Fuzzi, S., Gysel, M., Laaksonen, A., Lohmann, U., Mentel, T. F., Murphy, D. M., O'Dowd, C. D., Snider, J. R., and Weingartner, E. (2006).The Effect of Physical and Chemical Aerosol Properties on Warm Cloud Droplet Activation, *Atmospheric Chemistry and Physics*, *6*, 2593-2649.

Merikanto, J., Spracklen, D. V., Mann, G. W., Pickering, S. J., and Carslaw, K. S. (2009).Impact of Nucleation on Global Ccn, *Atmospheric Chemistry and Physics*, *9* (21), 8601-8616.

Moore, R. H., and Nenes, A. (2009).Scanning Flow Ccn Analysis - a Method for Fast Measurements of Ccn Spectra, *Aerosol Science and Technology*, *43* (12), 1192-1207.

Morawska, L., Wang, H., Ristovski, Z. D., Jayartne, E. R., Johnson, G., Cheung, H. C., Ling, X., and He, C. (2009).Jem Spotlight: Environmental Monitoring of Airborne Nanoparticles, *Journal of Environmental Monitoring*, *11* (10), 1758-1773.

Morrical, B. D., Fergenson, D. P., and Prather, K. A. (1998).Coupling Two-Step Laser Desorption/Ionization with Aerosol Time-of-Flight Mass Spectrometry for the Analysis of Individual Organic Particles, *Journal of the American Society for Mass Spectrometry*, *9* (10), 1068-1073.

Neubauer, K. R., Johnston, M. V., and Wexler, A. S. (1998).Humidity Effects on the Mass Spectra of Single Aerosol Particles, *Atmospheric Environment*, *32* (14-15), 2521-2529.

Noblitt, S. D., Lewis, G. S., Liu, Y., Hering, S. V., Collett, J. L., and Henry, C. S. (2009).Interfacing Microchip Electrophoresis to a Growth Tube Particle Collector for Semicontinuous Monitoring of Aerosol Composition, *Analytical Chemistry*, *81* (24), 10029-10037.

Panel on Aerosol Radiative Forcing and Climate Change, N. R. C. (1996). **A Plan for a Research Program on Aerosol Radiative Forcing and Climate Change**, National Academy Press, Washington, D.C.

Petters, M. D., and Kreidenweis, S. M. (2007).A Single Parameter Representation of Hygroscopic Growth and Cloud Condensation Nucleus Activity, *Atmospheric Chemistry and Physics*, *7* (8), 1961-1971.

Petzolda, A., Strömb, J., Ohlssonb, S., and Schrödera, F. P. (1998).Elemental Composition and Morphology of Ice-Crystal Residual Particles in Cirrus Clouds and Contrails, *Atmospheric Research*, *49* (1), 21-34.

Phares, D. J., Rhoads, K. P., and Wexler, A. S. (2002).Performance of a Single Ultrafine Particle Mass Spectrometer, *Aerosol Science and Technology*, *36* (5), 583-592.

Pierce, J. R., and Adams, P. J. (2006).Global Evaluation of Ccn Formation by Direct Emission of Sea Salt and Growth of Ultrafine Sea Salt, *Journal of Geophysical Research*, *111* (D06203), doi:10.1029/2005JD006186.

Pierce, J. R., and Adams, P. J. (2007).Efficiency of Cloud Condensation Nuclei Formation from Ultrafine Particles, *Atmospheric Chemistry and Physics*, *7*, 1367-1379.

Pierce, J. R., and Adams, P. J. (2009).Uncertainty in Global Ccn Concentrations from Uncertain Aerosol Nucleation and Primary Emission Rates, *Atmospheric Chemistry and Physics*, *9* (4), 1339-1356.

Pratt, K. A., Hatch, L. E., and Prather, K. A. (2009a).Seasonal Volatility Dependence of Ambient Particle Phase Amines, *Environmental Science & Technology*, *43* (14), 5276-5281.

Pratt, K. A., Mayer, J. E., Holecek, J. C., Moffet, R. C., Sanchez, R. O., Rebotier, T. P., Furutani, H. F., Gonin, M., Fuhrer, K., Su, Y. X., Guazzotti, S. A., and Prather, K. A. (2009b).Development and Characterization of an Aircraft Aerosol Time-of-Flight Mass Spectrometer, *Analytical Chemistry*, *81* (5), 1792-1800.

Pruppacher, H. R., and Klett, J. D. (1997). **Microphysics of Clouds and Precipitation**, Kluwer Academic Publishers, Norwell, MA.

Rhoads, K. P., Phares, D. J., Wexler, A. S., and Johnston, M. V. (2003).Size-Resolved Ultrafine Particle Composition Analysis, 1. Atlanta, *Journal of Geophysical Research*, *108* (D7), doi: 10.1029/2001jd001211.

Roberts, G. C., and Nenes, A. (2005).A Continuous-Flow Streamwise Thermal-Gradient Ccn Chamber for Atmospheric Measurements, *Aerosol Science and Technology*, *39*, 206-221.

Rose, D., Nowak, A., Achtert, P., Wiedensohler, A., Hu, M., Shao, M., Zhang, Y., Andreade, M. O., and Poschl, U. (2010).Cloud Condensation Nuclei in Polluted Air and Biomass Burning Smoke near the Mega-City Guangzhou, China - Part 1: Size Resolved Measurements and Implications for Modeling of Aerosol Particle Hygroscopicity and Ccn Activity, *Atmospheric Chemistry and Physics*, *10* (7), 3365-3383.

Sardar, S. B., Fine, P. M., Mayo, P. R., and Sioutas, C. (2005).Size-Fractionated Measurements of Ambient Ultrafine Particle Chemical Composition in Los Angeles Using the Nanomoudi, *Environmental Science & Technology*, *39* (4), 932-944.

Seinfeld, J. H., and Pandis, S. N. (1998). **Atmospheric Chemistry and Physics**, John Wiley & Sons, New York.

Shields, L., Suess, D. T., and Prather, K. A. (2007).Determination of Single Particle Mass Spectral Signatures from Heavy-Duty Diesel Vehicle Emissions for Pm2.5 Source Apportionment, *Atmospheric Environment*, *41* (18), 3841-3852.

Shields, L. G., Qin, X. Y., Toner, S. M., and Prather, K. A. (2008).Detection of Ambient Ultrafine Aerosols by Single Particle Techniques During the Soar 2005 Campaign, *Aerosol Science and Technology*, *42* (8), 674-684.

Shilling, J. E., King, S. M., Mochida, M., Worsnop, D. R., and Martin, S. T. (2007).Mass Spectral Evidence That Small Changes in Composition Caused by Oxidative Aging Processes Alter Aerosol Ccn Properties, *Journal of Physical Chemistry A*, *111* (17), 3358-3368.

Sierau, B., and Stratmann, F. (2003).A Condensation-Growth and Impaction Method for Rapid Off-Line Chemical-Characterization of Organic Submicrometer Atmospheric Aerosol Particles, *Journal of Aerosol Science*, *34* (2), 225-242.

Silva, P. J., Liu, D., Noble, C. A., and Prather, K. A. (1999).Size and Chemical Characterization of Individual Particles Resulting from Biomass Burning of Local Southern California Species, *Environmental Science & Technology*, *33* (18), 3068-3076.

Silva, P. J., and Prather, K. A. (2000).Interpretation of Mass Spectra from Organic Compounds in Aerosol Time-of-Flight Mass Spectrometry, *Analytical Chemistry*, *72* (15), 3553-3562.

Smith, J. N., Barsanti, K. C., Friedli, H. R., Ehn, M., Kulmala, M., Collins, D. R., Scheckman, J. H., Williams, B. J., and McMurry, P. H. (2010).Observations of Aminium Salts in Atmospheric Nanoparticles and Possible Climatic Implications, *Proceedings of the National Academy of Sciences of the United States of America*, *107* (15), 6634-6639.

Smith, J. N., Moore, K. F., McMurry, P. H., and Eisele, F. L. (2004).Atmospheric Measurements of Sub-20 Nm Diameter Particle Chemical Composition by Thermal Desporption Chemical Ionization Mass Spectrometry, *Aerosol Science and Technology*, *38* (2), 100-110.

Solomon, S., Qin, D., Manning, M., Chen, Z., Marquis, M., Averyt, K. B., Tignor, M., and Miller, H. L. (2007). Climate Change 2007: The Physical Science Basis. Contribution of Working Group I to the Fourth Assessment Report of the Intergovernmental Panel on Climate Change, Cambridge, United Kingdom and New York, USA.

Song, X. H., Hopke, P. K., Fergenson, D. P., and Prather, K. A. (1999).Classification of Single Particles Analyzed by Atofms Using an Artificial Neural Network, Art-2a, *Analytical Chemistry*, *71* (4), 860-865.

Spencer, M. T., and Prather, K. A. (2006).Using Atofms to Determine Oc/Ec Mass Fractions in Particles, *Aerosol Science and Technology*, *40* (8), 585-594.

Spencer, M. T., Shields, L. G., and Prather, K. A. (2007).Simultaneous Measurements of the Effective Density and Chemical Composition of Ambient Aerosol Particles, *Environmental Science & Technology*, *41* (4), 1303-1309.

Stroud, C. A., Bruintjes, R., Nemitz, E., Guenther, A. B., and Nandi, S. (2007).Cloud Activating Properties of Aerosol Observed During Celtic, *Journal of Atmospheric Sciences*, *64* (2), 441-459.

Su, Y. X., Sipin, M. F., Furutani, H. F., and Prather, K. A. (2004).Development and Characterization of an Aerosol Time-of-Flight Mass Spectrometer with Increased Detection Efficiency, *Analytical Chemistry*, *76*, 712-719.

Su, Y. X., Sipin, M. F., Prather, K. A., Gelein, R. M., Lunts, A., and Oberdorster, G. (2005).Atofms Characterization of Individual Model Aerosol Particles Used for Exposure Studies, *Aerosol Science and Technology, 39* (5), 400-407.

Su, Y. X., Sipin, M. F., Spencer, M. T., Qin, X. Y., Moffet, R. C., Shields, L. G., Prather, K. A., Venkatachari, P., Jeong, C. H., Kim, E., Hopke, P. K., Gelein, R. M., Utell, M. J., Oberdorster, G., Berntsen, J., Devlin, R. B., and Chen, L. C. (2006).Real-Time Characterization of the Composition of Individual Particles Emitted from Ultrafine Particle Concentrators, *Aerosol Science and Technology, 40* (6), 437-455.

Sullivan, R. C., Guazzotti, S. A., Sodeman, D. A., and Prather, K. A. (2007).Direct Observations of the Atmospheric Processing of Asian Mineral Dust, *Atmospheric Chemistry and Physics, 7* (5), 1213-1236.

Sullivan, R. C., Moore, M. J. K., Petters, M. D., Kreidenweis, S. M., Roberts, G. C., and Prather, K. A. (2009).Effect of Chemical Mixing State on the Hygroscopicity and Cloud Nucleation Properties of Calcium Mineral Dust Particles, *Atmospheric Chemistry and Physics, 9*, 3303-3316.

Sun, J. Y., Zhang, Q., Canagaratna, M. R., Zhang, Y. M., Ng, N. L., Sun, Y. L., Jayne, J. T., Zhang, X. C., Zhang, X. Y., and Worsnop, D. R. (2010).Highly Time- and Size-Resolved Characterization of Submicron Aerosol Particles in Beijing Using an Aerodyne Aerosol Mass Spectrometer, *Atmospheric Environment, 44* (1), 131-140.

Tiitta, P., Miettinen, P., Vaattovaara, P., Joutsensaari, T. P., Virtanen, A., Raatikainen, T., Aalto, P., Portin, H., Romakkaniemi, S., Kokkola, H., Lehtinen, K. E. J., Kulmala, M., and Laaksonen, A. (2010).Roadside Aerosol Study Using Hygroscopic, Organic and Volatility Tdmas: Characterization and Mixing State *Atmospheric Environment, 44* (7), 976-986.

Toner, S. M., Shields, L. G., Sodeman, D. A., and Prather, K. A. (2008).Using Mass Spectral Source Signatures to Apportion Exhaust Particles from Gasoline and Diesel Powered Vehicles in a Freeway Study Using Uf-Atofms, *Atmospheric Environment, 42* (3), 568-581.

Toner, S. M., Sodeman, D. A., and Prather, K. A. (2006).Single Particle Characterization of Ultrafine and Accumulation Mode Particles from Heavy Duty Diesel Vehicles Using Aerosol Time-of-Flight Mass Spectrometry, *Environmental Science & Technology, 40* (12), 3912-3921.

Twohy, C. H., and Anderson, J. R. (2008).Droplet Nuclei in Non-Precipitating Clouds: Composition and Size Matter, *Environmental Research Letters, 3* (4), 9.

Twohy, C. H., Anderson, J. R., and Crozier, P. A. (2005).Nitrogenated Organic Aerosols as Cloud Condensation Nuclei, *Geophysical Research Letters, 32*, L19805.

Twohy, C. H., and Gandrud, B. W. (1998).Electron Microscope Analysis of Residual Particles from Aircraft Contrails, *Geophysical Research Letters*, *25* (9), 1359-1362.

Utsunomiya, S., Jensen, K. A., Keeler, G. J., and Ewing, R. C. (2004).Direct Identification of Trace Metals in Fine and Ultrafine Particles in the Detroit Urban Atmosphere, *Environmental Science & Technology*, *38* (8), 2289-2297.

VanReken, T. M., Rissman, T. A., Roberts, G. C., Varutbangkul, V., Jonsson, H. H., Flagan, R. C., and Seinfeld, J. H. (2003).Toward Aerosol/Cloud Condensation Nuclei (Ccn) Closure During Crystal-Face, *Journal of Geophysical Research*, *108* (D20), 46333.

Wang, S. Y., Zordan, C. A., and Johnston, M. V. (2006).Chemical Characterization of Individual, Airborne Sub-10-Nm Particles and Molecules, *Analytical Chemistry*, *78* (6), 1750-1754.

Weber, R. J., Orsini, D., Daun, Y., Lee, Y. N., Klotz, P. J., and Brechtel, F. J. (2001).A Particle-into-Liquid Collector for Rapid Measurement of Aerosol Bulk Chemical Composition, *Aerosol Science and Technology*, *35* (3), 718-727.

Weingartner, E., Burtscher, H., and Baltensperger, U. (1997).Hygroscopic Properties of Carbon and Diesel Soot Particles, *Atmospheric Environment*, *31* (15), 2311-2327.

Wex, H., McFiggans, G., Henning, S., and Stratmann, F. (2010).Influence of External Mixing State of Atmospheric Aerosol on Derived Ccn Number Concentrations, *Geophysical Research Letters*, *37*, L10805.

Zelenyuk, A., Imre, D., and Cuadra-Rodriguez, L. A. (2006).Evaporation of Water from Particles in the Aerodynamic Lens Inlet: An Experimental Study, *Analytical Chemistry*, *78* (19), 6942-6947.

Zelenyuk, A., Imre, D., Earle, M., Easter, R., Korolev, A., Leaitch, R., Liu, P., Macdonald, A. M., Ovchinnikov, M., and Strapp, W. (2010).In Situ Characterization of Cloud Condensation Nuclei, Interstitial, and Background Particles Using the Single Particle Mass Spectrometer, Splat Ii, *Analytical Chemistry*, *82* (19), 7943–7951.

Zelenyuk, A., Yang, J., Choi, E., and Imre, D. (2009).Splat Ii: An Aircraft Compatible, Ultra-Sensitive, High Precision Instrument for in-Situ Characterization of the Size and Composition of Fine and Ultrafine Particles, *Aerosol Science and Technology*, *43* (5), 411-424.

Chapter 3. Quantitative comparison and aerosol mixing state in the western California Sierra Nevada foothills during pollution transport events in winter 2010

Aerosols affect the climate system and contribute to nutrient loading in remote ecosystems. Knowledge of the amount of soluble species present in individual particles as well as their mixing state is critical for predicting the environmental impacts of aerosols; however there is no single analytical technique that measures all of these parameters. In this study, a comparison was performed between complementary atmospheric measurements collected with the aerosol time-of-flight mass spectrometer (ATOFMS) and the particle-into-liquid sampler ion chromatography (PILS-IC) system during February-March, 2010 in the western foothills of the Sierra Nevada at Mariposa, California. ATOFMS provides the size (0.2-3.0 μm) and mixing state of individual particles, whereas PILS-IC quantifies the $PM_{2.5}$ mass concentrations of water-soluble ionic species in bulk aerosol, specifically nitrate, sulfate, and ammonium. In this work, the PILS-IC data were used to scale the ATOFMS mass spectral data to yield mass concentrations of ammonium, nitrate, and sulfate as a function of particle mixing state. The resulting ATOFMS and PILS-IC time series for ammonium and nitrate showed stronger correlations than those of sulfate, with correlation coefficients of 0.77, 0.80, and 0.53, respectively. Pollution transport events were observed which transported high concentrations of aged pollution particles comprised of internally mixed soot with organic carbon, ammonium, nitrate, and sulfate from the Central Valley to the otherwise pristine areas downwind in the Sierra Nevada foothills. These highly aged particles with soluble species contribute nutrients to the Sierra Nevada ecosystems through deposition. Furthermore, these transported particles are stronger absorbers of solar radiation and

have higher CCN activity than fresh soot, and could thus influence regional climate over the Sierra Nevada.

3.1 Introduction

Aerosols affect climate directly by absorbing and scattering solar and terrestrial radiation and indirectly by serving as cloud condensation nuclei (CCN) (Solomon et al., 2007). Increased numbers of CCN active particles can result in increased number of cloud droplets competing for the same amount of ambient water vapor; these smaller droplets may not grow large enough to precipitate, thus affecting cloud lifetime and regional precipitation patterns (McFiggans et al., 2006; Rosenfeld, 1999; Solomon et al., 2007). Orographic precipitation, the main source of water on the U.S. western coast, has been shown to have decreased during the past several decades east of the California Central Valley in the Sierra Nevada Mountains (Givati and Rosenfeld, 2004). Both the chemical composition and size of particles dictate their effects on climate. Particles internally mixed with secondary species, such as sulfate and nitrate, can have a stronger radiative forcing than particles externally mixed, as has been shown for soot (Chung et al., 2012; Jacobson, 2001b; Moffet and Prather, 2009). For two particles of the same chemical composition, the larger particle will be more CCN active. On the other hand, given two particles of the same size, the particle having a higher fraction of soluble species will have the higher CCN activity. Thus, knowing the association of chemical species within each individual particle, or mixing state, and particle size allows for more accurate prediction of their radiative properties and CCN activity.

In addition to playing a role in climate, aerosols also contribute nutrients, such as nitrogen, to ecosystems in the Sierra Nevada through wet and dry deposition, and therefore may lead to eutrophication of aquatic ecosystems, soil acidification, and changes in biodiversity, in addition to affecting the productivity of forests and the overall health of the ecosystems (Bytnerowicz and Fenn, 1996; Bytnerowicz and Riechers, 1995; Fenn et al., 2003a). Dry deposition typically contributes the largest component of total atmospheric N deposition downwind of polluted air basins in California (Bytnerowicz and Fenn, 1996), and therefore the deposition rates of nitrate

and ammonium are higher on the western Sierra Nevada slope than on the eastern side (Bytnerowicz et al., 1991; Bytnerowicz et al., 1992). Because N deposition in the Sierra Nevada is expected to continue increasing over time, there are concerns that significant long-term nitrogen deposition in the Sierra Nevada may lead to oversaturation and consequently to serious soil and water contamination in the Central Valley, which is one of the most agriculturally productive areas in the world (Bytnerowicz and Riechers, 1995; Fenn et al., 2003a).

Traditional analytical methods used to determine particle composition must collect many particles in order to obtain a statistically relevant mass measurement. With the mass of each component, which can then be converted to molarity, mass fraction, etc., it is possible to predict the environmental impacts of the particles, including their CCN (McFiggans et al., 2006) and optical properties (Dillner et al., 2001), and their contribution to nutrient dry deposition loadings. However, this traditional approach provides an average bulk composition view of particles that may not represent any single particle sampled, especially if particles are externally mixed.

The aerosol time-of-flight mass spectrometer (ATOFMS) measures the size-resolved mixing state of individual particles (Gard et al., 1998). ATOFMS data provides a qualitative measure of composition rather than the more commonly used mass concentrations; matrix effects, shot-to-shot variability of the desorption/ionization laser, and varying particle transmission efficiency across difference particle sizes contribute to the challenges associated with quantifying ATOFMS data (Allen et al., 2000; Morrical et al., 1998; Qin et al., 2006; Wenzel and Prather, 2004). Despite these instrumental challenges, ATOFMS datasets have been successfully scaled to provide mass concentrations through comparison with collocated mass measurements. Qin, et al. (2006) developed a method to correct the particle size transmission bias by scaling the number of particles measured with the ATOFMS by the particle concentrations of each size bin measured with a collocated aerodynamic particle sizer (APS) and multiplied it by an assumed particle density to arrive at mass concentration, which compared strongly (R^2 = 0.91) to $PM_{2.5}$ mass concentration measured with the beta attenuation

monitor (BAM) in the field. A comparison of scaled ATOFMS ammonium (NH_4^+) and nitrate (NO_3^-) ion signal to mass concentrations agreed strongly (R^2 = 0.72 and 0.81, respectively) with mass concentrations derived from co-located Teflon substrate cascade impactor measurements (Bhave et al., 2002). The scaled mass concentration of ATOFMS soot particles also resulted in reasonable correlations (R^2 = 0.61-0.68) compared to black carbon/elemental carbon mass concentrations from a multi-angle absorption photometer, an organic carbon/elemental carbon (OCEC) analyzer, and an aethalometer (Healy et al., 2012). Finally, a quantitative comparison of the ATOFMS against an aerosol mass spectrometer (AMS), gas particle ion chromatography (GPIC), and an OCEC analyzer yielded good correlations; specifically, the correlations between the mass concentrations of the ATOFMS and GPIC NH_4^+, NO_3^-, and sulfate (SO_4^{2-}) were strong (R = 0.85, 0.89, and 0.79, respectively) (Jeong et al., 2011). Furthermore, compared to collocated BAM measurements, Jeong, et al (2011) were able to successfully scale ATOFMS winter data from a rural site into mass concentrations based on linear regressions determined during summer at an urban site.

Previous source-apportionment studies utilizing the ATOFMS have been performed throughout California. Freeway studies have been able to differentiate between particulate emissions from heavy duty diesel vehicles (HDDV) and gasoline-powered passenger cars (Toner et al., 2008). Ault et al. (2010) identified unique particles emitted from ocean-faring ships combusting heavy fuel oil at the Port of Los Angeles. Particle emissions from residential night-time heating fires and large scale wildfires have also been analyzed (Muhle et al., 2007; Qin and Prather, 2006; Zauscher et al., 2012). Additionally, new particle formation events have been detected with an ATOFMS at a remote site in California (Creamean et al., 2011). The focus of this study is to identify the sources, using our knowledge our particulate sources in California, and mixing state of particles in the Sierra Nevada foothills; this area is of interest due to the observed decrease in orographic precipitation, which may be linked to aerosols.

During winter 2010, ground-based measurements in the western Sierra Nevada foothills at Mariposa, CA were conducted using a collocated ATOFMS and particle-

into-liquid sampler coupled to ion chromatography (PILS-IC). To our knowledge, these are the first single particle measurements in this area of the Sierra Nevada foothills. The findings presented herein indicate that pollution transport events bring a high concentration of aged carbonaceous aerosols coated with ammonium, nitrate, and sulfate from the Central Valley to the otherwise clean sampling site. Therefore, these aged transported aerosols may play a significant role in local ecology and regional climate.

3.2 Experimental Set-up

The sampling site (37.50931 N, 120.03752 W, 684 m altitude) was located in Mariposa, California, a rural town located on the western slope of the Sierra Nevada foothills, as shown in Figure 3.1. To the west of Mariposa is the California Central Valley, known for being one of the worst polluted areas in the U.S. due to high PM concentrations, especially during the winter due to the lowering of the boundary layer (Chow et al., 2006; Hall et al., 2008; MacDonald et al., 2006). The Sierra Nevada mountain range continues to rise in elevation to the east of Mariposa. Data was collected between 02/2/10 – 3/13/10. In addition to the ATOFMS and PILS-IC (described in detail below), 0.5-20 μm size distributions were measured with an aerodynamic particle sizer (APS, TSI model 3321) every minute and ambient gas-phase nitrous oxide (NO_x) concentrations were also monitored (TEI, model 42C). In addition, hourly $PM_{2.5}$ mass concentrations for 30 sites in the Central Valley and Sierra Nevada were compiled from the California Air Resources Board (http://www.arb.ca.gov) during this study. The data from all sites was interpolated in Igor Pro (WaveMetrics) to make $PM_{2.5}$ mass concentration contour maps. The air mass back trajectories were modeled with HYSPLIT 4.0 at four altitudes: 500, 1000, 1500 and 2500 m (Draxler and Hess, 1998).

3.2.1 Particle-into-liquid sampler coupled to ion chromatography (PILS-IC)

The PILS-IC system used in this study exposes atmospheric particles to water vapor creating a region of supersaturation in which the particles grow, thereby allowing the particles to be collected by impaction (Orsini et al., 2003; Weber et al., 2001). The ambient aerosol sample flow rate was 15.3 $Lmin^{-3}$ and a new chromatogram was started every 17. Following collection in the PILS the liquid sample was analyzed via IC using two Dionex ICS-1500 systems equipped with a pump, conductivity detector, and self-regenerating suppressor. The anion separation was conducted on a Dionex IonPac AS-14A column using an eluent of 1 mM sodium bicarbonate/8 mM sodium carbonate at a flowrate of 1 ml/min. A Dionex IonPac CS12A column employing an eluent of 20 mM methanesulfonic acid at a flowrate of 0.5 ml/min was used for cation analysis. Ambient samples were corrected for dilution, due to condensation within the instrument, by

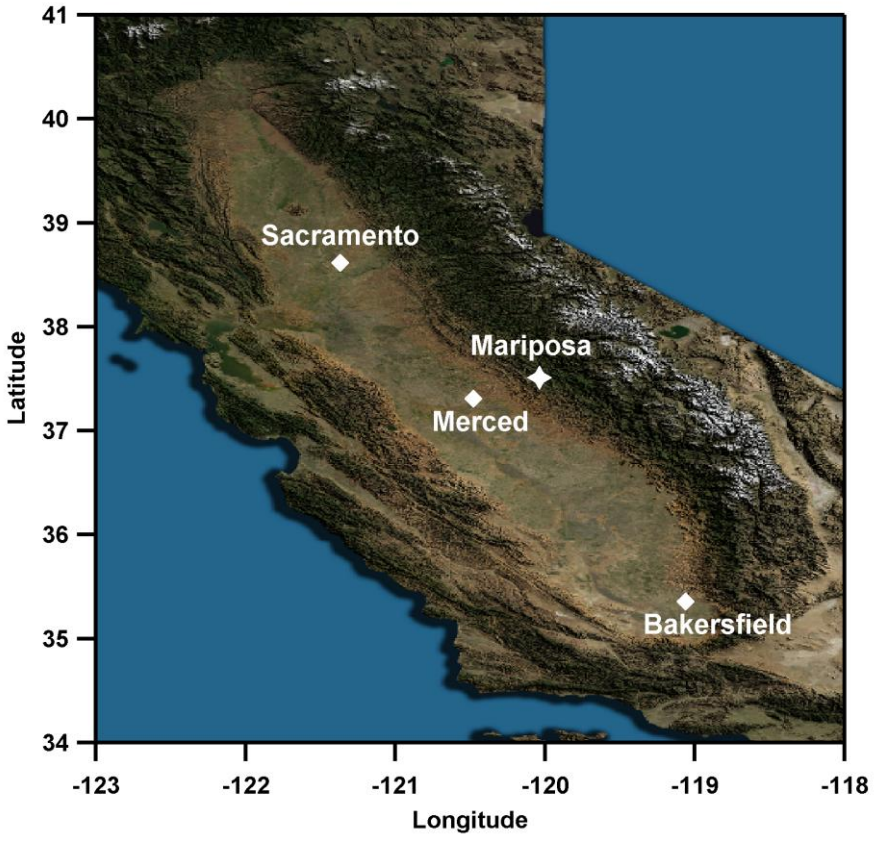

Figure 3.1: Map highlighting the location of the sampling site in Mariposa, California in the foothills of the California Sierra Nevada, which is above the Central Valley.

spiking the sample with a known concentration of lithium bromide in order to calculate the dilution factor. The PILS-IC sampled a range of soluble inorganic species during this study, such as calcium, chloride, and sodium, but the focus of this paper is on NH_4^+, NO_3^-, and SO_4^{2-} because they were most prevalent during this study. PILS-IC data was only collected until 3/10/10 because of instrumental problems

The PILS-IC used its own sampling line, which consisted of a 6.35 mm diameter and 2 m long un-insulated copper tube with a $PM_{2.5}$ cyclone placed upstream. Previous studies have determined that the PILS-IC detects particles as small as 30 nm with 95% collection efficiency (Orsini et al., 2003). Two denuders were placed in-line to remove ammonia (NH_3) and acidic gas-phase species (nitric acid, sulfur dioxide, oxalic acid, etc) in order to minimize their dissolution into the aqueous droplets. Water used in this study had a resistivity > 18.3 MΩ.

3.2.2 Aerosol time-of-flight mass spectrometer (ATOFMS)

The ATOFMS used in this study has a nozzle inlet that samples particles between 0.2-3.0 μm, acquiring the positive and negative ion mass spectra and size of individual particles (Gard et al., 1997). Particles enter the ATOFMS through a converging nozzle at a sample flow rate of 1 $Lmin^{-3}$ and are accelerated to their size dependent terminal velocity. Particles then scatter light from two continuous wave 532 nm lasers 6 cm apart. A timing circuit measures the time between the scattering pulses and fires a Nd:YAG laser at 266 nm at the appropriate time to desorb and ionize individual particles. Finally, positive and negative ion mass spectra are obtained using a dual-polarity reflectron time-of-flight mass spectrometer.

About 5 m away from the PILS-IC sampling line, an insulated 3 m long stainless steel sampling line with a 1.27 cm diameter was placed vertically outside the sampling trailer and secured to an insulated stainless steel manifold. Besides the ATOFMS, the APS and other instruments not mentioned herein were also sampling off this manifold. An insulated 0.95 mm diameter and 1 m long conductive silicone tube was used to connect the sampling manifold to the ATOFMS inlet.

3.2.2.1 ATOFMS Data Analysis

The ATOFMS mass spectra data were analyzed in the Matlab toolkit YAADA (http://www.yaada.org) and sorted into clusters with the neural network algorithm ART-2a based on similar mass spectral features with a vigilance factor of 0.85 (Song et al., 1999). ART-2a particle clusters of similar ion patterns of varying intensities were manually combined into 6 particle types: soot mixed with organic carbon (soot-OC), organic carbon (OC), biomass burning aerosol (BBA), dust, sea salt, and other. Particle types with low counts throughout the study were combined as one into the 'other' category and are described in the section titled Supplementary Information. Figure 3.2 shows the mass spectra of each particle type. The soot-OC particle type had peaks characteristic of soot, such as $^{12}C^+$, $^{24}C_2^+$, $^{36}C_3^+$, and of OC, including $^{27}C_2H_3^+$ and $^{43}C_2H_3O^+$ (Guazzotti et al., 2001a). The OC particle type was characterized by intense peaks at $^{27}C_2H_3^+$, $^{29}C_2H_5^+$, $^{37}C_3H^+$, and $^{43}C_2H_3O^+$ (Sodeman et al., 2005). BBA consisted of soot and OC peaks with a strong potassium ion peak at $^{39}K^+$ (Silva et al., 1999). The

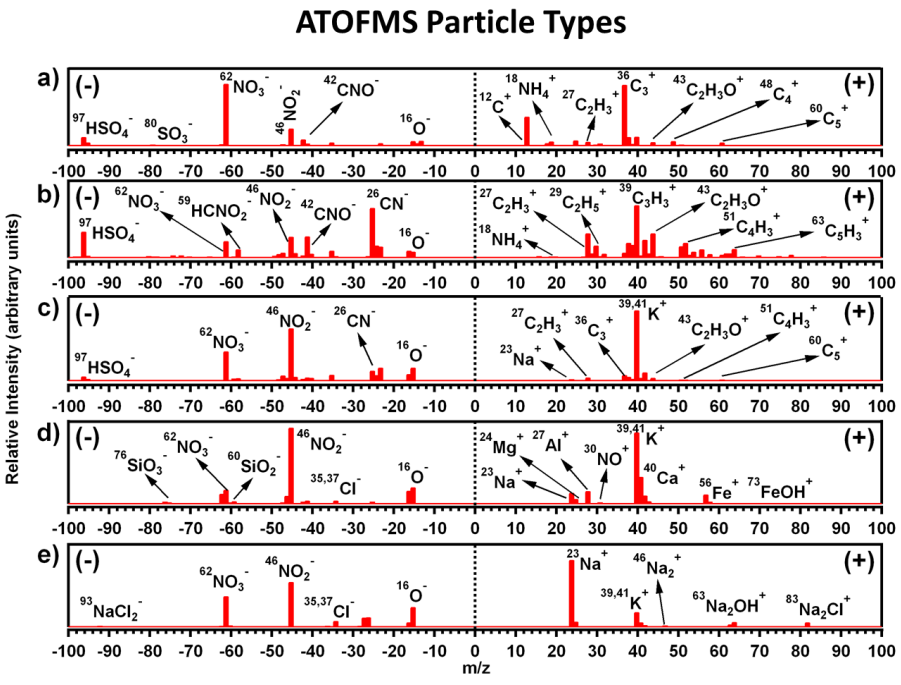

Figure 3.2: Mass spectra of the main particle types observed at Mariposa: a) Soot-OC, b) OC, c) biomass burning, d) dust, e) sea salt.

dust observed in this study had $^{39}K^+$, $^{40}Ca^+$, $^{54,56,57}Fe^+$, $^{73}FeOH^+$, $^{27}Al^+$, and aluminosilicate ($^{60}SiO_2/AlO(OH)^-$ and $^{76}SiO_3/ AlO_2(OH)^-$) ions in the mass spectra (Silva et al., 2000). The sea salt particle type exhibited intense $^{23}Na^+$ and $^{39}K^+$ ions and minor sodium chloride clusters ($^{81,83}Na_2Cl^+$ and $^{93,95,97}NaCl_2^-$) typical of sea salt (Gard et al., 1998; Noble and Prather, 1996). A total of 187,428 particles were chemically characterized during this study with 73.5% of those having dual-polarity mass spectra. Typically, positive mass spectra allow identification of the particle type whereas negative spectra provide information on the extent and type of chemical processing the particle has undergone in the atmosphere. While <36% of soot-OC and OC particles contained negative ion spectra, >80% of BBA, dust, and sea salt particles produced dual-polarity mass spectra. When particles are wet, either due to high ambient relative humidity and/or atmospheric processing, they generally produce less negative ion spectra (Neubauer et al., 1998).

The $^{18}NH_4^+$, $^{62}NO_3^-$, and $^{97}HSO_4^-$ ions have previously been shown to be indicators of ammonium, nitrate and sulfate (Bhave et al., 2002; Gard et al., 1997; Guazzotti et al., 2001b; Noble and Prather, 1996). Possible interference in the +18 m/z is discussed in section 3.6.2. Relative peak areas (RPA), the normalized intensity of a specific ion to the total peak areas of the whole mass spectrum, per particle type were analyzed herein because they tend to minimize the variability in peak intensity compared to absolute peak areas in particles of similar matrices (Gross et al., 2000). To study the mixing state of NH_4^+, NO_3^-, and SO_4^{2-} on individual particles, searches were performed on dual-polarity ATOFMS data for particles with only one, only two, all three, and none of these markers with RPA > 0.1 %. This low RPA was chosen because the peak area of $^{18}NH_4^+$ is typically small.

3.2.2.2 Scaling of ATOFMS Data

Particles in each of the six particle types (i) were binned by size (j) with bin widths of 100 nm for all sizes between from 200-2500 nm. First, the hourly averaged RPAs were determined for each particle type in every size bin. When calculating the RPA of positive ions ($^{18}NH_4^+$) all particles were used, whereas negative ions ($^{62}NO_3^-$

Table 3.1: Linear equation for transforming scaled RPA to mass concentration.

Species	NH_4^+	NO_3^-	SO_4^{2-}
m/z	+18	-62	-97
Slope	$2.44 \times 10^{-4} \pm 7.16 \times 10^{-6}$	$1.41 \times 10^{-5} \pm 4.25 \times 10^{-7}$	$3.15 \times 10^{-6} \pm 1.24 \times 10^{-7}$
Intercept	$8.56 \times 10^{-2} \pm 3.51 \times 10^{-2}$	$9.49 \times 10^{-2} \pm 4.16 \times 10^{-2}$	$1.83 \times 10^{-1} \pm 8.19 \times 10^{-3}$
R^2	0.77	0.80	0.53

and $^{97}HSO_4^-$) were averaged only over the particles with negative mass spectra and were applied to particles with no negative ion spectra because it was assumed that the lack of negative mass spectra was due to an artifact in the ion formation process caused by the presence of water on these particles. Separately, the corrected number of particles (NOP) in each particle type for each hour was determined by scaling particles chemically classified to the particle concentrations of each APS size bin in order to correct for particle transmission efficiency into the ATOFMS and instrument busy-time, following the procedure described previously by our group (Qin et al., 2006). Because of instrumental problems in the field, there were no size distributions of particles <500 nm, thus, the number scaling procedure for the smaller (<500 nm) size bins is not as precise as that described by Jeong et al. (2011). The scaled RPA was determined hourly for each of the markers ($^{18}NH_4^+$, $^{62}NO_3^-$ and $^{97}HSO_4^-$) separately, where D is the mid-point diameter of each size bin, j:

$$Scaled\ RPA = \sum_{i,j} \left[RPA_{i,j}\ NOP_{i,j}\ D_j^3 \right]$$

The D^3 factor is a correction for volumetric differences in observed peak areas among different sized particles; this factor may introduce biases if the whole particle is not fully ablated by the ATOFMS laser, as may be the case for particles > 1 μm (Bhave et al., 2002).

In order to compare these *scaled RPAs* with the mass concentrations determined with the PILS-IC, the PILS-IC data were averaged for each hour and the *scaled RPAs* were summed across all particle types and sizes. The NH_4^+, NO_3^- and SO_4^{2-} hourly-

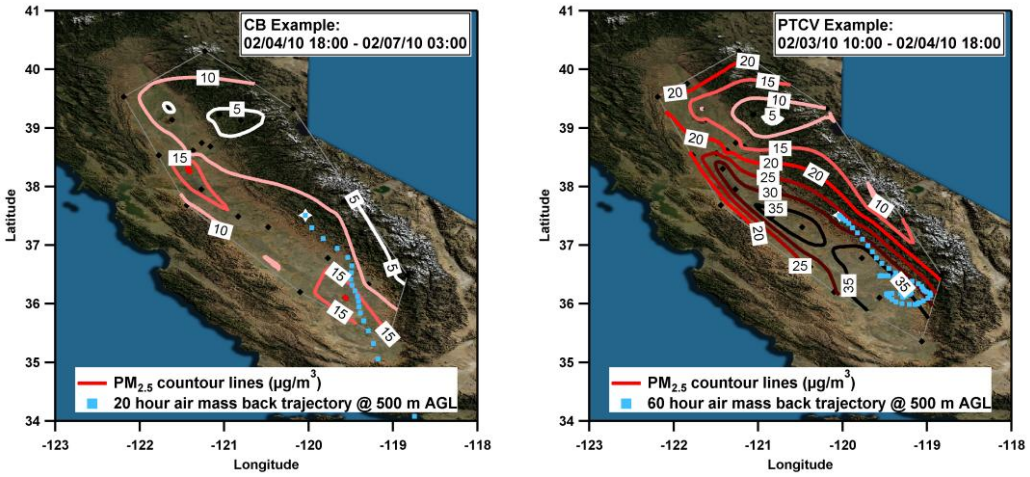

Figure 3.3: $PM_{2.5}$ contour maps and air mass back trajectories of an example of a) clean background and b) pollution transported from the Central Valley (PTCV).

averaged PILS-IC and *scaled RPA* were plotted against each other; the *scaled RPA* were then transformed into total hourly mass concentrations using the determined linear equations for each ion marker, given in Table 3.1.

In addition, transforming the *scaled RPA* to mass concentrations based on the PILS-IC data corrects for differences in chemical sensitivities of the ATOFMS data. Finally, to determine the mass concentrations of each species by particle type, the total mass concentrations were scaled by the fractional *scaled RPA* per particle type each hour.

3.3 Results and Discussion and Discussion

During the study, significant periods of pollution transport from the Central Valley (PTCV) occurred. These events were identified by analyzing the air mass back trajectories in HYSPLIT and by mapping the regional $PM_{2.5}$ during these periods, with examples shown in Figure 3.3 (Draxler and Hess, 1998). PTCV events were characterized by high $PM_{2.5}$ values valley-wide and transport from the Central Valley to the sampling site. Times not influenced by PTCV were considered background/local conditions. Major storms affecting the Central Valley (Western Region Headquarters, 2010a; Western Region Headquarters, 2010b) were included as background periods due to their similarities in particle size distributions and mass concentrations.

3.3.1 Comparison between PILS-IC and ATOFMS data

Figure 3.4 shows the relationship between *scaled RPA* and PILS-IC mass concentrations. The correlations between ATOFMS *scaled RPAs* of $^{18}NH_4^+$ and $^{62}NO_3^-$ were strong (R^2 = 0.77 and 0.80 respectively) with the PILS-IC ammonium and nitrate mass concentrations, whereas the correlation between the $^{97}HSO_4^-$ and PILS-IC sulfate was not as high (R^2 = 0.53). Instrumental differences between the ATOFMS and PILS-IC can help explain why the correlations in Figure 3.4 were not higher. The matrix effect, one of the instrumental biases that affects the ATOFMS but not the PILS-IC data, is the suppression of major components in the particle due to differences in ionization potentials between chemical species and charge transfer reactions (Reilly et al., 2000). For example, although the main component in BBA is OC, the BBA ATOFMS mass spectra are characterized by a large $^{39}K^+$ ion peak and minor carbonaceous peaks due to the low ionization potential of potassium (Reid et al., 2005; Silva et al., 1999). Another instrumental bias only affecting the ATOFMS results from the chemical dependence of different absorbing species to the 266 nm wavelength used to ablate the particles; for example, ammonium sulfate ($(NH_4)_2SO_4$) has a limited absorption at this wavelength (Kane and Johnston, 2001) thus, the ATOFMS may not fully detect $(NH_4)_2SO_4$ particles unless they are internally mixed with another species that strongly absorbs this wavelength (Wenzel et al., 2003; Yao et al., 2011). Although there is some $(NH_4)_2SO_4$ present in particles in this region, much less is found in California compared to other regions, such as the eastern U.S. Therefore, the mass scaling linear equation between the PILS-IC and ATOFMS sulfate may vary significantly between sulfate rich and poor regions. If there were periods with high concentrations of particles below the ATOFMS transmission range (<200 nm), only the PILS-IC would detect them; this could have been the case on the night of 2/10/10 when the ATOFMS mass concentrations were underestimated. Whereas data obtained by the ATOFMS is independent of solubility, only soluble components are measured with the PILS-IC. For example, because calcium sulfate is insoluble the PILS-IC would not detect sulfate associated with calcium dust, whereas the ATOFMS would. However,

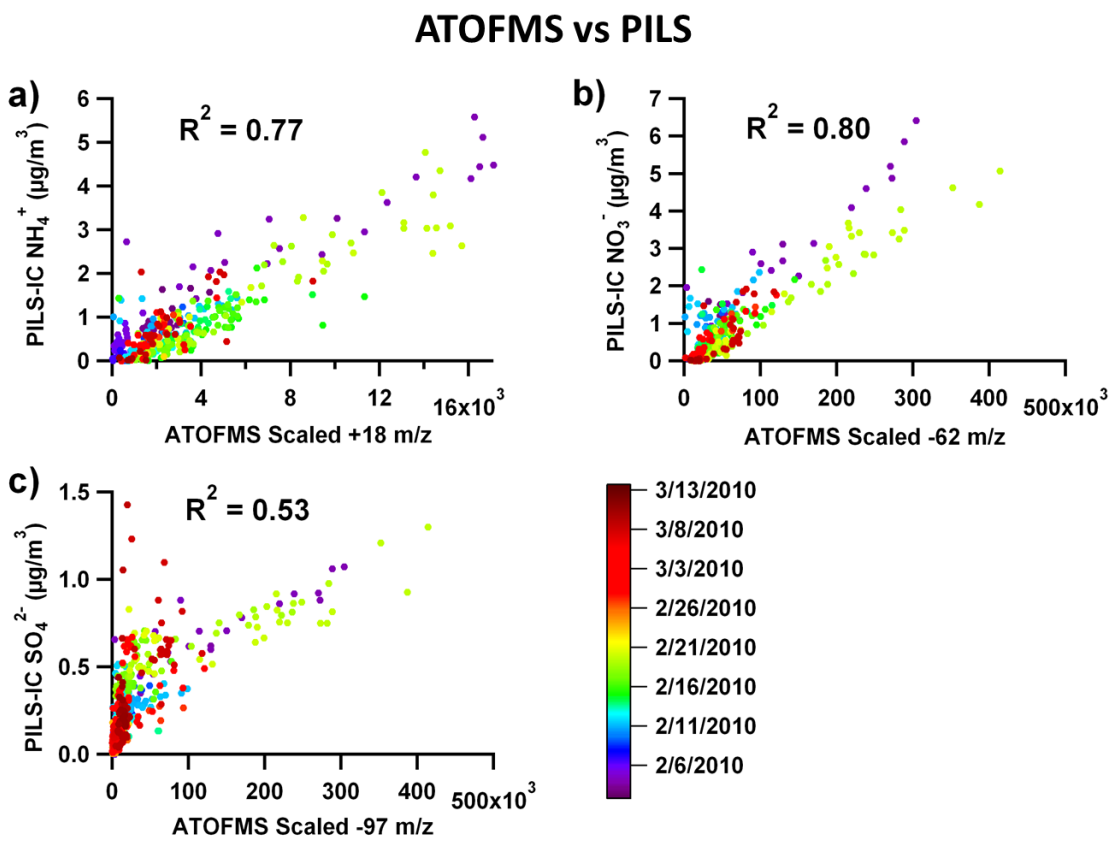

Figure 3.4: Scatter plots of PILS-IC and ATOFMS a) ammonium vs +18 m/z, b) nitrate vs -62 m/z, and c) sulfate vs -97 m/z.

because dust particles were not abundant in this study, this solubility effect would not be significant herein.

In order to fully understand the differences between measurements, comparisons between PILS-IC and ATOFMS measurements should be performed in a wide range of environments to see if similar correlations are obtained, which is not expected due to all these instrumental biases. However if similar, the correlations could be generalized and applied to other ATOFMS datasets without the need of a collocated PILS-IC in order to quantify previously measured ATOFMS peak area into mass concentrations, the same way Jeong, et al (2011) applied the linear regressions determined between scaled ATOFMS data and the GPIC from a winter urban site to data from a summer rural location.

3.3.2 Particle types and mixing state

The hourly PILS-IC and scaled ATOFMS mass concentrations of NH_4^+, NO_3^-, and SO_4^{2-} are shown in Figure 3.5, with PTCV periods highlighted in yellow. Time periods when no ambient PILS-IC and/or ATOFMS data were available are indicated by gaps. Overall, Figure 3.5 shows there was significantly more NH_4^+ and NO_3^- than SO_4^{2-}, as expected for this region based on previous measurements (Chow et al., 2006). However, based solely on the PILS-IC measurements, it is impossible to know whether these species were internally mixed on the same particles and which other species were also present on the particles; this information can be acquired by combining the ATOFMS and PILS-IC data. The highest mass concentrations of NH_4^+, NO_3^-, and SO_4^{2-}

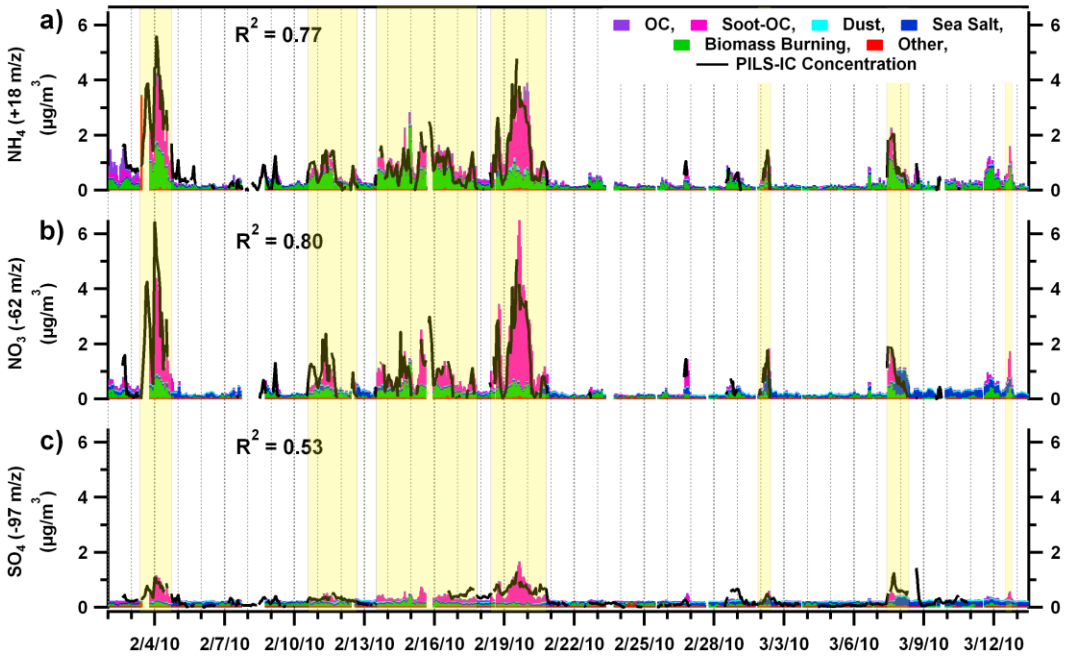

Figure 3.5: Hourly averaged temporal variation of PILS mass concentrations (in black lines) of a) ammonium, b) nitrate, and c) sulfate. In color are the corresponding mass concentrations estimated from the ATOFMS by particle types that contribute to these species. Yellow highlights periods of pollution transport from the Central Valley.

(with average and maximum values of 1.8, 2.1, and 0.6 versus 5.6, 6.4, and 1.4 µg/m^3 respectively) coincided with one another on 2/3/10-2/4/10, and 2/18/10-2/20/10, which

were PTCV events #1 and 4. In contrast, the mass concentrations were fairly low during background conditions, with average mass concentrations < 0.3 µg/m^3 for each of these secondary species.

Soot-OC concentrations were highest during periods characterized as PTCV (Figure 3.6a) comprising 51.6% of all PTCV particles; it is worth noting that if the ATOFMS counts had not been corrected for transmission biases, the high concentrations of soot-OC particles during PTCV events would have been missed. Further, the relative size distribution of soot-OC particles during PTCV events, shown in Figure 3.6c, indicates that these were large particles with a mode diameter of 750 nm, and therefore corroborating that these carbonaceous particles must have grown in size by acquiring secondary species during transport. Soot-OC particles were also present during background periods (Figure 3.6a) (20.3% by number), but these had smaller diameters and were thus less aged than soot-OC during PTCV events (Figure 3.6b). Soot-OC particles contributed to 44.4, 62.7 and 55.4 % of NH_4^+, NO_3^-, and SO_4^{2-} mass

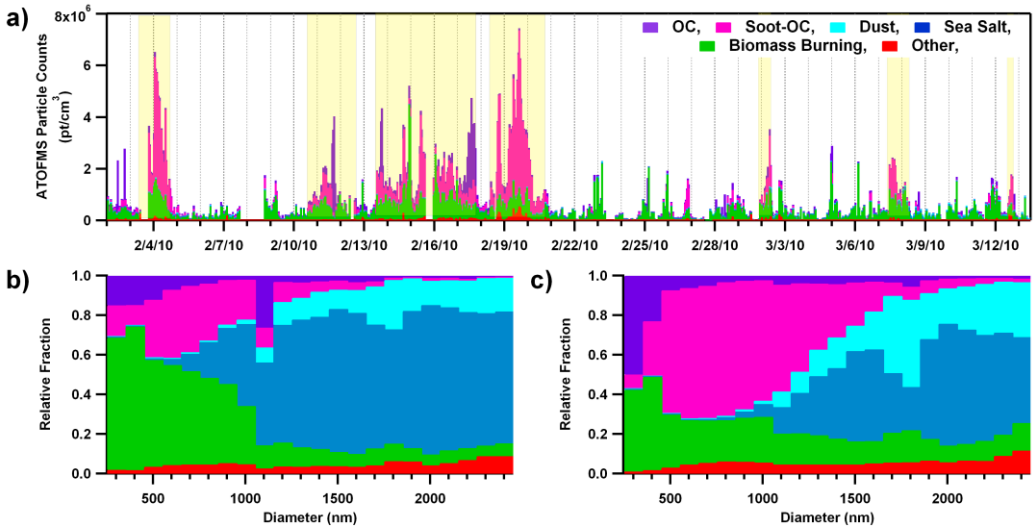

Figure 3.6: a) Temporal distribution of ATOFMS particle types and size distribution of particles during a) background periods and b) pollution transport events from the Central Valley. Pt refers to particles.

concentrations during PTCV events and 21.8, 13.8 and 19.2% during background periods. Figure 3.7 shows the relative fraction of particles mixed with NH_4^+, NO_3^-, and

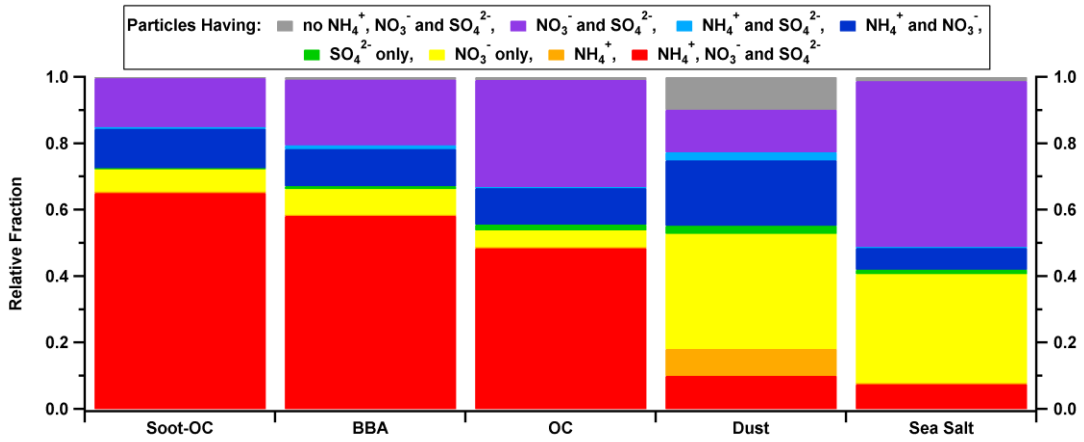

Figure 3.7: Distribution of mixing state of NH_4^+, NO_3^-, and SO_4^{2-} per particle type based on individual particles with relative peak areas greater than 0.1%.

SO_4^{2-} for different ATOFMS particle types, where each color represents a different regime: whether all three species, only two, just one, or none were found internally mixed on the same particle. Based on Figure 3.7, soot-OC was the particle type containing the highest percentage (65.1 %) of aerosols internally mixed with NH_4^+, NO_3^-, and SO_4^{2-}, and hence these were significantly atmospherically processed. Table 3.2, which lists the percentage of each particle type internally mixed with specific secondary species, shows that compared to other particle types, soot-OC also had the highest percentage of $^{62}NO_3^-$ and $^{18}NH_4^+$, 98.5 and 77.8%, confirming that soot-OC particles had the most ammonium and nitrate on them.

Table 3.2: Percent of dual polarity particles with relative peak areas of ion markers > 0.1%.

Ion	Soot-OC	OC	BBA	Dust	Sea Salt
$^{18}NH_4^+$	77.8	62.0	70.8	40.3	14.4
$^{62}NO_3^-$	98.5	97.1	97.0	77.2	97.1
$^{97}SO_4^{2-}$	80.6	82.8	80.0	27.6	59.0

The soot-OC particles were likely emitted directly from incomplete combustion processes initially as a soot core, which acquired secondary organic carbon and inorganic species during transport to Mariposa. Figure 3.8 shows high concentrations of the nitrate precursor, gas phase NO_x, at Mariposa during PTCV periods coincident with the high nitrate concentrations, confirming that NO_x was emitted in the Central Valley and transported to the foothills of the Sierra Nevada, as previously observed at a Sierra Nevada site further north and at higher altitude (Murphy et al., 2006). During transport NO_x is oxidized into nitric acid (HNO_3), which is then neutralized by ammonia, typically emitted in rural areas from animal husbandry and agriculture, forming particulate ammonium nitrate (NH_4NO_3) (Clarisse et al., 2010; Watson and Chow, 2002; Ying and Kleeman, 2009). Addition of soluble ammonium, nitrate, and sulfate onto soot-OC particles increases their hygroscopicity and hence their ability to nucleate clouds compared to less aged carbonaceous particles (Gunthe et al., 2011; Zaveri et al., 2010; Zuberi et al., 2005). Previous ground measurements in the Central Valley determined that carbonaceous aerosols were internally mixed with NH_4^+, NO_3^-, and

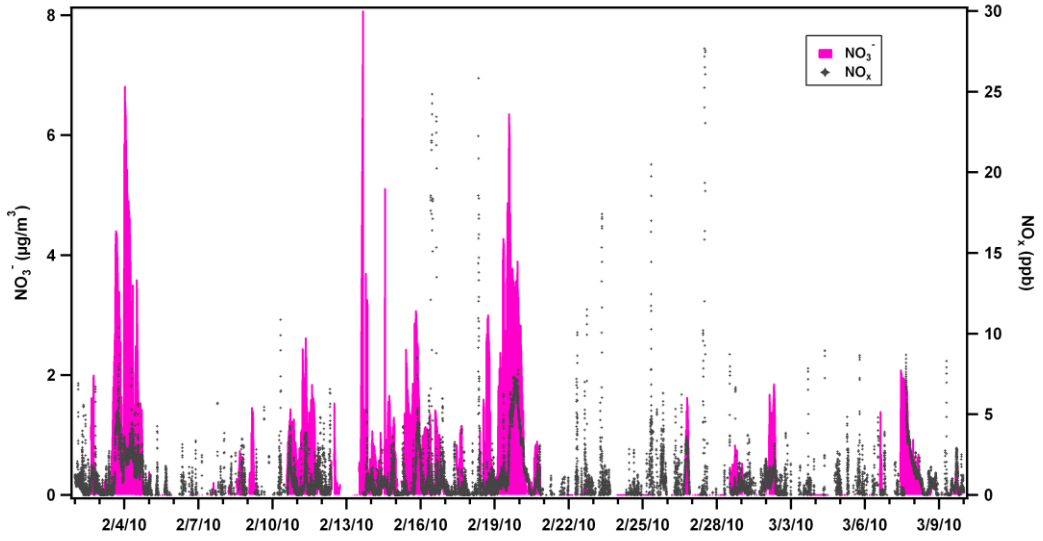

Figure 3.8: PILS-IC nitrate and NO_x temporal profiles. Nitrate was measured every 17 minutes and NO_x every 3 minutes.

SO_4^{2-}, especially during periods of stagnation (Whiteaker et al., 2002). The results presented herein show that these carbonaceous aerosols can also be transported to the

Sierra Nevada foothills, where they may act as CCN. Therefore, these aged soot-OC particles could be the CCN that were observed, but not identified in a previous aircraft study and hypothesized to be responsible for the suppression in orographic precipitation in this area (Rosenfeld et al., 2008). Decreased orographic precipitation in the Sierra Nevada translates into decreased water supply for the whole state of California. Measurements that show that aged soot particles are commonly transported to the Sierra Nevada foothills will help improve radiative budget predictions in this area since soot particles coated with organics, ammonium, nitrate, and sulfate are typically better absorbers of solar radiation compared to fresh soot (Chung et al., 2012; Jacobson, 2001b; Moffet and Prather, 2009). In addition, identification of these PTCV events with high concentrations of soot-OC particles containing significant amounts of NH_4^+ and NO_3^- can improve the estimated dry deposition fluxes of these N species in the Sierra Nevada wilderness, which are currently lacking (Bytnerowicz and Fenn, 1996; Fenn et al., 2003b).

BBA particles were the dominant particle type during background periods, making up 59.8% of all particles during these times, although they were also present during PTCV events contributing 30.0% to overall particle counts. During background periods, the size distribution of BBA was predominantly submicron (< 1 μm), whereas during PTCV events the BBA were larger, as shown in Figure 3.6b-c. Moreover, BBA counts tended to peak at night (Figure 3.6a), indicating biomass burning was used as a residential night-time heating source (Qin and Prather, 2006). Therefore, most BBA measured in this study were produced locally, although there were also some transported from the Central Valley. BBA contributed 50.8, 32.8 and 63.0% of the NH_4^+, NO_3^-, and SO_4^{2-} mass concentrations during background periods and 39.5, 21.7 and 37.3% during PTCV events. BBA had the second highest percentage (58.2%) of particles internally mixed with NH_4^+, NO_3^-, and SO_4^{2-} (Figure 3.7), indicating that even the locally produced BBA were aged by similar processes as soot-OC. A slightly smaller percentage of BBA had ammonium compared to soot-OC particles (70.8 vs 77.8%) (Table 3.2). Locally-produced BBA may actually have less ammonium than soot-OC because they are less atmospherically processed or have not yet been

neutralized by ammonia. However, the $^{18}NH_4^+$ ion is much less sensitive than $^{39}K^+$ in the ATOFMS system, so it is possible the ammonium ion in BBA was suppressed due to matrix effects.

BBA particles have been shown to be efficient CCN and previous studies have shown BBA can decrease precipitation (Reid et al., 2005; Vendrasco et al., 2009); thus, BBA may also act as CCN in the Sierra Nevada and may contribute to changes in precipitation. BBA scatter and absorb solar radiation efficiently, therefore knowledge of their abundance and mixing state will help constrain the regional radiation budget (Hobbs et al., 1997; Reid et al., 2005). Furthermore, knowledge of the mixing state and abundance of BBA can also improve the estimated dry deposition fluxes of nitrogen species in the Sierra Nevada.

OC particles were found in similar percentages during PTCV and background periods (13.5 vs 12.2%). As shown in previous studies, where there is extensive soot present, most OC is found as a coating on other particles rather than as externally mixed pure OC particles. During PTCV events, the relative size distribution of OC particles, with most particles < 350 nm, suggests most of these were produced locally, yet there is a tail in the size distribution of OC particles extending up to 2.5 µm indicating some of these were considerably aged OC particles (Figure 3.6). Therefore, there must have been a local source of OC particles, perhaps biogenic or due to a local activity at the airport, such as degreasing airplane components with solvents rich in volatile organic carbon species as was observed, in addition to OC particles being transported from the Central Valley. Furthermore, because OC particles were smaller than soot-OC particles during PTCV events, the soot-OC particles must have grown in size mostly from addition of NH_4NO_3 and not from secondary organic aerosol processing. Due to their lower particle concentrations, OC particles only contributed 8.3, 1.3 and 2.9% of the NH_4^+, NO_3^-, and SO_4^{2-} mass concentrations during PTCV events and 12.1, 2.6, and 3.9% during background periods. Approximately half of the OC particles were internally mixed with NH_4^+, NO_3^-, and SO_4^{2-} (Figure 3.7). However, less OC particles had ammonium (62.0%) compared to soot-OC (77.8%) (Table 3.2), which could be due

to matrix effects affecting OC particles more than soot-OC or simply that OC particles had not yet been neutralized. Although not as abundant as soot-OC and BBA particles, these OC particles can also serve as cloud nuclei in the Sierra Nevada because they were internally mixed with soluble species (Corrigan and Novakov, 1999; Novakov and Penner, 1993). Identifying the mixing state of OC particles in the Sierra Nevada foothills allows for better predictions of its optical properties, although these are still not well constrained (Fuzzi et al., 2006; Kanakidou et al., 2005). In addition, knowledge of the mixing state and abundance of OC particles allows for improved dry deposition fluxes of nitrogen in the Sierra Nevada.

The contribution of dust and sea salt to the overall counts was small, with dust comprising <1% and sea salt <4% of all particles during the study. Unlike the carbonaceous particles, dust was mainly internally mixed with NH_4^+ and NO_3^-, while sea salt particles were mostly internally mixed with NO_3^- and SO_4^{2-} (Figure 3.7). Because the focus of this study is on particles and sources that could be affecting clouds, further discussion of the mixing states of sea salt and dust during this campaign and the implications is given in sections 3.6.3.

3.4 Summary and Conclusions

Ambient aerosol measurements in the western foothills of the California Sierra Nevada were obtained in winter of 2010 using a variety of collocated instruments including a PILS-IC and an ATOFMS. While the ATOFMS provides the size and mixing state of individual particles, the PILS-IC quantifies the mass concentration of soluble ion species. ATOFMS peak areas of NH_4^+, NO_3^-, and SO_4^{2-} were scaled to mass concentrations. The PILS-IC ammonium and nitrate correlated strongly (R^2 = 0.77 and 0.80) with ATOFMS $^{18}NH_4^+$ and $^{62}NO_3^-$, while the correlation between sulfate with $^{97}HSO_4^-$ was not as strong (R^2 = 0.53). The imperfect correlations between ATOFMS and PILS-IC species may be explained by matrix effect, different solubility of chemical species, and the different sized particles each technique analyzes.

Pollution transport events from the Central Valley were shown to bring large concentrations of aged particles, mostly soot-OC, to the foothills of the Sierra Nevada. Although Soot-OC, BBA, and OC particles were all found to be internally mixed with NH_4^+, NO_3^-, and SO_4^{2-}, soot-OC particles had a higher fraction of internal mixing, and thus were the most aged particle type in this campaign. In contrast, dust was only internally mixed with NH_4^+ and NO_3^-, while sea salt particles were only internally mixed with NO_3^- and SO_4^{2-}. Therefore, the average bulk composition given by the PILS-IC cannot be assumed to be representative of all ambient aerosols since not all particles types were internally mixed with NH_4^+, NO_3^-, and SO_4^{2-} to the same degree. Furthermore, aerosols containing NH_4^+, NO_3^-, and SO_4^{2-} had different cores. Continued measurements of collocated PILS-IC and ATOFMS are encouraged in various environments and should include measurements of total mass concentrations and size distribution across smaller size particles than measured herein.

Particle mixing state is important for predicting its environmental effects. Dry deposition of particles transported from the Central Valley contribute nitrogen species to the soil and waterways in the Sierra Nevada, therefore affecting nutrient loading and overall health of the ecosystems. Internally mixed particles with ammonium, nitrate, and sulfate tend to have different radiative properties, and consequently the transport of high concentrations of aged soot-OC particles will need to be taken into account in regional climate modeling for more accurate radiative effects. Moreover, the high concentration of transported aged soot-OC particles sampled may be the unidentified CCN responsible for suppressing orographic precipitation downwind of the Central Valley. Although a separate paper will examine how the measurements presented herein can be related to CCN activity, long-term measurements in the foothills of the Sierra Nevada are encouraged to better understand the transport conditions and the effects of these aged soot-OC particles on orographic precipitation.

3.5 Acknowledgements

We are grateful to the Dr. Marty Ralphs's group at the National Oceanic and Atmospheric Administration for organizing logistics related to the sampling site and to

the Mariposa County Airport for allowing us to sample on site. Jake Lippman is acknowledged for assistance preparing instrumentation and collecting data during this study. We would also like to acknowledge Professor Wolfgang F. Rogge at the University of California Merced for access to Millipore ultrapure water during this study. This work was funded with a grant from the California Energy Commission and the U.S. Environmental Protection Agency PM Center Grant # R832415.

Chapter 3 contents are part of a manuscript in preparation, Melanie D. Zauscher, Kaitlyn J. Suski, John F. Cahill, Lindsay E. Hatch, Amy P. Sullivan, Jeffrey L. Collett, and Kimberly A. Prather.

3.6 Supplementary Information

3.6.1 Other Particle Types

The particle types grouped in the *other* category include soot, amines, biogenic, calcium rich, and K Na. Soot particles were identified by $C_n^{\pm}$ clusters, such as $^{12}C_1^{\pm}$, $^{24}C_2^{\pm}$, $^{36}C_3^{\pm}$. Amines particles were characterized by the ions $^{86}(C_2H_5)_2NCH_2^+$ and $^{101}(C_2H_5)_3N^+$. Biogenic particles had the $^{39}K^+$, phosphate ($^{79}PO_3^-$), and organic nitrogen ions ($^{26}CN^-$ and $^{42}CNO^-$) present in their mass spectra. The calcium rich particles mainly had calcium ions ($^{40}Ca^+$ and $^{56}CaO^+$, $^{57}CaOH^+$), while the K Na particles only had intense peaks at $^{39}K^+$ and $^{23}Na^+$ in their mass spectra.

3.6.2 Possible Interference at +18 m/z

Although +18 m/z could also be due to nitrogen containing organic species, because of the strong correlations between +18 m/z and NH_4^+ in this study it is correctly assigned to NH_4^+ (Silva and Prather, 2000) (Angelino et al., 2001; Silva and Prather, 2000). Furthermore, because of the lack of amine markers ($^{86}(C_2H_5)_2NCH_2^+$ and $^{101}(C_2H_5)_3N^+$) present on the particles during this study, coupled with the fact that the previous observations in San Joaquin Valley in Central California have shown a prevalence of NH_4NO_3, and the strong correlation between PILS-IC and ATOFMS ammonium, the interference at +18 from organic nitrogen is not significant in this study

(Chow et al., 2006; Chow et al., 2008). Moreover, the winter production of organic nitrogen species is at a minimum compared to the summer due decreased biogenic volatile organic emissions from lower temperatures and decreased solar radiation

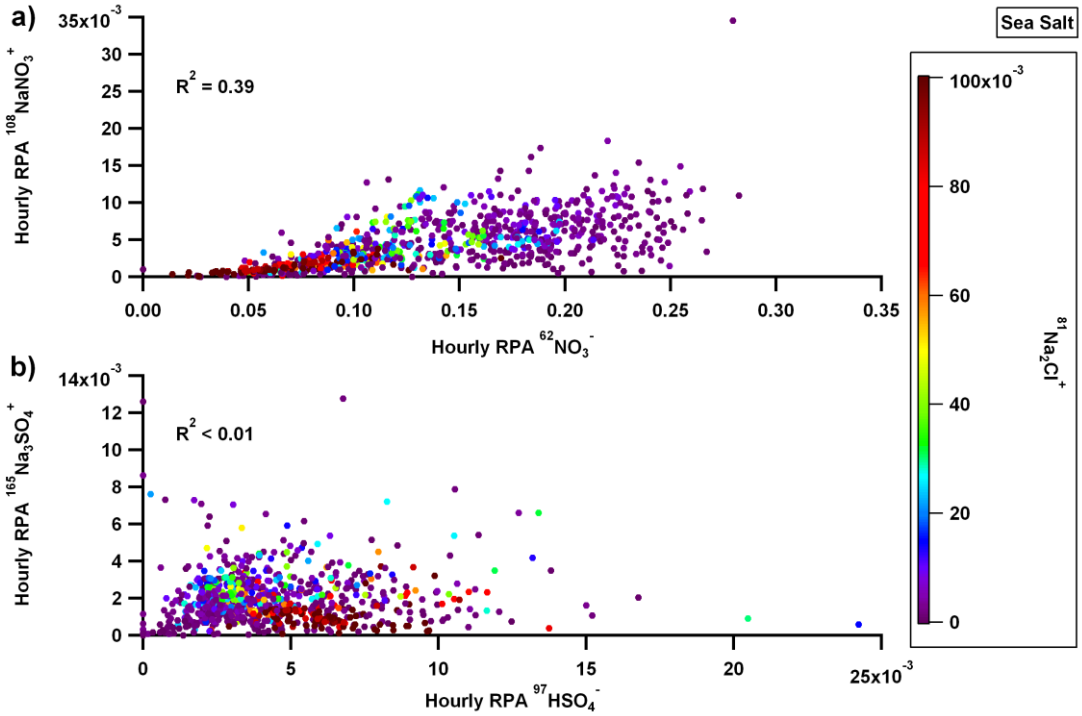

Figure 3.9: Sea salt particles hourly averaged mixing state a) $^{62}NO_3^-$ vs $^{108}NaNO_3^+$ and b) $^{97}HSO_4^-$ vs $^{165}Na_3SO_4^+$ with color representing $^{81}Na_2Cl^+$ from fresh sea salt.

(Murphy et al., 2006).

3.6.3 Mixing State and Implications of Sea Salt and Dust Particles

Unlike the carbonaceous aerosols, few (< 15%), sea salt particles were internally mixed with NH_4^+, and consequently fewer (<8%) were internally mixed with NH_4^+, NO_3^-, and SO_4^{2-}. Instead, the majority of sea salt aerosols were internally mixed with NO_3^- and SO_4^{2-}. Since 55% of all sea salt particles had the $^{108}NaNO_3^+$ ion present and it was found to be correlated with $^{62}NO_3^-$ and anti-related to $^{81}Na_2Cl^+$ (Figure 3.9), the NaCl in these sea salt aerosols must have heterogeneously reacted with nitrogen oxides, including HNO_3, during transport from the ocean to Mariposa (Gard et al., 1998;

Mamane and Gottlieb, 1990). 38% of sea salt aerosols had the $^{165}NaSO_4^+$ ion present, but it was not correlated with $^{97}HSO_4^-$ or $^{81}Na_2Cl^+$ (Figure 3.9) indicating that the sulfate present on these sea salt aerosols was likely due to sulfate naturally abundant in sea water, as previously observed (Gard et al., 1998). Aged sea salt is more hygroscopic than fresh sea salt particles because $NaNO_3$ is more hygroscopic than NaCl (Gibson et al., 2006). In addition, the presence of aqueous nitrate causes aged sea salt particles to absorb more solar radiation compared to fresh sea salt (Gibson et al., 2006; Hudson et al., 2007).

Dust aerosols exhibited unique mixing states compared to carbonaceous and sea salt particles, with the majority being internally mixed with nitrate (77%) and ammonium (40%) compared to sulfate (28%). Because more dust particles had nitrate than ammonium present, it is likely that the dust may have directly taken up nitric acid during transport from the Central Valley, which was then neutralized by NH_3 gas

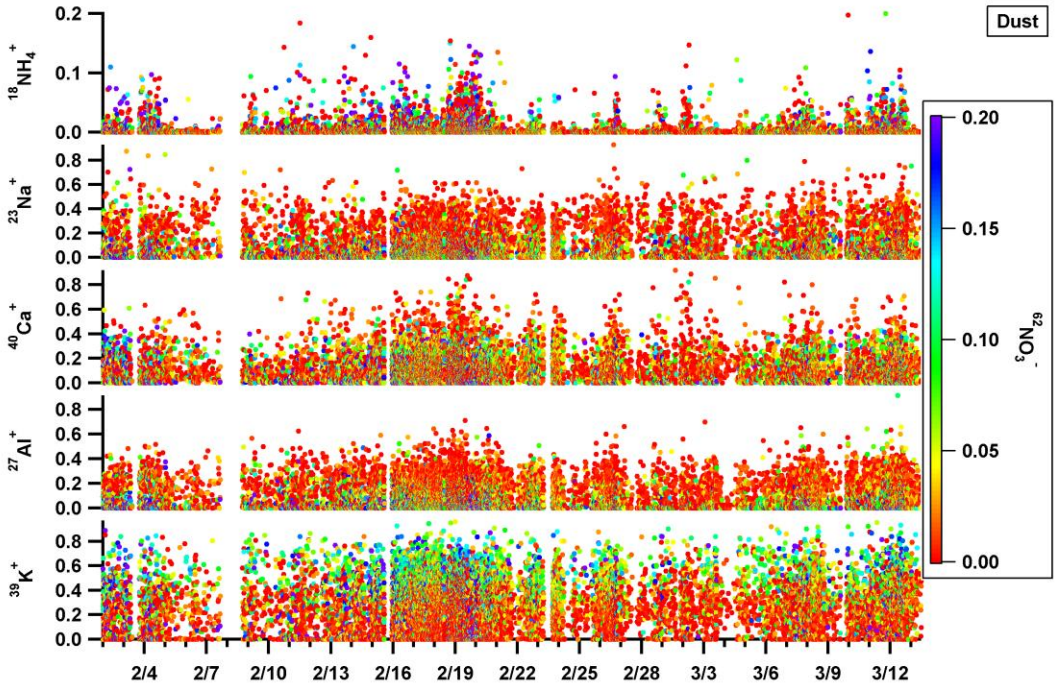

Figure 3.10: Individual dust particles mixing state with color representing $^{62}NO_3^-$.

forming NH_4NO_3 (Usher et al., 2003). Figure 3.10 shows increased $^{18}NH_4^+$ and $^{62}NO_3^-$

on dust particles only during PTCV events. Previous studies have shown dust particles internally mixed with NH_4NO_3 (Mamane and Gottlieb, 1990; Noble and Prather, 1996; Sullivan et al., 2007). 35% of dust nitrate was not associated with ammonium in this study, either because it was not present or because it was suppressed due to matrix effects. Larger peak areas of $^{62}NO_3^-$ were found on individual dust particles with larger peak areas of $^{39}K^+$, shown in Figure 3.10, indicating that the nitrate was also associated with potassium, perhaps as KNO_3, which can form from the heterogeneous reaction of HNO_3 with potassium chloride (KCl) (Jacobson, 2001a). In contrast, there were smaller RPAs of nitrate found on dust particles with larger RPAs of $^{23}Na^+$ and $^{27}Al^+$, indicating these species were less likely to be associated with nitrate. Based on Figure 3.10, there was no clear relationship between nitrate and $^{40}Ca^+$ in dust in this dataset, in contrast with previous observations (Sullivan et al., 2007; Usher et al., 2003). Dust particles that acquire nitrate coatings tend to be more spherical and larger, thus resulting in enhanced light scattering and CCN activity (Gibson et al., 2006; Li and Shao, 2009; Usher et al., 2003).

3.7 References

Allen, J. O., Fergenson, D. P., Gard, E. E., Hughes, L. S., Morrical, B. D., Kleeman, M. J., Gross, D. S., Galli, M. E., Prather, K. A., and Cass, G. R. (2000).Particle Detection Efficiencies of Aerosol Time of Flight Mass Spectrometers under Ambient Sampling Conditions, *Environmental Science & Technology*, *34* (1), 211-217.

Angelino, S., Suess, D. T., and Prather, K. A. (2001).Formation of Aerosol Particles from Reactions of Secondary and Tertiary Alkylamines: Characterization by Aerosol Time-of-Flight Mass Spectrometry, *Environmental Science & Technology*, *35* (15), 3130-3138.

Ault, A. P., Gaston, C., Wang, Y., Dominguez, G., Thiemens, M. H., and Prather, K. A. (2010).Characterization of the Single Particle Mixing State of Individual Ship Plume Events Measured at the Port of Los Angeles, *Environmental Science & Technology*, *44* (6), 1954-1961.

Bhave, P. V., Allen, J. O., Morrical, B. D., Fergenson, D. P., Cass, G. R., and Prather, K. A. (2002).A Field-Based Approach for Determining Atofms Instrument Sensitivities to Ammonium and Nitrate, *Environmental Science & Technology*, *36* (22), 4868-4879.

Bytnerowicz, A., Dawson, P. J., Morrison, C. L., and Poe, M. P. (1991).Deposition of Atmospheric Ions to Pine Branches and Surrogate Surfaces in the Vicinity of Emerald Lake Watershed, Sequoia National Park, *Atmospheric Environment Part a-General Topics, 25* (10), 2203-2210.

Bytnerowicz, A., Dawson, P. J., Morrison, C. L., and Poe, M. P. (1992).Atmospheric Dry Deposition on Pines in the Eastern Brook Lake Watershed, Sierra Nevada, California, *Atmospheric Environment Part a-General Topics, 26* (17), 3195-3201.

Bytnerowicz, A., and Fenn, M. E. (1996).Nitrogen Deposition in California Forests: A Review, *Environmental Pollution, 92* (2), 127-146.

Bytnerowicz, A., and Riechers, G. (1995).Nitrogenous Air-Pollutants in a Mixed-Conifer Stand of the Western Sierra Nevada, California, *Atmospheric Environment, 29* (12), 1369-1377.

Chow, J. C., Chen, L. W. A., Watson, J. G., Lowenthal, D. H., Magliano, K. A., Turkiewicz, K., and Lehrman, D. E. (2006).Pm2.5 Chemical Composition and Spatiotemporal Variability During the California Regional Pm10/Pm2.5 Air Quality Study (Crpaqs), *Journal of Geophysical Research-Atmospheres, 111* (D10), 17.

Chow, J. C., Watson, J. G., Lowenthal, D. H., and Magliano, K. L. (2008).Size-Resolved Aerosol Chemical Concentrations at Rural and Urban Sites in Central California, USA, *Atmospheric Research, 90* (2-4), 243-252.

Chung, C. E., Lee, K., and Muller, D. (2012).Effect of Internal Mixture on Black Carbon Radiative Forcing, *Tellus Series B-Chemical and Physical Meteorology, 64*, 1-13.

Clarisse, L., Shephard, M. W., Dentener, F., Hurtmans, D., Cady-Pereira, K., Karagulian, F., Van Damme, M., Clerbaux, C., and Coheur, P. F. (2010).Satellite Monitoring of Ammonia: A Case Study of the San Joaquin Valley, *Journal of Geophysical Research-Atmospheres, 115*, 15.

Corrigan, C. E., and Novakov, T. (1999).Cloud Condensation Nucleus Activity of Organic Compounds: A Laboratory Study, *Atmospheric Environment, 33* (17), 2661-2668.

Creamean, J. M., Ault, A. P., Ten Hoeve, J. E., Jacobson, M. Z., Roberts, G. C., and Prather, K. A. (2011).Measurements of Aerosol Chemistry During New Particle Formation Events at a Remote Rural Mountain Site, *Environmental Science & Technology, 45* (19), 8208-8216.

Dillner, A. M., Stein, C., Larson, S. M., and Hitzenberger, R. (2001).Measuring the Mass Extinction Efficiency of Elemental Carbon in Rural Aerosol, *Aerosol Science and Technology, 35* (6), 1009-1021.

Draxler, R. R., and Hess, G. D. (1998).An Overview of the Hysplit 4 Modelling System for Trajectories, Dispersion and Deposition, *Australian Meteorological Magazine*, *47* (4), 295-308.

Fenn, M. E., Baron, J. S., Allen, E. B., Rueth, H. M., Nydick, K. R., Geiser, L., Bowman, W. D., Sickman, J. O., Meixner, T., Johnson, D. W., and Neitlich, P. (2003a).Ecological Effects of Nitrogen Deposition in the Western United States, *Bioscience*, *53* (4), 404-420.

Fenn, M. E., Haeuber, R., Tonnesen, G. S., Baron, J. S., Grossman-Clarke, S., Hope, D., Jaffe, D. A., Copeland, S., Geiser, L., Rueth, H. M., and Sickman, J. O. (2003b).Nitrogen Emissions, Deposition, and Monitoring in the Western United States, *Bioscience*, *53* (4), 391-403.

Fuzzi, S., Andreae, M. O., Huebert, B. J., Kulmala, M., Bond, T. C., Boy, M., Doherty, S. J., Guenther, A., Kanakidou, M., Kawamura, K., Kerminen, V.-M., Lohmann, U., Russell, L. M., and Poschl, U. (2006).Critical Assesment of the Current State of Scientific Knowledge, Terminology, and Research Needs Concerning the Role of Organic Aerosols in the Atmosphere, Climate and Global Change, *Atmospheric Chemistry and Physics*, *6*, 2017-2038.

Gard, E., Mayer, J. E., Morrical, B. D., Dienes, T., Fergenson, D. P., and Prather, K. A. (1997).Real-Time Analysis of Individual Atmospheric Aerosol Particles: Design and Performance of a Portable Atofms, *Analytical Chemistry*, *69* (20), 4083-4091.

Gard, E. E., Kleeman, M. J., Gross, D. S., Hughes, L. S., Allen, J. O., Morrical, B. D., Fergenson, D. P., Dienes, T., Gaelli, M. E., Johnson, R. J., Cass, G. R., and Prather, K. A. (1998).Direct Observation of Heterogeneous Chemistry in the Atmosphere, *Science*, *279*, 1184-1187.

Gibson, E. R., Hudson, P. K., and Grassian, V. H. (2006).Physicochemical Properties of Nitrate Aerosols: Implications for the Atmosphere, *Journal of Physical Chemistry A*, *110* (42), 11785-11799.

Givati, A., and Rosenfeld, D. (2004).Quantifying Precipitation Suppression Due to Air Pollution, *Journal of Applied Meteorology*, *43* (7), 1038-1056.

Gross, D. S., Galli, M. E., Silva, P. J., and Prather, K. A. (2000).Relative Sensitivity Factors for Alkali Metal and Ammonium Cations in Single Particle Aerosol Time-of-Flight Mass Spectra, *Analytical Chemistry*, *72* (2), 416-422.

Guazzotti, S. A., Coffee, K. R., and Prather, K. A. (2001a).Continuous Measurements of Size-Resolved Particle Chemistry During Indoex-Intensive Field Phase 99, *Journal of Geophysical Research-Atmospheres*, *106* (D22), 28607-28627.

Guazzotti, S. A., Whiteaker, J. R., Suess, D., Coffee, K. R., and Prather, K. A. (2001b).Real-Time Measurements of the Chemical Composition of Size-

Resolved Particles During a Santa Ana Wind Episode, California USA, *Atmospheric Environment*, *35* (19), 3229-3240.

Gunthe, S. S., Rose, D., Su, H., Garland, R. M., Achtert, P., Nowak, A., Wiedensohler, A., Kuwata, M., Takegawa, N., Kondo, Y., Hu, M., Shao, M., Zhu, T., Andreae, M. O., and Poschl, U. (2011).Cloud Condensation Nuclei (Ccn) from Fresh and Aged Air Pollution in the Megacity Region of Beijing, *Atmospheric Chemistry and Physics*, *11* (21), 11023-11039.

Hall, J. V., Brajer, V., and Lurmann, F. W. (2008).Measuring the Gains from Improved Air Quality in the San Joaquin Valley, *Journal of Environmental Management*, *88* (4), 1003-1015.

Healy, R. M., Sciare, J., Poulain, L., Kamili, K., Merker, M., Muller, T., Wiedensohler, A., Eckhardt, S., Stohl, A., Sarda-Esteve, R., McGillicuddy, E., I.P., O. C., Sodeau, J. R., and Wenger, J. C. (2012).Sources and Mixing State of Size-Resolved Elemental Carbon Particles in a European Megacity: Paris, *Atmospheric Chemistry and Physics*, *12*, 1681-1700.

Hobbs, P. V., Reid, J. S., Kotchenruther, R. A., Ferek, R. J., and Weiss, R. (1997).Direct Radiative Forcing by Smoke from Biomass Burning, *Science*, *275* (5307), 1776-1778.

Hudson, P. K., Schwarz, J., Baltrusaitis, J., Gibson, E. R., and Grassian, V. H. (2007).A Spectroscopic Study of Atmospherically Relevant Concentrated Aqueous Nitrate Solutions, *Journal of Physical Chemistry A*, *111* (4), 544-548.

Jacobson, M. Z. (2001a).Global Direct Radiative Forcing Due to Multicomponent Anthropogenic and Natural Aerosols, *Journal of Geophysical Research-Atmospheres*, *106* (D2), 1551-1568.

Jacobson, M. Z. (2001b).Strong Radiative Heating Due to the Mixing State of Black Carbon in Atmospheric Aerosols, *Nature*, *409* (6821), 695-697.

Jeong, C. H., McGuire, M. L., Godri, K. J., Slowik, J. G., Rehbein, P. J. G., and Evans, G. J. (2011).Quantification of Aerosol Chemical Composition Using Continuous Single Particle Measurements, *Atmospheric Chemistry and Physics*, *11* (14), 7027-7044.

Kanakidou, M., Seinfeld, J. H., Pandis, S. N., Barnes, I., Dentener, F. J., Facchini, M. C., Van Dingenen, R., Ervens, B., Nenes, A., Nielsen, C. J., Swietlicki, E., Putaud, J. P., Balkanski, Y., Fuzzi, S., Horth, J., Moortgat, G. K., Winterhalter, R., Myhre, C. E. L., Tsigaridis, K., Vignati, E., Stephanou, E. G., and Wilson, J. (2005).Organic Aerosol and Global Climate Modelling: A Review, *Atmospheric Chemistry and Physics*, *5*, 1053-1123.

Kane, D. B., and Johnston, M. V. (2001).Enhancing the Detection of Sulfate Particles for Laser Ablation Aerosol Mass Spectrometry, *Analytical Chemistry*, *73* (22), 5365-5369.

Li, W. J., and Shao, L. Y. (2009).Observation of Nitrate Coatings on Atmospheric Mineral Dust Particles, *Atmospheric Chemistry and Physics*, *9* (6), 1863-1871.

MacDonald, C. P., McCarthy, M. C., Dye, T. S., Wheeler, N. J. M., Hafner, H. R., and Roberts, P. T. (2006).Transport and Dispersion During Wintertime Particulate Matter Episodes in the San Joaquin Valley, California, *Journal of the Air & Waste Management Association*, *56* (7), 961-976.

Mamane, Y., and Gottlieb, J. (1990).Heterogeneous Reaction of Nitrogen-Oxides on Sea Salt and Mineral Particles - a Single-Particle Approach, *Journal of Aerosol Science*, *21*, S225-S228.

McFiggans, G., Artaxo, P., Baltensperger, U., Coe, H., Facchini, M. C., Feingold, G., Fuzzi, S., Gysel, M., Laaksonen, A., Lohmann, U., Mentel, T. F., Murphy, D. M., O'Dowd, C. D., Snider, J. R., and Weingartner, E. (2006).The Effect of Physical and Chemical Aerosol Properties on Warm Cloud Droplet Activation, *Atmospheric Chemistry and Physics*, *6*, 2593-2649.

Moffet, R. C., and Prather, K. A. (2009).In-Situ Measurements of the Mixing State and Optical Properties of Soot with Implications for Radiative Forcing Estimates, *Proceedings of the National Academy of Sciences of the United States of America*, *106* (29), 11872-11877.

Morrical, B. D., Fergenson, D. P., and Prather, K. A. (1998).Coupling Two-Step Laser Desorption/Ionization with Aerosol Time-of-Flight Mass Spectrometry for the Analysis of Individual Organic Particles, *Journal of the American Society for Mass Spectrometry*, *9* (10), 1068-1073.

Muhle, J., Lueker, T. J., Su, Y., Miller, B. R., Prather, K. A., and Weiss, R. F. (2007).Trace Gas and Particulate Emissions from the 2003 Southern California Wildfires, *Journal of Geophysical Research-Atmospheres*, *112* (D3).

Murphy, J. G., Day, A., Cleary, P. A., Wooldridge, P. J., and Cohen, R. C. (2006).Observations of the Diurnal and Seasonal Trends in Nitrogen Oxides in the Western Sierra Nevada, *Atmospheric Chemistry and Physics*, *6*, 5321-5338.

Neubauer, K. R., Johnston, M. V., and Wexler, A. S. (1998).Humidity Effects on the Mass Spectra of Single Aerosol Particles, *Atmospheric Environment*, *32* (14-15), 2521-2529.

Noble, C. A., and Prather, K. A. (1996).Real-Time Measurement of Correlated Size and Composition Profiles of Individual Atmospheric Aerosol Particles, *Environmental Science & Technology*, *30* (9), 2667-2680.

Novakov, T., and Penner, J. E. (1993).Large Contribution of Organic Aerosols to Cloud Condensation Nuclei Concentrations, *Nature*, *365* (6449), 823-826.

Orsini, D. A., Ma, Y. L., Sullivan, A., Sierau, B., Baumann, K., and Weber, R. J. (2003).Refinements to the Particle-into-Liquid Sampler (Pils) for Ground and Airborne Measurements of Water Soluble Aerosol Composition, *Atmospheric Environment*, *37* (9-10), 1243-1259.

Qin, X., and Prather, K. A. (2006).Impact of Biomass Emissions on Particle Chemistry During the California Regional Particulate Air Quality Study, *International Journal of Mass Spectrometry*, *258*, 142-150.

Qin, X. Y., Bhave, P. V., and Prather, K. A. (2006).Comparison of Two Methods for Obtaining Quantitative Mass Concentrations from Aerosol Time-of-Flight Mass Spectrometry Measurements, *Analytical Chemistry*, *78* (17), 6169-6178.

Reid, J. S., Koppmann, R., Eck, T. F., and Eleuterio, D. P. (2005).A Review of Biomass Burning Emissions Part Ii: Intensive Physical Properties of Biomass Burning Particles, *Atmospheric Chemistry and Physics*, *5*, 799-825.

Reilly, P. T. A., Lazar, A. C., Gieray, R. A., Whitten, W. B., and Ramsey, J. M. (2000).The Elucidation of Charge-Transfer-Induced Matrix Effects in Environmental Aerosols Via Real-Time Aerosol Mass Spectral Analysis of Individual Airborne Particles, *Aerosol Science and Technology*, *33* (1-2), 135-152.

Rosenfeld, D. (1999).Trmm Observed First Direct Evidence of Smoke from Forest Fires Inhibiting Rainfall, *Geophysical Research Letters*, *26* (20), 3105-3108.

Rosenfeld, D., Woodley, W. L., Axisa, D., Freud, E., Hudson, J. G., and Givati, A. (2008).Aircraft Measurements of the Impacts of Pollution Aerosols on Clouds and Precipitation over the Sierra Nevada, *Journal of Geophysical Research-Atmospheres*, *113* (D15).

Silva, P. J., Carlin, R. A., and Prather, K. A. (2000).Single Particle Analysis of Suspended Soil Dust from Southern California, *Atmospheric Environment*, *34* (11), 1811-1820.

Silva, P. J., Liu, D., Noble, C. A., and Prather, K. A. (1999).Size and Chemical Characterization of Individual Particles Resulting from Biomass Burning of Local Southern California Species, *Environmental Science & Technology*, *33* (18), 3068-3076.

Silva, P. J., and Prather, K. A. (2000).Interpretation of Mass Spectra from Organic Compounds in Aerosol Time-of-Flight Mass Spectrometry, *Analytical Chemistry*, *72* (15), 3553-3562.

Sodeman, D. A., Toner, S. M., and Prather, K. A. (2005).Determination of Single Particle Mass Spectral Signatures from Light-Duty Vehicle Emissions, *Environmental Science & Technology*, *39* ((12)), 4569-4580.

Solomon, S., Qin, D., Manning, M., Chen, Z., Marquis, M., Averyt, K. B., Tignor, M., and Miller, H. L. (2007). Climate Change 2007: The Physical Science Basis. Contribution of Working Group I to the Fourth Assessment Report of the Intergovernmental Panel on Climate Change, Cambridge, United Kingdom and New York, USA.

Song, X. H., Hopke, P. K., Fergenson, D. P., and Prather, K. A. (1999).Classification of Single Particles Analyzed by Atofms Using an Artificial Neural Network, Art-2a, *Analytical Chemistry*, *71* (4), 860-865.

Sullivan, R. C., Guazzotti, S. A., Sodeman, D. A., and Prather, K. A. (2007).Direct Observations of the Atmospheric Processing of Asian Mineral Dust, *Atmospheric Chemistry and Physics*, *7* (5), 1213-1236.

Toner, S. M., Shields, L. G., Sodeman, D. A., and Prather, K. A. (2008).Using Mass Spectral Source Signatures to Apportion Exhaust Particles from Gasoline and Diesel Powered Vehicles in a Freeway Study Using Uf-Atofms, *Atmospheric Environment*, *42* (3), 568-581.

Usher, C. R., Michel, A. E., and Grassian, V. H. (2003).Reactions on Mineral Dust, *Chemical Reviews*, *103* (12), 4883-4939.

Vendrasco, E. P., Dias, P. L. S., and Freitas, E. D. (2009).A Case Study of the Direct Radiative Effect of Biomass Burning Aerosols on Precipitation in the Eastern Amazon, *Atmospheric Research*, *94* (3), 409-421.

Watson, J. G., and Chow, J. C. (2002).A Wintertime Pm2.5 Episode at the Fresno, Ca, Supersite, *Atmospheric Environment*, *36* (3), 465-475.

Weber, R. J., Orsini, D., Daun, Y., Lee, Y. N., Klotz, P. J., and Brechtel, F. (2001).A Particle-into-Liquid Collector for Rapid Measurement of Aerosol Bulk Chemical Composition, *Aerosol Science and Technology*, *35* (3), 718-727.

Wenzel, R. J., Liu, D. Y., Edgerton, E. S., and Prather, K. A. (2003).Aerosol Time-of-Flight Mass Spectrometry During the Atlanta Supersite Experiment: 2. Scaling Procedures, *Journal of Geophysical Research-Atmospheres*, *108* (D7).

Wenzel, R. J., and Prather, K. A. (2004).Improvements in Ion Signal Reproducibility Obtained Using a Homogeneous Laser Beam for on-Line Laser Desorption/Ionization of Single Particles, *Rapid Communications in Mass Spectrometry*, *18* (13), 1525-1533.

Western Region Headquarters, N. W. S. (2010a). Storm Data and Unusual Weather Phenomena - February 2010.

Western Region Headquarters, N. W. S. (2010b). Storm Data and Unusual Weather Phenomena - March 2010.

Whiteaker, J. R., Suess, D. T., and Prather, K. A. (2002).Effects of Meteorological Conditions on Aerosol Composition and Mixing State in Bakersfield, Ca, *Environmental Science & Technology*, *36* (11), 2345-2353.

Yao, X. H., Rehbein, P. J. G., Lee, C. J., Evans, G. J., Corbin, J., and Jeong, C. H. (2011).A Study on the Extent of Neutralization of Sulphate Aerosol through Laboratory and Field Experiments Using an Atofms and a Gpic, *Atmospheric Environment*, *45* (34), 6251-6256.

Ying, Q., and Kleeman, M. (2009).Regional Contributions to Airborne Particulate Matter in Central California During a Severe Pollution Episode, *Atmospheric Environment*, *43* (6), 1218-1228.

Zauscher, M. D., Wang, Y., Moore, M. J. K., C.J.;, G., and Prather, K. A. (2012).Mixing State and Aging of Individual Biomass Burning Aerosols During the 2007 San Diego Wildfires, *In prep*.

Zaveri, R. A., Barnard, J. C., Easter, R. C., Riemer, N., and West, M. (2010).Particle-Resolved Simulation of Aerosol Size, Composition, Mixing State, and the Associated Optical and Cloud Condensation Nuclei Activation Properties in an Evolving Urban Plume, *Journal of Geophysical Research-Atmospheres*, *115*, 19.

Zuberi, B., Johnson, K. S., Aleks, G. K., Molina, L. T., and Laskin, A. (2005).Hydrophilic Properties of Aged Soot, *Geophysical Research Letters*, *32* (1).

Chapter 4. Cloud condensation nuclei properties and aerosol composition in the foothills of California's Sierra Nevada

Ambient aerosol particles that can serve as cloud condensation nuclei (CCN) affect global climate and precipitation processes. The goal of this study was to identify the sources of CCN-active particles in the foothills of the California Sierra Nevada therefore, CCN activity and chemical composition of aerosols were measured at Mariposa, California in March, 2010; chemical measurements included black carbon and soluble inorganic mass concentrations and size-resolved composition of single particles using an aerosol time-of-flight mass spectrometer (ATOFMS). Pollution transport events and clean rural background conditions were observed. Both the total number and CCN concentrations were higher during regional pollution events compared to clean background conditions. Pollution aerosol transported from the Central Valley, which consisted of carbonaceous particles internally mixed with ammonium, nitrate, and sulfate, was observed to be the most hygroscopic with median (interquartile range) κ = 0.26 (0.16-0.50) during this study. During clean rural background conditions, particles were less hygroscopic with κ = 0.15 (0.06-0.29) and consisted mainly of biomass burning aerosols. Thus, during this study the CCN most likely influencing cloud microphysical properties in the central Sierra Nevada foothills are highly aged soot particles originating from the Central Valley.

4.1 Introduction

Aerosol particles affect climate directly through absorbing and reflecting solar and terrestrial radiation (Solomon et al., 2007). In addition, a subset of particles called cloud condensation nuclei (CCN) can nucleate cloud droplets (Solomon et al., 2007). Increased ambient CCN concentrations lead to increased cloud albedo, decreased cloud effective radius, increased cloud lifetime, and potentially to changes in precipitation

patterns (Albrecht, 1989; Lohmann and Feichter, 2005; Twomey, 1977). These so-called aerosol indirect effects contribute the largest uncertainty to our current understanding of climate change (Solomon et al., 2007). This uncertainty stems from the inability to accurately predict the spatial and temporal distribution of CCN concentrations and sources (Andreae and Rosenfeld, 2008; Pierce and Adams, 2009), from a lack of understanding of cloud formation processes and microphysics on regional scales (Khain et al., 2000), as well as how perturbations in CCN concentrations affect these processes.

Cloud droplets are formed when supersaturated water vapor spontaneously condenses onto particles. Particles that are more hygroscopic, a measure of particle water uptake, act as CCN at lower supersaturations (SS) compared to those that are less hygroscopic. Based on particle size and chemical composition, Kohler theory can predict which particles will activate to form cloud droplets at a given SS based on the water activity associated with water soluble aerosol constituents and the surface tension over the curved surface of the aerosol. The hygroscopicity parameter (κ), defined by Petters and Kreidenweis (2007), is a quantitative measure of aerosol water uptake used to compare hygroscopic growth and CCN activity between studies. Typical atmospherically relevant κ values range from ~0 for non-hygroscopic insoluble particles, such as fresh soot, to ~1.4 for the hygroscopic soluble NaCl salt, with average continental values ~0.3 ± 0.1 (Andreae and Rosenfeld, 2008; Gunthe et al., 2011; Kammermann et al., 2010; Rose et al., 2011; Rose et al., 2010).

Understanding aerosol-cloud interactions is particularly crucial for understanding changes in cloud microphysics, which can affect precipitation patterns. Accurately predicting orographic precipitation, the main source of water for the western coast of the United States, remains difficult due to the complexity of representing microphysical processes within clouds, model initialization errors, intricacy of dynamical interactions driven by spatial resolutions including topography and land use, and uncertainty in the multiple and variable sources of CCN (Colle and Zeng, 2004; Grubisic et al., 2005; Ralph et al., 2010; Stoelinga et al., 2003). Observations from the

past several decades have indicated a reduction in the amount of measured orographic precipitation in the California Sierra Nevada region downwind of the Central Valley (Givati and Rosenfeld, 2004), which suffers from poor air quality including high concentration of winter-time particulate matter (Chow et al., 2006). Rosenfeld et al. (2008) determined that the effective diameters of cloud droplets in the Sierra Nevada were negatively correlated to increasing CCN concentrations, which were hypothesized to be transported directly from the Central Valley, thus suggesting that anthropogenic pollution may be the cause of the reduced precipitation (Rosenfeld et al., 2008). However, this past study did not chemically identify these CCN particles or their source. Another main source of CCN in the atmosphere is from the growth of new particles formed in-situ (Laaksonen et al., 2005; Lihavainen et al., 2003); such new particle formation events followed by rapid growth and increased CCN activity were documented in a ground-based study at Sugar Pine Reservoir, a remote rural location in the Sierra Nevada foothills north of Sacramento (Creamean et al., 2011).

Combustion-generated aerosols, including fossil fuels and biomass burning, are a main source of global ambient particles (Andreae and Rosenfeld, 2008). The resulting carbonaceous particles, which include soot and organic carbon, account for more than 50% of global CCN number concentrations in modeling studies, especially in urban areas where new particle formation rates are low (Pierce and Adams, 2009; Spracklen et al., 2011). Although previous studies have shown that fresh soot particles are hydrophobic, they can become CCN active through aging processes that increase their soluble mass fraction, such as condensation of semi-volatile vapors, heterogeneous reactions, and coalescence with soluble inorganic particles (Zuberi et al., 2005). Modeling studies have determined that the CCN activity of particles evolving in an idealized urban plume increased three to four times in 6 hours as particles took up nitrate and ammonium (Zaveri et al., 2010). A previous ambient study in Mexico City identified elevated nitrate due to photochemistry as the main reason for the observed increased CCN activity of traffic-emitted particles (Wang et al., 2010). Previous ambient studies have shown that the highly aged air masses have the highest CCN activity (Furutani et al., 2008; Gunthe et al., 2011). Because of the abundance of

combustion-generated aerosols and the propensity for atmospheric aerosols to undergo atmospheric processing subsequent to their formation, it is crucial to quantify the CCN ability both of freshly emitted as well as atmospherically processed carbonaceous aerosols to decrease the uncertainty of the indirect effects of aerosols (Popovicheva et al., 2011).

This study seeks to identify the sources of CCN active particles in Mariposa, a rural area downwind of the Central valley located east of Merced, California in the foothills of the Sierra Nevada. Particle size, chemical composition, and CCN-derived hygroscopicity measurements obtained at Mariposa, CA during March, 2010 are presented. High concentrations of aged soot particles internally mixed with organic carbon and soluble ammonium, nitrate, and sulfate transported during pollution events in the Central Valley were more CCN active than particles found during clean rural background conditions. These findings support the hypothesis set forth in Rosenfeld et al. (2008) that the Central Valley is a major source of CCN-active particles and suggest that aerosol particles transported directly from the Central Valley are a major source of CCN active particles in the Sierra Nevada.

4.2 Experimental Methods

Ground-based measurements took place at Mariposa, California (37.51, -120.04W, 684 m above sea level) in the foothills of the Sierra Nevada. The sampling site was at the Mariposa County Airport, a rural airport rarely frequented by aircraft. In addition to the airport, local emissions may have been impacted by a fire station equipped with diesel vehicles that was also housed at the airport, a rural highway (Hwy 49) that was located ~200 m from the sampling site, and biomass burning events that were often observed within a few kilometers from the site, especially in the evenings. Attempts to remove these highly localized events from the analysis are described in section 4.2.1.1. The sampling lines and instrumental set-up are described in (Zauscher et al., 2012). Data shown herein is from March 1 – 13th, 2010 to coincide with the CCN and size distribution data.

Hourly particulate matter of diameter < 2.5 um ($PM_{2.5}$) mass concentrations for 28 sites in the Central Valley and Sierra Nevada were compiled from the California Air Resources Board (http://www.arb.ca.gov) during this study. We also measured $PM_{2.5}$ mass concentrations with a beta attenuation monitor (BAM 1020, MetOne Instruments) at the Mariposa and Sugar Pine sites. The data from all 30 sites was interpolated in Igor (WaveMetrics) to make $PM_{2.5}$ mass concentration contour maps in order to analyze the spatial and temporal of particulate pollution variability. In addition, the air mass back trajectories were modeled with HYSPLIT 4.0 using EDAS meteorological data at four altitudes: 500, 1000, 1500 and 2500 m (Draxler and Hess, 1998).

4.2.1 Instrumentation

4.2.1.1 Physical properties of aerosols

Particle size distributions of 10-600 nm and 0.5-20 μm were measured with a scanning mobility particle sizer (SMPS, TSI model 3936) every five minutes and an aerosol particle sizer (APS, TSI model 3321) every minute, respectively. The total particle condensation nuclei number concentrations (N_{CN}) were measured every second with a condensation particle counter (CPC, TSI model 3781), which has a lower size limit of 6 nm. CCN spectra were measured with a streamwise thermal gradient CCN counter (CCNc) (Roberts and Nenes, 2005), which records CCN number concentrations (N_{CCN}) every second while scanning supersaturation (SS) between 0.1-1.0% continuously with a complete up and down scan every 20 minutes. The CPC and CCNc sampling lines were in parallel with each other. The CCNc was calibrated in the field before, during, and after the study with ammonium sulfate aerosol (99.999%, Sigma Aldrich) using thermodynamics from the Aerosol Inorganic Model (AIM) and a surface tension of pure water at 298.15K (Wexler and Clegg, 2002).

Local transient sources, including airplanes and road traffic, were identified by rapid spikes > 10,000 pt/cm^3 in the N_{CN} compared to the baseline, and were removed from the analysis since the focus of this paper is not on these local anthropogenic sources. Despite the removal of these periods with obvious local influence, the N_{CCN}

and N_{CN} high temporal resolution (1 sec) contained high variability in measurements. Data was further filtered by removing periods for which the N_{CN} standard deviation was greater than 5% of the mean during each five minute SMPS scan. Because the N_{CN} measurements are more accurate than the total particle concentrations from the SMPS due to instrumental biases, the SMPS data was normalized to the averaged 3781 CPC concentrations during each SMPS scan. Similarly, the CN concentrations are more robust than the CCN concentrations, thus the N_{CCN} data was reduced by 10% compared to the N_{CN} data. The fraction of CCN active particles (f_{CCN}) was obtained from the filtered N_{CCN}/N_{CN} ratio, and instrumental noise was removed from the f_{CCN} data. The activation diameters (D_{act}) were estimated similarly to Furutani et al. (2008) using the total cumulative aerosol size distributions, N_{CN}, and N_{CCN} with an interpolation script written in the R programming language (http://www.r-project.org). κ was evaluated using the estimated D_{act} and the corresponding SS value using Petters' script (http://www4.ncsu.edu/~mdpetter/findkappa.pro) written in the interactive data language (IDL) based on Petters and Kreidenweis (2007) modified to run in R (http://atofms.ucsd.edu/content/findkappa.r). CCN properties, including D_{act} and κ, are presented per CCN scan in 12 SS bins ranging from 0.12 to 0.96%, with SS shown as subscript (i.e. $f_{CCNss\%}$, $\kappa_{ss\%}$).

4.2.1.2 Chemical properties of aerosols

Black carbon (BC) concentrations were measured with an aethalometer (Magee Scientific, Model AE31-7) at 880 nm wavelength every 5 minutes. The mass concentrations of soluble species (nitrate, ammonium, sulfate and chloride) of $PM_{2.5}$ were measured with a PILS-IC every 17 minutes (Lee et al., 2003; Weber et al., 2001) through 3/11/10. Real-time single particle size and chemical composition were measured with a standard inlet aerosol time-of-flight mass spectrometer (ATOFMS) (Gard et al., 1997). The particle's velocity, obtained from the time-of-flight between two 532-nm continuous wave lasers, was used to determine individual particle size. As the particle enters the dual polarity mass spectrometer, its known velocity was utilized to time the firing of a Q-switched 266-nm laser, which desorbs and ionizes the components from each particle. A mass spectrum is obtained when the positive and

negative ions are detected by a reflectron time-of-flight mass spectrometer. Because this work is focused on the CCN-active particles, which are typically formed from the 50-200 nm particles, only the submicron (<1000 nm) particles sampled with the ATOFMS (200-1000 nm) are presented.

The ATOFMS data was analyzed with the YAADA toolkit (http://www.yaada.org) for Matlab. Submicron particles were clustered with ART-2a, a neural network algorithm, which sorts and groups particles of similar mass spectra together, using a learning rate = 0.05, vigilance factor = 0.85 and 20 iterations (Song et al., 1999). The resulting clusters were further grouped manually based on similarities into 7 previously identified particle types, similar to those shown in Zauscher et al. (2012): elemental carbon or soot, organic carbon (OC), soot with organic carbon (soot-OC), biomass burning, sea salt, dust, and other (Gard et al., 1997; Noble and Prather, 1996; Silva et al., 1999). The sea salt particle type has the characteristic $^{23}Na^+$ and $^{39}K^+$ ions and sodium chloride clusters ($^{81, 83}Na_2Cl^+$ and $^{93, 95, 97}NaCl_2^-$) typical of sea salt. The soot particle type had peaks at carbon clusters, such as $^{12}C^+$, $^{24}C_2^+$, $^{+36}C_3^+$, etc. The OC particle type was characterized by intense peaks at $^{27}C_2H_3^+$, $^{29}C_2H_5^+$, $^{37}C_3H^+$, $^{39}C_3H_3^+$, and $^{43}C_2H_3O^+$. The soot-OC particle mass spectra contain a combination of the characteristic ions observed in of soot and OC particle types. The biomass burning particle type consists of soot-OC particles with a strong potassium ion peak at $^{39}K^+$ (Silva et al., 1999). Relative peak area (RPA) searches were performed for the following pre-established markers on all submicron particle types: ammonium ($^{18}NH_4^+$), nitrate ($^{30}NO^+$), chloride ($^{35}Cl^-$), and sulfate ($^{97}HSO_4^-$) (Bhave et al., 2002; Liu et al., 2000). ATOFMS data were compiled hourly.

4.3 Results/Discussion

Figure 4.1 shows the temporal evolution and variability in the particle size distributions, CCN activity, hygroscopicity, and particle chemical composition, including the bulk mass concentration of ionic soluble species from $PM_{2.5}$ measured

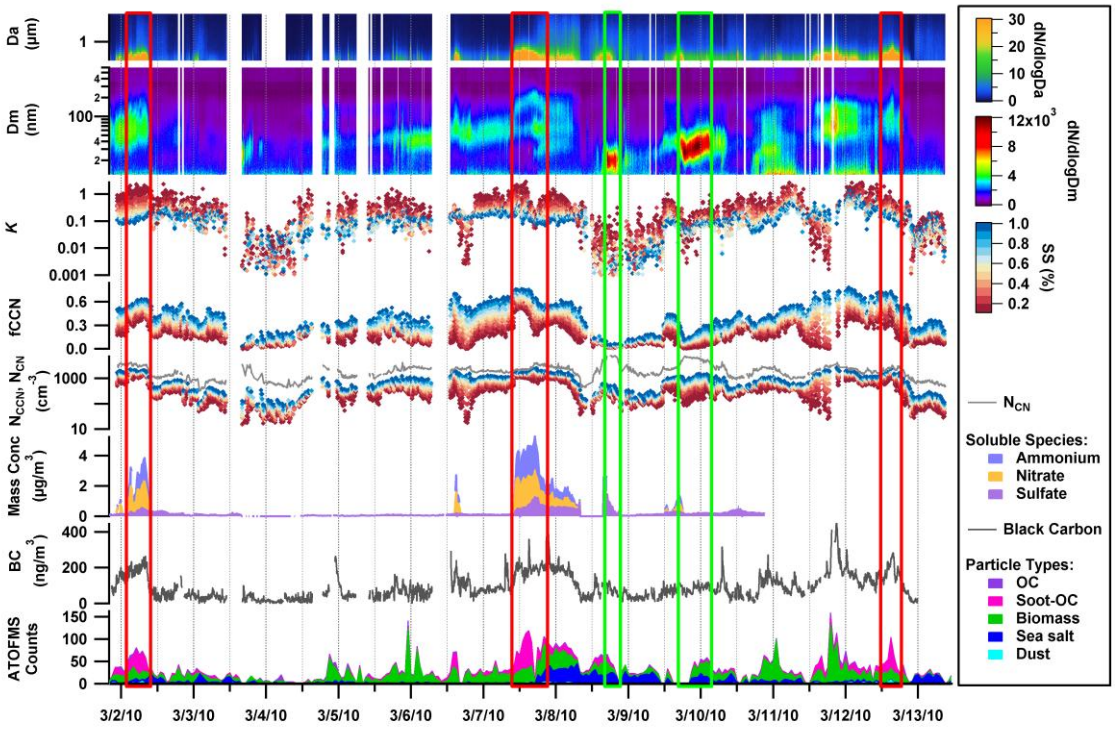

Figure 4.1: Size distributions, CCN and chemical properties of particles. Red boxes indicate pollution transport events, while green boxes highlight local events. The rest of the study is considered clean background.

with the PILS-IC, the submicron particle types measured with the ATOFMS, and the black carbon concentrations measured with the aethalometer. The submicron particles types, as determined with the ATOFMS, were dominated by biomass burning, sea salt, and soot-OC at different times (Figure 4.1). In addition, there was a minor fraction of OC and dust particles detected throughout this study. Particle chemistry and size did not exhibit diurnal patterns; however there were episodes with dramatically different characteristics. For example, the periods in red boxes had higher mass concentrations of black carbon (> 150 ng/m^3), nitrate (>1 μg/m^3), and ammonium (>0.5 μg/m^3), as well as

elevated submicron soot-OC particle counts, likely emitted from fossil fuel combustion, due to pollution transport from the Central Valley (PTCV). These polluted periods, which had larger particles than the rest of the study, were the most CCN active (f_{CCN} = 0.3-0.5). In contrast, the periods in the green boxes were relatively clean with low nitrate, ammonium, and BC mass concentrations but with high number concentrations of ultrafine particles (geometric mean diameter (GMD <42 nm) and $N_{CN} > 4500$ cm^{-3}; these ultrafine particles were freshly produced, and thus not large enough to act as CCN. Because these were mainly small particles, it was not possible to chemically analyze them with the instruments used in this campaign. These two ultrafine events, which are not discussed further, had low CCN activities (f_{CCN} = 0.04-0.2). During the rest of the study, conditions were also clean but characterized by lower N_{CN} (< 2500 cm^{-3}) overall, moderate fraction of CCN active particles (f_{CCN} = 0.1-0.4), and a prevalence of BBA. These clean condition periods were combined and labeled as 'clean rural background' (CB). Table 4.1 summarizes the particle properties for each of the events outlined above.

Figure 4.2 shows the average contour plot of $PM_{2.5}$ mass concentrations and representative air mass back trajectories for the three PTCV events highlighted in Figure 4.1 and the CB conditions. All three PTCV events, which lasted between 6 and 9 hours, coincided with pollution transported from the Central Valley. The average $PM_{2.5}$ contour map for all PTCV events (Figure 4.2b) highlights the increased $PM_{2.5}$ concentrations in the Central Valley between Sacramento and Corcoran decreasing radially from there. Previous work showed that high levels of $PM_{2.5}$ in the Central Valley were coincident with periods of air stagnation (Ying and Kleeman, 2009). The air mass back trajectories confirm not only that the air originated from the Central Valley but furthermore, that the air was stagnant for at least 60 hours over the Central Valley before arriving at Mariposa.

Table 4.1: Particle characteristics per event with median (interquartile range) unless otherwise noted. CB = clean rural background, PTCV = pollution transport from Central Valley.

Event	N_{CN} (cm^{-3})	SMPS GMD* (nm)	BC (ng/m^3)	NO_3^- ($\mu g/m^3$)	NH_4^+ ($\mu g/m^3$)	SO_4^{2-} ($\mu g/m^3$)
CB	1760 (1100-2420)	46 ± 3	64 (34-111)	BDL[¥]	BDL[¥]	0.11 (0.05-0.21)
PTCV1	3300 (3090-3620)	62 ± 2	189 (167-211)	1.18 (0.71-1.51)	0.98 (0.51-1.15)	0.35 (0.22-0.45)
PTCV2	2370 (2190-3270)	75 ± 3	190 (174-204)	1.69 (1.36-1.82)	1.84 (1.44-1.96)	0.62 (0.51-0.93)
PTCV3	2510 (2150-2810)	66 ± 3	173 (148-222)	NA[&]	NA[&]	NA[&]
PTCV all	2830 (2240-3330)	66 ± 2	189 (162-212)	1.51 (0.98-1.78)	1.32 (0.83-1.88)	0.50 (0.32-0.72)

*given with geometric mean, [¥]BDL = below detection limit, [&]NA = not applicable

High mass concentrations of ammonium and nitrate were mainly observed during PTCV events, which further supports the claim that pollution was transported from the valley to Mariposa since ammonium nitrate (NH_4NO_3) has been shown to be the most prevalent species by mass in the Central Valley during winter-time (Chow et al., 2006; MacDonald et al., 2006). NO_x, which oxidizes into nitric acid, is mainly emitted by traffic in urban areas of the Central Valley and transported downwind to rural regions. Once the nitric acid arrives in rural areas, it is neutralized by locally emitted ammonia (NH_3) produced by animal husbandry and agriculture (Clarisse et al., 2010), to form NH_4NO_3 in the particulate phase (Watson and Chow, 2002; Ying and Kleeman, 2009). BC concentrations were also high during PTCV periods indicating that these particles likely also originated from traffic emissions in urban areas of the Central Valley and were transported to the sampling site along with the NO_x and nitric acid. Because the data from all three PTCV events were similar, they were combined into one named PTCV to minimize the number of statistics reported in Table 4.2.

4.3.1 CCN properties and Hygroscopicity

Table 4.2 summarizes the CCN properties and κ during each event type. Both the number and fraction of CCN active particles were higher during PTCV than CB events across all supersaturations. The median CN and $CCN_{0.45\%}$ number concentrations were higher for pollution transport (2830 and 1404 cm^{-3}) versus the clean background (1760 and 430 cm^{-3}) conditions, resulting in $f_{CCN0.45\%}$ of 0.50 versus 0.27, respectively, with higher CCN activity at higher SS. Because at lower supersaturations only larger particles can be activated to CCN, it makes sense that during PTCV events, when the particles had larger diameters compared to those of CB events, more particles activated as CCN. The median estimated $Dact_{0.45\%}$ was larger during CB versus PTCV events (79

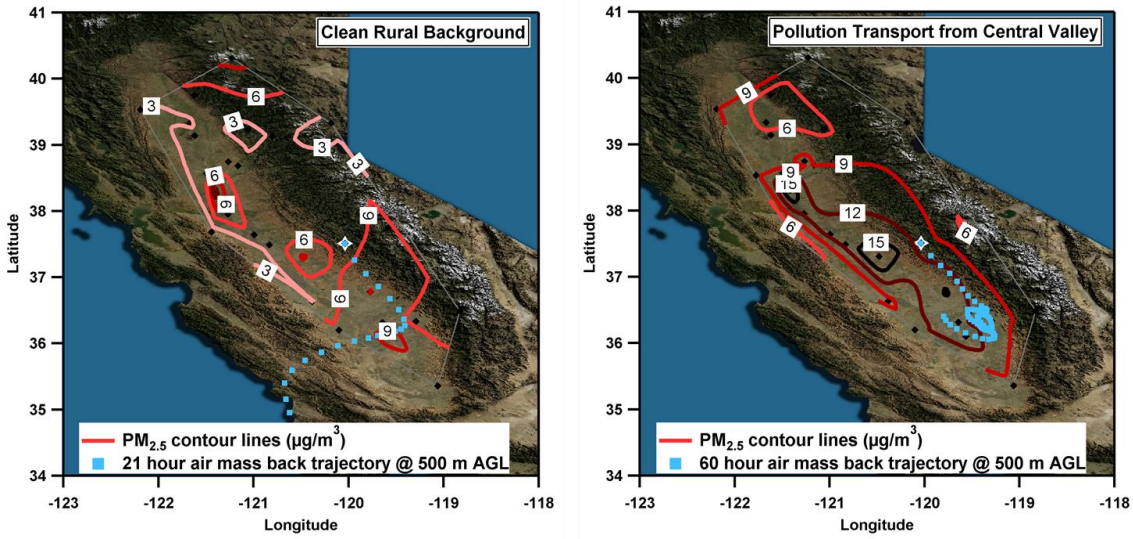

Figure 4.2: Average $PM_{2.5}$ contour maps and example modeled air mass back trajectories of a) clean background (3/2/10 12:00-3/3/10 12:00) and b) pollution transported from the Central Valley.

versus 66 nm), while the SMPS geometric mean diameter (GMD) was smaller (46 versus 66 nm), confirming that more particles were CCN active during PTCV in contrast with CB events. Furthermore, the particles were more hygroscopic during pollution transport events across all supersaturations, but more so at lower supersaturations. At SS=0.18%, the median κ was about three times higher meaning the particles were more hygroscopic during PTCV than CB events (0.75 vs 0.26), while

almost twice as hygroscopic at SS=0.45% (0.23 versus 0.14). This is an important observation because lower supersaturations, which are more likely to occur in the atmosphere, are more sensitive to chemical influences. At higher supersaturations, the hygroscopicity parameter seems to converge to similar values during both events, with $\kappa_{0.85\%}$ ~0.13. Across all supersaturations, the median (interquartile range) κ was 0.26 (0.16-0.50) versus 0.15 (0.06-0.29) for regional pollution transport events and clean rural background conditions.

Table 4.2: CCN properties per event type with median (interquartile range).

Variable	Event	Supersaturation (%)					
		0.18	**0.31**	**0.45**	**0.63**	**0.85**	**all**
N_{CCN} (cm^{-3})	CB	235 (114-433)	362 (160-592)	430 (179-743)	521 (212-860)	641 (260-1044)	367 (164-715)
	PTCV	1112 (860-1197)	1283 (1112-1433)	1404 (1303-1594)	1548 (1385-1770)	1683 (1539-1962)	1377 (1152-1629)
f_{CCN}	CB	0.18 (0.10-0.24)	0.23 (0.15-0.31)	0.27 (0.18-0.37)	0.32 (0.22-0.43)	0.39 (0.28-0.51)	0.25 (0.15-0.37)
	PTCV	0.38 (0.30-0.44)	0.45 (0.39-0.54)	0.50 (0.45-0.58)	0.55 (0.51-0.64)	0.62 (0.56-0.69)	0.51 (0.40-0.59)
D_{act} (nm)	CB	120 (95-180)	95 (78-132)	79 (68-106)	65 (57-89)	54 (48-68)	88 (63-128)
	PTCV	85 (76-105)	74 (68-80)	66 (62-71)	58 (54-61)	51 (46-54)	67 (56-81)
κ	CB	0.26 (0.07-0.54)	0.16 (0.06-0.31)	0.14 (0.06-0.22)	0.12 (0.05-0.18)	0.12 (0.06-0.17)	0.15 (0.06-0.29)
	PTCV	0.75 (0.41-1.04)	0.37 (0.29-0.44)	0.23 (0.19-0.28)	0.17 (0.14-0.21)	0.13 (0.11-0.18)	0.26 (0.16-0.50)

Overall, κ values estimated in this study had a broad range (0.07-1.01) (Table 4.2). It is likely the effects of the transient local sources were not fully removed. Other factors that may contribute to these broad values include: inaccurate multiple charge corrections applied to the SMPS size distributions, errors inverting the size distributions

to cumulative concentrations, depression in the CCNc supersaturation in the presence of high N_{CCN} (>1,000 cm^{-3}), coincident counts on the CPC and CCNc, and errors due to low N_{CCN} during clean conditions. Alternatively, broad κ values can be a result of rapidly changing air masses.

The κ values reported for this study fall within the range of those published by previous aircraft campaigns sampling in the boundary layer over the California Central Valley (κ~0.1-0.4) (Moore et al., 2012; Roberts et al., 2010; Sorooshian et al., 2008). Furthermore, CCN data from North American continental outflow to the Pacific Ocean during a separate aircraft study was used to estimate κ~0.05 (Roberts et al., 2006; Roberts et al., 2010). The range of these values may be explained if there were different levels of aged pollution during each campaign. For example, Gunthe et al. (2011) reported a higher κ value in Beijing, China during aged regional pollution in comparison to fresh city pollution (0.35 ± 0.05 versus 0.22 ± 0.07, respectively). This difference was explained by smaller, fresher, more hydrophobic soot and OC particles in the fresh city pollution in contrast to higher inorganic fractions, which are more hygroscopic, during the aged regional pollution (Gunthe et al., 2011). Similarly, particles measured at Mariposa during aged regional pollution had higher hygroscopicity (κ = 0.26 (0.16-0.50)) compared to those during clean rural background conditions (κ = 0.15 (0.06-0.29)). As discussed below, the higher kappa values during the aged regional pollution can also be explained by higher amounts of soluble inorganic species on the particles sampled in Mariposa compared to those of the clean rural background. The next section provides a more detailed investigation into the relationship between measured particle chemistry and CCN activity.

4.3.2 CCN activity comparison with particle chemistry

Table 4.3 summarizes the correlations between CCN activity and particle physical and chemical properties. The correlations between GMD and f_{CCN} were strong (R^2=0.57-0.81), with the weakest correlation (R^2=0.57) at the lowest SS where only larger particles become CCN; at SS>0.45%, the correlations were all strong (R^2=0.78-0.81) likely because more particles could activate at these supersaturations. In general,

chemistry plays less of a role at such high supersaturation values. Comparisons between particle chemistry measured with the aethalometer, ATOFMS, and PILS-IC and CCN properties were done using N_{CCN} rather than f_{CCN} because of the lower size cut-off (200 nm) of the ATOFMS and the low mass contributed by smaller particles. The strongest correlations between N_{CCN} and all particle chemical parameters were obtained with BC mass concentrations, which had R^2 = 0.67-0.79 across all SS bins. The lowest SS (0.18%) had the weakest correlation (R^2 = 0.67) between N_{CCN} and BC because at lower supersaturations only larger particles can serve as CCN and because smaller soot particles are less aged and hence less hygroscopic; median $Dact_{0.18\%}$ = 85 and 120 nm while GMD = 66 and 46 nm during PTCV and CB, respectively. Since BC concentrations were the most prevalent during PTCV, the GMD of all particles during PTCV events is likely representative of the size of BC during these periods; thus, the geometric mean diameter of the BC particles can be estimated to be ~66 nm. Therefore, the strongest correlation between N_{CCN} and BC (R^2 = 0.79) was at 0.45% SS probably because the GMD of all particles was the same as $Dact_{0.45\%}$ (66 nm) during PTCV events. Previous work has shown that aging increases the CCN activity and hygroscopicity of carbonaceous aerosols, including soot (Furutani et al., 2008; Gunthe et al., 2011; Khalizov et al., 2009; Popovicheva et al., 2011; Tritscher et al., 2011; Weingartner et al., 1997). Therefore, the BC sampled at Mariposa was likely aged because of the strong correlations between CCN and BC concentrations, which is confirmed with single particle data.

Table 4.3: Correlations (R^2) between N_{CCN} and particle properties. Red values highlight the strongest correlations.

Parameter	Supersaturation (%)				
	0.18	**0.31**	**0.45**	**0.63**	**0.85**
SMPS GMD (nm)*	0.57	0.72	0.79	*0.81*	0.78
Black Carbon (ng/m^3)	0.67	0.74	*0.79*	0.77	0.74
ATOFMS soot-OC (#)	0.48	*0.50*	0.49	0.45	0.41
NO_3^- ($\mu g/m^3$)	0.58	*0.61*	0.55	0.55	0.50
$^{30}NO^+$ (sum RPA)	0.47	0.51	*0.54*	0.53	0.50
NH_4^+ ($\mu g/m^3$)	0.35	0.41	0.38	0.41	0.39
$^{18}NH_4^+$ (sum RPA)	0.28	0.33	0.35	0.36	0.34
SO_4^{2-} ($\mu g/m^3$)	0.30	0.30	0.29	0.27	0.24
$^{97}HSO_4^-$ (sum RPA)	0.08	0.08	0.08	0.09	0.06

*Correlation with fCCN

As particles age, they grow in size due to acquisition of secondary species, such as soluble ammonium, nitrate, and sulfate and/or soluble to non-soluble OC species. Aged or atmospherically processed particles have a higher mass fraction of soluble secondary species, which increases their water uptake and hence CCN activity, according to Kohler theory. Increased water on particles suppresses the formation of negative ions when using a laser to desorb and ionize the particles, as is the case with the ATOFMS, resulting in the suppression of negative ion mass spectra (Neubauer et al., 1998). The lack of negative ion mass spectra on the majority (71 and 69%) of soot-OC and OC particles indicates that they had significant amounts of water associated with them and thus, were likely atmospherically processed. This processing would

theoretically increase their water uptake abilities (Moffet et al., 2008) making these particles more CCN active. Indeed, comparisons between N_{CCN} at all SS bins and the counts of the aged soot-OC particles (Table 4.2) showed fair correlations (R^2 = 0.39-0.50); these correlations would likely be stronger if the ATOFMS sampled particles < 200 nm. Soot-OC particles without negative polarity mass spectra had $^{18}NH_4^+$ and $^{30}NO^+$ in their positive mass spectra corroborating the that they were internally mixed with ammonium and nitrate, while those with dual polarity mass spectra had peaks at $^{62}NO_3^-$, $^{97}HSO_4^-$, and $^{125}H(NO_3)_2^-$ confirming the presence of nitrate and sulfate (Bhave et al., 2002). The fact that ~70% of these particles lacked negative spectra, confirms that they did take up water. This demonstrates that the higher mass of BC particles in this study were mostly aged soot-OC internally mixed with soluble species, which supports the strong observed correlations between N_{CCN} and BC.

In terms of soluble species, the correlations between PILS-IC nitrate mass concentrations and N_{CCN} were the strongest (R^2 = 0.452-0.612) across all supersaturations compared to those of sulfate and ammonium. At lower SS, which activate only larger more hygroscopic particles, the correlations between PILS-IC nitrate and N_{CCN} were stronger, likely because larger aged particles have more nitrate than smaller less atmospherically processed ones. The ATOFMS submicron nitrate correlations with N_{CCN} were comparable to those of the PILS-IC (R^2 = 0.47-0.54). In contrast, the correlations between PILS-IC sulfate mass concentrations and N_{CCN} were weak (R^2 = 0.234-0.320) because sulfate was found more readily on smaller particles, which would contribute less to the total sulfate mass making mass concentrations not the most representative parameter for comparison with N_{CCN}. There were no correlations between ATOFMS submicron sulfate and N_{CCN} (R^2 < 0.09) because most of the sulfate may have been in particles < 200 nm and also due to the low number of negative mass spectra obtained in this study, especially for aged soot-OC particles, which lead to no sulfate measurements. The correlations between PILS-IC and ATOFMS submicron ammonium and N_{CCN} across all supersaturations (R^2 = 0.307-0.415 and 0.28-0.36, respectively) were between those of nitrate and sulfate because the ammonium would be distributed over both large and small particles to neutralize the

nitrate and sulfate. For this study, the correlations between N_{CCN} with nitrate and ammonium PILS-IC and ATOFMS measurements indicate that the mixing state of aerosol particles is important in determining their CCN activity.

4.4 Conclusions

Physicochemical properties, including CCN-derived hygroscopicity, of ambient particles were measured at the Sierra Nevada foothills in March, 2010. Two main sources of CCN particles were identified. During regional transport events, which exhibited higher median total particle and CCN concentrations (N_{CN} = 2830 and N_{CCN} = 1377 cm^{-3}) and more hygroscopic and CCN-active particles (κ = 0.26 and f_{CCN} = 0.51) compared to clean background conditions, CCN were mostly characterized as soot particles mixed with soluble ammonium, nitrate, and sulfate. Locally produced biomass burning particles were identified as CCN during the clean rural background conditions, which had lower total particle and CCN concentrations (N_{CN} = 1760 and N_{CCN} = 367 cm^{-3}) and less hygroscopic and CCN-active particles (κ = 0.15 and f_{CCN} = 0.25) in contrast with polluted events. Because of the higher concentrations of particles and increase particle hygroscopicity during regional transport events, the transported aged soot particles may be significantly affecting regional cloud properties, thereby altering cloud albedo and potentially precipitation patterns. These observations validate the hypothesis set by Rosenfeld et al. (2008) that a major source of CCN particles in the Sierra Nevada foothills is Central Valley pollution. Although fresh soot particles do not serve as CCN, aged soot internally mixed with soluble inorganic species are CCN active thus, highlighting the important role that particle mixing state has in determining CCN activity. We encourage future long-term monitoring of CCN properties and CCN-sized particle composition at multiple sites across a transect of the Central Valley to the Sierra Nevada to further understand the conditions for pollution transport and its effects on regional orographic precipitation.

4.5 Acknowledgments

We are grateful to the National Oceanic and Atmospheric Administration for organizing logistics related to the sampling site and to the Mariposa County Airport for allowing us to sample on site. Jake Lippman is acknowledged for assistance preparing instrumentation and collecting data during this study. We would also like to acknowledge Professor Wolfgang F. Rogge at the University of California Merced for sharing his Millipore ultrapure water with us. The authors would like to thank Dr. Cassandra Gaston for comments that greatly improved the manuscript. This work was funded with a grant from the California Energy Commission and the U.S. Environmental Protection Agency PM Center Grant # R832415.

Chapter 4 contents are part of a manuscript in preparation, Melanie D. Zauscher, John F. Cahill, Kaitlyn J. Suski, Meagan J.K. Moore, Amy P. Sullivan, Jeffrey L. Collett, Kimberly A. Prather, and Gregory C. Roberts; Cloud condensation nuclei properties and aerosol composition in the foothills of California's Sierra Nevada.

4.6 References

Albrecht, B. A. (1989).Aerosols, Cloud Microphysics, and Fractional Cloudiness, *Science*, *245* (4923), 1227-1230.

Andreae, M. O., and Rosenfeld, D. (2008).Aerosol-Cloud-Precipitation Interactions. Part 1. The Nature and Sources of Cloud-Active Aerosols, *Earth Science Reviews*, *89*, 13-41.

Bhave, P. V., Allen, J. O., Morrical, B. D., Fergenson, D. P., Cass, G. R., and Prather, K. A. (2002).A Field-Based Approach for Determining Atofms Instrument Sensitivities to Ammonium and Nitrate, *Environmental Science & Technology*, *36* (22), 4868-4879.

Chow, J. C., Chen, L. W. A., Watson, J. G., Lowenthal, D. H., Magliano, K. A., Turkiewicz, K., and Lehrman, D. E. (2006).Pm2.5 Chemical Composition and Spatiotemporal Variability During the California Regional Pm10/Pm2.5 Air Quality Study (Crpaqs), *Journal of Geophysical Research-Atmospheres*, *111* (D10), 17.

Clarisse, L., Shephard, M. W., Dentener, F., Hurtmans, D., Cady-Pereira, K., Karagulian, F., Van Damme, M., Clerbaux, C., and Coheur, P. F.

(2010).Satellite Monitoring of Ammonia: A Case Study of the San Joaquin Valley, *Journal of Geophysical Research-Atmospheres*, *115*, 15.

Colle, B. A., and Zeng, Y. G. (2004).Bulk Microphysical Sensitivities within the Mm5 for Orographic Precipitation. Part I: The Sierra 1986 Event, *Monthly Weather Review*, *132* (12), 2780-2801.

Creamean, J. M., Ault, A. P., Ten Hoeve, J. E., Jacobson, M. Z., Roberts, G. C., and Prather, K. A. (2011).Measurements of Aerosol Chemistry During New Particle Formation Events at a Remote Rural Mountain Site, *Environmental Science & Technology*, *45* (19), 8208-8216.

Draxler, R. R., and Hess, G. D. (1998).An Overview of the Hysplit 4 Modelling System for Trajectories, Dispersion and Deposition, *Australian Meteorological Magazine*, *47* (4), 295-308.

Furutani, H. F., Dall'osto, M., Roberts, G. C., and Prather, K. A. (2008).Assessment of the Relative Importance of Atmospheric Aging on Ccn Activity Derived from Field Observations, *Atmospheric Environment*, *42*, 3130-3142.

Gard, E., Mayer, J. E., Morrical, B. D., Dienes, T., Fergenson, D. P., and Prather, K. A. (1997).Real-Time Analysis of Individual Atmospheric Aerosol Particles: Design and Performance of a Portable Atofms, *Analytical Chemistry*, *69* (20), 4083-4091.

Givati, A., and Rosenfeld, D. (2004).Quantifying Precipitation Suppression Due to Air Pollution, *Journal of Applied Meteorology*, *43* (7), 1038-1056.

Grubisic, V., Vellore, R. K., and Huggins, A. W. (2005).Quantitative Precipitation Forecasting of Wintertime Storms in the Sierra Nevada: Sensitivity to the Microphysical Parameterization and Horizontal Resolution, *Monthly Weather Review*, *133* (10), 2834-2859.

Gunthe, S. S., Rose, D., Su, H., Garland, R. M., Achtert, P., Nowak, A., Wiedensohler, A., Kuwata, M., Takegawa, N., Kondo, Y., Hu, M., Shao, M., Zhu, T., Andreae, M. O., and Poschl, U. (2011).Cloud Condensation Nuclei (Ccn) from Fresh and Aged Air Pollution in the Megacity Region of Beijing, *Atmospheric Chemistry and Physics*, *11* (21), 11023-11039.

Kammermann, L., Gysel, M., Weingartner, E., and Baltensperger, U. (2010).13-Month Climatology of the Aerosol Hygroscopicity at the Free Tropospheric Site Jungfraujoch (3580 M A.S.L.), *Atmospheric Chemistry and Physics*, *10* (22), 10717-10732.

Khain, A., Ovtchinnikov, M., Pinsky, M., Pokrovsky, A., and Krugliak, H. (2000).Notes on the State-of-the-Art Numerical Modeling of Cloud Microphysics, *Atmospheric Research*, *55* (3-4), 159-224.

Khalizov, A. F., Zhang, R. Y., Zhang, D., Xue, H. X., Pagels, J., and McMurry, P. H. (2009).Formation of Highly Hygroscopic Soot Aerosols Upon Internal Mixing with Sulfuric Acid Vapor, *Journal of Geophysical Research-Atmospheres, 114*.

Laaksonen, A., Hamed, A., Joutsensaari, J., Hiltunen, L., Cavalli, F., Junkermann, W., Asmi, A., Fuzzi, S., and Facchini, M. C. (2005).Cloud Condensation Nucleus Production from Nucleation Events at a Highly Polluted Region, *Geophysical Research Letters*, *32* (6).

Lee, Y. N., Weber, R., Ma, Y., Orsini, D., Maxwell-Meier, K., Blake, D., Meinardi, S., Sachse, G., Harward, C., Chen, T. Y., Thornton, D., Tu, F. H., and Bandy, A. (2003).Airborne Measurement of Inorganic Ionic Components of Fine Aerosol Particles Using the Particle-into-Liquid Sampler Coupled to Ion Chromatography Technique During Ace-Asia and Trace-P, *Journal of Geophysical Research-Atmospheres*, *108* (D23).

Lihavainen, H., Kerminen, V. M., Komppula, M., Hatakka, J., Aaltonen, V., Kulmala, M., and Viisanen, Y. (2003).Production of "Potential" Cloud Condensation Nuclei Associated with Atmospheric New-Particle Formation in Northern Finland, *Journal of Geophysical Research-Atmospheres*, *108* (D24).

Liu, D. Y., Prather, K. A., and Hering, S. V. (2000).Variations in the Size and Chemical Composition of Nitrate-Containing Particles in Riverside, Ca, *Aerosol Science and Technology*, *33* (1), 71-86.

Lohmann, U., and Feichter, J. (2005).Global Indirect Aerosol Effects: A Review, *Atmospheric Chemistry and Physics*, *5*, 715-737.

MacDonald, C. P., McCarthy, M. C., Dye, T. S., Wheeler, N. J. M., Hafner, H. R., and Roberts, P. T. (2006).Transport and Dispersion During Wintertime Particulate Matter Episodes in the San Joaquin Valley, California, *Journal of the Air & Waste Management Association*, *56* (7), 961-976.

Moffet, R. C., Qin, X. Y., Rebotier, T., Furutani, H., and Prather, K. A. (2008).Chemically Segregated Optical and Microphysical Properties of Ambient Aerosols Measured in a Single-Particle Mass Spectrometer, *Journal of Geophysical Research-Atmospheres*, *113* (D12).

Moore, R. H., Cerully, K., Bahreini, R., Brock, C. A., Middlebrook, A. M., and Nenes, A. (2012).Hygroscopicity and Composition of California Ccn During Summer 2010, *Journal of Geophysical Research-Atmospheres*, *117*.

Neubauer, K. R., Johnston, M. V., and Wexler, A. S. (1998).Humidity Effects on the Mass Spectra of Single Aerosol Particles, *Atmospheric Environment*, *32* (14-15), 2521-2529.

Noble, C. A., and Prather, K. A. (1996).Real-Time Measurement of Correlated Size and Composition Profiles of Individual Atmospheric Aerosol Particles, *Environmental Science & Technology*, *30* (9), 2667-2680.

Petters, M. D., and Kreidenweis, S. M. (2007).A Single Parameter Representation of Hygroscopic Growth and Cloud Condensation Nucleus Activity, *Atmospheric Chemistry and Physics*, *7* (8), 1961-1971.

Pierce, J. R., and Adams, P. J. (2009).Uncertainty in Global Ccn Concentrations from Uncertain Aerosol Nucleation and Primary Emission Rates, *Atmospheric Chemistry and Physics*, *9* (4), 1339-1356.

Popovicheva, O. B., Persiantseva, N. M., Kireeva, E. D., Khokhlova, T. D., and Shonija, N. K. (2011).Quantification of the Hygroscopic Effect of Soot Aging in the Atmosphere: Laboratory Simulations, *Journal of Physical Chemistry A*, *115* (3), 298-306.

Ralph, F. M., Sukovich, E., Reynolds, D., Dettinger, M., Weagle, S., Clark, W., and Neiman, P. J. (2010).Assessment of Extreme Quantitative Precipitation Forecasts and Development of Regional Extreme Event Thresholds Using Data from Hmt-2006 and Coop Observers, *Journal of Hydrometeorology*, *11* (6), 1286-1304.

Roberts, G., Mauger, G., Hadley, O., and Ramanathan, V. (2006).North American and Asian Aerosols over the Eastern Pacific Ocean and Their Role in Regulating Cloud Condensation Nuclei, *Journal of Geophysical Research*, *111* (D13205), doi:10.1029/2005JD006661

Roberts, G. C., Day, D. A., Russell, L. M., Dunlea, E. J., Jimenez, J. L., Tomlinson, J. M., Collins, D. R., Shinozuka, Y., and Clarke, A. D. (2010).Characterization of Particle Cloud Droplet Activity and Composition in the Free Troposphere and the Boundary Layer During Intex-B, *Atmospheric Chemistry and Physics*, *10* (14), 6627-6644.

Roberts, G. C., and Nenes, A. (2005).A Continuous-Flow Streamwise Thermal-Gradient Ccn Chamber for Atmospheric Measurements, *Aerosol Science and Technology*, *39*, 206-221.

Rose, D., Gunthe, S. S., Su, H., Garland, R. M., Yang, H., Berghof, M., Cheng, Y. F., Wehner, B., Achtert, P., Nowak, A., Wiedensohler, A., Takegawa, N., Kondo, Y., Hu, M., Zhang, Y., Andreae, M. O., and Poeschl, U. (2011).Cloud Condensation Nuclei in Polluted Air and Biomass Burning Smoke near the Mega-City Guangzhou, China -Part 2: Size-Resolved Aerosol Chemical Composition, Diurnal Cycles, and Externally Mixed Weakly Ccn-Active Soot Particles, *Atmospheric Chemistry and Physics*, *11* (6), 2817-2836.

Rose, D., Nowak, A., Achtert, P., Wiedensohler, A., Hu, M., Shao, M., Zhang, Y., Andreade, M. O., and Poschl, U. (2010).Cloud Condensation Nuclei in Polluted

Air and Biomass Burning Smoke near the Mega-City Guangzhou, China - Part 1: Size Resolved Measurements and Implications for Modeling of Aerosol Particle Hygroscopicity and Ccn Activity, *Atmospheric Chemistry and Physics*, *10* (7), 3365-3383.

Rosenfeld, D., Woodley, W. L., Axisa, D., Freud, E., Hudson, J. G., and Givati, A. (2008).Aircraft Measurements of the Impacts of Pollution Aerosols on Clouds and Precipitation over the Sierra Nevada, *Journal of Geophysical Research-Atmospheres*, *113* (D15).

Silva, P. J., Liu, D., Noble, C. A., and Prather, K. A. (1999).Size and Chemical Characterization of Individual Particles Resulting from Biomass Burning of Local Southern California Species, *Environmental Science & Technology*, *33* (18), 3068-3076.

Solomon, S., Qin, D., Manning, M., Chen, Z., Marquis, M., Averyt, K. B., Tignor, M., and Miller, H. L. (2007). Climate Change 2007: The Physical Science Basis. Contribution of Working Group I to the Fourth Assessment Report of the Intergovernmental Panel on Climate Change, Cambridge, United Kingdom and New York, USA.

Song, X. H., Hopke, P. K., Fergenson, D. P., and Prather, K. A. (1999).Classification of Single Particles Analyzed by Atofms Using an Artificial Neural Network, Art-2a, *Analytical Chemistry*, *71* (4), 860-865.

Sorooshian, A., Murphy, S. N., Hersey, S., Gates, H., Padro, L. T., Nenes, A., Brechtel, F. J., Jonsson, H., Flagan, R. C., and Seinfeld, J. H. (2008).Comprehensive Airborne Characterization of Aerosol from a Major Bovine Source, *Atmospheric Chemistry and Physics*, *8* (17), 5489-5520.

Spracklen, D. V., Carslaw, K. S., Poschl, U., Rap, A., and Forster, P. M. (2011).Global Cloud Condensation Nuclei Influenced by Carbonaceous Combustion Aerosol, *Atmospheric Chemistry and Physics*, *11* (17), 9067-9087.

Stoelinga, M. T., Hobbs, P. V., Mass, C. F., Locatelli, J. D., Collie, B. A., Houze, R. A., Rangno, A. L., Bond, N. A., Smull, B. F., Rasmussen, R. M., Thompson, G., and Colman, B. R. (2003).Improvement of Microphysical Parameterization through Observational Verification Experiment, *Bulletin of the American Meteorological Society*, *84* (12), 1807-+.

Tritscher, T., Juranyi, Z., Martin, M., Chirico, R., Gysel, M., Heringa, M. F., DeCarlo, P. F., Sierau, B., Prevot, A. S. H., Weingartner, E., and Baltensperger, U. (2011).Changes of Hygroscopicity and Morphology During Ageing of Diesel Soot, *Environmental Research Letters*, *6* (3).

Twomey, S. (1977).Influence of Pollution on Shortwave Albedo of Clouds, *Journal of the Atmospheric Sciences*, *34* (7), 1149-1152.

Wang, J., Cubison, M. J., Aiken, A. C., Jimenez, J. L., and Collins, D. R. (2010).The Importance of Aerosol Mixing State and Size-Resolved Composition on Ccn Concentration and the Variation of the Importance with Atmospheric Aging of Aerosols, *Atmospheric Chemistry and Physics*, *10* (15), 7267-7283.

Watson, J. G., and Chow, J. C. (2002).A Wintertime Pm2.5 Episode at the Fresno, Ca, Supersite, *Atmospheric Environment*, *36* (3), 465-475.

Weber, R. J., Orsini, D., Daun, Y., Lee, Y. N., Klotz, P. J., and Brechtel, F. (2001).A Particle-into-Liquid Collector for Rapid Measurement of Aerosol Bulk Chemical Composition, *Aerosol Science and Technology*, *35* (3), 718-727.

Weingartner, E., Burtscher, H., and Baltensperger, U. (1997).Hygroscopic Properties of Carbon and Diesel Soot Particles, *Atmospheric Environment*, *31* (15), 2311-2327.

Wexler, A. S., and Clegg, S. L. (2002).Atmospheric Aerosol Models for Systems Including Ions H+, Nh4+, Na+, So42-, No3-, Cl-, Br- and H2o, *Journal of Geophysical Research*, *107* (D14), 4207.

Ying, Q., and Kleeman, M. (2009).Regional Contributions to Airborne Particulate Matter in Central California During a Severe Pollution Episode, *Atmospheric Environment*, *43* (6), 1218-1228.

Zauscher, M. D., Suski, K. J., Cahill, J. F., Hatch, L. E., Sullivan, A. P., Collett, J. L., and Prather, K. A. (2012).Quantitative Comparison and Aerosol Mixing State in the Western California Sierra Nevada Foothills During Pollution Transport Events in Winter 2010, *In prep*.

Zaveri, R. A., Barnard, J. C., Easter, R. C., Riemer, N., and West, M. (2010).Particle-Resolved Simulation of Aerosol Size, Composition, Mixing State, and the Associated Optical and Cloud Condensation Nuclei Activation Properties in an Evolving Urban Plume, *Journal of Geophysical Research-Atmospheres*, *115*, 19.

Zuberi, B., Johnson, K. S., Aleks, G. K., Molina, L. T., and Laskin, A. (2005).Hydrophilic Properties of Aged Soot, *Geophysical Research Letters*, *32* (1).

Chapter 5. Mixing state and aging of individual biomass burning aerosols during the 2007 San Diego Wildfires

Biomass burning aerosols (BBA) affect regional air quality, human health, and climate. The goals of this opportunistic study during the 2007 San Diego Wildfires, which burned > 360,000 acres, were to determine the impact of wildfires on local air quality and analyze BBA aging. Size-resolved mixing state of individual particles was measured in real-time with an ultrafine aerosol time-of-flight mass spectrometer (ATOFMS). This is the first analysis of BBA aging during local wildfires via single-particle mass spectrometry. Particulate mass concentrations were high county-wide due to BBA, with 84% of 120-400 nm particles by number being BBA, with maximum $PM_{0.4}$ = 148 $\mu g/m^3$. Results from single particle analysis and positive matrix factorization (PMF) of BBA chemical markers are discussed. For example, potassium chloride (KCl), indicative of fresh BBA, was only seen at the beginning of the wildfires when the size mode of particles was <120 nm. Evidence of heterogeneous reactions between potassium salts with nitric and sulfuric acids resulting in potassium nitrate (KNO_3) and potassium sulfate (K_2SO_4) was observed for the first time with continuous high temporal resolution. Knowledge of how BBA mixing state evolves is important for determining the climate and health impacts of wildfires.

5.1 Introduction

Biomass burning leads to substantial atmospheric emissions of trace gases and high number and mass concentrations of biomass burning aerosols (BBA), which significantly impact air quality, human health, and climate on regional scales (Andreae and Merlet, 2001; Crutzen and Andreae, 1990; Reid et al., 2005). BBA have been associated with respiratory and cardiovascular symptoms (Arbex et al., 2007; Arbex et al., 2010) including during the 2003 Southern California wildfires when increased $PM_{2.5}$ concentrations were correlated to increased emergency room visits for asthma and other respiratory problems (Delfino et al., 2009; Kunzli et al., 2006; Viswanathan et al., 2006). In addition, BBA perturb climate by scattering and absorbing solar radiation and by serving as cloud condensation and ice nuclei (Crutzen and Andreae, 1990; Grell et al., 2011; Penner et al., 1992; Petters et al., 2009a; Petters et al., 2009b; Roberts et al., 2003). To understand the full range of environmental impacts of BBA particle mixing state is needed (Furukawa and Takahashi, 2011; Jacobson, 2001; Lighty et al., 2000; Pratt et al., 2010; Zhou et al., 2003); however, the majority of previous biomass burning studies have focused on bulk aerosol properties (Reid et al., 2005).

The physicochemical properties of freshly emitted BBA change rapidly due to evolution in flame conditions and as a result of the interactions of BBA with gas phase species in the biomass burning plume and other regional pollutants as the plume becomes diluted and mixed. Furthermore, photochemical reactions, cloud processing, and coagulation are important pathways in transforming BBA. These processes cause the diameter of fresh BBA to grow from ~100-160 nm to ~120-230 nm (Reid et al., 2005). The composition of BBA depends strongly on fire type. The hotter flaming fires produce particles containing higher fractions of inorganic material, including potassium (K) along with increased soot content, while the lower temperature smoldering fires emit more organic carbon rich aerosol (Allen and Miguel, 1995; Posfai et al., 2003; Reid et al., 2005; Yamasoe et al., 2000). However, the chemical composition of BBA is also transformed through aging processes. Fresh BBA are characterized by potassium chloride (KCl) salts, which heterogeneously react with secondary acids, such as nitric

acid ($HNO_{3(g)}$) and sulfuric acid ($H_2SO_{4(g)}$) (Gaudichet et al., 1995; Li et al., 2003); thus as the BBA ages, KCl is replaced with potassium nitrate (KNO_3) and potassium sulfate (K_2SO_4). In addition to K, levoglucosan, which is emitted directly from the thermal breakdown of cellulose, is an established tracer for BBA (Fraser and Lakshmanan, 2000; Simoneit et al., 1999). However, recent studies have determined that the amount of levoglucosan produced during biomass burning depends on fuel and fire type (Gao et al., 2003; Hedberg and Johansson, 2006; Mazzoleni et al., 2007; Sullivan et al., 2008) and have shown levoglucosan decomposes through photo-oxidation, exposure to hydroxyl radical and oligomerization (Hennigan et al., 2011; Hennigan et al., 2010; Holmes and Petrucci, 2006); thus levoglucosan may not be as robust a biomass burning tracer as originally postulated. Water soluble organic carbon species, such as oxalic acid, are also of interest in BBA since their presence may affect the CCN activity of particles (Furukawa and Takahashi, 2011; Pratt et al., 2010; Sullivan and Prather, 2007; Yu, 2000). Thus, there is a need to characterize both freshly emitted BBA and the evolution of composition of these particles as they are processed in the atmosphere, and to identify stable makers that can be used to accurately differentiate BBA from other particles.

For the past few decades, the frequency of wildfires and land area burned has increased in the western U.S. due to regional warming, earlier spring arrival, and increased droughts (Park et al., 2007; Westerling et al., 2006). Between 2001-2004, ~30% of the annual $PM_{2.5}$ in the western U.S. originated from biomass burning (Park et al., 2007). Specifically, southern California experienced major wildfire seasons recently in 2003 and 2007, where the majority of the landscape burned was chaparral shrublands (Clinton et al., 2006; Keeley et al., 2004; Keeley et al., 2009). During the 2003 Southern California Wildfires, which burned > 742,000 acres, PM_{10} increased 3-4 times compared to non-fire conditions (Keeley et al., 2004; Phuleria et al., 2005).

In October 2007, wildfires burned > 360,000 acres in San Diego County releasing large concentrations of particulate matter and gases into the atmosphere (EG&G Technical Services, 2007). The rapid and dry easterly Santa Ana winds

contributed to the propagation of the wildfires. Estimated perimeters of the wildfires are shown in Figure 5.1. The goals of this study were to investigate the impact of the 2007 San Diego Wildfires on regional air quality and to analyze the aging of individual BBA. Single particle sampling during urban wildfires this intense has not been done previously. Positive matrix factorization (PMF) and single particle analysis were utilized to associate different primary and secondary chemical markers of BBA in order to try to identify formation mechanisms for some of these markers. To our knowledge, this is the first study that uses positive matrix factorization analysis to investigate the

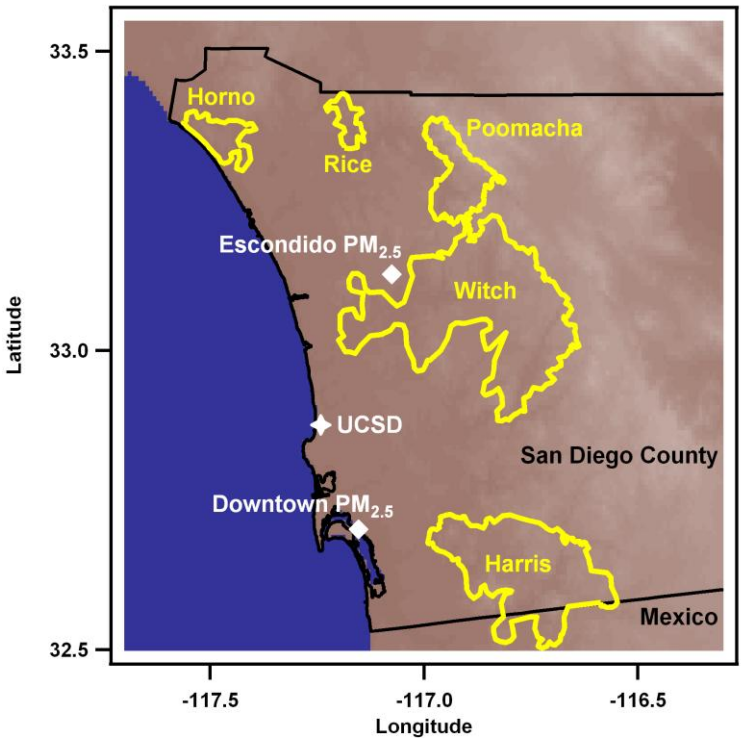

Figure 5.1: Map of wildfire perimeters in San Diego County, October, 2007 and sampling sites. Aerosol physiochemical properties were measured at the University of California San Diego (UCSD). Gas phase and particulate matter mass concentrations were obtained from the California Air Resources Board (CARB) while meteorological data was obtained from the California Irrigation Management Information System (CIMIS), respectively.

chemical evolution of single-particles from the same source.

5.2 Experimental Section

Ambient aerosol sampling was conducted at Urey Hall (32°52'31.66"N, 117°14'28.64"W) at the University of California, San Diego (UCSD) from 10/22/07 12:00 - 11/01/07 12:00. Given the opportunistic nature of this study, measurements commenced one day after the Witch fire began (10/21/07 11:00). All times are given in local time (PDT). During the first week of the fires, the public was urged to stay home and most public institutions and private businesses were closed (EG&G Technical Services, 2007); therefore the contribution of aerosols from mobile sources was primarily limited to emergency vehicles during this time.

5.2.1 Peripheral Instrumentation

The size distributions of 10-590 nm and 0.6-20 μm particles were measured every five minutes with a scanning mobility particle sizer (SMPS, TSI 3936) and every minute with an aerodynamic particle sizer (APS, TSI, 3321) at UCSD. Hourly concentrations of $PM_{2.5}$ mass were obtained from the California Air Resources Board (CARB) for Escondido and downtown San Diego sites. The SMPS and APS size resolved concentrations measured at UCSD were transformed into $PM_{2.5}$, $PM_{1.0}$ and $PM_{0.12\text{-}0.4}$ mass concentrations, assuming spherical particles with density of 1.2 g/cm^3, appropriate for BBA (Reid et al., 2005). Meteorological data were obtained from the California Irrigation Management Information System (CIMIS) network at three different sites: Escondido, downtown San Diego, and Torrey Pines. All the sampling sites are identified in Figure 5.1. Escondido, downtown San Diego, and Torrey Pines sites are ~30, 20 and 3 km away from UCSD, respectively.

5.2.2 ATOFMS Instrument and Data Analysis

Individual particle size (120-1000 nm) and composition measurements were obtained in real-time with an ultrafine aerosol time of flight mass spectrometer (ATOFMS), without the MOUDI pre-cut (Su et al., 2004). Briefly, particles enter the ATOFMS through an aerodynamic focusing lens and are accelerated to their size-dependent terminal velocities before traversing two 532 nm continuous wave lasers

beams 6-cm apart. The determined particle velocity is used to time the firing of a Q-switched 266 nm laser, which desorbs and ionizes the chemical constituents of each particle. The generated positive and negative ions are detected using a dual polarity reflectron time-of-flight mass spectrometer.

Although 120-1000 nm particles were sampled with the ATOFMS, only 120-400 nm particles were analyzed herein due to the prevalence of BBA in this size range. Mass spectra were obtained for a total of 900,143 particles in the 120-400 nm aerodynamic diameter size range. The mass spectra were analyzed in the YAADA (http://www.yaada.org) toolkit for Matlab and were subsequently clustered with the neural network algorithm ART-2a, which separates the main particle types into clusters based on their unique ion patterns (Song et al., 1999). Parameters used in ART-2a were: vigilance factor of 0.85, learning rate of 0.05 and iteration number of 20. The particle clusters were named based on the most intense ion peaks detected and do not necessarily reflect all of the chemical species present. Clusters of similar ion patterns of varying intensities were manually combined, resulting in a total of 4 major classes previously identified: BBA (Guazzotti et al., 2003; Silva et al., 1999), heavy fuel oil (HFO) (Ault et al., 2010; Healy et al., 2009), organic carbon (OC) (Silva and Prather, 2000; Spencer and Prather, 2006), and soot (Spencer and Prather, 2006; Toner et al., 2006).

The identified peaks at each m/z were based on the most likely assignment. Due to ambiguity and interference, several markers could not be used in this study. The most intense peak in BBA is from the potassium ion, $^{39}K^+$. Although the +39 m/z could also the $^{39}C_3H_3^+$ organic marker, the majority of it is likely to be from $^{39}K^+$ due to its high ionization potential and known large emissions during biomass burning (Andreae, 1983;

Table 5.1: The 20 BBA markers used in this study.

Species	Marker
Ammonium	$^{18}NH_4^+$
Organic carbon fragment	$^{27}C_2H_3^+$
Organic carbon fragment	$^{43}C_2H_3O^+$
Amine fragment	$^{86}(C_2H_5)_2NCH_2^+$
Potassium chloride	$^{113}K_2Cl^+$
Potassium nitrate	$^{140}K_2NO_3^+$
Potassium bisulfate	$^{175}K_2HSO_4^+$
Potassium sulfate	$^{213}K_3SO_4^+$
Organic nitrogen fragment	$^{26}CN^-$
Organic nitrogen fragment	$^{42}CNO^-$
Nitrite	$^{46}NO_2^-$
Acetate	$^{59}CH_3COO^-$
Nitrate	$^{62}NO_3^-$
Acrylate or Methylglyoxyl	$^{71}C_3H_3O_2^-$
Glyoxylate or Propanoate	$^{73}C_2HO_3^-/C_3H_5O_2^-$
Glycolate	$^{75}C_2H_3O_3^-$
Pyruvate	$^{87}C_3H_3O_3^-$
Oxalate	$^{89}HC_2O_4^-$
Bisulfate	$^{97}HSO_4^-$
Nitric Acid	$^{125}HNO_3NO_3^-$

Gross et al., 2000; Silva et al., 1999). It should be noted that the strong signal at $^{39}K^+$ on BBA often causes distinct cross talk interference in the negative mass spectra between -

33 – -38 m/z. Thus due to the prevalence of cross talk, the chloride ions ($^{35,37}Cl^-$) were not utilized in this study. In addition, due to significant interference of nitrite ($^{46}NO_2^-$) from its intense broad peak, the formate ion ($^{45}HCO_2^-$) was not utilized in this analysis either.

The relative peak areas (RPA), defined as the normalized peak area of one ion to the sum of all peak areas in the whole mass spectrum, minimizes the variability in peak intensity compared to absolute peak areas in particles of the same matrix (Gross et al., 2000). The average RPA of 120-400 nm BBA were determined for 20 markers listed in Table 5.1, including common species observed by the ATOFMS, such as nitrate ($^{62}NO_3^-$), sulfate ($^{97}HSO_4^-$), ammonium ($^{18}NH_4^+$) and hydrogen oxalate ($^{89}HC_2O_4^-$) (Moffet et

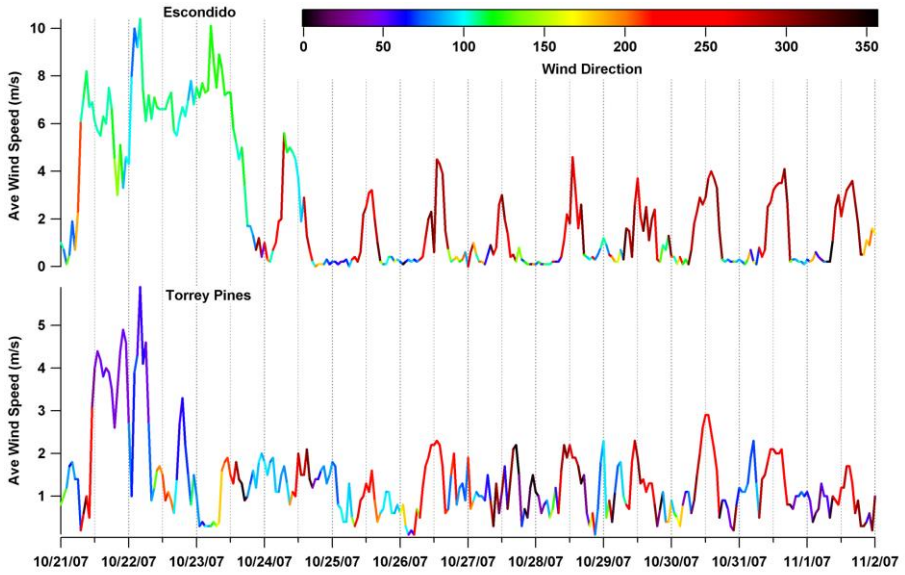

Figure 5.2: Wind Patterns from Escondido and Torrey Pines sites through the CIMIS network.

al., 2008; Noble and Prather, 1996; Pratt et al., 2011; Sullivan and Prather, 2007; Yang et al., 2009), in addition to potassium chloride ($^{113}K_2Cl^+$), potassium nitrate ($^{140}K_2NO_3^+$) and potassium sulfate ($^{213}K_3SO_4^+$), which have been previously identified in biomass burning studies (Pratt et al., 2011; Silva et al., 1999). The average RPA were determined independently every 15 minutes and by particle size every 10 nm.

5.2.3 Positive Matrix Factorization Analysis

In order to complement single particle data analysis, positive matrix factorization (PMF) of the chemical markers was also performed. A multivariate receptor model that implicitly assumes temporally covarying species have the same origin, PMF is used to determine source factors (Kim et al., 2003; Polissar et al., 1998; Reff et al., 2007). PMF has been used extensively with aerosol data, typically with speciated mass concentrations, although it has also been used with ATOFMS data previously (Eatough et al., 2008; Healy et al., 2010; McGuire et al., 2011). These previous studies with ATOFMS data used PMF to elucidate source emissions, chemical processing and transport of particle types determined with the ATOFMS. In contrast, this current study focuses on the aging and evolution of the mixing state of BBA. The Environmental Protection Agency's (USEPA) PMF 3.0 model (USEPA, 2008) was used to generate source factors based on the 15 minute averaged RPAs for the 20 primary and secondary BBA markers in Table 5.1. These species were utilized because

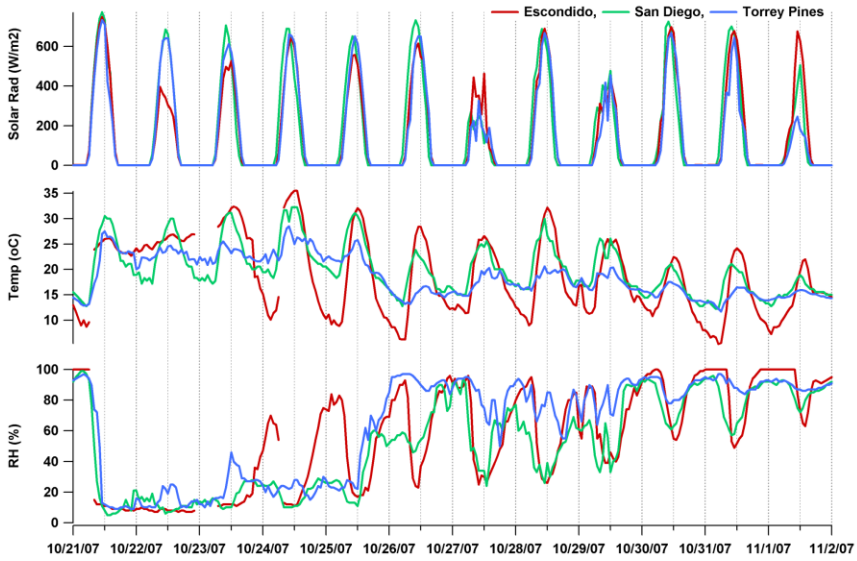

Figure 5.3: Meteorological data from Escondido, San Diego and Torrey Pines sites through the CIMIS network.

of their relevance in biomass burning and abundance during the 2007 San Diego Wildfires. Previous ATOFMS particle type counts used in PMF has been assigned an uncertainty of 15% (Eatough et al., 2008; Healy et al., 2010). For this study, the 15%

uncertainty was doubled in order to apply it to RPA since the ATOFMS laser shot-to-shot fluctuations may affect the resulting individual mass spectra peaks more than the determined particle types. PMF solutions with 3-13 factors were explored, and the 11 factor solution was chosen as the best one because the measured versus predicted RPA of chemical species in the PMF model had the strongest correlations (R^2 = 0.94-0.99) while providing the most physically meaningful factors (Reff et al., 2007; USEPA, 2008). Further details considered during data preparation and PMF analyses are given in the supporting information.

5.3 Results and Discussion

Figure 5.2 and Figure 5.3 show the wind speed and direction, temperature, relative humidity and solar radiation during this study. Intense easterly Santa Ana winds were observed during the first two days of the study (10/21/07-10/23/07 16:00) in conjunction with high temperature, low humidity, and fast wind speed. This period

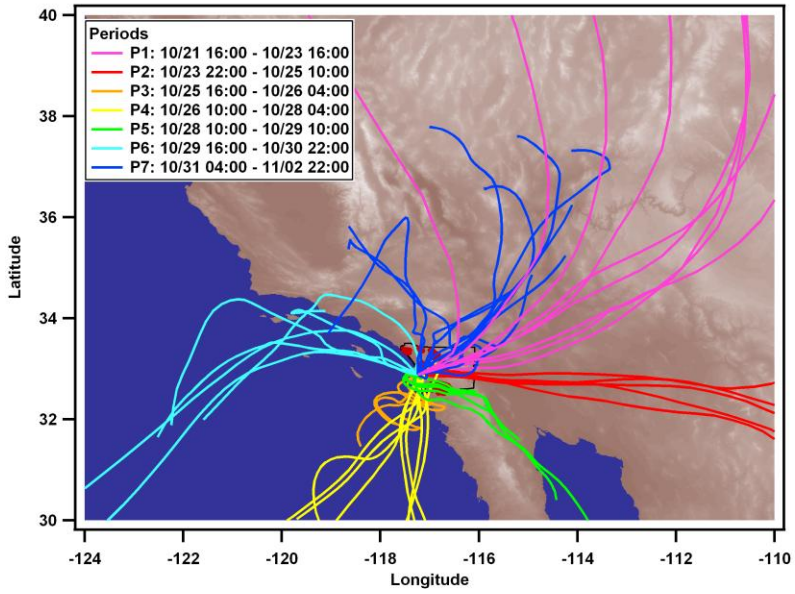

Figure 5.4: Air mass back trajectories during study determined using HYSPLIT at 1000 m altitude.

exhibited the most active wildfires, which were propagated by the Santa Ana winds towards the more populated western side of San Diego County. The air mass back

trajectories modeled with HYSPLIT 4.0 (Draxler and Hess, 1998), shown in Figure 5.4, indicate that during the intense Santa Ana winds, UCSD was directly downwind of the Witch fire, the largest fire during the study. Following this period, the winds shifted so that the air mass back trajectories originated further south and did not pass over dense wildfire emissions. The wildfire emissions flowed offshore until the afternoon of 10/25 (Figure 5.5), when the wind shifted again originating slightly offshore, although remaining fairly stagnant; the relative humidity (RH) remained low (<45%) at Torrey Pines until this time when it increased to > 90%. Between 10/26 10:00 and 10/28 4:00 the air continued to flow onshore but from further away. During this period, there was a significant fog event on 10/27/07, which limited the amount of solar radiation (Figure 5.3). During 10/28 10:00 – 10/29 10:00, the air masses sampled passed above the Harris fire, which burned along the border with Mexico. Towards the end of the study, between 10/29 16:00 - 10/30 22:00, the air mass sampled at UCSD passed close to the Ports of Los Angeles and Long Beach bringing aged BBA onshore possibly mixed with ocean faring ship and port emissions. Finally, after 10/31 the air came through Riverside, California.

5.3.1 Peripheral Data

Figure 5.5: MODIS image from 10/23/10 11:45. Red dots indicate active fires.

Figure 5.6 shows the SMPS size distribution as a function of size and time. The highest particle concentrations were between 60-400 nm during the most intense wildfire period between 10/22/07-10/23/07 confirming this was a period when UCSD received the most wildfire emissions. Specifically, there was a spike in SMPS 120-400 nm particle number concentrations on 10/22/07 20:00-22:00 going from ~10,000 to ~40,000 cm^{-3} and back to ~10,000 cm^{-3}. Additionally, the mode of the particles shifted rapidly on 10/22/07-10/23/07 (Figure 5.6) increasing from ~100 to ~170 nm between 10/22/07 10:00-18:00, decreasing back to ~100 nm by 10/22/07 23:00. The mode increased again from 10/22/07 23:00 to 10/23/07 9:00, at which time the size mode remained stable at ~140 nm. The size mode decreased to ~100 nm on the morning of 10/25/07 and then increased to ~180 nm coinciding with the increase of RH on the afternoon of 10/25/07. After 10/27/07, the effects of wildfires were less evident on the particle size distributions and periodically an ultrafine mode was observed, indicative of local traffic emissions. The observed particle diameter modes of 100-180 nm at the beginning of this study are comparable to the range of previously measured BBA between 100-230 nm depending on their age (Muhle et al., 2007; Phuleria et al., 2005; Reid et al., 2005). The broad size range observed indicates BBA were physicochemically processed to different degrees during transport from the wildfires to the sampling site at UCSD or alternatively that flaming versus smoldering took place during burning (Hossain et al., 2012). Detailed analysis linking chemical markers of fresh and aged BBA with the shifts in size distribution are described below.

Figure 5.6 shows the $PM_{2.5}$ measured at Escondido and downtown San Diego along with the estimated mass concentrations from UCSD. Overall, the $PM_{2.5}$ concentrations were higher at Escondido than at UCSD and downtown, due to the proximity of the Witch and Poomacha fires to the Escondido site (Figure 5.1). However, the national air quality air standard (NAAQS) 24-hour average $PM_{2.5}$ exposure limit of 35 $\mu g/m^3$ was exceeded at all sites, with hourly maximum values as high as 397, 177, and 110 $\mu g/m^3$ at Escondido, UCSD, and downtown, respectively. Because of the variability and extreme values in mass concentrations during the wildfires, median values were more appropriate than the mean. During 10/22/07-10/23/07 16:00, when

the wildfires were most intense and air mass trajectories passed through the Witch fire before arriving at UCSD, the $PM_{2.5}$ concentrations were the highest county-wide with median (interquartile range) values of 72.0 (43.0-186.0), 47.6 (35.1-61.7), and 42.0 (29.5-48.3) $\mu g/m^3$ at Escondido, UCSD, and downtown, respectively. In contrast, the annual 2007 average $PM_{2.5}$ concentrations were 15.0 ± 17.5 and 10.9 ± 9.1 $\mu g/m^3$ at Escondido and downtown. Therefore, the 2007 wildfires emitted high fine aerosol mass concentrations dangerous to public health to communities downwind of the wildfires. Compared to other times during this study, estimated $PM_{1.0}$ and $PM_{0.1\text{-}0.4}$ from particle size concentrations at UCSD were also the highest throughout the period of intense wildfires (10/22/07-10/23/07 16:00) with median (interquartile range) values of 44.5 (30.9-56.3) and 37.7 (26.6-48.5), and maximum values of 168, and 148 $\mu g/m^3$, respectively. The majority of particle mass was due to particles < 400 nm. For example, during the period of intense wildfires total $PM_{0.1\text{-}0.4}$ mass concentrations contributed to 81.2% of the $PM_{2.5}$ and 87.5% of $PM_{1.0}$ at UCSD. This is contrary to normal ambient aerosols in which larger particles contribute the majority of particle mass, an important observation since particle size can play a role in adverse health effects (Ramgolam et al., 2009; Schwartz and Neas, 2000; Stoelzel et al., 2007).

Muhle et al (2007) estimated $PM_{2.5}$ concentrations at UCSD during the 2003 wildfires as high as 250 $\mu g/m^3$, higher concentrations than those estimated during the 2007 wildfires. The higher $PM_{2.5}$ concentrations in 2003 were due to different fire and meteorological conditions, in addition to fire proximity. Previous measurements during a Santa Ana event at UCSD's Scripps Institution of Oceanography (SIO) pier determined that 30 minute-averaged $PM_{2.5}$ was only 7 $\mu g/m^3$ (Guazzotti et al., 2001), indicating that the high mass concentrations observed during the 2003 and 2007 wildfires were not caused by the Santa Ana event alone, but rather by the wildfires themselves. In contrast, the estimated $PM_{1.0}$ was as high as 30 $\mu g/m^3$ during a previous period of pollution transport from the ports of Los Angeles and Long Beach to the SIO pier (Ault et al., 2009). Therefore, large wildfires, with maximum $PM_{1.0}$ concentrations of 177 and 250 $\mu g/m^3$ during 2007 and 2003 wildfires, can contribute > 5 times higher

submicron aerosol mass concentrations than regional pollution transport events in San Diego.

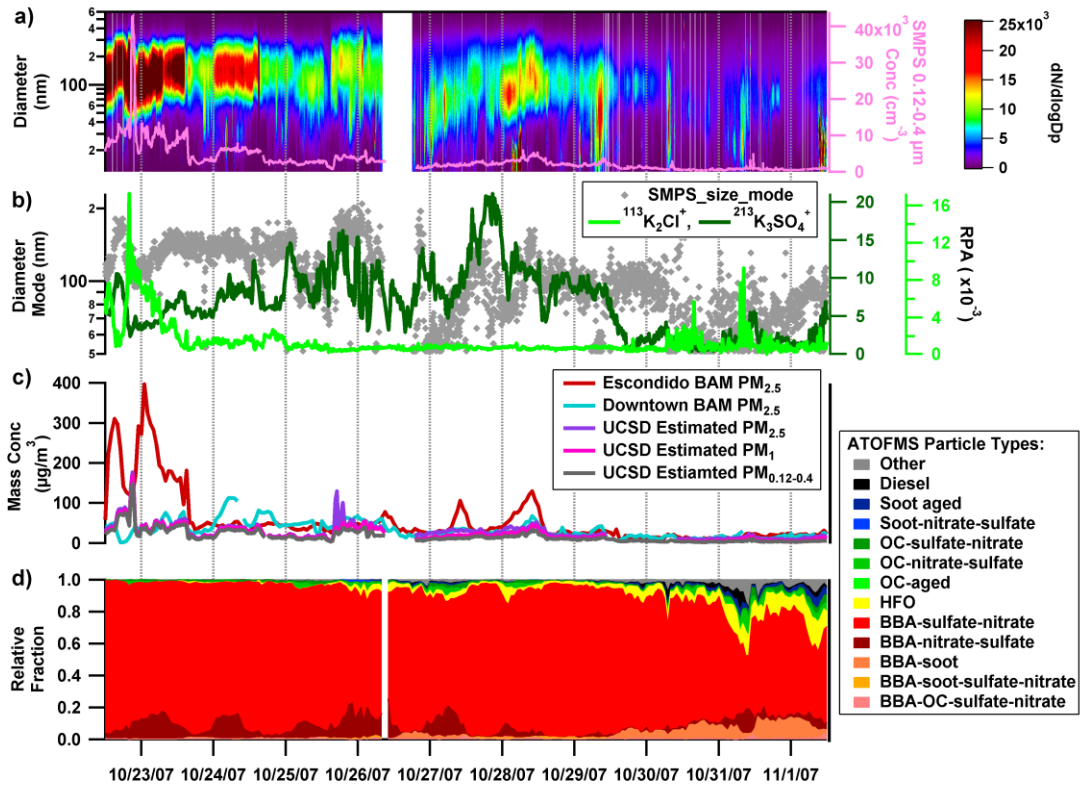

Figure 5.6: a) 10-600 nm ambient particle size distribution from SMPS , b) SMPS mode diameter with $^{113}K_2Cl^+$ and $^{213}K_3SO_4^+$, c) mass concentrations, and d) temporal distribution of 120-400 nm ambient particle types measured with the ATOFMS. White space indicates no data obtained in that time period.

5.3.2 Particle Types and Mixing State of BBA

Figure 5.6 shows the temporal variation of particle types between 120-400 nm. In addition to BBA, the main particles types observed were OC, soot, and HFO. After 10/30/07, OC (green) and soot (blue) begin to grow in. The HFO particle type, emitted from combusting HFO in ocean-faring ships, became more prevalent after 10/31/07. Because the remaining particle types were made up < 2% of particle numbers, they were combined into the "other" category.

Although all BBA mass spectra have similar characteristics, including $^{39}K^+$ and carbonaceous markers (Silva et al., 1999), five different BBA particle types were observed in this study based on the strength of the carbonaceous markers, $^{62}NO_3^-$, and $^{97}HSO_4^-$, with mass spectra shown in Figure 5.7. The BBA-sulfate-nitrate particle type, where the $^{97}HSO_4^-$ ion peak intensity was slightly greater than that of $^{62}NO_3^-$, was present throughout the study and represented 91% of all BBA. The BBA-nitrate-sulfate particle type, which contained more intense $^{62}NO_3^-$ than $^{97}HSO_4^-$ peaks, contributed 6% to all BBA by number. As shown in Figure 5.6, BBA-nitrate-sulfate peaked in the day probably due to the photochemical formation of nitrate. The BBA-soot particle type, which only contributed ~1% to all BBA numbers, had moderately intense $^{12n}C_n^+$ peaks, and was more prevalent during the last 3 days of the study. Perhaps, during this time there was coagulation and cloud processing of BBA with combustion particles from the LA and LB ports and Riverside. The lack of negative mass spectra in the BBA-soot particle type supports that these were wet, and thus aged particles (Neubauer et al., 1998). The BBA-soot-sulfate-nitrate had similar positive mass spectra as the BBA-soot type, but with peaks at $^{97}HSO_4^-$ and $^{62}NO_3^-$. The BBA-OC-sulfate-nitrate particle type had moderately intense OC peaks, such as $^{27}C_2H_3^+$ and $^{43}C_2H_3O^+$, with a very intense $^{97}HSO_4^-$ peak. The BBA-OC-sulfate-nitrate and the BBA-soot-sulfate-nitrate particle type made up only 0.6 and 0.4% of all BBA particles, respectively. Previous single particle aerosol mass spectrometer studies have also identified different BBA particle types during ambient measurements (Bi et al., 2011; McGuire et al., 2011). Combining all of the BBA particle types together, BBA represented ~84% of all particle numbers sampled during this study, although nearly 100% of all particles were BBA until 10/25/07.

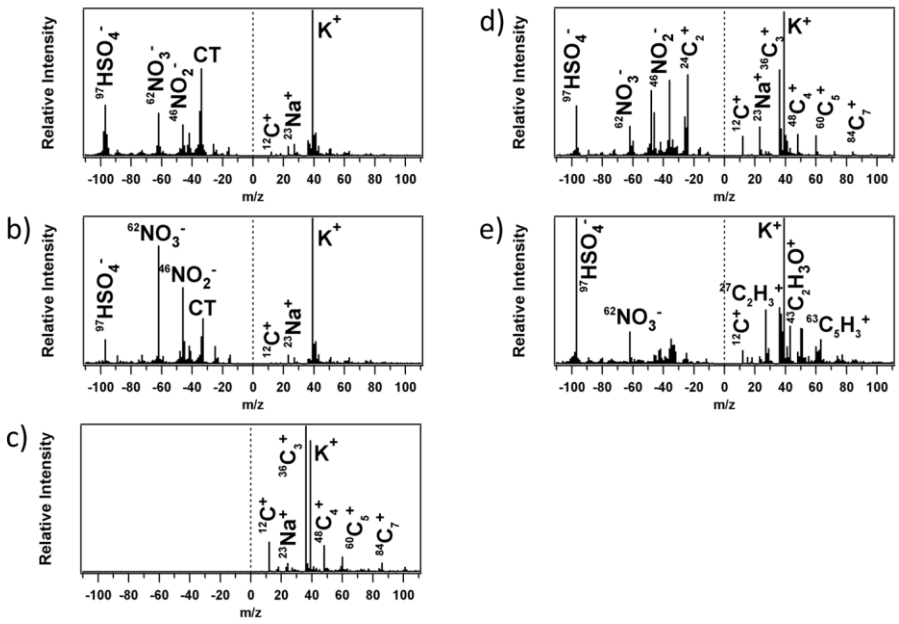

Figure 5.7: Mass spectra of the different types of 100-400nm particles types detected during 2007 San Diego Wildfires: a) BB sulfate nitrate, b) BB nitrate sulfate, c) BB soot, d) BB soot sulfate nitrate, and e) BB OC sulfate nitrate. CT refers to cross talk interference.

It should be noted that since the BBA were not sampled directly above the wildfires, but after their transport to UCSD; the particles sampled in this study were aged to various degrees. A known marker for fresh BBA, $^{113}K_2Cl^+$ (Li et al., 2003; Liu et al., 2000; Posfai et al., 2003) peaked on 10/22/07 when particles with the smallest SMPS size mode (~100 nm) were detected indicating the presence of fresh BBA (Figure 5.6). However, when the SMPS size mode increased to ~170 nm, also on 10/22/07, $^{113}K_2Cl^+$ decreased while $^{213}K_3SO_4^+$ increased, thus indicating these were more aged BBA; therefore confirming the use of these chemical markers to determine the aging of BBA. Potassium salts were prevalent in most BBA with > 50, 60 and 70% of BBA having $^{140}K_2NO_3^+$, $^{113}K_2Cl^+$, and $^{213}K_3SO_4^+$, respectively. Potassium salts were found to be internally mixed together in 43, 52 and 49% of BBA as $^{113}K_2Cl^+$ and $^{140}K_2NO_3^+$, $^{113}K_2Cl^+$ and $^{213}K_3SO_4^+$, and $^{140}K_2NO_3^+$ and $^{213}K_3SO_4^+$, respectively; 36% of BBA had all three potassium salts internally mixed.

In this study, BBA were internally mixed with either $^{62}NO_3^-$ or $^{97}HSO_4^-$, both acidic species, in roughly equal percentages by number (82 versus 80%), within the range of previous observations (21-100% and 92-100%, respectively) (Pratt et al., 2010; Pratt et al., 2011). Furthermore, 73% of BBA by number had $^{97}HSO_4^-$ and $^{62}NO_3^-$ internally mixed together. The occurrence of the $^{125}HNO_3NO_3^-$ peak, which may indicate the presence of nitric acid, was found on almost half of the BBA sampled and was more intense on 10/25/07 coincident with increased RH. Previous studies have observed 21-59% of BBA number fraction internally mixed with $^{125}HNO_3NO_3^-$ (Pratt et al., 2011). 69% of BBA were internally mixed with oxalate, a weak acid, in contrast with 28-94% in previous studies (Moffet et al., 2008; Pratt et al., 2010; Pratt et al., 2011). $^{18}NH_4^+$, which is basic, was found on 76% of BBA particle numbers, whereas previous studies have only detected $^{18}NH_4^+$ internally mixed in 8-58% of BBA (Pratt et al., 2010; Pratt et al., 2011). In addition, 76% of BBA were internally mixed with

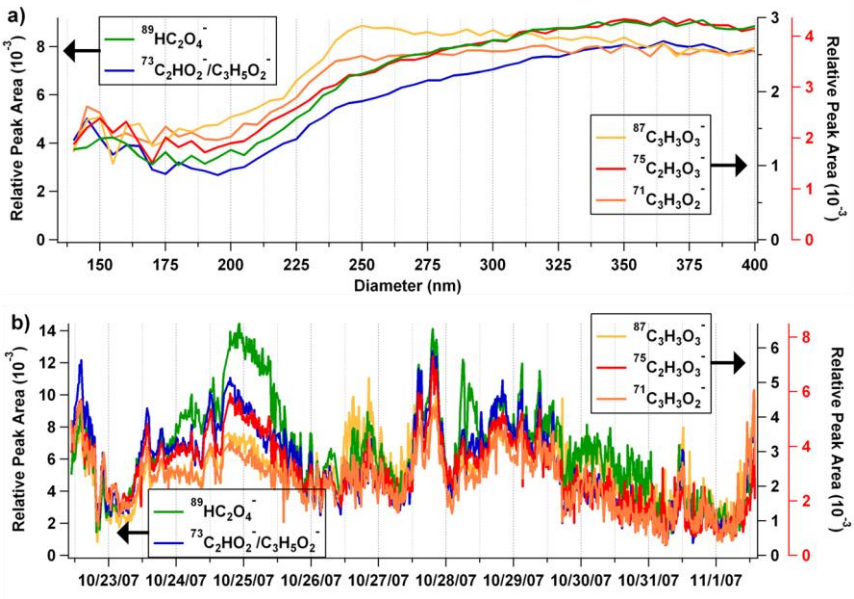

Figure 5.8: Distributions of the relative peak areas of organic acids in BBA by a) size and b) time.

amines, also basic, based on the presence of the $^{86}(C_2H_5)_2NCH_2^+$ fragment (Angelino et al., 2001). The percentages of BBA internally mixed with all these species depend on fire conditions, regionally background pollutant levels, and meteorology.

In this study, 44%, 46%, 54%, and 65% of BBA mass spectra had peaks at $^{71}C_3H_3O_2^-$, $^{73}C_2HO_3^-/C_3H_5O_2^-$, $^{75}C_2H_3O_3^-$, and $^{87}C_3H_3O_3^-$ likely due to organic acid anions, such as oxalate ($^{89}HC_2O_4^-$), which typically produce negative molecular ions (Sullivan and Prather, 2007). However, previous ATOFMS work concluded that the presence of $^{45}HCO_2^-$, $^{59}CH_3COO^-$, and $^{71}C_3H_3O_2^-$ were uniquely indicative of levoglucosan (Silva et al., 1999). Nonetheless, the $^{45}HCO_2^-$ and $^{59}CH_3COO^-$ markers are evincive of formate and acetate ions, and thus could be the resulting fragments of multiple organic carbon species. As explained in section 2.2, the $^{45}HCO_2^-$ marker was not used in this study due to interference. Furthermore, previous studies with organic meat burning and plant detritus standards showed that the $^{71}C_3H_3O_2^-$ peak is not unique

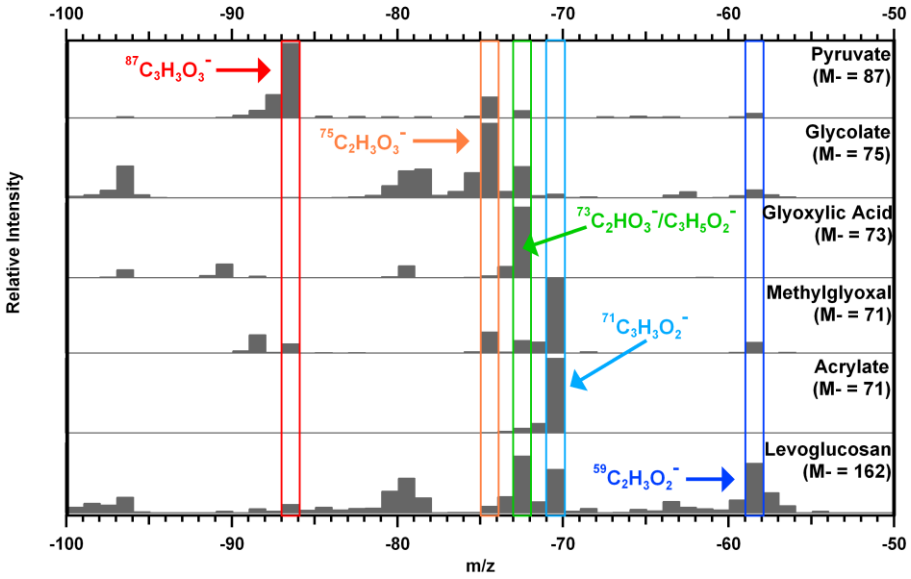

Figure 5.9: Mass Spectra of Organic Acid Standards

to levoglucosan (Silva, 2000; Silva and Prather, 2000). Because levoglucosan is primarily emitted from biomass burning, it should be found across all BBA sizes. However, the size distribution of BBA with $^{71}C_3H_3O_2^-$ is shifted toward particles >225 nm (Figure 5.8), and thus the $^{71}C_3H_3O_2^-$ marker on BBA in this study must be mostly secondary in nature. These results suggest that the -59 and -71 m/z peaks observed in BBA during this study were not representative of levoglucosan. In order to try to

identify the $^{71}C_3H_3O_2^-$, $^{73}C_2HO_3^-/C_3H_5O_2^-$, $^{75}C_2H_3O_3^-$, and $^{87}C_3H_3O_3^-$ peaks, organic standards were analyzed with the ATOFMS. Figure 5.9 shows representative mass spectra of acrylate, glyoxalate, and other standards, in addition to levoglucosan, highlighting that multiple compounds can produce peaks these peaks; thus using the ATOFMS as the single indentifying technique, it is not possible to identify the source of these ions, yet it is likely that these peaks resulted from secondary organic acids. For more information on how these standards were analyzed and a discussion of the results see section 5.6.3.

5.3.3 PMF Factors and Single Particle Analysis

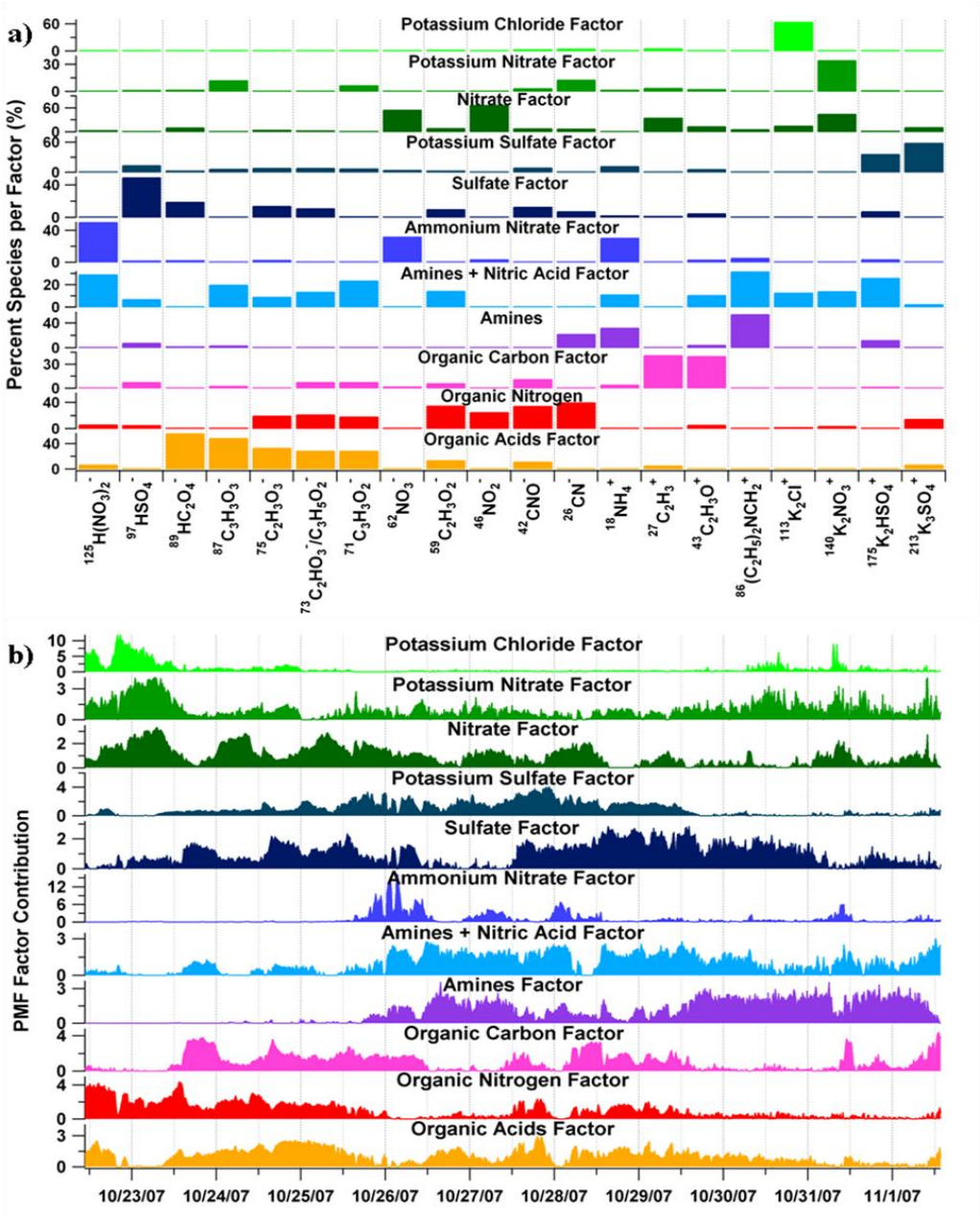

Figure 5.10: The PMF results with 11 factors a) the source profiles, where each profile was named based on the most abundant species, and b) temporal distribution of each factor.

PMF analysis determines which species co-vary at the same time and groups these species into different factors. The profiles and temporal distribution of the solution with 11 PMF factors for 120-400 nm BBA are shown in Figure 5.10 and

described in the following sections. The PMF factors were named based on the most abundant species present. All species were separated into multiple factors. Each factor may have a unique formation mechanism based on its formation, meteorology and/or environmental conditions. The size and temporal profiles of representative chemical markers for each PMF factor are shown in Figure 5.11.

5.3.3.1 Inorganic Species

The *potassium chloride, potassium nitrate, and potassium sulfate factors* were mainly associated with $^{113}K_2Cl^+$, $^{140}K_2NO_3^+$, and $^{213}K_3SO_4^+$, respectively, as shown in Figure 5.10. The *potassium chloride factor*, which peaked on 10/22/07 (Figure 5.10), was assigned as the freshest BBA sampled. $^{140}K_2NO_3^+$ and $^{213}K_3SO_4^+$, which are indicative of more aged BBA, peaked at different times than $^{113}K_2Cl^+$ (Figure 5.11). Following the decline of $^{113}K_2Cl^+$, there was a steady increase of $^{140}K_2NO_3^+$ on 10/22/07 until it peaked on the morning of 10/23/07, indicating that the majority of KCl was first transformed to KNO_3 through heterogeneous reactions with $HNO_{3(g)}$. $^{213}K_3SO_4^+$ peaked between 10/25/07-10/30/07, indicating that potassium salts in BBA were further transformed to K_2SO_4 by reaction with $H_2SO_{4(g)}$. Particles grow in size as they coagulate or as secondary species condense onto them. A comparison of the size distribution of particles containing $^{113}K_2Cl^+$, $^{140}K_2NO_3^+$ and $^{213}K_3SO_4^+$ (Figure 5.11) highlights that the smaller and hence fresher particles are those with KCl and KNO_3 compared to the larger and hence more aged particles with K_2SO_4. Fresh (*potassium chloride factor*), slightly aged (*potassium nitrate factor*), and moderately aged (*potassium sulfate factor*) plumes from the San Diego wildfires were sampled during this study as characterized by the temporal and size distribution of potassium salts in BBA. Figure 5.11 shows that the size distributions of the non-potassium salt markers, with the exception of $^{62}NO_3^-$ and $^{43}C_2H_3O^+$, were larger than those of $K_3SO_4^+$. These larger and hence more aged BBA were characterized by the lack of potassium salts. It is likely that these aged BBA still contained potassium salts, but that they were coated with significant amounts of secondary species therefore, masking their presence when analyzed with the ATOFMS. Thus, in addition to the fresh, slightly aged, and moderately aged BBA, aged BBA were also sampled in this study.

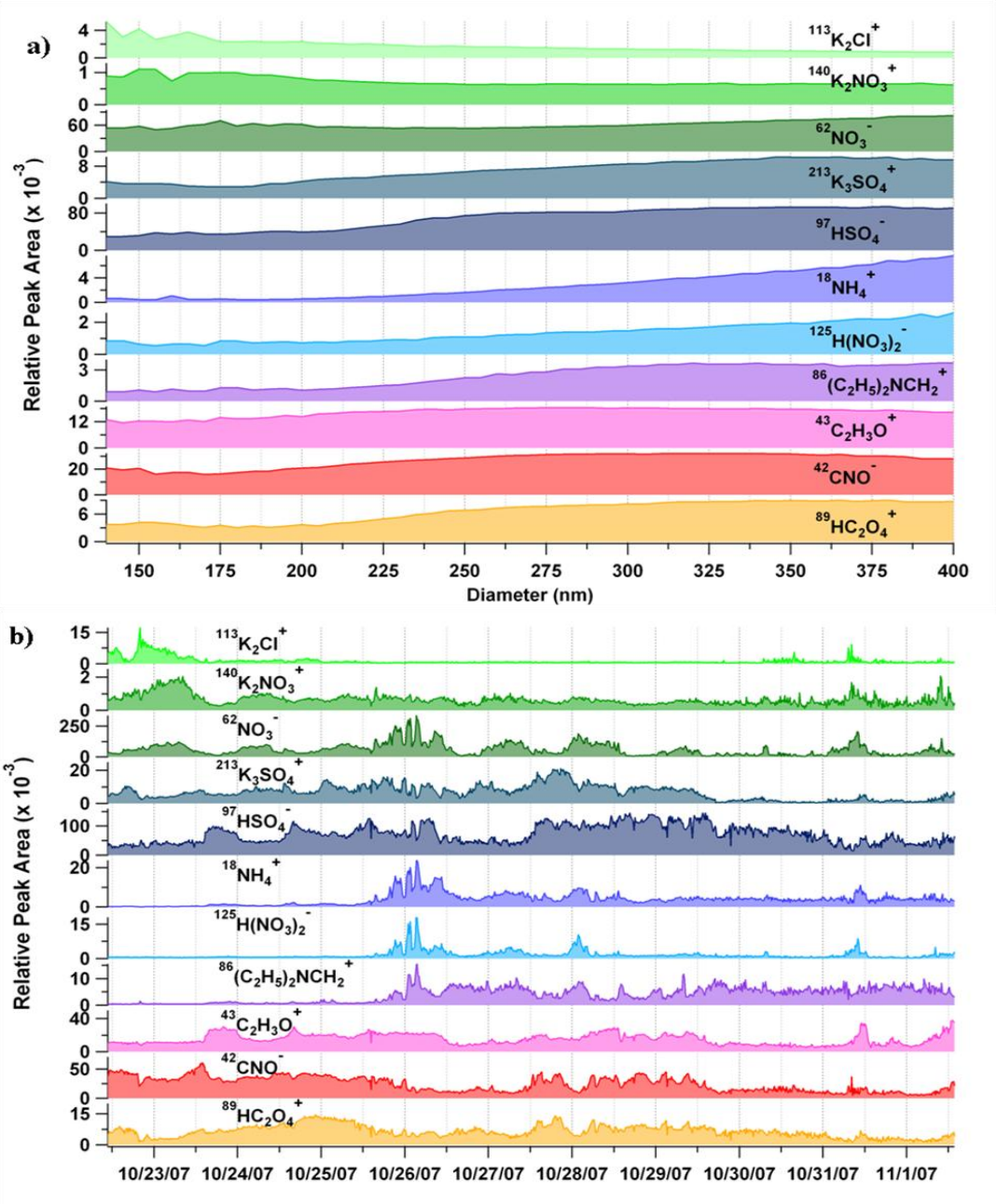

Figure 5.11: a) Size and b) temporal distribution of the BBA relative peak areas most representative of each factor.

Although particulate phase nitrate and sulfate are typically secondary species, they can be primarily emitted during biomass burning. Because $^{62}NO_3^-$ was found fairly uniformly across all sizes whereas $^{97}HSO_4^-$ was found predominantly in BBA > 225 nm (Figure 5.11), it can be concluded that $^{62}NO_3^-$ was present in all stages of aging while

$^{97}HSO_4^-$ was only found in aged BBA. This conclusion is supported by a previous aircraft study of BBA over Wyoming, which also determined that aged BBA contained more $^{97}HSO_4^-$ compared with $^{62}NO_3^-$ (Pratt et al., 2010). In contrast, a previous study in Mexico City observed more $^{62}NO_3^-$ than $^{97}HSO_4^-$ in aged BBA (Moffet et al., 2008). The difference in the abundance of HSO_4^- versus $^{62}NO_3^-$ in aged BBA is caused by the atmospheric aging processes that the BBA undergo, which depend on the concentrations of different precursor gas phase species and meteorological conditions. For example, high humidity and increased cloud-cover were likely more abundant in the air mass during the aircraft BBA study in order for extensive cloud processing of BBA to occur, whereas in the Mexico City study there were probably higher concentrations of $NO_{x(g)}$ and solar radiation leading to increased photochemistry.

Overall, the *nitrate factor* and *sulfate factor* followed the temporal variations of $^{62}NO_3^-$ and $^{97}HSO_4^-$, respectively (Figure 5.10). BBA $^{62}NO_3^-$ exhibited a diurnal pattern at the beginning of the fires reaching a maximum in the mid-morning and decreasing at noon when temperature was the highest. Thus, the likely mechanism involved in this diurnal pattern is partly explained by the semi-volatile nature of nitrate, which makes the ambient temperature an important driver for its partitioning between the gas and particulate phases. The NO_x temporal distribution (Figure 5.12) was characterized with a maximum during the mid-morning and a smaller one at night. Thus, in addition to temperature, photochemistry must be playing a role. Despite the thick haze over San Diego County during the wildfires, solar radiation still had a strong diurnal profile overall (Figure 5.3), and thus photochemistry probably initiated the rapid conversion of $NO_{x(g)}$, likely emitted directly from the wildfires, to $HNO_{3(g)}$, which would then partition to the particulate phase as nitrate (Fiedler et al., 2011). The addition of nitrate to BBA is representative of BBA aging due to interaction with wildfire co-emissions in the presence of the appropriate meteorological conditions.

When the RH increased on 10/25/07 (Figure 5.3), the *nitrate factor* no longer tracked $^{62}NO_3^-$, which spiked in parallel with $^{125}HNO_3NO_3^-$ suggesting that these were acidic BBA. Instead, PMF analysis separated this $^{62}NO_3^-$ spike into the *ammonium nitrate factor* (Figure 5.10) since the measurements of $^{18}NH_4^+$ and $^{125}HNO_3NO_3^-$ also followed the same temporal trend as $^{62}NO_3^-$ during this period. Although the $^{18}NH_4^+$ was more strongly associated with $^{97}HSO_4^-$ than $^{62}NO_3^-$during the rest of the study indicating the presence of ammonium sulfate ($(NH_4)_2SO_4$), when the *ammonium nitrate factor* spiked there was a prevalence of ammonium nitrate (NH_4NO_3), as evidenced by Figure 5.13 and as previously observed in BBA (Fiedler et al., 2011; Song et al., 2005). A more thorough description of Figure 5.13 is included in section 5.6.2. Gaseous NH_3 and HNO_3, both found in biomass burning plumes (Lefer et al., 1994; Lobert et al.,

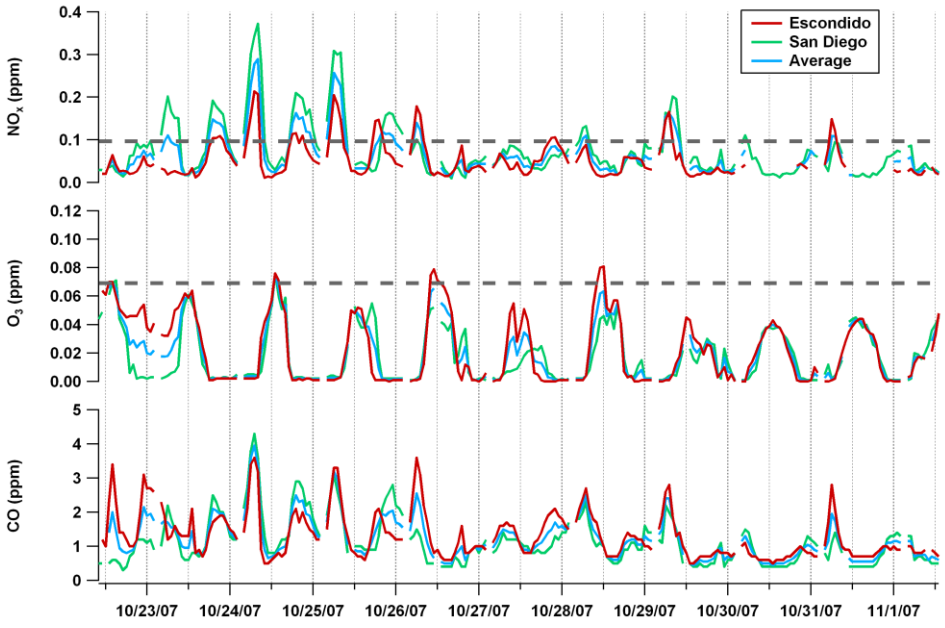

Figure 5.12: Gas phase concentrations and PM2.5 mass concentration. Dashed lines indicate U.S. EPA Federal standards. Data from CARB.

1991; Streets et al., 2003; Talbot et al., 1994; Yokelson et al., 1997), react together to form particulate phase NH_4NO_3, which only remains on the particle due to high humidity during this time since it volatilizes at low RH (Stelson and Seinfeld, 1982a; Stelson and Seinfeld, 1982b). Alternatively, BBA may uptake HNO_3 directly; the nitric

acid uptake coefficient on mineral dust particles has also been shown to be a function of RH (Vlasenko et al., 2006), and the same effect likely occurs on BBA.

In contrast to $^{62}NO_3^-$, the $^{97}HSO_4^-$ remained low from the beginning of the study until the afternoon of 10/23, probably due to the low $SO_{2(g)}$ emissions from the wildfires and its long conversion time to the particulate phase, especially during low RH conditions (<40%) which were present until 10/25 even during the night due to the Santa Ana winds; between 10/23-10/26 $^{97}HSO_4^-$ peaked mostly in the afternoons. Once the Santa Ana conditions ended on 10/25, the RH increased to > 90%; however, sulfate did not increase with the increased RH as expected if it were not produced through in-cloud processing of $SO_{2(g)}$ during this time, which is usually the main formation pathway. Since $SO_{2(g)}$ is the precursor, $SO_{2(g)}$ may have homogeneously reacted with OH radicals in the gas phase eventually forming sulfate (Warneck, 1999). Previous studies have measured and estimated much higher concentrations of OH radicals in biomass burning plumes than in background air masses highlighting the plausibility of

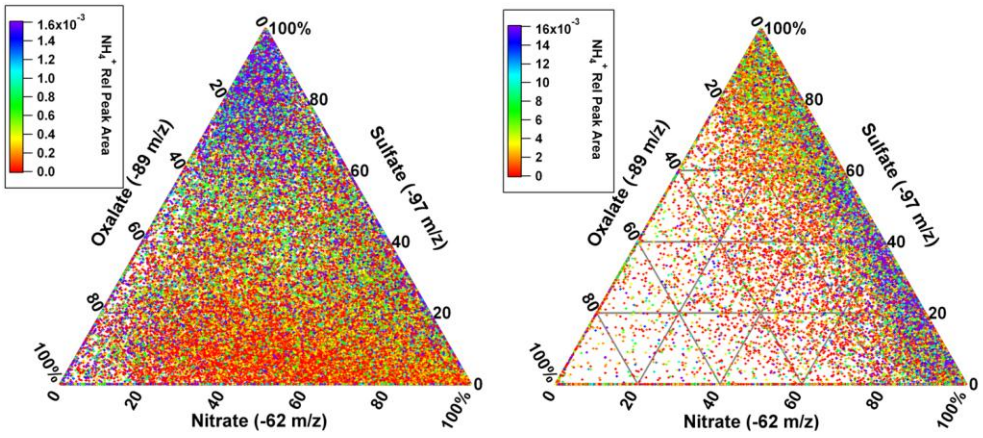

Figure 5.13: Ternary plots show the mixing state of ammonium, sulfate, nitrate, and oxalate in 100-400 nm BBA during a) the beginning of the fires (10/22/07 10:00-10/23/07 17:53) and b) during spike in nitric acid (10/25/07 12:00 - 10/26/07 12:00). There were 99,999 and 69,255 particles during each period, respectively. Each point on the plots represents a single particle.

this explanation (Yokelson et al., 2009). An additional spike of $^{97}HSO_4^-$ occurred on 10/27 coinciding with the presence of a fog event. The sampled air mass came from the ocean after 10/25/07 based on the back trajectories (Figure 5.4), and was consistent with

the presence of the HFO particle type associated with ships (Figure 5.6). Additionally, because shipping is a more significant source of $SO_{2(g)}$ than biomass burning (Smith et al., 2011), the $^{97}HSO_4^-$ detected on BBA must have originated from $SO_{2(g)}$ emitted from the ships around the ports of San Diego, Los Angeles and Long Beach facilitating the formation of sulfate through cloud processing during this time. Therefore, addition of sulfate to BBA, summarized in the *sulfate factor*, is representative of BBA aging upon interaction with regional pollutants.

5.3.3.2 Organic Carbon Species

As illustrated in Figure 5.10, PMF analysis separated organic carbon markers into 4 distinct factors described below with species given in order of prevalence. The *organic carbon factor* was mainly composed of $^{43}C_2H_3O^+$ and $^{27}C_2H_3^+$, which are stable organic carbon fragments resulting from the ionization of larger organic carbon species. Unfortunately, it is not possible to determine the parent molecule from these fragments only that they represent organic carbon species. The *organic carbon factor* tracked the temporal profile of the *sulfate factor* during the first half of the sampling period very well (Figure 5.10) suggesting that the organic species represented by the $^{43}C_2H_3O^+$ and $^{27}C_2H_3^+$ fragments were formed from reactions of other organic species with OH, which was hypothesized to also produce $^{97}HSO_4^-$ during this time.

The *organic nitrogen factor* was comprised of $^{26}CN^-$, $^{42}CNO^-$, $^{59}C_2H_3O_2^-$, and $^{46}NO_2^-$ and was more prevalent at the beginning of the wildfires. The $^{26}CN^-$ and $^{42}CNO^-$ markers, which can be the resulting fragment of many nitrogen containing organic carbon species, have also been observed in biogenic particles such as plant detritus and bacteria (Pratt et al., 2009; Silva, 2000; Silva and Prather, 2000). Heterocyclic nitrogen compounds, including some naturally produced by plants and living organisms, and water soluble organic nitrogen species have been previous measured in BBA (Laskin et al., 2009; Ma and Hays, 2008; Mace et al., 2003). Previous work has also observed significant gas phase hydrogen cyanide (HCN) and isocyanic acid (HCNO) emitted in fresh biomass burning (Roberts et al., 2011; Simpson et al., 2011; Veres et al., 2010; Yokelson et al., 2009); however, based on the vapor pressure of these species it is

unlikely they would partition to the particulate phase. Thus, it is likely that the $^{26}CN^-$ and $^{42}CNO^-$ markers are resulting fragments of organic nitrogen biogenic material involved in biomass pyrolysis. Furthermore, rapid formation of gas phase acetic acid, which would be seen in BBA as $^{59}C_2H_3O_2^-$ when sampled with the ATOFMS, and other organic acids has been observed in relatively young biomass burning plumes (Gao et al., 2003; Legrand et al., 2007; Miyazaki et al., 2009; Yokelson et al., 2009). Thus, it is likely that the species found in the *organic nitrogen factor* were either emitted directly in the particulate phase or they were rapidly produced from gas phase precursors emitted during flaming conditions which partitioned rapidly into the particulate phase as the smoke plume cooled during transport.

The *amines factor* consisted mainly of $^{86}(C_2H_5)_2NCH_2^+$ with minor contributions from $^{18}NH_4^+$ and $^{26}CN^-$, which were both likely also amine fragments during this time. It is interesting that the *amines and organic nitrogen factors* were split into two, but based on their temporal and size profiles this makes sense. While the *organic nitrogen factor* was prevalent at the beginning of the fires, the *amines factor* spiked after the increase in RH on 10/25. In controlled laboratory burns, gas phase amines have been observed to be emitted during biomass burning, typically during the smoldering phase (Andreae and Merlet, 2001; Lobert et al., 1991). Therefore, amines remained in the gas phase while the RH was low, as shown by previous work (Angelino et al., 2001; Rehbein et al., 2011), and partitioned to the particulate phase once the RH increased to > 90%.

The *organic acids factor*, which had contributions from $^{89}HC_2O_4^-$, $^{87}C_3H_3O_3^-$, $^{75}C_2H_3O_3^-$, $^{73}C_2HO_3^-$/$^{73}C_3H_5O_2^-$, and $^{71}C_3H_3O_2^-$, peaked between 10/23/07-10/26/07 and 10/27/07-10/31/07. These organic acids, tracked each other very well temporally and by size (Figure 5.8) indicating a similar formation mechanism among organic acids, which may have varied during the sampling period due to changing meteorological conditions and differing concentrations of gas phase precursors. The organic acids at the beginning of the wildfires were likely primary or a result of fast secondary production, as has been previously observed (Gao et al., 2003; Legrand et al., 2007; Miyazaki et al., 2009). However, organic acids spiked between 10/27/07-10/31/07 coinciding with the period

when the air mass back trajectories came from offshore, and thus the BBA sampled during this time had significantly more time to age. Therefore, the organic acids from this period could have formed through slow gas-to-particle conversion of VOCs emitted during biomass burning which further oxidized into the organic acids (Narukawa et al., 1999; Timonen et al., 2010). Although it is not possible to identify each organic species present in BBA when only using the ATOFMS, the four different organic carbon factors identified in this study indicate that data obtained can still be used to learn about different processes that occur in biomass burning.

5.4 Summary and conclusions

Throughout the 2007 wildfires, San Diego was impacted by elevated $PM_{2.5}$ concentrations county-wide exceeding the NAAQS short-term limit of 35 $\mu g/m^3$. During the intense wildfire period, > 80% of $PM_{2.5}$ and $PM_{1.0}$ mass estimated at UCSD was due to particles in the 120-400 nm range, with $PM_{0.1\text{-}0.4}$ as high as 148 $\mu g/m^3$. This is an important observation since smaller particles may contribute to more adverse health problems than larger ones (Ramgolam et al., 2009; Stoelzel et al., 2007).

Comprised of five different particle types, BBA contributed to 84% of all 120-400 nm particle numbers chemically analyzed during this study. BBA were aged based on wildfire co-emissions, regional pollutants, and the aid of meteorological conditions. PMF and single particle analysis were used to study the aging of BBA. Fresh, slightly aged, moderately aged, and aged BBA were differentiated using the presence of unique chemical markers such as $^{113}K_2Cl^+$, $^{140}K_2NO_3^+$ and $^{213}K_3SO_4^+$, and secondary species, such as sulfate and the lack of potassium salts. Four main organic carbon PMF factors were identified: *organic carbon, organic nitrogen, amines, and organic acids,* indicating different temporal profiles and hence differing formation mechanisms. The mixing state and size of BBA determines their hygroscopicity and cloud nucleating properties, hence affecting the climate impact of BBA. For a thorough analysis of the hygroscopicity of the particles during the 2007 San Diego Wildfires the reader is referred to (Moore et al., 2012).

Further studies will sample southern California wildfires and prescribed burns to learn more about the evolution of chaparral BBA. While we expect that BBA in areas affected by different regional pollutants and meteorological conditions will exhibit different aging processes at different rates, efforts will focus on more detailed characterization of the composition of fresh BBA from wildfires in urban communities by sampling as close as safely possible during future wildfires. In addition, it would be greatly beneficial to sample ultrafine (<100 nm) BBA (Figure 5.1) with the combined growth tube ATOFMS approach to investigate mixing state differences in individual particles smaller than can currently be sampled with the ATOFMS alone (Zauscher et al., 2011). Furthermore, new methods for on-line sampling of BBA would be useful, such as the aerosol chip electrophoresis (ACE) system (Noblitt et al., 2009) and the two-dimensional gas chromatography thermal desorption (2D-TAG) instrument (Worton et al., 2012), in order to complement the capabilities of ATOFMS measurements.

5.5 Acknowledgements

The authors would like to acknowledge Dr. Andrew Ault, Joe Mayer, Dr. Ryan Sullivan, and Maggie Yandell for help collecting data during the 2007 San Diego Wildfires and John Cahill for comments that greatly improved the manuscript. We are also grateful for data collected by the California Air Resources Board (CARB) and the California Irrigation Management Information System networks. Funding for this study was provided by CARB Grant # 04-336 and the U.S. Environmental Protection Agency PM Center Grant # R832415.

Chapter 5 contents are part of a manuscript in preparation, Melanie D. Zauscher, Ying Wang, Meagan J.K. Moore, Cassandra J. Gaston and Kimberly A. Prather; Mixing state and aging of individual biomass burning aerosols during the 2007 San Diego Wildfires.

5.6 Supplemental Materials

5.6.1 PMF Factors

The Positive Matrix Factorization (PMF) model used was the USEPA PMF 3.0. The guidelines presented in the Fundamentals & User Guide were followed during the analysis (USEPA, 2008). However, instead of using PMF for determining the source of aerosols, we used PMF in this study to group chemical markers from the same source, namely biomass burning. The 20 marker species from BBA utilized in this PMF analysis were chosen because of their relevance in biomass burning aerosols and abundance during the 2007 San Diego Wildfires. The signal-to-noise ratio of all species was > 2.3 indicating that the variability in the measurements was real and therefore all 20 marker species were categorized as strong in the PMF model (USEPA, 2008). In 245 hourly samples, there was only one missing value across all species on 10/26/07 9:00, which was replaced with the geometric mean value of the preceding and following 3 hours of the missing value for each species. The PMF base model was set-up with a random seed and 20 runs, which all converged.

Table 5.2: Q values for PMF Analysis with different number of factors. [a]Qrobust with Fpeak = 0

# of Factors	R^2 between observed and predicted species	Q_{robust} [a]	Q_{theory} (EPA2.0)	Q_{theory} (EPA1.0)
3	0.00-0.90	15,476	16,192	19,120
4	0.47-0.90	9,738	15,216	19,120
5	0.51-0.95	7,478	14,240	19,120
6	0.57-0.97	5,571	13,264	19,120
7	0.67-0.98	4,106	12,288	19,120
8	0.72-0.98	3,112	11,312	19,120
9	0.75-0.98	2,544	10,336	19,120
10	0.85-0.99	2,057	9,360	19,120
11	0.89-0.99	1,696	8,384	19,120
12	0.90-0.99	1,371	7,408	19,120
13	0.91-0.99	1,086	6,432	19,120

Solutions for 3-13 factors were considered and the relevant Q values for each of these cases are shown in Table 5.2. In all solutions explored $Q_{theory} > Q_{robust}$, although it is recommended that $Q_{theory} \approx Q_{robust}$ (USEPA, 2008). The 3 factor solution had the closest Q_{theory} to Q_{robust}, but the three factors were completely inadequate in describing the temporal variability of the species. As the number of factors increased, Q_{robust} decreased at a faster rate than Q_{theory} (EPA2.0) while the predicted species better match the observed species in time. Because the correlations between observed and predicted variables were strong ($R^2 > 0.89$), the residuals were between -2 and 2, and the resulting factors made physical sense, we chose the 11 factor PMF solution as the final one (Reff et al., 2007). We could have chosen the 12 or 13 factor solution. However, the 12 and 13 factor solutions did not have improved correlations between observed and predicted species. Furthermore, these solutions had multiple factors with similar composition profiles and temporal distributions split into two. For example, the 12 factor solution had a nitric acid, an ammonium, and the ammonium nitrate factor. These observations

led us to believe these split factors were unrealistic and less physically meaningful and thus, we opted for the 11 factor solution. For the chosen 11 factor solution, Q_{theory}= 19,120 or 8,384, depending on whether the PMF1.0 or 2.0 definition of Q is used (Chan et al., 2011; USEPA, 2008). The 11 factor solution at F_{peak}=0 had Q_{robust}=Q_{true}=1696. The G-space was used to investigate rotational ambiguity in the factor solutions by varying F_{peak} between -0.5-0.5.(Paatero et al., 2005) The solution which removed the oblique edges between every pair of factors was for F_{peak} = -0.1 and is presented herein, thus changing the Q values to Q_{true}=1696.2 and Q_{robust}=1698.2. Because we were using PMF analysis in a way that has not been used before, it is possible that the recommendation that $Q_{theory} \approx Q_{robust}$ is not appropriate here.

5.6.2 Insights from Chemical Markers

Figure 5.13 shows the mixing state of $^{18}NH_4^+$, $^{62}NO_3^-$, $^{97}HSO_4^-$ and $^{89}HC_2O_4^-$ on individual BBA particles during two different periods. In each ternary plot, BBA containing mostly nitrate would be towards the right vertex, mostly sulfate towards the top vertex, and mostly oxalate towards the left vertex; the color represents different amounts of ammonium. Each ternary plot represents a different period chosen to represent different conditions, the beginning of the fires (10/22/07 10:00 – 10/23/07 17:53) and a period when nitric acid spiked (10/25/07 12:00 – 10/26/07 12:00). The number of BBA from the beginning of the fires was cut-off at 99,999 in order to make the amount of data manageable for the ternary plot. During the beginning of the fires, there was a greater distribution in the mixing state of BBA compared with the nitric acid spike period. At the beginning of the fires, there were particles with mostly oxalate, mostly sulfate, mostly nitrate, and particles internally mixed with different amounts of all three species. During the high nitric acid period, the majority of particles had significant amounts of nitrate, little oxalate and a broad distribution of sulfate. The distribution of ammonium was also different during both periods. In the beginning of the fires, higher amounts of $^{18}NH_4^+$ were predominantly associated with sulfate only BBA indicating that during this period, and most of the fires (not shown), ammonium was predominantly found as $(NH_4)_2SO_4$ and not NH_4NO_3. During the nitric acid spike,

higher amounts of $^{18}NH_4^+$ were mostly associated with nitrate. Because sulfuric acid is a stronger acid than nitric acid, there must not have been enough sulfuric acid to neutralize the ammonium during this period. Thus, during the nitric acid spike, there was a prevalence of NH_4NO_3 over $(NH_4)_2SO_4$, which has been observed before in BBA (Fiedler et al., 2011; Song et al., 2005).

5.6.3 Organic acid standards

Solutions of sodium pyruvate (Fisher), sodium glycolate (Acros), sodium propanoate (Spectrum), glyoxylic acid (Acros), methylglyoxal (Sigma), zinc acrylate (Aldrich), in addition to levoglucosan (Acros), were made with ultra-pure water and atomized to generate particles. The particles were dried downstream with diffusion dryers before entering the ATOFMS inlet. At least 2,000 mass spectra were obtained per standard for statistical significance. A representative negative mass spectrum for each standard is shown in Figure 5.9. The pyruvate, glycolate and glyoxylate generated a molecular ion at -87, -75, and -73 m/z, respectively, whereas the molecular ion from methylglyoxal and acrylate was at -71 m/z. Most standards also had small peaks at -59 and -45 m/z in their mass spectra. Because negative molecular ions from different standards known to be present in BBA were formed at -71 and -73 m/z, it is not possible to attribute these peaks to a specific compound. Thus, in addition to levoglucosan fragments, the peaks at -71, -73, -75, and -87 m/z could be the resulting ions of several organic acids.

5.6.4 Peripheral Data

Figure 5.12 shows the gas phase concentrations measured at Escondido and San Diego California Air Resources Board (CARB) sites from 10/11/07 until 11/01/07. Overall, the NO_x was higher at San Diego site compared to Escondido. The concentrations of nitrogen oxides (NO_x) exceeded the 1-hour NAAQS (0.1 ppm) during a few periods between 10/23/07-10/25/07. The highest NO_x reported was 0.37 ppm at the San Diego site at 10/24/07 8:00 compared to 0.21 ppm at Escondido an hour before. It is interesting that the NOx concentrations were higher at the San Diego site than at

Escondido during the 12 days after the first wildfire, with an average of 0.07 ± 0.06 versus 0.05 ± 0.04 ppm, respectively. The 10 days preceding the wildfires, the NOx concentrations were 0.03 ± 0.04 and 0.02 ± 0.02 ppm at San Diego and Escondido, respectively. There was no statistically significant (using p-test) difference for the daily profiles of O_3 before and after the wildfires started. At the beginning of the wildfires (10/21/07 morning thru the afternoon of 10/23/07), O_3 remained high at Escondido, but the rest of the time the O_3 was typical of a non-fires period with a strong diurnal pattern. A modeling study showed that the O_3 from the 2007 California wildfires peaked over the ocean because by the time the precursors generated O_3 the winds had blown the air mass offshore.(Pfister et al., 2008) Carbon monoxide (CO) concentrations were fairly low overall, but roughly twice as high from 10/11/07-10/20/07 compared to 10/21/07-11/1/07.

The amount of nitrogen present in the fuel and the type of fire determines how much $NO_{x(g)}$ and $NH_{3(g)}$ are formed (Reid et al., 2005). $NO_{x(g)}$ and $NH_{3(g)}$ preferentially form during flaming and smoldering conditions, respectively (Andreae and Merlet, 2001). Unfortunately, we cannot compare $NH_{3(g)}$ to $NO_{x(g)}$ because $NH_{3(g)}$ was not measured during the 2007 San Diego Wildfires. Both $NO_{x(g)}$ and $NH_{3(g)}$ may eventually partition into the particle phase as $^{62}NO_3^-$ and $^{18}NH_4^+$, respectively. Another gas species of interest is $SO_{2(g)}$, which can oxidize into $H_2SO_{4(g)}$ and eventually partition into the particle phase as SO_4^{2-}.

ınterestingly, $NO_{x(g)}$ and $CO_{(g)}$ peaked in the morning and then at night on 10/23/07-10/26/07. The night-time peak is probably due to a lower nocturnal boundary layer, whereas the morning peak is likely a result of photochemistry. The hypothesized low nocturnal boundary layer would trap the wildfire emissions from diluting and mixing with the rest of the troposphere and hence concentrate the emissions. Although there is some $SO_{2(g)}$ emitted from biomass burning, previous studies found it less significant than the emitted $NO_{x(g)}$ (Andreae and Merlet, 2001; Fiedler et al., 2011; Song et al., 2005; Streets et al., 2003). In San Diego County, only the San Diego CARB site measured the concentration of $SO_{2(g)}$ and it was low and stable during this study,

indicating that biomass burning in Southern California does not generate substantial emissions of $SO_{2(g)}$ or it reacts very quickly.

5.7 References

Allen, A. G., and Miguel, A. H. (1995).Biomass Burning in the Amazon - Characterization of the Ionic Component of Aerosols Generated from Flaming and Smoldering Rain-Forest and Savanna, *Environmental Science & Technology*, *29* (2), 486-493.

Andreae, M. O. (1983).Soot Carbon and Excess Fine Potassium: Long-Range Transport of Combustion-Derived Aerosols, *Science*, *220* (4602), 1148-1151.

Andreae, M. O., and Merlet, P. (2001).Emission of Trace Gases and Aerosols from Biomass Burning, *Global Biogeochemical Cycles*, *15* (4), 955-966.

Angelino, S., Suess, D. T., and Prather, K. A. (2001).Formation of Aerosol Particles from Reactions of Secondary and Tertiary Alkylamines: Characterization by Aerosol Time-of-Flight Mass Spectrometry, *Environmental Science & Technology*, *35* (15), 3130-3138.

Arbex, M. A., Martins, L. C., de Oliveira, R. C., Pereira, L. A. A., Arbex, F. F., Cancado, J. E. D., Saldiva, P. H. N., and Braga, A. L. F. (2007).Air Pollution from Biomass Burning and Asthma Hospital Admissions in a Sugar Cane Plantation Area in Brazil, *Journal of Epidemiology and Community Health*, *61* (5), 395-400.

Arbex, M. A., Saldiva, P. H. N., Pereira, L. A. A., and Braga, A. L. F. (2010).Impact of Outdoor Biomass Air Pollution on Hypertension Hospital Admissions, *Journal of Epidemiology and Community Health*, *64* (7), 573-579.

Ault, A. P., Gaston, C., Wang, Y., Dominguez, G., Thiemens, M. H., and Prather, K. A. (2010).Characterization of the Single Particle Mixing State of Individual Ship Plume Events Measured at the Port of Los Angeles, *Environmental Science & Technology*, *44* (6), 1954-1961.

Ault, A. P., Moore, M. J. K., Furutani, H. F., and Prather, K. A. (2009).Impact of Emissions from the Los Angeles Port Region on San Diego Air Quality During Regional Transport Events, *Environmental Science & Technology*, *43* (10), 3500-3506.

Bi, X. H., Zhang, G. H., Li, L., Wang, X. M., Li, M., Sheng, G. Y., Fu, J. M., and Zhou, Z. (2011).Mixing State of Biomass Burning Particles by Single Particle Aerosol Mass Spectrometer in the Urban Area of Prd, China, *Atmospheric Environment*, *45* (20), 3447-3453.

Chan, Y. C., Hawas, O., Hawker, D., Vowles, P., Cohen, D. D., Stelcer, E., Simpson, R., Golding, G., and Christensen, E. (2011).Using Multiple Type Composition Data and Wind Data in Pmf Analysis to Apportion and Locate Sources of Air Pollutants, *Atmospheric Environment, 45* (2), 439-449.

Clinton, N. E., Gong, P., and Scott, K. (2006).Quantification of Pollutants Emitted from Very Large Wildland Fires in Southern California, USA, *Atmospheric Environment, 40* (20), 3686-3695.

Crutzen, P. J., and Andreae, M. O. (1990).Biomass Burning in the Tropics - Impact on Atmospheric Chemistry and Biogeochemical Cycles, *Science, 250* (4988), 1669-1678.

Delfino, R. J., Brummel, S., Wu, J., Stern, H., Ostro, B., Lipsett, M., Winer, A., Street, D. H., Zhang, L., Tjoa, T., and Gillen, D. L. (2009).The Relationship of Respiratory and Cardiovascular Hospital Admissions to the Southern California Wildfires of 2003, *Occupational and Environmental Medicine, 66* (3), 189-197.

Draxler, R. R., and Hess, G. D. (1998).An Overview of the Hysplit 4 Modelling System for Trajectories, Dispersion and Deposition, *Australian Meteorological Magazine, 47* (4), 295-308.

Eatough, D. J., Grover, B. D., Woolwine, W. R., Eatough, N. L., Long, R., and Farber, R. (2008).Source Apportionment of 1 H Semi-Continuous Data During the 2005 Study of Organic Aerosols in Riverside (Soar) Using Positive Matrix Factorization, *Atmospheric Environment, 42* (11), 2706-2719.

EG&G Technical Services, I. (2007). San Diego County Firestorms after Action Report.

Fiedler, V., Arnold, F., Ludmann, S., Minikin, A., Hamburger, T., Pirjola, L., Dornbrack, A., and Schlager, H. (2011).African Biomass Burning Plumes over the Atlantic: Aircraft Based Measurements and Implications for H(2)So(4) and Hno(3) Mediated Smoke Particle Activation, *Atmospheric Chemistry and Physics, 11* (7), 3211-3225.

Fraser, M. P., and Lakshmanan, K. (2000).Using Levoglucosan as a Molecular Marker for the Long-Range Transport of Biomass Combustion Aerosols, *Environmental Science & Technology, 34* (21), 4560-4564.

Furukawa, T., and Takahashi, Y. (2011).Oxalate Metal Complexes in Aerosol Particles: Implications for the Hygroscopicity of Oxalate-Containing Particles, *Atmospheric Chemistry and Physics, 11* (9), 4289-4301.

Gao, S., Hegg, D. A., Hobbs, P. V., Kirchstetter, T. W., Magi, B. I., and Sadilek, M. (2003).Water-Soluble Organic Components in Aerosols Associated with Savanna Fires in Southern Africa: Identification, Evolution, and Distribution, *Journal of Geophysical Research-Atmospheres, 108* (D13), 16.

Gaudichet, A., Echalar, F., Chatenet, B., Quisefit, J. P., Malingre, G., Cachier, H., Buatmenard, P., Artaxo, P., and Maenhaut, W. (1995).Trace-Elements in Tropical African Savanna Biomass Burning Aerosols, *Journal of Atmospheric Chemistry*, *22* (1-2), 19-39.

Grell, G., Freitas, S. R., Stuefer, M., and Fast, J. (2011).Inclusion of Biomass Burning in Wrf-Chem: Impact of Wildfires on Weather Forecasts, *Atmospheric Chemistry and Physics*, *11* (11), 5289-5303.

Gross, D. S., Galli, M. E., Silva, P. J., and Prather, K. A. (2000).Relative Sensitivity Factors for Alkali Metal and Ammonium Cations in Single Particle Aerosol Time-of-Flight Mass Spectra, *Analytical Chemistry*, *72* (2), 416-422.

Guazzotti, S. A., Suess, D. T., Coffee, K. R., Quinn, P. K., Bates, T. S., Wisthaler, A., Hansel, A., Ball, W. P., Dickerson, R. R., Neususess, C., Crutzen, P. J., and Prather, K. A. (2003).Characterization of Carbonaceous Aerosols Outflow from India and Arabia: Biomass/Biofuel Burning and Fossil Fuel Combustion, *Journal of Geophysical Research*, *108* (D15), 4485, doi:10.1029/2002JD003277.

Guazzotti, S. A., Whiteaker, J. R., Suess, D., Coffee, K. R., and Prather, K. A. (2001).Real-Time Measurements of the Chemical Composition of Size-Resolved Particles During a Santa Ana Wind Episode, California USA, *Atmospheric Environment*, *35* (19), 3229-3240.

Healy, R. M., Hellebust, S., Kourtchev, I., Allanic, A., O'Connor, I. P., Bell, J. M., Healy, D. A., Sodeau, J. R., and Wenger, J. C. (2010).Source Apportionment of Pm2.5 in Cork Harbour, Ireland Using a Combination of Single Particle Mass Spectrometry and Quantitative Semi-Continuous Measurements, *Atmospheric Chemistry and Physics*, *10* (19), 9593-9613.

Healy, R. M., O'Connor, I. P., Hellebust, S., Allanic, A., Sodeau, J. R., and Wenger, J. C. (2009).Characterisation of Single Particles from in-Port Ship Emissions, *Atmospheric Environment*, *43* (40), 6408-6414.

Hedberg, E., and Johansson, C. (2006).Is Levoglucosan a Suitable Quantitative Tracer for Wood Burning? Comparison with Receptor Modeling on Trace Elements in Lycksele, Sweden, *Journal of the Air & Waste Management Association*, *56* (12), 1669-1678.

Hennigan, C. J., Miracolo, M. A., Engelhart, G. J., May, A. A., Presto, A. A., Lee, T., Sullivan, A. P., McMeeking, G. R., Coe, H., Wold, C. E., Hao, W. M., Gilman, J. B., Kuster, W. C., de Gouw, J., Schichtel, B. A., Collett, J. L., Jr., Kreidenweis, S. M., and Robinson, A. L. (2011).Chemical and Physical Transformations of Organic Aerosol from the Photo-Oxidation of Open Biomass Burning Emissions in an Environmental Chamber, *Atmospheric Chemistry and Physics*, *11* (15), 7669-7686.

Hennigan, C. J., Sullivan, A. P., Collett, J. L., and Robinson, A. L. (2010).Levoglucosan Stability in Biomass Burning Particles Exposed to Hydroxyl Radicals, *Geophysical Research Letters*, *37*, 4.

Holmes, B. J., and Petrucci, G. A. (2006).Water-Soluble Oligomer Formation from Acid-Catalyzed Reactions of Levoglucosan in Proxies of Atmospheric Aqueous Aerosols, *Environmental Science & Technology*, *40* (16), 4983-4989.

Hossain, A. M. M. M., Park, S., Kim, J.-S., and Park, K. (2012).Volatility and Mixing States of Ultrafine Particles from Biomass Burning, *Journal of Hazardous Materials*, *205*, 189-197.

Jacobson, M. Z. (2001).Strong Radiative Heating Due to the Mixing State of Black Carbon in Atmospheric Aerosols, *Nature*, *409* (6821), 695-697.

Keeley, J. E., Fotheringham, C. J., and Moritz, M. A. (2004).Lessons from the October 2003 Wildfires in Southern California, *Journal of Forestry*, *102* (7), 26-31.

Keeley, J. E., Safford, H., Fotheringham, C. J., Franklin, J., and Moritz, M. (2009).The 2007 Southern California Wildfires: Lessons in Complexity, *Journal of Forestry*, *107* (6), 287-296.

Kim, E., Hopke, P. K., and Edgerton, E. S. (2003).Source Identification of Atlanta Aerosol by Positive Matrix Factorization, *Journal of the Air & Waste Management Association*, *53* (6), 731-739.

Kunzli, N., Avol, E., Wu, J., Gauderman, W. J., Rappaport, E., Millstein, J., Bennion, J., McConnell, R., Gilliland, F. D., Berhane, K., Lurmann, F., Winer, A., and Peters, J. M. (2006).Health Effects of the 2003 Southern California Wildfires on Children, *American Journal of Respiratory and Critical Care Medicine*, *174* (11), 1221-1228.

Laskin, A., Smith, J. S., and Laskin, J. (2009).Molecular Characterization of Nitrogen-Containing Organic Compounds in Biomass Burning Aerosols Using High-Resolution Mass Spectrometry, *Environmental Science & Technology*, *43* (10), 3764-3771.

Lefer, B. L., Talbot, R. W., Harriss, R. C., Bradshaw, J. D., Sandholm, S. T., Olson, J. O., Sachse, G. W., Collins, J., Shipham, M. A., Blake, D. R., Klemm, K. I., Klemm, O., Gorzelska, K., and Barrick, J. (1994).Enhancement of Acidic Gases in Biomass Burning Impacted Air Masses over Cananda, *Journal of Geophysical Research-Atmospheres*, *99* (D1), 1721-1737.

Legrand, M., Preunkert, S., Oliveira, T., Pio, C. A., Hammer, S., Gelencser, A., Kasper-Giebl, A., and Laj, P. (2007).Origin of C-2-C-5 Dicarboxylic Acids in the European Atmosphere Inferred from Year-Round Aerosol Study Conducted at a West-East Transect, *Journal of Geophysical Research-Atmospheres*, *112* (D23), 14.

Li, J., Posfai, M., Hobbs, P. V., and Buseck, P. R. (2003).Individual Aerosol Particles from Biomass Burning in Southern Africa: 2. Compositions and Aging of Inorganic Particles, *Journal of Geophysical Research, 108(D13)* (8484), doi:10.1029/2002JD002310.

Lighty, J. S., Veranth, J. M., and Sarofim, A. F. (2000).Combustion Aerosols: Factors Governing Their Size and Composition and Implications to Human Health, *Journal of the Air & Waste Management Association, 50* (9), 1565-1618.

Liu, X. D., Van Espen, P., Adams, F., Cafmeyer, J., and Maenhaut, W. (2000).Biomass Burning in Southern Africa: Individual Particle Characterization of Atmospheric Aerosols and Savanna Fire Samples, *Journal of Atmospheric Chemistry, 36* (2), 135-155.

Lobert, J. M., Scharffe, D. H., Hao, W. M., Kuhlbusch, T. A., Seuwen, R., Warneck, P., and P.J., C. (1991). Experimental Evaluation of Biomass Burning Emissions: Nitrogen and Carbon Containing Compounds, in *Global Biomass Burning: Atmospheric, Climatic and Biospheric Implications*, edited by J.S. Levine, pp. 289-304, MIT Press, Cambridge.

Ma, Y. L., and Hays, M. D. (2008).Thermal Extraction-Two-Dimensional Gas Chromatography-Mass Spectrometry with Heart-Cutting for Nitrogen Heterocyclics in Biomass Burning Aerosols, *Journal of Chromatography A, 1200* (2), 228-234.

Mace, K. A., Artaxo, P., and Duce, R. A. (2003).Water-Soluble Organic Nitrogen in Amazon Basin Aerosols During the Dry (Biomass Burning) and Wet Seasons, *Journal of Geophysical Research-Atmospheres, 108* (D16), 10.

Mazzoleni, L. R., Zielinska, B., and Moosmueller, H. (2007).Emissions of Levoglucosan, Methoxy Phenols, and Organic Acids from Prescibed Burns, Laboratory Combustion of Wildland Fuels, and Residential Wood Combustion, *Environmental Science & Technology, 41* (7), 2115-2122.

McGuire, M. L., Jeong, C. H., Slowik, J. G., Chang, R. Y. W., Corbin, J. C., Lu, G., Mihele, C., Rehbein, P. J. G., Sills, D. M. L., Abbatt, J. P. D., Brook, J. R., and Evans, G. J. (2011).Elucidating Determinants of Aerosol Composition through Particle-Type-Based Receptor Modeling, *Atmospheric Chemistry and Physics, 11* (15), 8133-8155.

Miyazaki, Y., Aggarwal, S. G., Singh, K., Gupta, P. K., and Kawamura, K. (2009).Dicarboxylic Acids and Water-Soluble Organic Carbon in Aerosols in New Delhi, India, in Winter: Characteristics and Formation Processes, *Journal of Geophysical Research-Atmospheres, 114*, 12.

Moffet, R. C., de Foy, B., Molina, L. T., Molina, M. J., and Prather, K. A. (2008).Measurement of Ambient Aerosols in Northern Mexico City by Single Particle Mass Spectrometry, *Atmospheric Chemistry and Physics, 8*, 4499-4516.

Moore, M. J. K., Sullivan, R. C., Roberts, G. C., Wang, Y., Zauscher, M. D., and Prather, K. A. (2012).A Comparison of Single Particle Mixing State and Ccn Activity During the 2007 and 2008 San Diego Wildfires, *in preparation*.

Muhle, J., Lueker, T. J., Su, Y., Miller, B. R., Prather, K. A., and Weiss, R. F. (2007).Trace Gas and Particulate Emissions from the 2003 Southern California Wildfires, *Journal of Geophysical Research-Atmospheres*, *112* (D3).

Narukawa, M., Kawamura, K., Takeuchi, N., and Nakajima, T. (1999).Distribution of Dicarboxylic Acids and Carbon Isotopic Compositions in Aerosols from 1997 Indonesian Forest Fires, *Geophysical Research Letters*, *26* (20), 3101-3104.

Neubauer, K. R., Johnston, M. V., and Wexler, A. S. (1998).Humidity Effects on the Mass Spectra of Single Aerosol Particles, *Atmospheric Environment*, *32* (14-15), 2521-2529.

Noble, C. A., and Prather, K. A. (1996).Real-Time Measurement of Correlated Size and Composition Profiles of Individual Atmospheric Aerosol Particles, *Environmental Science & Technology*, *30* (9), 2667-2680.

Noblitt, S. D., Lewis, G. S., Liu, Y., Hering, S. V., Collett, J. L., and Henry, C. S. (2009).Interfacing Microchip Electrophoresis to a Growth Tube Particle Collector for Semicontinuous Monitoring of Aerosol Composition, *Analytical Chemistry*, *81* (24), 10029-10037.

Paatero, P., Hopke, P. K., Begum, B. A., and Biswas, S. K. (2005).A Graphical Diagnostic Method for Assessing the Rotation in Factor Analytical Models of Atmospheric Pollution, *Atmospheric Environment*, *39* (1), 193-201.

Park, R. J., Jacob, D. J., and Logan, J. A. (2007).Fire and Biofuel Contributions to Annual Mean Aerosol Mass Concentrations in the United States, *Atmospheric Environment*, *41* (35), 7389-7400.

Penner, J. E., Dickinson, R. E., and Oneill, C. A. (1992).Effects of Aerosol from Biomass Burning on the Global Radiation Budget, *Science*, *256* (5062), 1432-1434.

Petters, M. D., Carrico, C. M., Kreidenweis, S. M., Prenni, A. J., DeMott, P. J., Collett, J. L., and Moosmuller, H. (2009a).Cloud Condensation Nucleation Activity of Biomass Burning Aerosol, *Journal of Geophysical Research-Atmospheres*, *114*, 16.

Petters, M. D., Parsons, M. T., Prenni, A. J., DeMott, P. J., Kreidenweis, S. M., Carrico, C. M., Sullivan, A. P., McMeeking, G. R., Levin, E., Wold, C. E., Collett, J. L., and Moosmueller, H. (2009b).Ice Nuclei Emissions from Biomass Burning, *Journal of Geophysical Research*, *114* (D07209), doi:10.1029/2008JD011532.

Pfister, G. G., Wiedinmyer, C., and Emmons, L. K. (2008).Impacts of the Fall 2007 California Wildfires on Surface Ozone: Integrating Local Observations with Global Model Simulations, *Geophysical Research Letters*, *35* (19), 5.

Phuleria, H. C., Fine, P. M., Zhu, Y. F., and Sioutas, C. (2005).Air Quality Impacts of the October 2003 Southern California Wildfires, *Journal of Geophysical Research-Atmospheres*, *110* (D7).

Polissar, A. V., Hopke, P. K., and Paatero, P. (1998).Atmospheric Aerosol over Alaska - 2. Elemental Composition and Sources, *Journal of Geophysical Research-Atmospheres*, *103* (D15), 19045-19057.

Posfai, M., Simonics, R., Li, J., Hobbs, P. V., and Buseck, P. R. (2003).Individual Aerosol Particles from Biomass Burning in Southern Africa: 1. Compositions and Size Distributions of Carbonaceous Particles, *Journal of Geophysical Research*, *108* (D13), 8483, doi:10.1029/2002JD002291.

Pratt, K. A., DeMott, P. J., French, J. R., Wang, Z., Westphal, D. L., Heymsfield, A. J., Twohy, C. H., Prenni, A. J., and Prather, K. A. (2009).In Situ Detection of Biological Particles in Cloud Ice-Crystals, *Nature Geoscience*, *2* (6), 397-400.

Pratt, K. A., Heymsfield, A. J., Twohy, C. H., Murphy, S. M., DeMott, P. J., Hudson, J. G., Subramanian, R., Wang, Z. E., Seinfeld, J. H., and Prather, K. A. (2010).In Situ Chemical Characterization of Aged Biomass-Burning Aerosols Impacting Cold Wave Clouds, *Journal of the Atmospheric Sciences*, *67* (8), 2451-2468.

Pratt, K. A., Murphy, S. M., Subramanian, R., DeMott, P. J., Kok, G. L., Campos, T., Rogers, D. C., Prenni, A. J., Heymsfield, A. J., Seinfeld, J. H., and Prather, K. A. (2011).Flight-Based Chemical Characterization of Biomass Burning Aerosols within Two Prescribed Burn Smoke Plumes, *Atmospheric Chemistry and Physics*, *11* (24), 12549-12565.

Ramgolam, K., Favez, O., Cachier, H., Gaudichet, A., Marano, F., Martinon, L., and Baeza-Squiban, A. (2009).Size-Partitioning of an Urban Aerosol to Identify Particle Determinants Involved in the Proinflammatory Response Induced in Airway Epithelial Cells, *Particle and Fibre Toxicology*, *6*, 12.

Reff, A., Eberly, S. I., and Bhave, P. V. (2007).Receptor Modeling of Ambient Particulate Matter Data Using Positive Matrix Factorization: Review of Existing Methods, *Journal of the Air & Waste Management Association*, *57* (2), 146-154.

Rehbein, P. J. G., Jeong, C. H., McGuire, M. L., Yao, X. H., Corbin, J. C., and Evans, G. J. (2011).Cloud and Fog Processing Enhanced Gas-to-Particle Partitioning of Trimethylamine, *Environmental Science & Technology*, *45* (10), 4346-4352.

Reid, J. S., Koppmann, R., Eck, T. F., and Eleuterio, D. P. (2005).A Review of Biomass Burning Emissions Part Ii: Intensive Physical Properties of Biomass Burning Particles, *Atmospheric Chemistry and Physics*, *5*, 799-825.

Roberts, G. C., Nenes, A., Seinfeld, J. H., and Andreae, M. O. (2003).Impact of Biomass Burning on Cloud Properties in the Amazon Basin, *Journal of Geophysical Research-Atmospheres*, *108* (D2), 19.

Roberts, J. M., Veres, P. R., Cochran, A. K., Warneke, C., Burling, I. R., Yokelson, R. J., Lerner, B., Gilman, J. B., Kuster, W. C., Fall, R., and de Gouw, J. (2011).Isocyanic Acid in the Atmosphere and Its Possible Link to Smoke-Related Health Effects, *Proceedings of the National Academy of Sciences of the United States of America*, *108* (22), 8966-8971.

Schwartz, J., and Neas, L. M. (2000).Fine Particles Are More Strongly Associated Than Coarse Particles with Acute Respiratory Health Effects in Schoolchildren, *Epidemiology*, *11* (1), 6-10.

Silva, P. J. (2000). Source Profiling and Apportionment of Airborne Particles: A New Approach Using Aerosol Time-of-Flight Mass Spectrometry, University of California Riverside, Riverside.

Silva, P. J., Liu, D., Noble, C. A., and Prather, K. A. (1999).Size and Chemical Characterization of Individual Particles Resulting from Biomass Burning of Local Southern California Species, *Environmental Science & Technology*, *33* (18), 3068-3076.

Silva, P. J., and Prather, K. A. (2000).Interpretation of Mass Spectra from Organic Compounds in Aerosol Time-of-Flight Mass Spectrometry, *Analytical Chemistry*, *72* (15), 3553-3562.

Simoneit, B. R. T., Schauer, J. J., Nolte, C. G., Oros, D. R., Elias, V. O., Fraser, M. P., Rogge, W. F., and Cass, G. R. (1999).Levoglucosan, a Tracer for Cellulose in Biomass Burning and Atmospheric Particles, *Atmospheric Environment*, *33* (2), 173-182.

Simpson, I. J., Akagi, S. K., Barletta, B., Blake, N. J., Choi, Y., Diskin, G. S., Fried, A., Fuelberg, H. E., Meinardi, S., Rowland, F. S., Vay, S. A., Weinheimer, A. J., Wennberg, P. O., Wiebring, P., Wisthaler, A., Yang, M., Yokelson, R. J., and Blake, D. R. (2011).Boreal Forest Fire Emissions in Fresh Canadian Smoke Plumes: C(1)-C(10) Volatile Organic Compounds (Vocs), Co(2), Co, No(2), No, Hcn and Ch(3)Cn, *Atmospheric Chemistry and Physics*, *11* (13), 6445-6463.

Smith, S. J., van Aardenne, J., Klimont, Z., Andres, R. J., Volke, A., and Arias, S. D. (2011).Anthropogenic Sulfur Dioxide Emissions: 1850-2005, *Atmospheric Chemistry and Physics*, *11* (3), 1101-1116.

Song, C. H., Ma, Y., Orsini, D., Kim, Y. P., and Weber, R. J. (2005).An Investigation into the Ionic Chemical Composition and Mixing State of Biomass Burning Particles Recorded During Trace-P P3b Flight # 10, *Journal of Atmospheric Chemistry*, *51* (1), 43-64.

Song, X. H., Hopke, P. K., Fergenson, D. P., and Prather, K. A. (1999).Classification of Single Particles Analyzed by Atofms Using an Artificial Neural Network, Art-2a, *Analytical Chemistry*, *71* (4), 860-865.

Spencer, M. T., and Prather, K. A. (2006).Using Atofms to Determine Oc/Ec Mass Fractions in Particles, *Aerosol Science and Technology*, *40* (8), 585-594.

Stelson, A. W., and Seinfeld, J. H. (1982a).Relative-Humidity and Ph-Dependence of the Vapor-Pressure of Ammonium-Nitrate Nitric Acid-Solutions at 25-Degrees-C, *Atmospheric Environment*, *16* (5), 993-1000.

Stelson, A. W., and Seinfeld, J. H. (1982b).Relative Humidity and Temperature Dependence of the Ammonium Nitrate Dissociation Constant, *Atmospheric Environment*, *16* (5), 983-992.

Stoelzel, M., Breitner, S., Cyrys, J., Pitz, M., Woelke, G., Kreyling, W., Heinrich, J., Wichmann, H. E., and Peters, A. (2007).Daily Mortality and Particulate Matter in Different Size Classes in Erfurt, Germany, *Journal of Exposure Science and Environmental Epidemiology*, *17* (5), 458-467.

Streets, D. G., Yarber, K. F., Woo, J. H., and Carmichael, G. R. (2003).Biomass Burning in Asia: Annual and Seasonal Estimates and Atmospheric Emissions, *Global Biogeochemical Cycles*, *17* (4), 20.

Su, Y. X., Sipin, M. F., Furutani, H. F., and Prather, K. A. (2004).Development and Characterization of an Aerosol Time-of-Flight Mass Spectrometer with Increased Detection Efficiency, *Analytical Chemistry*, *76*, 712-719.

Sullivan, A. P., Holden, A. S., Patterson, L. A., McMeeking, G. R., Kreidenweis, S. M., Malm, W. C., Hao, W. M., Wold, C. E., and Collett, J. L. (2008).A Method for Smoke Marker Measurements and Its Potential Application for Determining the Contribution of Biomass Burning from Wildfires and Prescribed Fires to Ambient Pm2.5 Organic Carbon, *Journal of Geophysical Research*, *113* (D22302), doi:10.1029/2008JD010216.

Sullivan, R. C., and Prather, K. A. (2007).Investigations of the Diurnal Cycle and Mixing State of Oxalic Acid in Individual Particles in Asian Aerosol Outflow, *Environmental Science & Technology*, *41* (23), 8062-8069.

Talbot, R. W., Bradshaw, J. D., Sandholm, S. T., Singh, H. B., Sachse, G. W., Collins, J., Gregory, G. L., Anderson, B., Blake, D., Barrick, J., Browell, E. V., Klemm, K. I., Lefer, B. L., Klemm, O., Gorzelska, K., Olson, J., Herlth, D., and Ohara, D. (1994).Summertime Distribution and Relations of Reactive Odd Nitrogen Species and Noy in the Troposphere over Canada, *Journal of Geophysical Research-Atmospheres*, *99* (D1), 1863-1885.

Timonen, H., Aurela, M., Carbone, S., Saarnio, K., Saarikoski, S., Makela, T., Kulmala, M., Kerminen, V. M., Worsnop, D. R., and Hillamo, R. (2010).High Time-

Resolution Chemical Characterization of the Water-Soluble Fraction of Ambient Aerosols with Pils-Toc-Ic and Ams, *Atmospheric Measurement Techniques*, *3* (4), 1063-1074.

Toner, S. M., Sodeman, D. A., and Prather, K. A. (2006).Single Particle Characterization of Ultrafine and Accumulation Mode Particles from Heavy Duty Diesel Vehicles Using Aerosol Time-of-Flight Mass Spectrometry, *Environmental Science & Technology*, *40* (12), 3912-3921.

USEPA (2008). Epa Positive Matrix Factorization (Pmf) 3.0 Fundamentals & User Guide, USEPA Office of Research and Development.

Veres, P., Roberts, J. M., Burling, I. R., Warneke, C., de Gouw, J., and Yokelson, R. J. (2010).Measurements of Gas-Phase Inorganic and Organic Acids from Biomass Fires by Negative-Ion Proton-Transfer Chemical-Ionization Mass Spectrometry, *Journal of Geophysical Research-Atmospheres*, *115*, 15.

Viswanathan, S., Eria, L., Diunugala, N., Johnson, J., and McClean, C. (2006).An Analysis of Effects of San Diego Wildfire on Ambient Air Quality, *Journal of the Air & Waste Management Association*, *56* (1), 56-67.

Vlasenko, A., Sjogren, S., Weingartner, E., Stemmler, K., Gaggeler, H. W., and Ammann, M. (2006).Effect of Humidity on Nitric Acid Uptake to Mineral Dust Aerosol Particles, *Atmospheric Chemistry and Physics*, *6*, 2147-2160.

Warneck, P. (1999).The Relative Importance of Various Pathways for the Oxidation of Sulfur Dioxide and Nitrogen Dioxide in Sunlit Continental Fair Weather Clouds, *Physical Chemistry Chemical Physics*, *1* (24), 5471-5483.

Westerling, A. L., Hidalgo, H. G., Cayan, D. R., and Swetnam, T. W. (2006).Warming and Earlier Spring Increase Western Us Forest Wildfire Activity, *Science*, *313* (5789), 940-943.

Worton, D. R., Kreisberg, N. M., Isaacman, G., Teng, A. P., McNeish, C., Gorecki, T., Hering, S. V., and Goldstein, A. H. (2012).Thermal Desorption Comprehensive Two-Dimensional Gas Chromatography: An Improved Instrument for in-Situ Speciated Measurements of Organic Aerosols, *Aerosol Science and Technology*, *46* (4), 380-393.

Yamasoe, M. A., Artaxo, P., Miguel, A. H., and Allen, A. G. (2000).Chemical Composition of Aerosol Particles from Direct Emissions of Vegetation Fires in the Amazon Basin: Water-Soluble Species and Trace Elements, *Atmospheric Environment*, *34*, 1641-1653.

Yang, F., Chen, H., Wang, X. N., Yang, X., Du, J. F., and Chen, J. M. (2009).Single Particle Mass Spectrometry of Oxalic Acid in Ambient Aerosols in Shanghai: Mixing State and Formation Mechanism, *Atmospheric Environment*, *43* (25), 3876-3882.

Yokelson, R., Crounse, J. D., DeCarlo, P., Karl, T., Urbanski, S., Atlas, E., Campos, T., Shinozuka, Y., Kapustin, V. N., Clarke, A. D., Weinheimer, A., Knapp, D. J., Montzka, D. D., Holloway, J., Weibring, P., Flocke, F., Zheng, W., Toohey, D., Wennberg, P. O., Wiedinmyer, C., Mauldin, L., Freid, A., Richter, D., Walega, J., Jimenez, J. L., Adachi, K., Buseck, P. R., Hall, S. R., and Shetter, R. (2009).Emissions from Biomass Burning in the Yucatan, *Atmospheric Chemistry and Physics*, *9*, 5785-5812.

Yokelson, R. J., Susott, R., Ward, D. E., Reardon, J., and Griffith, D. W. T. (1997).Emissions from Smoldering Combustion of Biomass Measured by Open-Path Fourier Transform Infrared Spectroscopy, *Journal of Geophysical Research-Atmospheres*, *102* (D15), 18865-18877.

Yu, S. C. (2000).Role of Organic Acids (Formic, Acetic, Pyruvic and Oxalic) in the Formation of Cloud Condensation Nuclei (Ccn): A Review, *Atmospheric Research*, *53* (4), 185-217.

Zauscher, M. D., Moore, M. J. K., Lewis, G. S., Hering, S. V., and Prather, K. A. (2011).Approach for Measuring the Chemistry of Individual Particles in the Size Range Critical for Cloud Formation, *Analytical Chemistry*, *83* (6), 2271-2278.

Zhou, Y. M., Zhong, C. Y., Kennedy, I. M., Leppert, V. J., and Pinkerton, K. E. (2003).Oxidative Stress and Nf Kappa B Activation in the Lungs of Rats: A Synergistic Interaction between Soot and Iron Particles, *Toxicology and Applied Pharmacology*, *190* (2), 157-169.

Chapter 6. Impact of Central Valley emissions on local aerosols sampled at San Pedro Bay Ports

6.1 Abstract

Port communities are heavily impacted by air pollution from multiple sources. In an effort to understand the health effects of particles produced from shipping and trucking emissions, measurements of the size-resolved chemical mixing state of individual 100-1300 nm particles using aerosol time-of-flight mass spectrometry were carried out at the San Pedro Bay Ports in May, 2011. The main particle types observed were soot particles internally mixed with organic carbon aged to varying degrees and biomass burning aerosol, in addition to minor contributions from ships, organic carbon, and sea salt particles. Locally produced fresh soot and diesel particles from trucks comprised > 40% by number of all 100-200 nm particles. Surprisingly, 59% of all ambient particles measured contained amine markers, which is significant due to the adverse health problems attributed to amines. The air mass back trajectories indicate that transport pollution from the Central Valley was one source of amines at the port complex, which was unexpected and has not been shown before. Additionally, particulate trimethylamine spiked during a clean marine period suggesting a local, yet unknown, source of amines. During this study, amines partitioned to the particulate phase as alkylaminium sulfate salts. Identifying the sources of amines and understanding their partitioning to the particle phase is important in order to accurately predict regional air quality.

6.2 Introduction

Emissions from ocean-faring ships contribute to aerosol loadings in port regions and are known to induce negative health effects (Agrawal et al., 2009; Ariola et al.,

2008; Contini et al., 2011; Minguillon et al., 2008; Pandolfi et al., 2011). Modeling studies have concluded that 60,000-87,000 premature deaths can be attributed to shipping emissions worldwide (Corbett et al., 2007; Winebrake et al., 2009). The largest port complex in the U.S. is the combination of the neighboring Port of Los Angeles and Port of Long Beach, known as the San Pedro Bay Ports (SPBP), through which more than 40% of all U.S. containerized imports enter the country with imports projected to double by 2020 (Geske, 2006). In addition to shipping emissions, communities downwind of SPBP have been found to be heavily impacted by heavy duty diesel truck (HDDT) emissions (Kozawa et al., 2009). Diesel exhaust has been designated as a carcinogen, while diesel particulate matter has been identified as a toxic air contaminant that can affect lung function and exacerbate cardiovascular problems (Kagawa, 2002; McCreanor et al., 2007; Scheepers and Bos, 1992). In addition, epidemiological studies have concluded that premature cardiopulmonary mortality is associated with living near a major roadway (Hoek et al., 2002). Furthermore, preterm birth and low birth weight have both been correlated with traffic related air toxics in Los Angeles (Wilhelm et al., 2011; Wilhelm et al., 2012).

Recent changes in fuel and emission regulations have improved air quality significantly at ports in California. Specifically, the requirement of ocean-faring ships to switch to low sulfur marine diesel oil (MDO) from high sulfur heavy fuel oil (HFO) within 44.5 km of the California coast and the speed reduction program have reduced the emissions of total particulate matter, particulate matter containing heavy metals and sulfate, and black carbon (BC) (Geske, 2006; Khan et al., 2012; Lack et al., 2011). HFO fuel contains high concentrations of heavy metals, such as vanadium and nickel, naturally present in crude oil that are concentrated during the refining process (Allouis et al., 2003). Particulate matter with vanadium and nickel, which appear to act synergistically, has been associated with cardiovascular problems (Campen et al., 2001; Zhang et al., 2009). In addition to declining ship emissions, the truck emission control regulations at Californian ports have drastically reduced overall $PM_{2.5}$, BC, NO_x and CO emissions by accelerating fleet turnover and the retrofitting of older trucks with diesel particulate filters (Bishop et al., 2012; Dallmann et al., 2011). However, Bishop

et al. (2012) observed a 20% increase in ammonia gas emissions at SPBP due to replacement of 11% of HDDT with liquefied natural gas trucks. Both the emission reductions from regulating ship fuel and speed close to the populated SPBP region and the overall reduction in HDDT emissions should lead to improved health benefits in the local communities (Winebrake et al., 2009). However, as the number of ships and trucks at the port complex continues to increase in time due to increased commerce, attention to the emissions must continue as well.

Once these particles are emitted, their chemical composition can change with time through condensation, coagulation, photochemistry, and heterogeneous reactions with other gas phase species and particles in the atmosphere. The acquisition of other chemical components will lead to alteration of the particle's chemical and physical properties, potentially altering its toxicology. Herein we report measurements of size-resolved chemical mixing state of particles sampled at SPBP during May, 2011. Surprisingly, a large fraction of combustion-generated aerosol was found to be mixed with organic nitrogen, such as amines. These particles are of interest because organic nitrogen species are known to cause adverse health effects, including clotting (McGuinnes et al., 2011; Nemmar et al., 2002), difficulty breathing, and cancer (Albrecht and Stephenson, 1988; de Vocht et al., 2009; Greim et al., 1998; Pira et al., 2010). Attempts were made to identify the sources of the observed organic nitrogen.

6.3 **Experimental Set-Up**

Sampling was performed at the Southern California Marine Institute (SCMI) situated on the western side of Terminal Island on the SPBP; this is the same location as a previous study from our group (Ault et al., 2010), where more information about the site can be found. Data presented herein was collected over the period 5/12/11-5/16/11. The size distributions of 10-590 nm particles were measured every five minutes with a scanning mobility particle sizer (SMPS, TSI 3936) and 0.6-20 μm particles every minute with an aerodynamic particle sizer (APS, TSI, 3321). In addition, meteorological data, $PM_{2.5}$, O_3, and NO_2 data from the SPBP clean air action plan (CAAP) monitoring sites was obtained from http://caap.airsis.com/. Air mass

trajectories were modeled every 2 hours for 60 hours backwards in time starting at SCMI with HYSPLIT 4.0 at 500 m above ground level (Draxler and Hess, 1998). The resulting trajectories were clustered within the HYSPLIT program yielding 5 separate back trajectory periods. The mean and 95% confidence interval were calculated from all the trajectories in each cluster.

Real-time single particle chemistry and size were measured with an ultrafine aerosol time-of-flight mass spectrometer (ATOFMS) (Su et al., 2004). This version of the instrument has an aerodynamic focusing lens that collimates the particles as they enter, allowing particles 100-1500 nm to be detected. After passing the lens, particles

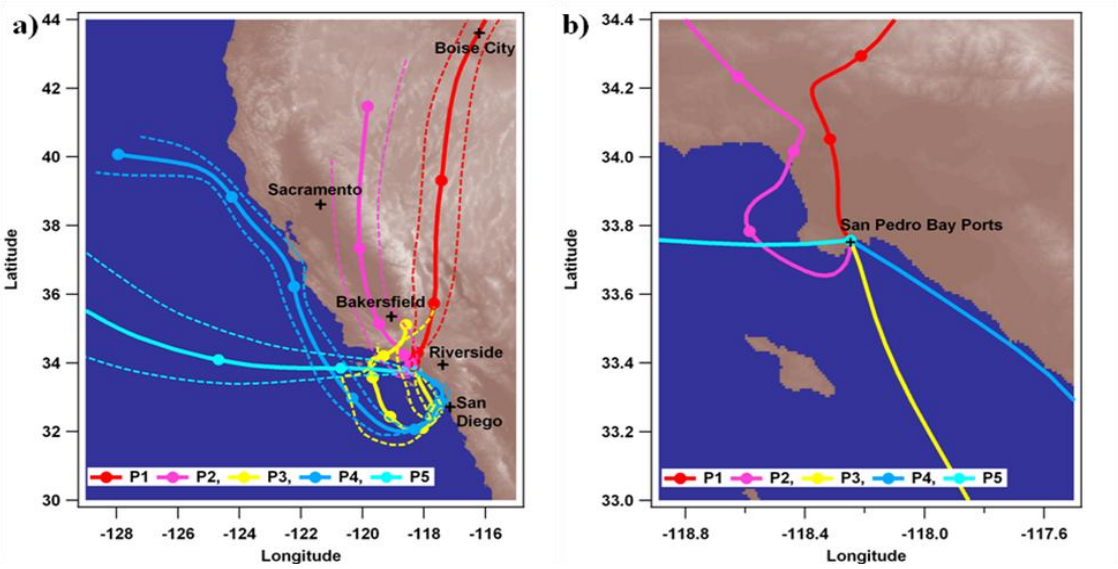

Figure 6.1: Figure 1: HYSPLIT back trajectories clustered into 5 periods (P) with a) zoomed out with 95% confidence intervals (given by dashed lines), and b) zoomed in. Every dot marker on the trajectories represents 12 hours.

cross the beams of two 532-nm wavelength continuous wave lasers, used to calculate speed and particle size, which sets the timing of a pulsed 266-nm laser that desorbs and ionizes the particle constituents. A dual-polarity reflectron time-of-flight mass spectrometer records positive and negative mass spectra from these generated ions.

ATOFMS data were analyzed with the YAADA (http://www.yaada.org) Matlab toolkit and clustered according to similar mass spectral patterns with the neural network algorithm ART-2a using vigilance factor of 0.85, learning rate of 0.05 and iteration number of 20 (Song et al., 1999). ART-2a clusters were further combined manually into 10 main particle types based on similar ion patterns of varying intensities: diesel, soot, soot mixed with organic carbon (soot-OC), soot-OC aged, OC, organic nitrogen (ON), biomass burning aerosol (BBA), sea salt, heavy fuel oil (HFO), and other. Potassium, sodium, aluminum, and iron rich particles were combined into the "other" category since they represented a minor fraction of total aerosol (<5%) throughout this study. A total of 820,675 particles were clustered in this study of which over 98% were chemically identified. Nearly 33% of total particles had dual-polarity mass spectra. Typically, positive mass spectra allow identification of the particle type, whereas the ion negative spectra yield evidence on the extent and type of atmospheric processing the particle has undergone. When particles are wet, either due to high ambient relative humidity or chemical processing, they tend to produce fewer negative ion spectra (Neubauer et al., 1998). Peak identifications herein correspond to the most probable ion per mass-to-charge (*m/z*). Previous ATOFMS studies have identified $^{59}N(CH_3)_3^+$ as the molecular ion of trimethylamine (TMA), and both $^{58}NHCH_2C_2H_5^+$ and $^{86}NCH_2(C_2H_5)_2^+$ as a stable fragments resulting from the desorption/ionization of other alkylamines, including dimethylamine (DMA), triethylamine (TEA), and diethylamine (DEA) (Angelino et al., 2001; Rehbein et al., 2011). Relative peak areas (RPA), which are the normalized peak intensities of a specific ion to the total peak areas of the whole mass spectrum, were used in this study to identify particles containing amines. ATOFMS data is presented in 30-minute averages.

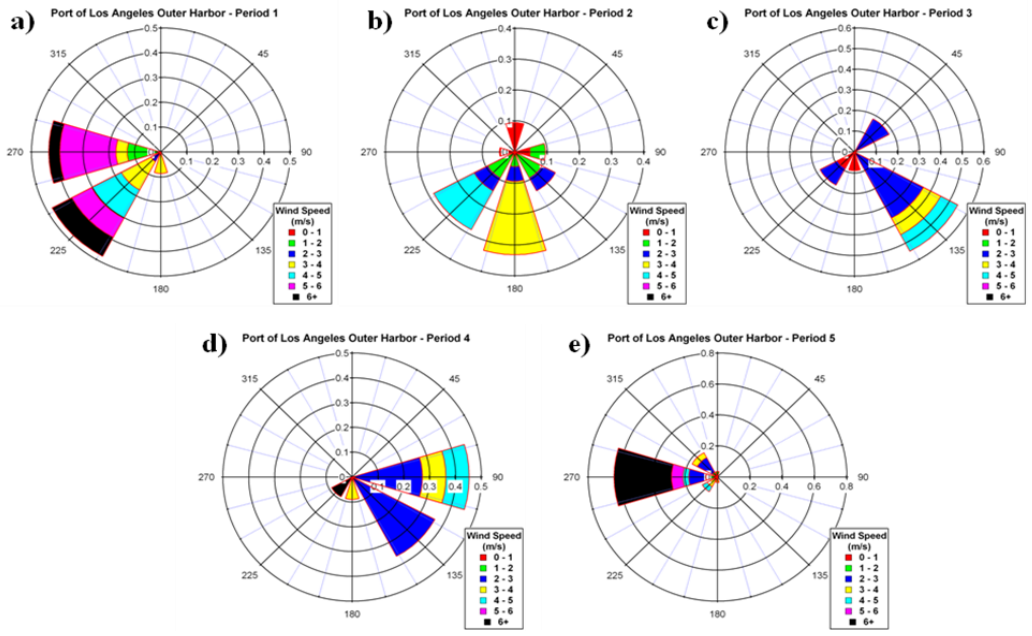

Figure 6.2 Wind rose plots showing wind direction with color representing wind speed during a) Period 1, b) Period 2, c) Period 3, d) Period 4, and e) Period 5.

6.4 Results and Discussion

Figure 3.1 shows the average air mass back trajectory per cluster calculated with HYSPLIT (Draxler and Hess, 1998). Although this was a short study in duration, there were five distinct periods identified by back trajectory clusters. Period 1 (P1) was between 5/11 23:00 - 5/12 21:00 during which time the air came through Nevada and eastern California. During period 2 (P2, 5/12 23:00 - 5/13 17:00), the air passed through California's Central Valley, which is one of the most productive agricultural areas in the world and is known to have some of the most polluted levels of $PM_{2.5}$ and smog in the U.S. (Hall et al., 2008). Period 3 (P3), from 5/13 19:00 - 5/14 03:00, was characterized by stagnant conditions. During period 4 (P4), between 5/14 05:00 - 5/14 13:00, the air mass back trajectories originated near the northern California coast and proceeded along the California coast with a loop through San Diego before reaching SPBP. Period 5 (P5) was from 5/15 03:00 - 5/16 12:00 and came directly from the Pacific Ocean. Because

the air mass back trajectories between 5/14/11 15:00- 5/15/11 1:00 varied significantly, this time was not assigned to a period.

The wind rose plots, shown in Figure 6.2, illustrate the frequency of wind direction and speed, for each period identified through the air mass back trajectories. The air mass back trajectories of periods 2-5 depicted in Figure 3.1b correspond with the dominant wind direction measured near the sampling site as shown in Figure 6.2. However, the wind direction in period 1 does not seem to match the air mass back trajectory, which is likely due to a discrepancy of the winds at 500 m used in the

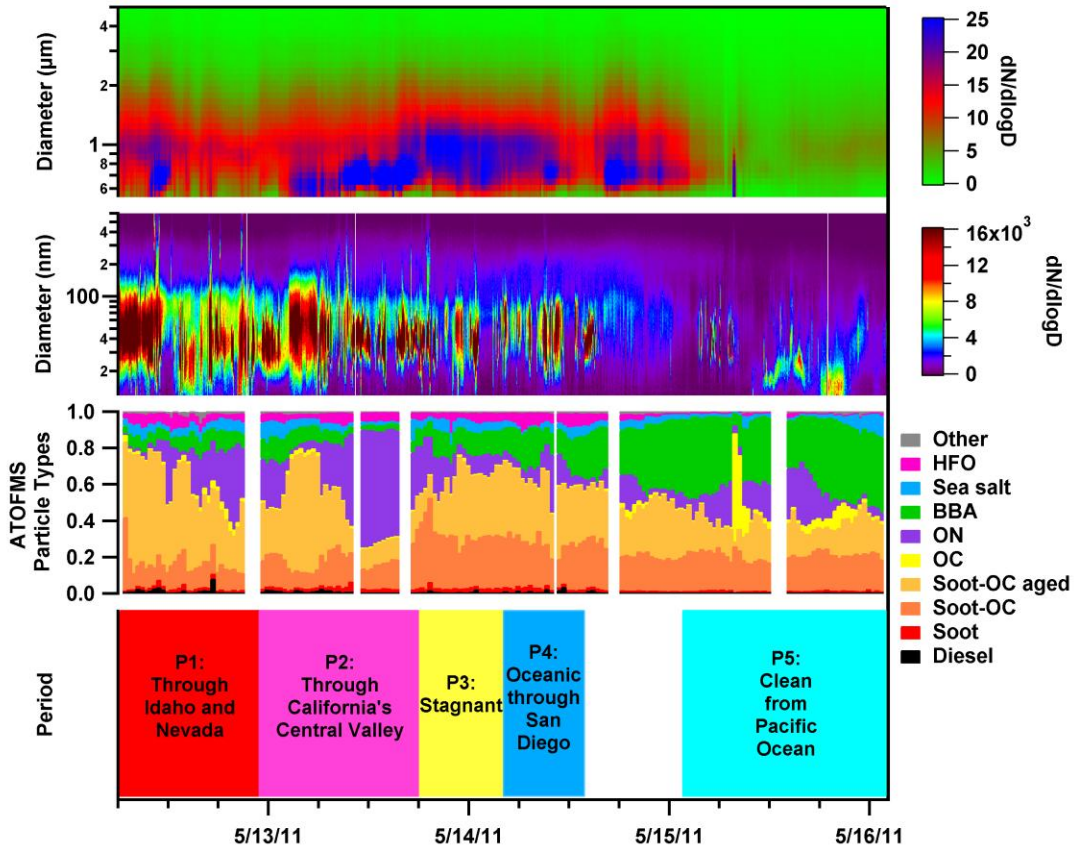

Figure 6.3: Size distributions of aerosols and ATOFMS relative fraction of particle types with periods highlighted. HFO = high fuel oil, BBA = biomass burning aerosol, ON = organic nitrogen, and OC = organic carbon

HYSPLIT model compared to the surface winds measured by the CAAP air quality monitoring network.

6.4.1 **Overall particle temporal and size trends**

Figure 3.2 shows the temporal distribution of particle size and composition with each period identified. Between 5/12/11-5/15/11 the ultrafine (<100 nm) particle counts were high and did not follow any diurnal trend indicating a significant contribution of local emissions from trucks and ships as expected for the SPBP complex (Moore et al., 2009). Port operations are being expanded to run 24-hours 7-days a week, although fewer trucks were visible during late night hours and the weekend (5/14-5/15), as confirmed by decreased particle concentrations during these times in Figure 3.2. Particles 0.6-2.5 μm, which typically have undergone more atmospheric processing than smaller particles, also did not exhibit any diurnal patterns and were more concentrated until 5/15/11. After 5/15/11 and coinciding with the period of air coming directly from the Pacific Ocean, the air was clean with low particle counts at all sizes compared to the rest of the study. Again, no daily trend was observed with the ATOFMS-derived particle types. Average mass spectra of each particle type are shown in Figure 6.4. It should be noted that during this study the negative ion mass spectra had significant interference noise from intense positive ions, referred to as cross talk (CT), perhaps due to the negative ion detector surface being considerably degraded.

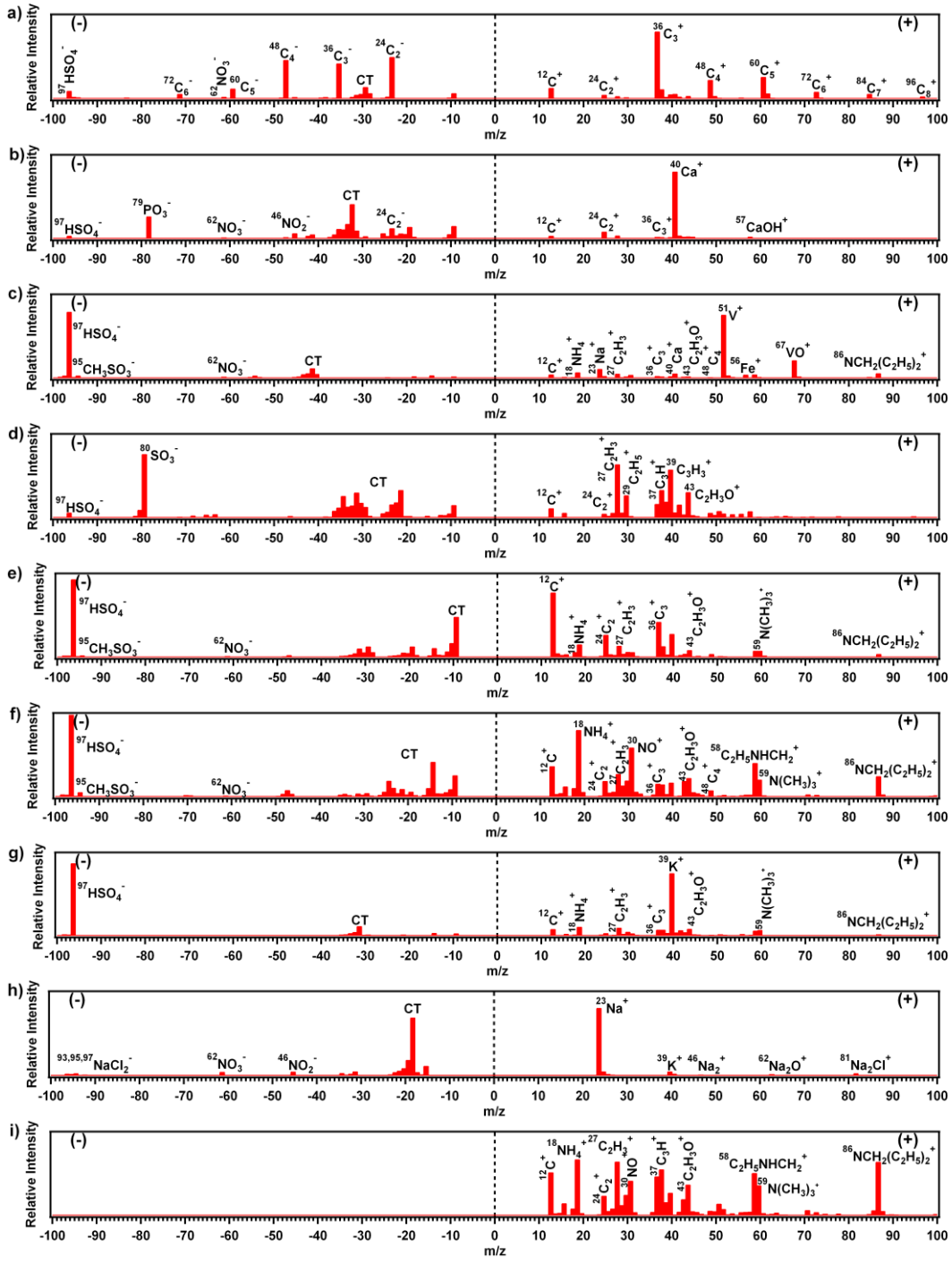

Figure 6.4 Average mass spectra for each of the particle types observed in this study. a) soot, b) diesel, c) ships burning heavy fuel oil, d) organic carbon (OC), e) soot-OC, f) soot-OC aged, g) biomass burning, h) sea salt, and i) organic nitrogen. CT = cross talk, which is interference from ions in the opposite polarity.

Soot particles, identified by $C_n^{+/-}$ clusters internally mixed with sulfate ($^{97}HSO_4^-$), are indicative of all types of combustion, including diesel and gasoline powered vehicles. Particles emitted from HDDT have previously been identified as soot particles with a strong calcium ion ($^{40}Ca^+$) peak internally mixed with phosphate ($^{79}PO_3^-$), and are referred to as diesel herein because they are also be produced from ships burning low sulfur fuel (Ault et al., 2010; Toner et al., 2006); thus the diesel and soot particles measured in this study were likely emitted from HDDT and ships within and near the port complex. Over 40% of 100-200 nm particles sampled at SPBP were fresh soot and diesel, as shown in Figure 3.3; if the ATOFMS had sampled particles < 100 nm, this percentage would have been larger because most particles emitted from combustion engines are typically ultrafine (Burtscher, 2005; Lighty et al., 2000).

Carbonaceous particles with intense $^{51}V^+$ and $^{67}VO^+$ peaks have been previously identified as those originating from ships burning HFO, which has the higher content of vanadium than MDO (Ault et al., 2010; Healy et al., 2009). The size distribution of these ship particles spans almost the whole range from 160-1300 nm, whereas particles emitted from ships are typically ultrafine (Murphy et al., 2009). Thus, the ship particles detected were likely emitted from the ocean-faring ships outside the 44.5 km low sulfur regulation limit and transported to the sampling site during which they were atmospherically processed; smaller contributions from ship emissions closer to the port burning low sulfur fuel but with leftover HFO in the fuel and engine system after the switch to low sulfur fuel are also possible (Gaston et al., 2012a; Lack et al., 2011). Most ship particles were internally mixed with ammonium ($^{18}NH_4^+$), nitrate ($^{30}NO^+$), and $^{97}HSO_4^-$ confirming that they were aged. Only 4% of all sampled particles at SPBP were identified as being emitted from ships. Fewer vanadium-rich ship particles were observed during this study than at the same site in 2007 most likely due to regulatory changes (2009) for ships near the California coast, as further investigated in (Gaston et al., 2012a).

The OC particle type was characterized by intense peaks at $^{27}C_2H_3^+$, $^{29}C_2H_5^+$, $^{37}C_3H^+$, and $^{43}C_2H_3O^+$ (Sodeman et al., 2005), which were internally mixed with nitrate ($^{62}NO_3^-$) and $^{97}HSO_4^-$. The relative fraction of OC particles was low throughout the

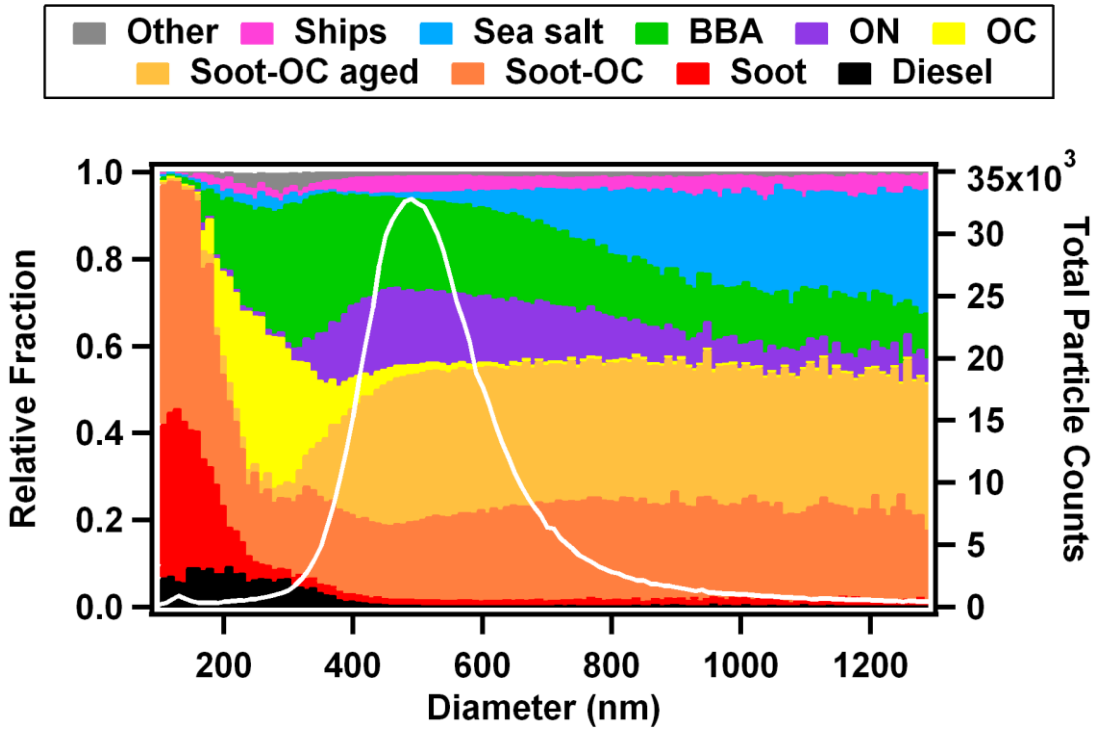

Figure 6.5: Relative fraction of particle types by size. White line represents total particle counts per size. BBA = biomass burning aerosol, ON = organic nitrogen, and OC = organic carbon.

study, comprising only 3% of all particles, except for a one-hour spike on the morning of 5/15/11 7:30-8:30 am from an unknown local source. Because the size range of the OC particles was 200-400 nm, these were less aged particles than those at larger sizes. The soot-OC particle type, a combination of both soot and OC markers (Guazzotti et al., 2001), had a mode at 140 nm, but extended all the way up to 1300 nm; these particles were internally mixed with $^{97}HSO_4^-$, nitrate ($^{30}NO^+$), ammonium ($^{18}NH_4^+$), $^{59}N(CH_3)_3^+$ and $^{86}NCH_2(C_2H_5)_2^+$. Soot-OC particles with $^{18}NH_4^+$ and $^{30}NO^+$ as the most intense peaks were named soot-OC aged; these particles had diameters > 300 nm. Soot-OC and soot-OC aged particles were the most prevalent during the whole study, accounting for 20 and 31% by number of all particles sampled, but especially before 5/15/11. Both

soot-OC particle types likely originated from trucks at the SPBP and freeways nearby, as well as being transported from areas further inland allowing time for these particles to undergo chemical processing. Biomass burning aerosol (BBA) consisted of soot-OC particles with a strong potassium ion peak at $^{39}K^+$ (Silva et al., 1999) and were internally mixed with $^{97}HSO_4^-$, $^{18}NH_4^+$, and amines. BBA particles had a mode at 300 nm and extended all the way to 1300 nm, which is much larger than fresh BBA (100-160 nm) indicating these were aged BBA (Reid et al., 2005). Overall, 21% of all particles by number were BBA, but these were more prevalent after 5/15/11 coincident with the clean marine period. Therefore, these aged BBA must have been transported from fires on land to the ocean before being transported and sampled at SPBP.

The sea salt particle type was characterized by intense $^{23}Na^+$ and $^{39}K^+$ ions with small sodium chloride clusters ($^{81,83}Na_2Cl^+$ and $^{93,95,97}NaCl_2^-$) (Gard et al., 1998; Noble and Prather, 1996). Some of the sea salt particles also had nitrate present in the form of $^{62}NO_3^-$ and $^{108}NaNO_3^+$ suggesting this sea salt has been aged through heterogeneous reactions with HNO_3 and/or N_2O_5 (Gard et al., 1998). Because sea salt particles are typically supermicron (> 1000 nm) and the transmission efficiency of the ATOFMS decreases for particles > 800 nm, it is not surprising that sea salt only made up 4% by number of all particles sampled during this study; at the larger sizes (> 1000 nm), sea salt comprised > 30% by number of all particles sampled.

Particles that had the most intense peaks at $^{58}NHCH_2C_2H_5^+$, $^{59}N(CH_3)_3^+$, or $^{86}NCH_2(C_2H_5)_2^+$ were designated as organic nitrogen (ON) because it is likely these amine markers suppressed organic carbon peaks in the mass spectra (Hatch et al., 2012) and also because alkylamines can undergo oxidation to form other organic nitrogen containing compounds, such as amides and imines (De Haan et al., 2009; Malloy et al., 2009; Murphy et al., 2007; Silva et al., 2008). Of note was the significant concentration of ON particles (15% by number) measured at SPBP in this study, especially during P2, because of their association with adverse health effects. There are several known natural and anthropogenic amine sources including animal husbandry (Mosier et al., 1973; Schade and Crutzen, 1995; Sorooshian et al., 2008a), industrial sources (Fuselli et al.,

1982), vehicle exhaust (Angelino et al., 2001; Cadle and Mulawa, 1980; Key et al., 2011), landfill and sewage treatment plants (Chang et al., 2003; Leach et al., 1999), biomass burning (Schade and Crutzen, 1995; Takahama et al., 2011), and marine sources (Facchini et al., 2008). Gaston et al. (2012b) identified particles characterized by an intense $^{59}N(CH_3)_3^+$ peak during a research cruise off the California coast when the air was coming from the SPBP and attributed the source of this particle to an unknown amine source emitted at the port complex. During P2, the organic nitrogen source most likely originated from dairy farms and agricultural emissions in the Central Valley, as Sorooshian et al. (2008a) previously observed, that partitioned to the particulate phase during transport. In addition, the size of the ON particles (250-1300 with a mode at 450 nm) is similar to cloud/fog processed particles (400-2000 nm) (Dall'Osto et al., 2009; Li et al., 2011; Whiteaker and Prather, 2003; Yao et al., 2003). Because amines are basic, one mechanism for alkylamines to enter the particle phase is through the formation of alkylaminium salts through acid-base reactions with nitric (HNO_3) or sulfuric (H_2SO_4) acids (Angelino et al., 2001; Murphy et al., 2007). In addition, alkylamines can heterogeneously react with ammonium salts by displacing ammonia (Bzdek et al., 2010b; Qiu et al., 2011). Although less likely due to their basic nature, amines can also condense onto aqueous particles as neutral species (Ge et al., 2011b; Pratt et al., 2009). Although mixing state could help determine the history, source, and partitioning mechanism of the ON particles measured, the mixing state of ON particles with respect to $^{97}HSO_4^-$ and $^{62}NO_3^-$ could not be examined because they yielded no negative-ion mass spectra due to their increased water content. However, since these particles were wet, it is likely that they obtained sulfate through aqueous processing.

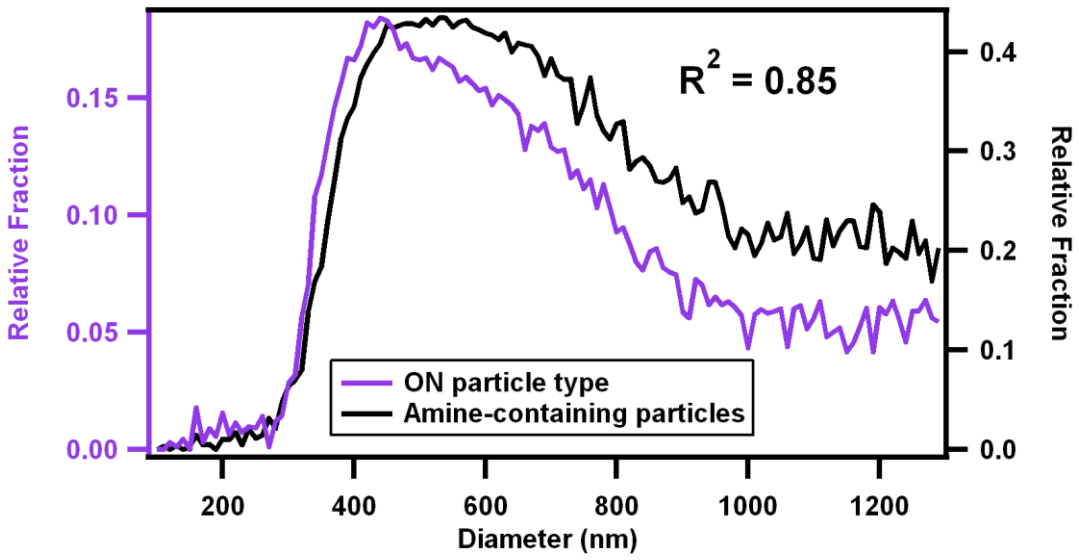

Figure 6.6: Size distribution of ON and amine-containing particles

6.4.2 Amine-containing particles

Overall, 59% of all particles sampled, including the ON particle type, during this study had amine markers $^{59}N(CH_3)_3^+$ or $^{86}NCH_2(C_2H_5)_2^+$ present in their mass spectra with RPA > 2%, hereafter referred to as amine-containing particles. 89, 46, 38, 34, and 4% of all soot-OC aged, HFO, soot-OC, BBA, and sea salt particles met this criterion. Because the amine markers were found on such a variety of particle types, it confirms that the particulate amines were formed through secondary processes. Amine-containing particles were comprised of soot-OC aged (47%), ON (25%), soot-OC (13%), BBA (12%), and HFO (3%). The size distributions of the ON particle type and amine-containing particles had a strong correlation (R^2 = 0.85) (Figure 3.4), suggesting the same secondary processes were involved in adding amines to these particles; thus the ON particles were likely, soot-OC aged, soot-OC, BBA, and HFO particles further aged and coated more thickly with amines. Since amine molecules often have lower ionization potentials than other molecules, it is likely that these markers could suppress other key organic peaks in the mass spectra and lead to their identification as ON (Reilly et al., 2000; Watanabe and Mottl, 1957). In order to analyze the mixing state of aerosols with ON markers, only the 100,361 dual-polarity, amine-containing particles

(38% of all dual-polarity particles) were used; 30-minute average relative peak areas (RPA) were calculated for these particles. Figure 3.5 shows the average RPA of dual polarity, amine-containing particles with each period highlighted.

In amine-containing particles, $^{86}NCH_2(C_2H_5)_2^+$ peaked during P2 indicating that amines were transported from the Central Valley area during this time (Figure 3.5). Although it is expected that ammonium would also be found on particles originating from the Central Valley perhaps it was not observed during this time perhaps because it was displaced by amines, as previously shown (Bzdek et al., 2010a; Qiu et al., 2011). During P2, $^{97}HSO_4^-$ correlated strongly (R = 0.80) with $^{86}NCH_2(C_2H_5)_2^+$ indicating that alkylaminium sulfate salts, which are less volatile than neutral amines (Pratt et al., 2009), were formed through acid-base reactions. Because $^{86}NCH_2(C_2H_5)_2^+$ began increasing at 8:30 am and peaked at noon, photochemistry may have been involved in forming the sulfuric acid that neutralized the amines. $^{62}NO_3^-$ and $^{30}NO^+$ also spiked during P2 but at nighttime and before the $^{86}NCH_2(C_2H_5)_2^+$ spike (Figure 3.5); $^{62}NO_3^-$ and $^{86}NCH_2(C_2H_5)_2^+$ were fairly anticorrelated (R = -0.40) suggesting no alkylaminium nitrate salts were formed during this time despite this being the highest $^{62}NO_3^-$ peak area during the study.

Figure 3.5 also shows that $^{59}N(CH_3)_3^+$ peaked in amine-containing particles during the Pacific Ocean/clean period (P5) suggesting that TMA may have originated from marine biogenic activity. Previous studies have found amines on marine aerosol particles during periods of high biological activity and have attributed the presence of these amines to secondary production of alkylaminium sulfate salts (Facchini et al., 2008; Gibb et al., 1999; Miyazaki et al., 2011; Mueller et al., 2009; Sorooshian et al.,

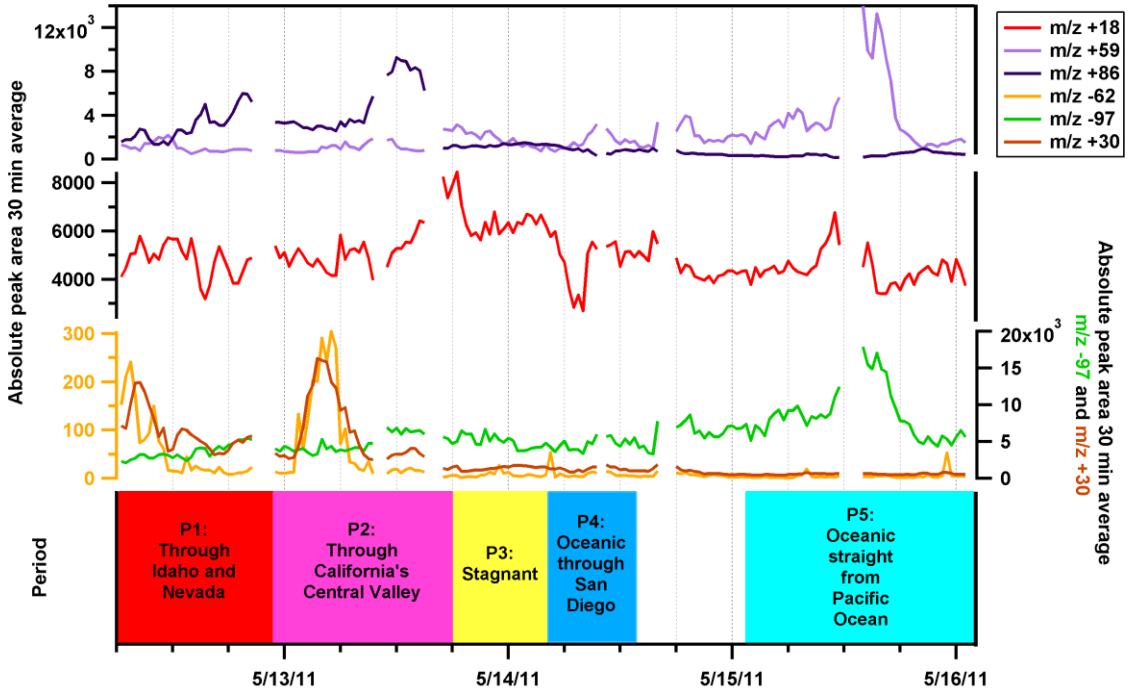

Figure 6.7: Peak areas of all amine-containing particles averaged every 30 minutes.

2009); however only Gibb et al. (1999) identified TMA on sea salt particles and these were in the Arabian Sea, while Van Neste et al. (1987) also found gaseous TMA over the Pacific Ocean in Hawaii. Figure 3.6 shows the oceanic chlorophyll-a concentrations along the California coast during this study, with highest concentrations (2.5-30 mg/m^3) between Channel Islands National Park and the Santa Barbara coast; the air mass back trajectory (Figure 3.1) shows that the air during P5 came through here. However, these were not high chlorophyll concentrations, and therefore P5 was not a high biological activity period. Methanesulfonate (MSA, $^{95}CH_3SO_3^-$), which is also an indicator of marine biogenic activity (Gaston et al., 2010), was fairly correlated (R = 0.30) with

$^{59}N(CH_3)_3^+$ during P5; however previous studies have indicated that MSA and amines emitted during marine biological activity have different seasonal cycles and do not always correlate (Facchini et al., 2008; Mueller et al., 2009). Alternatively, the amine source during this period could be due to biomass burning or an unknown port emission not observed during the other periods; such sources might include leaks from refineries producing amines and/or amine leaks used in refineries for removal of hydrogen sulfide and carbon dioxide from liquid petroleum gas near SPBP, fuel additives used in gasoline (Zerda et al., 2001), and in diesel fuels (Anastopoulos et al., 2005; Serdari et al., 2000), possibly including HFO and MDO, and in selective catalyst reduction systems on HDDV (Stanciulescu et al., 2010), and fish processing (Rappert and Muller, 2005). Similarly to the $^{86}NCH_2(C_2H_5)_2^+$ spike during P2, there was also a strong correlation (R = 0.97) between the $^{59}N(CH_3)_3^+$ and $^{97}HSO_4^-$ during P5 indicating the presence of trimethylaminium sulfate salts. During P5, $^{59}N(CH_3)_3^+$ also peaked in the daytime (10:30-18:30) indicating that the unknown TMA source(s) is (are) active only during the daytime and/or the involvement of photochemistry in forming sulfuric acid needed to form the trimethylaminium salt.

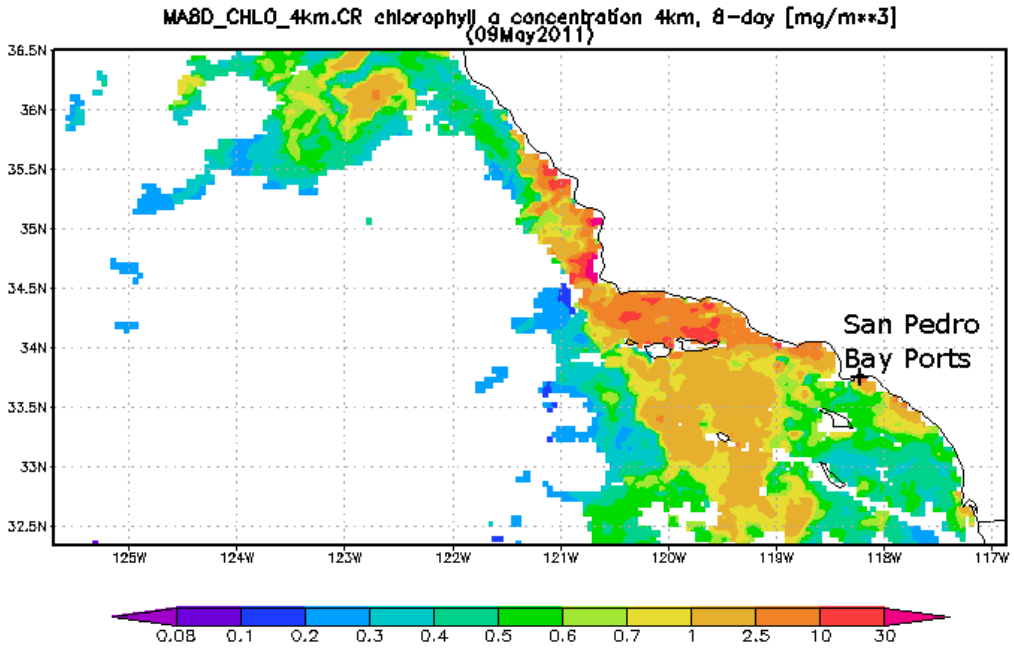

Figure 6.8: Chlorophyll-a concentrations off the California coast. Data from GIOVANNI: http://disc.sci.gsfc.nasa.gov/giovanni

Although ammonia is typically found in the atmosphere at higher concentrations than amines, amines are in general less volatile and more basic than ammonia (Ge et al., 2011a). Thus, amines can be more prevalent in the particulate phase. Ammonia, which partitions to the particle phase as ammonium, is emitted from increasing LNG trucks at the SPBP port (Bishop et al., 2012), in nearby freeway traffic (Battye et al., 2003; Livingston et al., 2009; Nowak et al., 2012), from the ocean (Anderson et al., 2003), and can also be transported from agricultural areas, such as the Central Valley (Anderson et al., 2003; Battye et al., 2003; Clarisse et al., 2010; Sorooshian et al., 2008b). During P5, $^{18}NH_4^+$ and $^{59}N(CH_3)_3^+$ were not correlated (R = -0.08), with $^{18}NH_4^+$ spiking after the peak in $^{59}N(CH_3)_3^+$. Figure 3.5 shows that during P5 there was no correlation (R = 0.06) between $^{18}NH_4^+$ and $^{97}HSO_4^-$ suggesting higher concentrations of trimethylaminium sulfate than ammonium sulfate. This finding is surprising, assuming similar ambient concentrations of TMA other simple alkylamines, because based on thermodynamic data, such as its low Henry's law constant (Ge et al., 2011b), TMA is one of the least likely amines to partition to the particulate phase. One possible

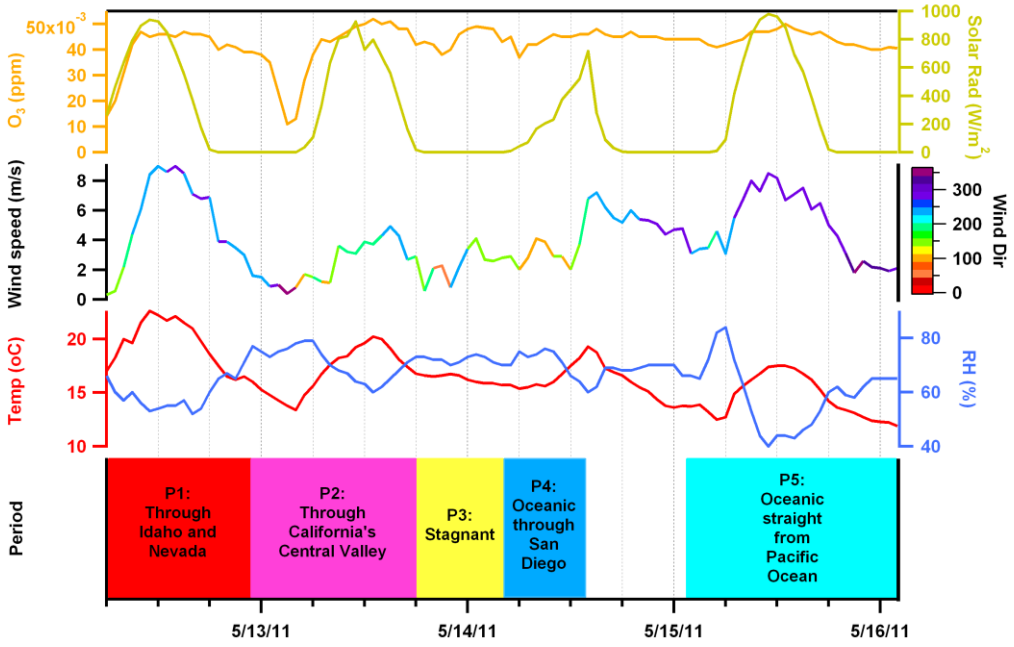

Figure 6.9: Meteorological data from San Pedro Bay Ports Clean Air Action Plan (http://caap.airsis.com) Outer Harbor site.

explanation is that TMA may have displaced ammonia from ammonium sulfate (Bzdek et al., 2010b; Qiu et al., 2011), but if this were the case then there should be a correlation between $^{18}NH_4^+$ and $^{97}HSO_4^-$ prior to that between $^{59}N(CH_3)_3^+$ and $^{97}HSO_4^-$, which was not observed perhaps because the displacement reaction occurred before the air mass was sampled at SPBP. An alternative explanation is that during this time ambient gas-phase concentrations of TMA were higher than ammonia, but there were no measurements to support this.

A comparison between dual-polarity amine-containing particles and dual-polarity particles not-containing amines was performed. The $^{97}HSO_4^-$ peak areas were higher in particles not-containing amines compared to that of amine-containing particles, although $^{97}HSO_4^-$ trends were similar. This observation shows that amines did not partition to all sulfate-containing particles. Amine-containing particles had higher $^{18}NH_4^+$ peak areas than particles not-containing amines, which can be explained because ~50% of the amine-containing particles were comprised of aged particles types, such soot-OC aged. The $^{62}NO_3^-$ peak areas were low throughout the study, especially for the amine-containing particles, but the trends were similar across all particles. The low $^{62}NO_3^-$ peak areas may be explained by the instrumental configuration used in this study, which saw significant amounts of cross talk interference. For that reason the positive ion marker for nitrate, $^{30}NO^+$, was also shown in Figure 3.8. The temporal

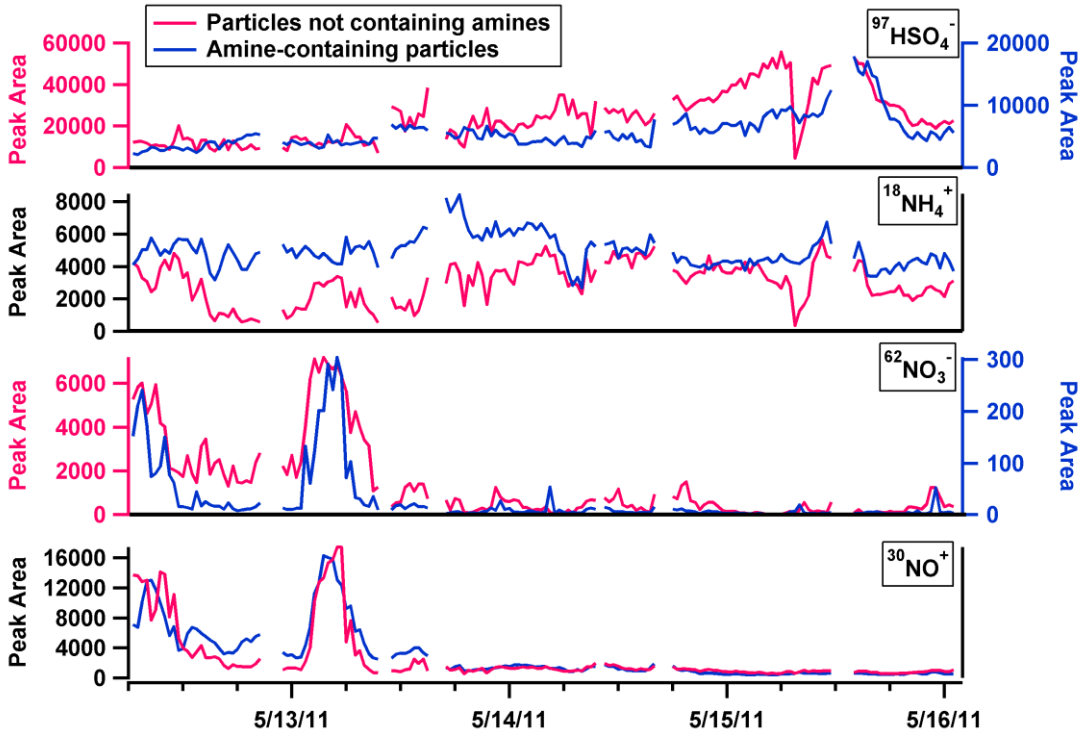

Figure 6.10: Peak areas of amine-containing particles and particles not containing amines averaged every 30 minutes.

trends between $^{62}NO_3^-$ and $^{30}NO^+$ were similar, with both peaking on the early morning of 5/13/11.Thus, despite its low peak areas, $^{62}NO_3^-$ is still representative.

6.5 Summary and Conclusions

Ambient particles were chemically analyzed at the San Pedro Bay Ports in May, 2011. The main 100-1300 nm particle types observed were soot-OC aged to different extents and biomass burning aerosols. However, fresh soot and diesel particles emitted in the port complex contributed > 40% by number to 100-200 nm particles. In addition, 15% by number of all particles sampled were classified as ON, while 59% of all particles contained amine markers. These measurements represent the first observations of secondary organic nitrogen on particles in the Los Angeles/Long Beach ports to our knowledge. The high number of ON and amine-containing particles measured during this study is worrisome and warrants further research. Although previous studies have identified SPBP emissions transported to other areas up to 160 km downwind during regional transport events (Agrawal et al., 2009; Ault et al., 2009; Gaston et al., 2010; Pratt and Prather, 2009), to our knowledge no other study has identified transport of secondary organic nitrogen particles, some of which originated from California's Central Valley, to the SPBP. The mixing of these two air masses, each already known to be harmful to human health, could result in an even greater risk to nearby populated regions. It is worth quantifying in future work how often air from the polluted Central Valley is transported to SPBP. Additionally, other possible amine sources at the port complex should be investigated. Furthermore, toxicological studies should be performed to determine if amines internally mixed with diesel and HFO particles, as observed during this study, play synergistic roles that may exacerbate the negative health outcomes of these particles.

Due to the strong correlations between amine markers with sulfate on amine-containing particles during different periods, amines partitioned to the particulate phase as alkylaminium sulfate salts during this study, as observed in previous field experiments (Creamean et al., 2011; Facchini et al., 2008; Pratt et al., 2009; Smith et al., 2010). In contrast, smog chamber experiments have shown that oxidation chemistry of

amines producing SOA may dominate over acid/base chemistry (Murphy et al., 2007; Silva et al., 2008; Tan et al., 2002); therefore Ge et al. (2011a) concluded that gas/particle partitioning behavior of amines is still uncertain and that both acid/base reactions and oxidation processes can be significant. Further research designed to understand the gas/particle partitioning of amines is required to accurately predict amine and agricultural impacts on air quality in California.

6.6 Acknowledgements

The authors acknowledge the Southern California Marine Institute for hosting us. Help from John Cahill, Elizabeth Fitzgerald, Dr. Defeng Zhao, and Dr. Luis Cuadra-Rodriguez, UCSD and Dr. Arantza Eiguren-Fernandez, Aerosol Dynamics, Inc. with trailer transport and set-up is greatly appreciated. Additionally, we are thankful for the thoughtful comments from John Cahill and Lindsay Hatch, UCSD and Clinton MacDonald, Sonoma Technology, Inc that greatly improved this manuscript. We acknowledge the NOAA Air Resources Laboratory for the provision of the HYSPLIT transport model used in this publication. Chlorophyll a analyses and visualizations used in this study were produced with the Giovanni online data system, developed and maintained by the NASA GES DISC. This work was funded by the U.S. Environmental Protection Agency PM Center Grant # R832415.

Chapter 6 contents are part of a manuscript in preparation, Melanie D. Zauscher, and Kimberly A. Prather, Impact of Central Valley emissions on local aerosols sampled at San Pedro Bay Ports.

6.7 References

Agrawal, H., Eden, R., Zhang, X., Fine, P. M., Katzenstein, A., Miller, J. W., Ospital, J., Teffera, S., and Cocker, D. R. (2009).Primary Particulate Matter from Ocean-Going Engines in the Southern California Air Basin, *Environmental Science & Technology*, *43* (14), 5398-5402.

Albrecht, W. N., and Stephenson, R. L. (1988).Health-Hazards of Tertiary Amine Catalysts, *Scandinavian Journal of Work Environment & Health*, *14* (4), 209-219.

Allouis, C., Beretta, F., and D'Alessio, A. (2003).Structure of Inorganic and Carbonaceous Particles Emitted from Heavy Oil Combustion, *Chemosphere*, *51* (10), 1091-1096.

Anastopoulos, G., Lois, E., Karonis, D., Kalligeros, S., and Zannikos, F. (2005).Impact of Oxygen and Nitrogen Compounds on the Lubrication Properties of Low Sulfur Diesel Fuels, *Energy*, *30* (2-4), 415-426.

Anderson, N., Strader, R., and Davidson, C. (2003).Airborne Reduced Nitrogen: Ammonia Emissions from Agriculture and Other Sources, *Environment International*, *29* (2-3), 277-286.

Angelino, S., Suess, D. T., and Prather, K. A. (2001).Formation of Aerosol Particles from Reactions of Secondary and Tertiary Alkylamines: Characterization by Aerosol Time-of-Flight Mass Spectrometry, *Environmental Science & Technology*, *35* (15), 3130-3138.

Ariola, V., Bernardoni, V., Calzolai, G., Chiari, M., Cuccia, E., Lucarelli, F., Mazzei, F., Nava, S., Prati, P., Valli, G., and Vecchi, R. (2008).Nuclear Techniques and the Particulate Matter Pollution in Big Harbours, *Nuovo Cimento Della Societa Italiana Di Fisica C-Geophysics and Space Physics*, *31* (4), 527-536.

Ault, A. P., Gaston, C., Wang, Y., Dominguez, G., Thiemens, M. H., and Prather, K. A. (2010).Characterization of the Single Particle Mixing State of Individual Ship Plume Events Measured at the Port of Los Angeles, *Environmental Science & Technology*, *44* (6), 1954-1961.

Ault, A. P., Moore, M. J. K., Furutani, H. F., and Prather, K. A. (2009).Impact of Emissions from the Los Angeles Port Region on San Diego Air Quality During Regional Transport Events, *Environmental Science & Technology*, *43* (10), 3500-3506.

Battye, W., Aneja, V. P., and Roelle, P. A. (2003).Evaluation and Improvement of Ammonia Emissions Inventories, *Atmospheric Environment*, *37* (27), 3873-3883.

Bishop, G. A., Schuchmann, B. G., and Stedman, D. H. (2012).Emission Changes Resulting from the San Pedro Bay, California Ports Truck Retirement Program, *Environmental Science & Technology*, *46* (1), 551-558.

Burtscher, H. (2005).Physical Characterization of Particulate Emissions from Diesel Engines: A Review, *Journal of Aerosol Science*, *36* (7), 896-932.

Bzdek, B. R., Ridge, D. P., and Johnston, M. V. (2010a).Amine Exchange into Ammonium Bisulfate and Ammonium Nitrate Nuclei, *Atmospheric Chemistry and Physics Discussions*, *10*, 45-68.

Bzdek, B. R., Ridge, D. P., and Johnston, M. V. (2010b).Size-Dependent Reactions of Ammonium Bisulfate Clusters with Dimethylamine, *Journal of Physical Chemistry A, 114* (43), 11638-11644.

Cadle, S. H., and Mulawa, P. A. (1980).Low Molecular Weight Aliphatic-Amines in Exhaust from Catalyst Equipped Cars, *Environmental Science & Technology*, *14* (6), 718-723.

Campen, M. J., Nolan, J. P., Schladweiler, M. C. J., Kodavanti, U. P., Evansky, P. A., Costa, D. L., and Watkinson, W. P. (2001).Cardiovascular and Thermoregulatory Effects of Inhaled Pm-Associated Transition Metals: A Potential Interaction between Nickel and Vanadium Sulfate, *Toxicological Sciences*, *64* (2), 243-252.

Chang, I. H., Lee, C. G., and Lee, D. S. (2003).Development of an Automated Method for Simultaneous Determination of Low Molecular Weight Aliphatic Amines and Ammonia in Ambient Air by Diffusion Scrubber Coupled to Ion Chromatography, *Analytical Chemistry*, *75* (22), 6141-6146.

Clarisse, L., Shephard, M. W., Dentener, F., Hurtmans, D., Cady-Pereira, K., Karagulian, F., Van Damme, M., Clerbaux, C., and Coheur, P. F. (2010).Satellite Monitoring of Ammonia: A Case Study of the San Joaquin Valley, *Journal of Geophysical Research-Atmospheres*, *115*, 15.

Contini, D., Gambaro, A., Belosi, F., De Pieri, S., Cairns, W. R. L., Donateo, A., Zanotto, E., and Citron, M. (2011).The Direct Influence of Ship Traffic on Atmospheric Pm(2.5), Pm(10) and Pah in Venice, *Journal of Environmental Management*, *92* (9), 2119-2129.

Corbett, J. J., Winebrake, J. J., Green, E. H., Kasibhatla, P., Eyring, V., and Lauer, A. (2007).Mortality from Ship Emissions: A Global Assessment, *Environmental Science & Technology*, *41* (24), 8512-8518.

Creamean, J. M., Ault, A. P., Ten Hoeve, J. E., Jacobson, M. Z., Roberts, G. C., and Prather, K. A. (2011).Measurements of Aerosol Chemistry During New Particle Formation Events at a Remote Rural Mountain Site, *Environmental Science & Technology*, *45* (19), 8208-8216.

Dall'Osto, M., Harrison, R. M., Coe, H., and Williams, P. (2009).Real-Time Secondary Aerosol Formation During a Fog Event in London, *Atmospheric Chemistry and Physics*, *9* (7), 2459-2469.

Dallmann, T. R., Harley, R. A., and Kirchstetter, T. W. (2011).Effects of Diesel Particle Filter Retrofits and Accelerated Fleet Turnover on Drayage Truck Emissions at the Port of Oakland, *Environmental Science & Technology*, *45* (24), 10773-10779.

De Haan, D. O., Tolbert, M. A., and Jimenez, J. L. (2009).Atmospheric Condensed-Phase Reactions of Glyoxal with Methylamine, *Geophysical Research Letters*, *36*.

de Vocht, F., Sobala, W., Wilczynska, U., Kromhout, H., Szeszenia-Dabrowska, N., and Peplonska, B. (2009).Cancer Mortality and Occupational Exposure to Aromatic Amines and Inhalable Aerosols in Rubber Tire Manufacturing in Poland, *Cancer Epidemiology*, *33* (2), 94-102.

Draxler, R. R., and Hess, G. D. (1998).An Overview of the Hysplit 4 Modelling System for Trajectories, Dispersion and Deposition, *Australian Meteorological Magazine*, *47* (4), 295-308.

Facchini, M. C., Decesari, S., Rinaldi, M., Carbone, C., Finessi, E., Mircea, M., Fuzzi, S., Moretti, F., Tagliavini, E., Ceburnis, D., and O'Dowd, C. D. (2008).Important Source of Marine Secondary Organic Aerosol from Biogenic Amines, *Environmental Science & Technology*, *42* (24), 9116-9121.

Fuselli, S., Benedetti, G., and Mastrangeli, R. (1982).Determination of Methylamines in Air Using Activated-Charcoal Traps and Gas-Chromatographic Analysis with an Alkali Flame Detector (Afd), *Atmospheric Environment*, *16* (12), 2943-2946.

Gard, E. E., Kleeman, M. J., Gross, D. S., Hughes, L. S., Allen, J. O., Morrical, B. D., Fergenson, D. P., Dienes, T., Gaelli, M. E., Johnson, R. J., Cass, G. R., and Prather, K. A. (1998).Direct Observation of Heterogeneous Chemistry in the Atmosphere, *Science*, *279*, 1184-1187.

Gaston, C. J., Ault, A. P., Zauscher, M. D., Furutani, H., Cahill, J. F., Collins, D. B., Suski, K. J., and Prather, K. A. (2012a).Changes in the Single-Particle Composition of Ship Emissions in California: Impact of Stricter Regulations on Shipping Emissions, *In prep*.

Gaston, C. J., Pratt, K. A., Qin, X. Y., and Prather, K. A. (2010).Real-Time Detection and Mixing State of Methanesulfonate in Single Particles at an Inland Urban Location During a Phytoplankton Bloom, *Environmental Science & Technology*, *44* (5), 1566-1572.

Gaston, C. J., Quinn, P. K., Bates, T. S., and Prather, K. A. (2012b).The Impact of Shipping, Agricultural, and Urban Emissions on Single Particle Chemistry Observed Aboard the R/V Atlantis During Calnex *In prep*.

Ge, X. L., Wexler, A. S., and Clegg, S. L. (2011a).Atmospheric Amines - Part I. A Review, *Atmospheric Environment*, *45* (3), 524-546.

Ge, X. L., Wexler, A. S., and Clegg, S. L. (2011b).Atmospheric Amines - Part Ii. Thermodynamic Properties and Gas/Particle Partitioning, *Atmospheric Environment*, *45* (3), 561-577.

Geske, D. M. (2006).Port of L.A. Ships in Air Quality Plan, *Diesel Progress*, *72* (9).

Gibb, S. W., Mantoura, R. F. C., and Liss, P. S. (1999).Ocean-Atmosphere Exchange and Atmospheric Speciation of Ammonia and Methylamines in the Region of the Nw Arabian Sea, *Global Biogeochemical Cycles*, *13* (1), 161-177.

Greim, H., Bury, D., Klimisch, H. J., Oeben-Negele, M., and Zeigler-Skylakakis, Z. (1998).Toxicity of Aliphatic Amines: Structure-Activity Relationship, *Chemosphere*, *36* (2), 271-295.

Guazzotti, S. A., Coffee, K. R., and Prather, K. A. (2001).Continuous Measurements of Size-Resolved Particle Chemistry During Indoex-Intensive Field Phase 99, *Journal of Geophysical Research-Atmospheres*, *106* (D22), 28607-28627.

Hall, J. V., Brajer, V., and Lurmann, F. W. (2008).Measuring the Gains from Improved Air Quality in the San Joaquin Valley, *Journal of Environmental Management*, *88* (4), 1003-1015.

Hatch, L. E., Pratt, K. A., Huffman, J. A., Jimenez, J. L., and Prather, K. A. (2012).Impacts of Aging on Laser/Desorption Ionization in Single Particle Mass Spectrometers, *In prep*.

Healy, R. M., O'Connor, I. P., Hellebust, S., Allanic, A., Sodeau, J. R., and Wenger, J. C. (2009).Characterisation of Single Particles from in-Port Ship Emissions, *Atmospheric Environment*, *43* (40), 6408-6414.

Hoek, G., Brunekreef, B., Goldbohm, S., Fischer, P., and van den Brandt, P. A. (2002).Association between Mortality and Indicators of Traffic-Related Air Pollution in the Netherlands: A Cohort Study, *Lancet*, *360* (9341), 1203-1209.

Kagawa, J. (2002).Health Effects of Diesel Exhaust Emissions - a Mixture of Air Pollutants of Worldwide Concern, *Toxicology*, *181*, 349-353.

Key, D., Stihle, J., Petit, J. E., Bonnet, C., Depernon, L., Liu, O., Kennedy, S., Latimer, R., Burgoyne, M., Wanger, D., Webster, A., Casunuran, S., Hidalgo, S., Thomas, M., Moss, J. A., and Baum, M. M. (2011).Integrated Method for the Measurement of Trace Nitrogenous Atmospheric Bases, *Atmospheric Measurement Techniques*, *4* (12), 2795-2807.

Khan, M. Y., Giordano, M., Gutierrez, J., Welch, W. A., Asa-Awuku, A., Miller, J. W., and Cocker, D. R., III (2012).Benefits of Two Mitigation Strategies for Container Vessels: Cleaner Engines and Cleaner Fuels, *Environmental Science & Technology*, *46* (9), 5049-5056.

Kozawa, K. H., Fruin, S. A., and Winer, A. M. (2009).Near-Road Air Pollution Impacts of Goods Movement in Communities Adjacent to the Ports of Los Angeles and Long Beach, *Atmospheric Environment*, *43* (18), 2960-2970.

Lack, D. A., Cappa, C. D., Langridge, J., Bahreini, R., Buffaloe, G., Brock, C., Cerully, K., Coffman, D., Hayden, K., Holloway, J., Lerner, B., Massoli, P., Li, S. M., McLaren, R., Middlebrook, A. M., Moore, R., Nenes, A., Nuaaman, I., Onasch, T. B., Peischl, J., Perring, A., Quinn, P. K., Ryerson, T., Schwartz, J. P., Spackman, R., Wofsy, S. C., Worsnop, D., Xiang, B., and Williams, E. (2011).Impact of Fuel Quality Regulation and Speed Reductions on Shipping Emissions: Implications for Climate and Air Quality, *Environmental Science & Technology*, *45* (20), 9052-9060.

Leach, J., Blanch, A., and Bianchi, A. C. (1999).Volatile Organic Compounds in an Urban Airborne Environment Adjacent to a Municipal Incinerator, Waste Collection Centre and Sewage Treatment Plant, *Atmospheric Environment*, *33* (26), 4309-4325.

Li, W., Li, P., Sun, G., Zhou, S., Yuan, Q., and Wang, W. (2011).Cloud Residues and Interstitial Aerosols from Non-Precipitating Clouds over an Industrial and Urban Area in Northern China, *Atmospheric Environment*, *45* (15), 2488-2495.

Lighty, J. S., Veranth, J. M., and Sarofim, A. F. (2000).Combustion Aerosols: Factors Governing Their Size and Composition and Implications to Human Health, *Journal of the Air & Waste Management Association*, *50* (9), 1565-1618.

Livingston, C., Rieger, P., and Winer, A. (2009).Ammonia Emissions from a Representative in-Use Fleet of Light and Medium-Duty Vehicles in the California South Coast Air Basin, *Atmospheric Environment*, *43* (21), 3326-3333.

Malloy, Q. G. J., Qi, L., Warren, B., Cocker, D. R., Erupe, M. E., and Silva, P. J. (2009).Secondary Organic Aerosol Formation from Primary Aliphatic Amines with No3 Radical, *Atmospheric Chemistry and Physics*, *9* (6), 2051-2060.

McCreanor, J., Cullinan, P., Nieuwenhuijsen, M. J., Stewart-Evans, J., Malliarou, E., Jarup, L., Harrington, R., Svartengren, M., Han, I., Ohman-Strickland, P., Chung, K. F., and Zhang, J. F. (2007).Respiratory Effects of Exposure to Diesel Traffic in Persons with Asthma, *New England Journal of Medicine*, *357* (23), 2348-2358.

McGuinnes, C., Duffin, R., Brown, S., Mills, N. L., Megson, I. L., MacNee, W., Johnston, S., Lu, S. L., Tran, L., Li, R. F., Wang, X., Newby, D. E., and Donaldson, K. (2011).Surface Derivatization State of Polystyrene Latex Nanoparticles Determines Both Their Potency and Their Mechanism of Causing Human Platelet Aggregation in Vitro, *Toxicological Sciences*, *119* (2), 359-368.

Minguillon, M. C., Arhami, M., Schauer, J. J., and Sioutas, C. (2008).Seasonal and Spatial Variations of Sources of Fine and Quasi-Ultrafine Particulate Matter in Neighborhoods near the Los Angeles-Long Beach Harbor, *Atmospheric Environment*, *42* (32), 7317-7328.

Miyazaki, Y., Kawamura, K., Jung, J., Furutani, H., and Uematsu, M. (2011).Latitudinal Distributions of Organic Nitrogen and Organic Carbon in Marine Aerosols over the Western North Pacific, *Atmospheric Chemistry and Physics*, *11* (7), 3037-3049.

Moore, K., Krudysz, M., Pakbin, P., Hudda, N., and Sioutas, C. (2009).Intra-Community Variability in Total Particle Number Concentrations in the San Pedro Harbor Area (Los Angeles, California), *Aerosol Science and Technology*, *43* (6), 587-603.

Mosier, A. R., Andre, C. E., and Viets, F. G. (1973).Identification of Aliphatic-Amines Volatilized from Cattle Feedyard, *Environmental Science & Technology*, *7* (7), 642-644.

Mueller, C., Iinuma, Y., Karstensen, J., van Pinxteren, D., Lehmann, S., Gnauk, T., and Herrmann, H. (2009).Seasonal Variation of Aliphatic Amines in Marine Sub-Micrometer Particles at the Cape Verde Islands, *Atmospheric Chemistry and Physics*, *9* (24), 9587-9597.

Murphy, S. M., Agrawal, H., Sorooshian, A., Padro, L. T., Gates, H., Hersey, S., Welch, W. A., Jung, H., Miller, J. W., Cocker, D. R., Nenes, A., Jonsson, H. H., Flagan, R. C., and Seinfeld, J. H. (2009).Comprehensive Simultaneous Shipboard and Airborne Characterization of Exhaust from a Modern Container Ship at Sea, *Environmental Science & Technology*, *43* (13), 4626-4640.

Murphy, S. M., Sorooshian, A., Kroll, J. H., Ng, N. L., Chhabra, P., Tong, C., Surratt, J. D., Knipping, E., Flagan, R. C., and Seinfeld, J. H. (2007).Secondary Aerosol Formation from Atmospheric Reactions of Aliphatic Amines, *Atmospheric Chemistry and Physics*, *7* (9), 2313-2337.

Nemmar, A., Hoylaerts, M. F., Hoet, P. H. M., Dinsdale, D., Smith, T., Xu, H. Y., Vermylen, J., and Nemery, B. (2002).Ultrafine Particles Affect Experimental Thrombosis in an in Vivo Hamster Model, *American Journal of Respiratory and Critical Care Medicine*, *166* (7), 998-1004.

Neubauer, K. R., Johnston, M. V., and Wexler, A. S. (1998).Humidity Effects on the Mass Spectra of Single Aerosol Particles, *Atmospheric Environment*, *32* (14-15), 2521-2529.

Noble, C. A., and Prather, K. A. (1996).Real-Time Measurement of Correlated Size and Composition Profiles of Individual Atmospheric Aerosol Particles, *Environmental science & technology*, *30* (9), 2667-2680.

Nowak, J. B., Neuman, J. A., Bahreini, R., Middlebrook, A. M., Holloway, J. S., McKeen, S. A., Parrish, D. D., Ryerson, T. B., and Trainer, M. (2012).Ammonia Sources in the California South Coast Air Basin and Their Impact on Ammonium Nitrate Formation, *Geophysical Research Letters*, *39*.

Pandolfi, M., Gonzalez-Castanedo, Y., Alastuey, A., de la Rosa, J. D., Mantilla, E., de la Campa, A. S., Querol, X., Pey, J., Amato, F., and Moreno, T. (2011).Source Apportionment of Pm(10) and Pm(2.5) at Multiple Sites in the Strait of Gibraltar by Pmf: Impact of Shipping Emissions, *Environmental Science and Pollution Research*, *18* (2), 260-269.

Pira, E., Piolatto, G., Negri, E., Romano, C., Boffetta, P., Lipworth, L., McLaughlin, J. K., and La Vecchia, C. (2010).Bladder Cancer Mortality of Workers Exposed to Aromatic Amines: A 58-Year Follow-Up, *Journal of the National Cancer Institute*, *102* (14), 1096-1099.

Pratt, K. A., Hatch, L. E., and Prather, K. A. (2009).Seasonal Volatility Dependence of Ambient Particle Phase Amines, *Environmental Science & Technology*, *43* (14), 5276-5281.

Pratt, K. A., and Prather, K. A. (2009).Real-Time, Single-Particle Volatility, Size, and Chemical Composition Measurements of Aged Urban Aerosols, *Environmental Science & Technology*, *43* (21), 8276-8282.

Qiu, C., Wang, L., Lal, V., Khalizov, A. F., and Zhang, R. (2011).Heterogeneous Reactions of Alkylamines with Ammonium Sulfate and Ammonium Bisulfate, *Environmental Science & Technology*, *45* (11), 4748-4755.

Rappert, S., and Muller, R. (2005).Odor Compounds in Waste Gas Emissions from Agricultural Operations and Food Industries, *Waste Management*, *25* (9), 887-907.

Rehbein, P. J. G., Jeong, C. H., McGuire, M. L., Yao, X. H., Corbin, J. C., and Evans, G. J. (2011).Cloud and Fog Processing Enhanced Gas-to-Particle Partitioning of Trimethylamine, *Environmental Science & Technology*, *45* (10), 4346-4352.

Reid, J. S., Koppmann, R., Eck, T. F., and Eleuterio, D. P. (2005).A Review of Biomass Burning Emissions Part Ii: Intensive Physical Properties of Biomass Burning Particles, *Atmospheric Chemistry and Physics*, *5*, 799-825.

Reilly, P. T. A., Lazar, A. C., Gieray, R. A., Whitten, W. B., and Ramsey, J. M. (2000).The Elucidation of Charge-Transfer-Induced Matrix Effects in Environmental Aerosols Via Real-Time Aerosol Mass Spectral Analysis of Individual Airborne Particles, *Aerosol Science and Technology*, *33* (1-2), 135-152.

Schade, G. W., and Crutzen, P. J. (1995).Emission of Aliphatic-Amines from Animal Husbandry and Their Reactions - Potential Source of N2o and Hcn, *Journal of Atmospheric Chemistry*, *22* (3), 319-346.

Scheepers, P. T. J., and Bos, R. P. (1992).Combustion of Diesel Fuel from a Toxicological Perspective 2: Toxicity, *International Archives of Occupational and Environmental Health*, *64* (3), 163-177.

Serdari, A., Lois, E., and Stournas, S. (2000).The Role of Amines as Diesel Fuel Extenders, *Journal of the Institute of Energy*, *73* (495), 94-99.

Silva, P. J., Erupe, M. E., Price, D., Elias, J., Malloy, Q. G. J., Li, Q., Warren, B., and Cocker, D. R. (2008).Trimethylamine as Precursor to Secondary Organic Aerosol Formation Via Nitrate Radical Reaction in the Atmosphere, *Environmental Science & Technology*, *42* (13), 4689-4696.

Silva, P. J., Liu, D., Noble, C. A., and Prather, K. A. (1999).Size and Chemical Characterization of Individual Particles Resulting from Biomass Burning of Local Southern California Species, *Environmental Science & Technology*, *33* (18), 3068-3076.

Smith, J. N., Barsanti, K. C., Friedli, H. R., Ehn, M., Kulmala, M., Collins, D. R., Scheckman, J. H., Williams, B. J., and McMurry, P. H. (2010).Observations of Aminium Salts in Atmospheric Nanoparticles and Possible Climatic Implications, *Proceedings of the National Academy of Sciences of the United States of America*, *107* (15), 6634-6639.

Sodeman, D. A., Toner, S. M., and Prather, K. A. (2005).Determination of Single Particle Mass Spectral Signatures from Light-Duty Vehicle Emissions, *Environmental Science & Technology*, *39* ((12)), 4569-4580.

Song, X. H., Hopke, P. K., Fergenson, D. P., and Prather, K. A. (1999).Classification of Single Particles Analyzed by Atofms Using an Artificial Neural Network, Art-2a, *Analytical Chemistry*, *71* (4), 860-865.

Sorooshian, A., Murphy, S. M., Hersey, S., Gates, H., Padro, L. T., Nenes, A., Brechtel, F. J., Jonsson, H., Flagan, R. C., and Seinfeld, J. H. (2008a).Comprehensive Airborne Characterization of Aerosol from a Major Bovine Source, *Atmospheric Chemistry and Physics Discussions*, *8*, 10415-10479.

Sorooshian, A., Murphy, S. N., Hersey, S., Gates, H., Padro, L. T., Nenes, A., Brechtel, F. J., Jonsson, H., Flagan, R. C., and Seinfeld, J. H. (2008b).Comprehensive Airborne Characterization of Aerosol from a Major Bovine Source, *Atmospheric Chemistry and Physics*, *8* (17), 5489-5520.

Sorooshian, A., Padro, L. T., Nenes, A., Feingold, G., McComiskey, A., Hersey, S. P., Gates, H., Jonsson, H. H., Miller, S. D., Stephens, G. L., Flagan, R. C., and Seinfeld, J. H. (2009).On the Link between Ocean Biota Emissions, Aerosol, and Maritime Clouds: Airborne, Ground, and Satellite Measurements Off the Coast of California, *Global Biogeochemical Cycles*, *23*, 15.

Stanciulescu, M., Charland, J. P., and Kelly, J. F. (2010).Effect of Primary Amine Hydrocarbon Chain Length for the Selective Catalytic Reduction of Nox from Diesel Engine Exhaust, *Fuel*, *89* (9), 2292-2298.

Su, Y. X., Sipin, M. F., Furutani, H. F., and Prather, K. A. (2004).Development and Characterization of an Aerosol Time-of-Flight Mass Spectrometer with Increased Detection Efficiency, *Analytical Chemistry, 76*, 712-719.

Takahama, S., Schwartz, R. E., Russell, L. M., Macdonald, A. M., Sharma, S., and Leaitch, W. R. (2011).Organic Functional Groups in Aerosol Particles from Burning and Non-Burning Forest Emissions at a High-Elevation Mountain Site, *Atmospheric Chemistry and Physics, 11* (13), 6367-6386.

Tan, P. V., Evans, G. J., Tsai, J., Owega, S., Fila, M. S., and Malpica, O. (2002).On-Line Analysis of Urban Particulate Matter Focusing on Elevated Wintertime Aerosol Concentrations, *Environmental Science & Technology, 36* (16), 3512-3518.

Toner, S. M., Sodeman, D. A., and Prather, K. A. (2006).Single Particle Characterization of Ultrafine and Accumulation Mode Particles from Heavy Duty Diesel Vehicles Using Aerosol Time-of-Flight Mass Spectrometry, *Environmental Science & Technology, 40* (12), 3912-3921.

Van Neste, A., Duce, R. A., and Lee, C. (1987).Methylamines in the Marine Atmosphere, *Geophysical Research Letters, 14* (7), 711-714.

Watanabe, K., and Mottl, J. R. (1957).Ionization Potentials of Ammonia and Some Amines, *Journal of Chemical Physics, 26* (6), 1773-1774.

Whiteaker, J. R., and Prather, K. A. (2003).Hydroxymethanesulfonate as a Tracer for Fog Processing of Individual Aerosol Particles, *Atmospheric Environment, 37*, 1033-1043.

Wilhelm, M., Ghosh, J. K., Su, J., Cockburn, M., Jerrett, M., and Ritz, B. (2011).Traffic-Related Air Toxics and Preterm Birth: A Population-Based Case-Control Study in Los Angeles County, California, *Environmental Health, 10*, 12.

Wilhelm, M., Ghosh, J. K., Su, J., Cockburn, M., Jerrett, M., and Ritz, B. (2012).Traffic-Related Air Toxics and Term Low Birth Weight in Los Angeles County, California, *Environmental Health Perspectives, 120* (1), 132-138.

Winebrake, J. J., Corbett, J. J., Green, E. H., Lauer, A., and Eyring, V. (2009).Mitigating the Health Impacts of Pollution from Oceangoing Shipping: An Assessment of Low-Sulfur Fuel Mandates, *Environmental Science & Technology, 43* (13), 4776-4782.

Yao, X. H., Lau, A. P. S., Fang, M., Chan, C. K., and Hu, M. (2003).Size Distributions and Formation of Ionic Species in Atmospheric Particulate Pollutants in Beijing, China: 2 - Dicarboxylic Acids, *Atmospheric Environment, 37* (21), 3001-3007.

Zerda, T. W., Yuan, X., and Moore, S. M. (2001).Effects of Fuel Additives on the Microstructure of Combustion Engine Deposits, *Carbon, 39* (10), 1589-1597.

Zhang, Z. H., Chau, P. Y. K., Lai, H. K., and Wong, C. M. (2009).A Review of Effects of Particulate Matter-Associated Nickel and Vanadium Species on Cardiovascular and Respiratory Systems, *International Journal of Environmental Health Research, 19* (3), 175-185.

Chapter 7. Conclusions and future directions

7.1 Conclusions

7.1.1 Development of method to extend lower size limit of ATOFMS

This work was motivated by the need to develop new analytical techniques to characterize the chemical mixing state of ultrafine particles in order to study the links between particles and human health and the physicochemical properties of particles and their impacts on cloud formation and climate. The goal to develop a method that can determine the composition of ultrafine particles was achieved by first growing them with water vapor through a supersaturated condensational growth tube (GT) (Hering and Stolzenburg, 2005) prior to entering the ATOFMS. In this manner, grown ultrafine particles as small as 38 nm can be optically detected and subsequently chemically analyzed by the ATOFMS. By using a differential mobility analyzer upstream of the GT-ATOFMS, it is possible to size select particles. Experiments, which were performed with chemical standards and ambient particles, confirm that this novel GT-ATOFMS technique does not change the chemistry of particles through aqueous processing due to the added water. However, the added water does inhibit the production of negative ion mass spectra (Neubauer et al., 1998), so this technique does not obtain the complete chemical composition of the ultrafine particles. Nonetheless, cecause it is analytically challenging to determine the composition of ultrafine particles in the atmosphere, this new method that chemically analyzes ultrafine particles is important for moving the field to the next level. This GT-ATOFMS technique can be used in future studies in the laboratory and throughout the world.

7.1.2 Mixing state of aerosols and CCN properties in the Sierra Nevada foothills

In an effort to understand how air pollution may be contributing to reduced orographic precipitation in the Sierra Nevada mountains east of the Central Valley, a field campaign was conducted in February and March, 2010 at Mariposa, California to analyze the physicochemical properties, including CCN-derived hygroscopicity, of ambient aerosols. These properties have not been measured before in the Sierra Nevada foothills east of Merced, California. A secondary goal of this study was to quantify ATOFMS measurements in order to extract more information from the collected data to better accomplish the primary goal. Particle chemical mixing state data was quantified for the first time by using measurements from a collocated aerodynamic particle sampler (APS) and PILS-IC. The APS provides representative particle size concentrations, while the PILS-IC quantifies the mass concentration of soluble ion species in bulk $PM_{2.5}$. ATOFMS peak areas of NH_4^+, NO_3^-, and SO_4^{2-} were scaled to mass concentrations by correcting for size and chemical biases in the ATOFMS measurements. The PILS-IC ammonium and nitrate correlated strongly (R^2 = 0.77 and 0.80) with ATOFMS $^{18}NH_4^+$ and $^{62}NO_3^-$, while the correlation between sulfate with $^{97}HSO^{4-}$ was not as strong (R^2 = 0.53). Coupling the ATOFMS and PILS-IC chemical measurements allowed us to determine how the mass concentrations of soluble species were distributed among different particle types. Several pollution transport events from the Central Valley were observed to bring large concentrations of highly aged soot particles internally mixed with soluble NH_4^+, NO_3^-, and SO_4^{2-} to the foothills of the Sierra Nevada; these particles were likely aged during transport. Biomass burning aerosols, also internally mixed with NH_4^+, NO_3^-, and SO_4^{2-} but to a lesser degree than the highly aged soot particles, were additionally detected during this study, mainly during clean rural background conditions. Dust and sea salt were sampled as well, but in smaller numbers; dust was internally mixed with NH_4^+ and NO_3^-, and sea salt with NO_3^- and SO_4^{2-}. Because different particles types with unique cores were internally mixed

with NH_4^+, NO_3^-, and SO_4^{2-} to various degrees, the average bulk composition given by the PILS-IC was not representative of all ambient aerosols in this study.

Differences in estimated hygroscopicity, propensity of particles to act as CCN, and overall CCN number concentrations varied between pollution transport events from the Central Valley and clean rural background conditions. Median total particle and CCN concentrations were higher during aged regional pollution (N_{CN} = 2830 and N_{CCN} = 1377 cm^{-3}) compared to clean rural background conditions N_{CN} = 1760 and N_{CCN} = 367 cm^{-3}). Additionally, particles were more hygroscopic and CCN active during the pollution transport events (κ = 0.26 and f_{CCN} = 0.51) in contrast to those from clean rural background (κ = 0.15 and f_{CCN} = 0.25). We identified these CCN active and hygroscopic particles as highly aged soot particles internally mixed with soluble species acquired during transport from the Central Valley to the Sierra Nevada. Whereas fresh soot particles do not serve as CCN (Tritscher et al., 2011; Weingartner et al., 1997), these highly aged soot particles internally mixed with soluble NH_4^+, NO_3^-, and SO_4^{2-} were CCN active thus, emphasizing the crucial role that particle mixing state plays in determining CCN activity. These observations support the hypothesis set forth by Rosenfeld et al. (2008) that a major source of CCN particles in the Sierra Nevada foothills, which may be affecting orographic precipitation, is Central Valley pollution. Transport of high concentrations of CCN active particles can change regional cloud properties by decreasing cloud droplet radii, leading to changes in cloud albedo and potentially altering precipitation patterns (Albrecht, 1989; Lohmann, 2006; Tao et al., 2012; Twomey, 1977). Long-term effects of these transport events on local precipitation patterns needs to be investigated.

Overall, this study is significant for various reasons. Using the ATOFMS and PILS-IC data together, pollution transport events were detected for the first time, to our knowledge, bringing high concentrations of aged soot particles internally mixed with ammonium, nitrate, and sulfate from the Central Valley to the Sierra Nevada. Furthermore, single-particle chemical analysis coupled to CCN measurements showed that these transported soot particles were more hygroscopic and CCN-active than

particles measured during clean rural background conditions. Because of these observations, we were able to identify for the first time the composition and sources of particles that may be affecting regional precipitation. Finally, the method outlined for quantifying ATOFMS data via comparison with PILS-IC measurements can be used in future studies to improve our knowledge of atmospheric chemistry.

7.1.3 Aging and mixing state of biomass burning aerosols during wildfires

The goals of this opportunistic study were to evaluate the impacts of the 2007 San Diego Wildfires on regional air quality and to analyze the aging and mixing state of biomass burning aerosols. Over 300,000 acres burned in October, 2007. Measured and estimated size-resolved particulate matter mass concentrations county-wide were high, especially during the first two days of the fires, exceeding the 24-hour average U.S. national ambient air quality standard $PM_{2.5}$ limit of 35 $\mu g/m^3$. More than 80% of $PM_{2.5}$ and $PM_{1.0}$ mass was due to particles < 400 nm, with $PM_{0.4}$ mass concentrations reaching as high as 148 $\mu g/m^3$. This is a significant observation because smaller particles may lead to increased health problems compared to larger ones (Ramgolam et al., 2009; Stoelzel et al., 2007).

During this study, 84% of all 120-400 nm chemically analyzed particles with the ATOFMS were biomass burning aerosols. Single-particle analysis and positive matrix factorization (PMF) of these biomass burning particles identified rapid atmospheric aging, including heterogeneous reactions transforming KCl into KNO_3 and K_2SO_4 (Gaudichet et al., 1995; Li et al., 2003), which were coupled to rapid changes in the mode of the particle size distributions. Positive matrix factorization analysis identified four organic carbon factors: organic carbon, organic nitrogen, amines, and organic acids thus, indicating different formation mechanisms and temporal profiles for each. The extent and timing of biomass burning aerosols aging depended on concentrations of wildfire co-emissions and regional pollutants, as well as meteorological conditions. It is vital to understand the aging processes biomass burning aerosol undergo because the resulting physicochemical changes impact the phase, morphology, hygroscopicity, and

optical properties of the particles. Therefore, it is essential to properly incorporate aging wildfire emissions into air quality, weather and climate models (Grell et al., 2011; Hodzic et al., 2007).

The importance of this study stems from being able to analyze real-world wildfire emissions as they age due to regional pollutants and meteorology, in addition to wildfire co-emissions. Although laboratory controlled burns do provide insights into biomass burning emissions, they lack the complex nature inherent in all atmospheric processes. In addition, this was the first single-particle analysis of rapid biomass burning aerosols aging in intense coastal urban fires. Furthermore, being able to identify the size range of particles responsible for the majority of the particulate mass concentrations is crucial for determining the health impacts of wildfires. Lastly, this study showed a unique use of positive matrix factorization applied to analyze the aging of single-particles from the same source.

7.1.4 Impact of Central Valley emissions on local aerosols at port complex

As part of a health effects study of shipping and trucking particles, the physicochemical properties of ambient aerosols were measured at the Port of Los Angeles in May, 2011. Over 40% of the 100-200 nm particles were composed of fresh soot and diesel particles. The majority of the 100-1300 nm particles sampled were aged soot particles to varying degrees, with minor contributions from ships, organic carbon, biomass burning, and sea salt particles. Although several particles types were observed, ~60% of all 100-1300 nm particles contained amine markers. The high number of amine-containing particles is worrisome from a health perspective because amine particles can induce clots (McGuinnes et al., 2011; Nemmar et al., 2002). One source of amines was attributed to transport from the Central Valley through modeling of the air mass back trajectories. To our knowledge, this is the first study to identify transport of amines from the Central Valley to the Los Angeles air basin. Local, yet unknown, amine sources at the port are also likely. Amines partitioned to the particle phase as alkylaminium sulfate salts.

7.1.5 Overall conclusions

This dissertation shows a novel technique that allows the detection of ultrafine particles with the ATOFMS and a method to quantify ion peak areas into mass concentrations. These new methods can now be used by other scientists to continue expanding our knowledge of atmospheric chemistry, and other scientific fields. Additionally, this dissertation describes three different ambient studies with the underlying goal to characterize aerosols in order to understand how they might impact air quality, cloud properties, precipitation, and human health. The results shed light on how atmospheric processing and transport of air masses affect the physicochemical properties of aerosols thus, altering their climate and health impacts.

Although the field campaigns described in this dissertation all took place in California, the results are applicable to other areas worldwide. For example, reduced orographic precipitation has been observed in other regions besides in the Sierra Nevada downwind of the Central Valley, such as in mountains downwind of urban centers in Israel (Givati and Rosenfeld, 2004). Therefore, it is likely that aged anthropogenic aerosol pollution is also transported to the mountains affecting cloud properties in this area of Israel, similarly to pollution from the Central Valley affecting regional precipitation in the Sierra Nevada mountains. As far as wildfires and biomass burning, they occur globablly, and the results from the analysis of the 2007 San Diego Wildfires are generally applicable to all biomass burning. For example, the largest contribution of particulate mass during intense biomass burning should be due to particles < 400 nm. However, the timing and extent of aging of biomass burning aerosols are more relevant to fires at other coastal urban communities with similar chaparral landscape, such as other regions in southern California, Greece and Italy. Finally, there are shipping ports throughout the world that are located nearby to agricultural areas that may emit gas phase amines, such as Cork, Ireland (Healy et al., 2009). In these areas, there may be a similar large fraction of particles emitted from trucks and ocean faring ships at the port that are internally mixed with amines, as was observed at the Port of Los Angeles.

7.2 Future directions

While the research described in this dissertation has extended our knowledge of the physicochemical properties of aerosols, specifically within California, and how they might impact climate and human health, questions remain. A brief description of suggested future work follows.

7.2.1 Development of method to extend lower size limit of ATOFMS

In order to fully take advantage of the GT-ATOFMS method, obtaining dual-polarity mass spectra should be the goal. Therefore, the development of two-step desorption/ionization for the ATOFMS is crucial. However, the use of the GT-ATOFMS technique should continue to be used in order to learn more about ultrafine particles in diverse environments therefore, improving the knowledge of the environmental impacts of aerosols. For example, using the GT-ATOFMS in parallel with CCN measurements will increase our understanding of the spatial and temporal variability of the sources and composition of CCN thereby, decreasing the uncertainties associated with the indirect effect of aerosols. Furthermore, using a collocated aerosol chip electropheresis (ACE) system in these CCN studies would complement the data obtained with the GT-ATOFMS with high temporal resolution (1 minute) mass concentrations of soluble organic and inorganic species on ultrafine particles, which is ultimately needed to predict CCN activity (Noblitt et al., 2009). Ultimately, a method to convert soluble ultrafine species to mass concentrations, similar to the quantification of ATOFMS data described in Chapter 3, would be needed. In addition to CCN applications, health studies can also immensly benefit from being able to identify the composition of ultrafine aerosols. Therefore, the GT-ATOFMS should be used in ultrafine ambient exposure experiments (Kim et al., 2001) in order to better understand how particle composition may be related to the measured biological responses. Furthermore, the GT-ATOFMS technique could be used to better characterize the ultrafine particles humans are exposed to in real-life both indoors, at home and through occupational exposure, and outdoors. For example, the GT-ATOFMS could be used analyze the composition of metal-working and welding particles (Elihn and Berg, 2009)

in addition to incense burning (See et al., 2007). Finally, this technique is not limited to applications withing the fields of atmospheric chemistry, climate, and environmental health. The GT-ATOFMS technique is a powerful tool that scientists can apply to material science and nanotechnology as well.

7.2.2 Mixing state of aerosols and CCN properties in the Sierra Nevada foothills

Although this study made important observations, more research is needed to be able to predict and model CCN-active pollution transport from the Central Valley to the Sierra Nevada. Conditions leading to pollution transport events need to be characterized so these events can be predicted, compared with current observations, and used for modeling regional cloud microphysics and precipitation over the past couple of decades. Therefore, further measurements should be collected, including particle size-resolved mixing state and CCN properties, along different transects of the Sierra Nevada – Central Valley and during different seasons in order to better understand the processes and CCN sources involved in this area. Similar aircraft measurements during regional pollution events would also be beneficial in order to improve our knowledge of what is occurring at cloud-level. Understanding the exact impact of this aerosol pollution on cloud properties and precipitation will take time due to the complexity involved.

7.2.3 Aging and mixing state of biomass burning aerosols during wildfires

Sampling during future wildfires with the GT-ATOFMS technique (Zauscher et al., 2011) will be beneficial in order to analyze the mixing state of ultrafine biomass burning particles. It is also worth comparing the results of this analysis with those of other wildfires in order to build a biomass burning aerosol aging model that can be used to predict air quality and climate impacts resulting from the evolution of biomass burning particles. Future studies should also analyze fires from different fuel types in order to establish differences in particle composition. In order to identify the various organic carbon components on biomass burning aerosols, future sampling should be

performed with other real-time analytical techniques, such as the aerosol chip electrophoresis (ACE) (Noblitt et al., 2009) and the two-dimensional gas chromatography thermal desorption system (Worton et al., 2012) to complement the ATOFMS measurements.

7.2.4 Impact of Central Valley emissions on local aerosols at port complex

Several issues remain worth exploring. First, it is essential to identify and quantify local amine sources at the port area. Second, further research in order to understand gas-to-particle partitioning of amines is needed. Therefore, continued field measurements at the Port of Los Angeles with different analytical techniques capable of identifying the amines present in the particle and gas phases are encouraged. We also recommend ATOFMS analysis of particulate emissions from gasoline and diesel fuels with amine-based additives and from diesel vehicles using diesel particulate filters and selective catalyst reduction systems since the resulting particles may now be different than those sampled during previous source identification studies (Shields et al., 2007; Sodeman et al., 2005; Toner et al., 2006). It is also important to quantify how often air pollution from the Central Valley is transported to the Los Angeles basin in order to understand its impact on regional air quality. The CCN activity of these amine particles should also be explored. Finally, toxicological studies of amine-containing particles should be investigated, including possible synergistic roles between amines and metal containing particles, such as those emitted from combusting heavy fuel oil in ocean faring ships.

7.3 References

Albrecht, B. A. (1989).Aerosols, Cloud Microphysics, and Fractional Cloudiness, *Science*, *245* (4923), 1227-1230.

Elihn, K., and Berg, P. (2009).Ultrafine Particle Characteristics in Seven Industrial Plants, *Annals of Occupational Hygiene*, *53* (5), 475-484.

Gaudichet, A., Echalar, F., Chatenet, B., Quisefit, J. P., Malingre, G., Cachier, H., Buatmenard, P., Artaxo, P., and Maenhaut, W. (1995).Trace-Elements in

Tropical African Savanna Biomass Burning Aerosols, *Journal of Atmospheric Chemistry, 22* (1-2), 19-39.

Givati, A., and Rosenfeld, D. (2004).Quantifying Precipitation Suppression Due to Air Pollution, *Journal of Applied Meteorology, 43* (7), 1038-1056.

Grell, G., Freitas, S. R., Stuefer, M., and Fast, J. (2011).Inclusion of Biomass Burning in Wrf-Chem: Impact of Wildfires on Weather Forecasts, *Atmospheric Chemistry and Physics, 11* (11), 5289-5303.

Healy, R. M., O'Connor, I. P., Hellebust, S., Allanic, A., Sodeau, J. R., and Wenger, J. C. (2009).Characterisation of Single Particles from in-Port Ship Emissions, *Atmospheric Environment, 43* (40), 6408-6414.

Hering, S. V., and Stolzenburg, M. R. (2005).A Method for Particle Size Amplification by Water Condensation in a Laminar, Thermally Diffusive Flow, *Aerosol Science and Technology, 39* (5), 428-436.

Hodzic, A., Madronich, S., Bohn, B., Massie, S., Menut, L., and Wiedinmyer, C. (2007).Wildfire Particulate Matter in Europe During Summer 2003: Meso-Scale Modeling of Smoke Emissions, Transport and Radiative Effects, *Atmospheric Chemistry and Physics, 7* (15), 4043-4064.

Kim, S., Jaques, P. A., Chang, M. C., Froines, J. R., and Sioutas, C. (2001).Versatile Aerosol Concentration Enrichment System (Vaces) for Simultaneous in Vivo and in Vitro Evaluation of Toxic Effects of Ultrafine, Fine and Coarse Ambient Particles - Part I: Development and Laboratory Characterization, *Journal of Aerosol Science, 32* (11), 1281-1297.

Li, J., Posfai, M., Hobbs, P. V., and Buseck, P. R. (2003).Individual Aerosol Particles from Biomass Burning in Southern Africa: 2. Compositions and Aging of Inorganic Particles, *Journal of Geophysical Research, 108(D13)* (8484), doi:10.1029/2002JD002310.

Lohmann, U. (2006).Aerosol Effects on Clouds and Climate, *Space Science Reviews, 125* (1-4), 129-137.

McGuinnes, C., Duffin, R., Brown, S., Mills, N. L., Megson, I. L., MacNee, W., Johnston, S., Lu, S. L., Tran, L., Li, R. F., Wang, X., Newby, D. E., and Donaldson, K. (2011).Surface Derivatization State of Polystyrene Latex Nanoparticles Determines Both Their Potency and Their Mechanism of Causing Human Platelet Aggregation in Vitro, *Toxicological Sciences, 119* (2), 359-368.

Nemmar, A., Hoylaerts, M. F., Hoet, P. H. M., Dinsdale, D., Smith, T., Xu, H. Y., Vermylen, J., and Nemery, B. (2002).Ultrafine Particles Affect Experimental Thrombosis in an in Vivo Hamster Model, *American Journal of Respiratory and Critical Care Medicine, 166* (7), 998-1004.

Neubauer, K. R., Johnston, M. V., and Wexler, A. S. (1998).Humidity Effects on the Mass Spectra of Single Aerosol Particles, *Atmospheric Environment*, *32* (14-15), 2521-2529.

Noblitt, S. D., Lewis, G. S., Liu, Y., Hering, S. V., Collett, J. L., and Henry, C. S. (2009).Interfacing Microchip Electrophoresis to a Growth Tube Particle Collector for Semicontinuous Monitoring of Aerosol Composition, *Analytical Chemistry*, *81* (24), 10029-10037.

Ramgolam, K., Favez, O., Cachier, H., Gaudichet, A., Marano, F., Martinon, L., and Baeza-Squiban, A. (2009).Size-Partitioning of an Urban Aerosol to Identify Particle Determinants Involved in the Proinflammatory Response Induced in Airway Epithelial Cells, *Particle and Fibre Toxicology*, *6*, 12.

Rosenfeld, D., Woodley, W. L., Axisa, D., Freud, E., Hudson, J. G., and Givati, A. (2008).Aircraft Measurements of the Impacts of Pollution Aerosols on Clouds and Precipitation over the Sierra Nevada, *Journal of Geophysical Research-Atmospheres*, *113* (D15).

See, S. W., Balasubramanian, R., and Joshi, U. M. (2007).Physical Characteristics of Nanoparticles Emitted from Incense Smoke, *Science and Technology of Advanced Materials*, *8* (1-2), 25-32.

Shields, L., Suess, D. T., and Prather, K. A. (2007).Determination of Single Particle Mass Spectral Signatures from Heavy-Duty Diesel Vehicle Emissions for Pm2.5 Source Apportionment, *Atmospheric Environment*, *41* (18), 3841-3852.

Sodeman, D. A., Toner, S. M., and Prather, K. A. (2005).Determination of Single Particle Mass Spectral Signatures from Light-Duty Vehicle Emissions, *Environmental Science & Technology*, *39* ((12)), 4569-4580.

Stoelzel, M., Breitner, S., Cyrys, J., Pitz, M., Woelke, G., Kreyling, W., Heinrich, J., Wichmann, H. E., and Peters, A. (2007).Daily Mortality and Particulate Matter in Different Size Classes in Erfurt, Germany, *Journal of Exposure Science and Environmental Epidemiology*, *17* (5), 458-467.

Tao, W. K., Chen, J. P., Li, Z. Q., Wang, C., and Zhang, C. D. (2012).Impact of Aerosols on Convective Clouds and Precipitation, *Reviews of Geophysics*, *50*, 62.

Toner, S. M., Sodeman, D. A., and Prather, K. A. (2006).Single Particle Characterization of Ultrafine and Accumulation Mode Particles from Heavy Duty Diesel Vehicles Using Aerosol Time-of-Flight Mass Spectrometry, *Environmental Science & Technology*, *40* (12), 3912-3921.

Tritscher, T., Juranyi, Z., Martin, M., Chirico, R., Gysel, M., Heringa, M. F., DeCarlo, P. F., Sierau, B., Prevot, A. S. H., Weingartner, E., and Baltensperger, U.

(2011).Changes of Hygroscopicity and Morphology During Ageing of Diesel Soot, *Environmental Research Letters*, *6* (3).

Twomey, S. (1977).Influence of Pollution on Shortwave Albedo of Clouds, *Journal of the Atmospheric Sciences*, *34* (7), 1149-1152.

Weingartner, E., Burtscher, H., and Baltensperger, U. (1997).Hygroscopic Properties of Carbon and Diesel Soot Particles, *Atmospheric Environment*, *31* (15), 2311-2327.

Worton, D. R., Kreisberg, N. M., Isaacman, G., Teng, A. P., McNeish, C., Gorecki, T., Hering, S. V., and Goldstein, A. H. (2012).Thermal Desorption Comprehensive Two-Dimensional Gas Chromatography: An Improved Instrument for in-Situ Speciated Measurements of Organic Aerosols, *Aerosol Science and Technology*, *46* (4), 380-393.

Zauscher, M. D., Moore, M. J. K., Lewis, G. S., Hering, S. V., and Prather, K. A. (2011).Approach for Measuring the Chemistry of Individual Particles in the Size Range Critical for Cloud Formation, *Analytical Chemistry*, *83* (6), 2271-2278.

Appendix 1. Determining the upper size limit of fully ablated particles using aerosol time-of-flight mass spectrometry

A1.1 Objective

During size selection of standard metal particles with the growth-tube ultrafine aerosol time-of-flight mass spectrometer (GT-UF-ATOFMS) approach described in Chapter 2 and Zauscher et al. (2011), it was observed that smaller particles generated smaller peak areas. Therefore, the objective of this analysis shifted to determine the particle size at which the whole particle was no longer fully desorbed/ionized by the laser desorption/ionization (LDI) in the ATOFMS.

A1.2 Experimental Methods

Laboratory measurements were conducted using particles generated from a standard solution of lead nitrate ($Pb(NO_3)_2$) (99+%, Aldrich). The $Pb(NO_3)_2$ particles were sent through two diffusion dryers filled with silica gel to dry the particles. Particles were size selected with the differential mobility analyzer (DMA, TSI 3080-L) based on mobility diameter (D_m) prior to GT-ATOFMS sampling. The dry vacuum aerodynamic diameters (D_{va}) were calculated from the D_m using the density of $Pb(NO_3)_2$ (4.53 g/cm^3) assuming the particles were spherical, following DeCarlo, et al (2004). Although 50-425 nm D_m particles were size selected, the D_{va} of these particles was between 230-1930 nm. Average and 95th percent confidence intervals for $^{208}Pb^+$ peak areas were calculated per particle size sampled using the YAADA toolkit for Matlab. Table A1-1summarizes the particles sampled. All particles were sampled from the same $Pb(NO_3)_2$ solution during the same day (12/X/2008).

Table A1-1. Properties of $Pb(NO_3)_2$ particles sampled.

D_m (µm)	D_{va} (µm)	$^{208}Pb^+$ Average Peak Area	$^{208}Pb^+$ Peak Area 95th Percent Confidence Interval	Number of Particles Sampled
0.050	0.23	7548	5149	501
0.060	0.27	4363	2114	1185
0.070	0.32	3548	327	1206
0.080	0.36	10003	3032	1086
0.090	0.41	13029	2530	1124
0.100	0.45	21434	3082	1015
0.120	0.54	38027	3755	1055
0.140	0.63	59654	4981	1070
0.160	0.72	73187	5394	1102
0.180	0.82	89942	6557	1021
0.200	0.91	104253	7105	983
0.220	1.00	120413	5991	1519
0.240	1.09	156764	6320	1887
0.260	1.18	179128	7492	1500
0.280	1.27	211149	14793	516
0.300	1.36	243871	11240	1021
0.320	1.45	269685	9403	1812
0.340	1.54	262835	20472	424
0.360	1.63	271281	22261	400
0.380	1.72	260006	24235	367
0.400	1.81	266997	27635	319
0.425	1.93	271267	18714	672

Because of the interest in determining at what size particles are no longer fully ablated and since particle volume is proportional to diameter cubed, assuming particles were spherical, D_{va} was cubed in order to compare with average peak areas.

A1.3 Results

Figure A1.1 shows average peak area of $^{208}Pb^{+}$ as a function of D_{va} cubed. The

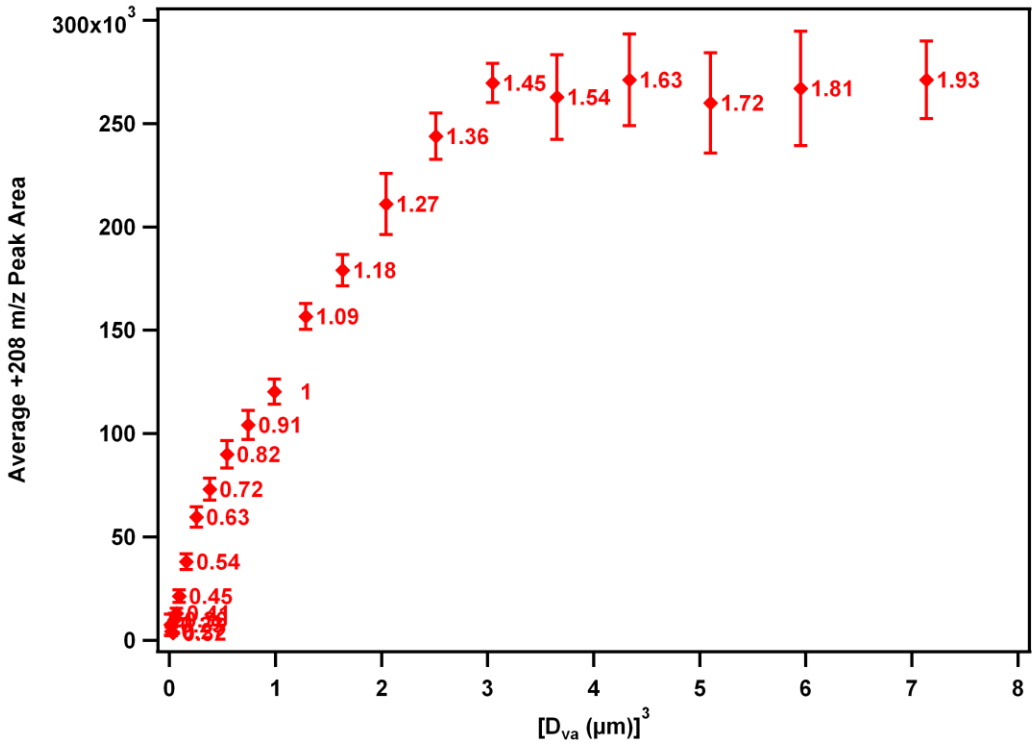

Figure A1.1: Average peak area of $^{208}Pb^{+}$ per particle vacuum aerodynamic diameter cubed. Error bars represent 95th percent confidence intervals. The numbers next to diamonds are the D_{va} of each size sampled.

peak area of $^{208}Pb^{+}$ in $Pb(NO_3)_2$ particles increased steadily until D_{va} reached 1.45 µm. The average peak area plateaued for particles with D_{va} > 1.45 µm, with the 95th percent confidence interval increasing for larger particles due to a smaller number of particles being sampled as shown in Table A1-1. It should be noted that the average peak areas for $^{208}Pb^{+}$ are still within the dynamic range of the data acquisition boards since

maximum peak areas observed during this study were > 800,000. Thus, from this analysis it can be concluded that $Pb(NO_3)_2$ particles with D_{va} < 1.45 µm were fully desorbed/ionized. Although the LDI beam is typically 0.4-0.8 mm wide in the ATOFMS (Wenzel and Prather, 2004), the power density of the beam is not strong enough to ablate particles > 1.45 µm. Previous studies have shown that a larger fraction of smaller particles are ablated than that of larger particles and that at higher laser irradiances a greater fraction of the particle can be desorbed/ionized (Bhave et al., 2002; Carson et al., 1997; Dall'Osto et al., 2006; Schoolcraft et al., 2000). Carranza and Hahn, (2002) showed that using laser induced breakdown spectroscopy (LIBS) silica particles up to 2.1 µm were fully ablated, which is the same order of magnitude as that determined in the current study.

A1.4 Summary

$Pb(NO_3)_2$ particles were size selected and analyzed with the GT-ATOFMS. Because the average peak areas of $^{208}Pb^+$ increased with D_{va}^3 until particles were 1.45 µm and then plateaued for larger particles, it appears that particles with D_{va} < 1.45 µm were fully ablated in contrast to particles D_{va} > 1.45 µm. These experiments should be repeated with different standards, such as iron, vanadium, titanium, sodium, and potassium, as well as mixed particles to see test if similar sized particles are also fully ablated.

A1.5 Acknowledgements

We are grateful to Manuel Ruidíaz and Maggie Yandell for help during sampling. John Cahill is acknowledged for useful discussions. Susanne Hering and Gregory Lewis, Aerosol Dynamics Inc. are acknowledged for collaborating with us and providing the growth tube used during this study. This work was funded with a grant from the U.S. Environmental Protection Agency PM Center Grant # R832415.

A1.6 References

Bhave, P. V., Allen, J. O., Morrical, B. D., Fergenson, D. P., Cass, G. R., and Prather, K. A. (2002).A Field-Based Approach for Determining Atofms Instrument Sensitivities to Ammonium and Nitrate, *Environmental Science & Technology*, *36* (22), 4868-4879.

Carranza, J. E., and Hahn, D. W. (2002).Assessment of the Upper Particle Size Limit for Quantitative Analysis of Aerosols Using Laser-Induced Breakdown Spectroscopy, *Analytical Chemistry*, *74* (21), 5450-5454.

Carson, P. G., Johnston, M. V., and Wexler, A. S. (1997).Real-Time Monitoring of the Surface and Total Composition of Aerosol Particles, *Aerosol Science and Technology*, *26* (4), 291-300.

Dall'Osto, M., Harrison, R. M., Beddows, D. C. S., Freney, E. J., Heal, M. R., and Donovan, R. J. (2006).Single-Particle Detection Efficiencies of Aerosol Time-of-Flight Mass Spectrometry During the North Atlantic Marine Boundary Layer Experiment, *Environmental Science & Technology*, *40* (16), 5029-5035.

DeCarlo, P., Slowik, J., Worsnop, D. R., Davidovits, P., and Jimenez, J. L. (2004).Particle Morphology and Density Characterization by Combined Mobility and Aerodynamic Diameter Measurements. Part 1: Theory *Aerosol Science and Technology*, *38* (12), 1185-1205.

Schoolcraft, T. A., Constable, G. S., Zhigilei, L. V., and Garrison, B. J. (2000).Molecular Dynamics Simulation of the Laser Disintegration of Aerosol Particles, *Analytical Chemistry*, *72* (21), 5143-5150.

Wenzel, R. J., and Prather, K. A. (2004).Improvements in Ion Signal Reproducibility Obtained Using a Homogeneous Laser Beam for on-Line Laser Desorption/Ionization of Single Particles, *Rapid Communications in Mass Spectrometry*, *18* (13), 1525-1533.

Zauscher, M. D., Moore, M. J. K., Lewis, G. S., Hering, S. V., and Prather, K. A. (2011).Approach for Measuring the Chemistry of Individual Particles in the Size Range Critical for Cloud Formation, *Analytical Chemistry*, *83* (6), 2271-2278.

Appendix 2. Single-particle ultrafine sampling at the California Sierra Nevada foothills

A2.1 Objective

The goal of this study was to use the growth-tube aerosol time-of-flight mass spectrometer (GT-ATOFMS) technique discussed in Chapter 2 and Zauscher et al. (2011) to sample 50-150 nm particles that may be acting as cloud condensation nuclei (CCN) in the Sierra Nevada foothills during the field campaign described in Chapters 3 & 4. Thus, the mixing state of these particles was investigated.

A2.2 Experimental Methods

Measurements were conducted at the Mariposa-Yosemite Airport located in the western Sierra Nevada foothills in March, 2010. During this study the ATOFMS used had a converging nozzle, which only detects particles > 200 nm, instead of the UF-ATOFMS that is outfitted with an aerodynamic focusing lens inlet as described in Chapter 1. Therefore, some modifications were made to the GT-ATOFMS interface, as it was previously only used with the UF-ATOFMS. One modification was to add a centerline tube into the nozzle, both of which were kept heated to room temperature to prevent condensation of water, connected to the growth tube output to keep the grown particles from diffusing and drying in the larger space of the nozzle. Also, filtered, humidified sheath flow was added to the inner area between the nozzle and the added centerline tube, in order to maintain the flow rate needed (1 Lm^{-3}) into the instrument and to keep the particles from drying out when these different air masses mixed within the ATOFMS. The differential mobility analyzer (DMA, TSI 3081) was utilized to size select particles prior to the GT-ATOFMS. During GT-ATOFMS sampling, several sizes were selected in order to compare mixing states across different sizes.

The ATOFMS data was analyzed using the YAADA program within Matlab and subsequently clustered into particle types using a neural network algorithm. The particle types, named based on previously identified types, are the same as in Chapters 3 & 4 except for the soot and soot with lead particle types. The leaded soot is likely emitted from low-leaded fuel used in aviation. The error within particle types was calculated based on X statistics. In addition to particles types, ATOFMS peak areas were also analyzed for ammonium (+18 m/z), nitrate (+30 m/z), and amines (+86 m/z). Because of the lack of negative ion mass spectra when sampling with GT-ATOFMS due to the added water (Neubauer et al., 1998), sulfate could not be analyzed in these particles.

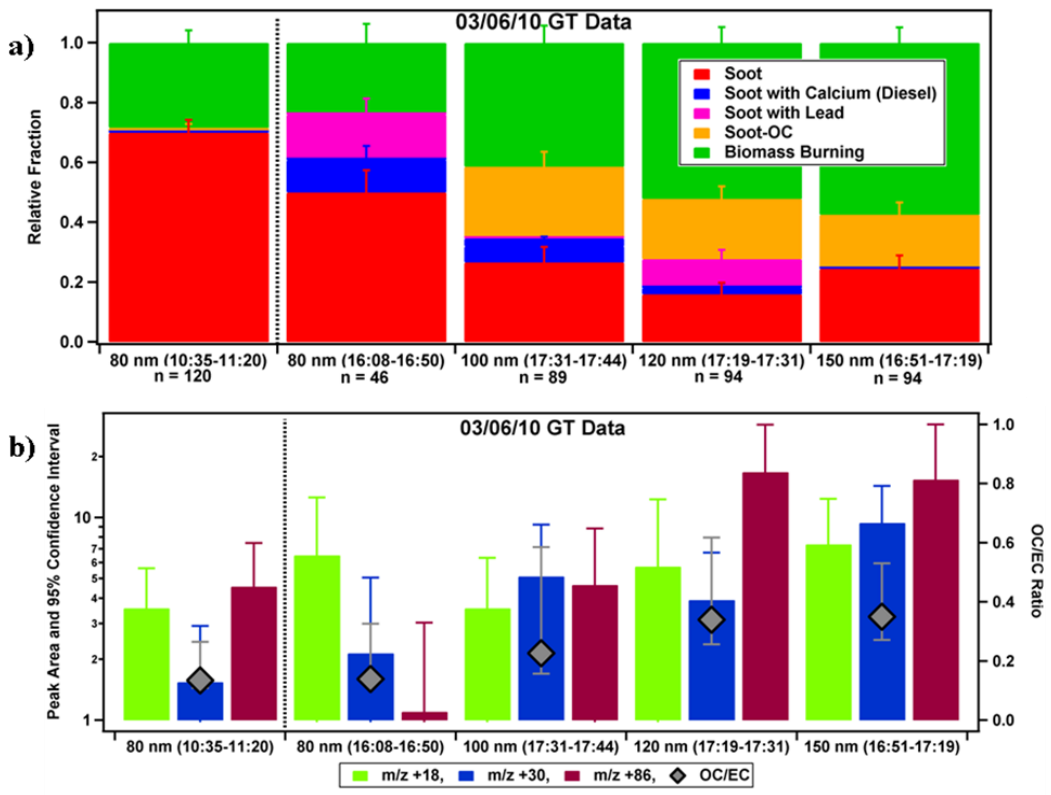

Figure A2.1: Results during March 6, 2010 of a) particle types and b) peak areas of ammonium (+18 m/z), nitrate (+30), and amines (+86 m/z) and OC/EC ratio by particle size sampled with the GT-ATOFMS.

The average peak areas are shown with 95% confidence intervals. The organic carbon (OC) to elemental carbon (EC) peak area ratios were also calculated following Spencer and Prather (2006), with the median values shown with the respective interquatile range.

A2.3 Results

Figure 3.1 shows the particle composition of 80, 100, 120, and 150 nm particles sampled with the GT-ATOFMS on 03/06/10. 80 nm particles were sampled both in the morning and afternoon. In the morning, 80 nm particles had a higher fraction of soot and biomass burning particles, while in the afternoon there were also soot with lead and soot with calcium (diesel) particles sampled. In the afternoon, 80, 100, 120, and 150 nm

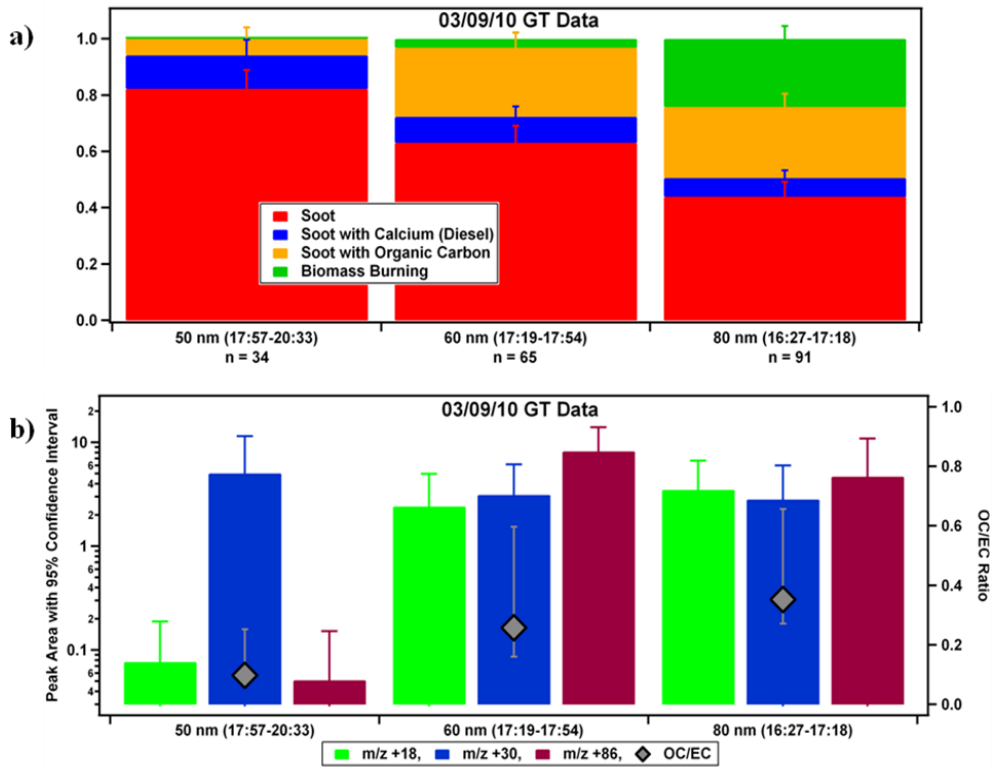

Figure A2.2: Results during March 9, 2010 of a) particle types, and b) peak areas of ammonium (+18 m/z), nitrate (+30), and amines (+86 m/z) and OC/EC ratio by particle size sampled with the GT-ATOFMS.

particles were sampled. These show increasing biomass burning fractions with increasing particle size. Similarly, there was a decreasing fraction of soot particles with increasing particle size, except for the 150 nm particles, which had a soot fraction similar to that of 80 nm. Besides the afternoon 80 nm particles, the only other particle size that had leaded-soot particles was 120 nm. These samples were not contiguous in time or in size, so there may have just been spurious soot with lead emissions. The median OC/EC ratio double from the smallest particles (50 nm, 0.13) to the largest ones (150 nm, 0.35), probably due to the increased biomass burning fraction and also because larger particles have been more atmospherically processed than smaller particles. The 80 nm particles had the smallest ammonium, nitrate, and amine peak areas overall, although the afternoon sample had less amines.

On 03/09/10, 50, 60, and 80 nm particles were sampled with the GT-ATOFMS as well, as shown in Figure 3.2. Smaller particles had a higher fraction of soot particles and a smaller fraction of biomass burning with increasing particle size, as similarly observed on 03/06/10 (Figure 3.1). The fraction of soot-OC particles also increased with increased particle size. The 50 nm particles had significantly less ammonium and amines than the larger particles, but the peak area of nitrate was similar among these three particle sizes. The 60 and 80 nm particles also had similar ammonium and amine peaks areas. The OC/EC ratio also increased with increasing particle size from 0.1 to 0.35.

A2.4 Summary

Chemical analysis of 50-150 nm particles was successfully obtained at the foothills of the Sierra Nevada via the GT-ATOFMS method. Smaller particles had higher fractions of soot particles, while larger particles had higher fractions of biomass burning aerosols. Smaller particles often had smaller peak areas than larger particles; they also had smaller OC/EC ratios indicating smaller particles were fresher.

A2.5 Acknowledgements

We are grateful to the Mariposa-Yosemite Airport for hosting us during this study. Susanne Hering and Gregory Lewis, Aerosol Dynamics Inc. are acknowledged for collaborating with us and providing the growth tube used during this study. This work was funded with a grant from the U.S. Environmental Protection Agency PM Center Grant # R832415 and the California Energy Commission.

A2.6 References

Neubauer, K. R., Johnston, M. V., and Wexler, A. S. (1998).Humidity Effects on the Mass Spectra of Single Aerosol Particles, *Atmospheric Environment*, *32* (14-15), 2521-2529.

Spencer, M. T., and Prather, K. A. (2006).Using Atofms to Determine Oc/Ec Mass Fractions in Particles, *Aerosol Science and Technology*, *40* (8), 585-594.

Zauscher, M. D., Moore, M. J. K., Lewis, G. S., Hering, S. V., and Prather, K. A. (2011).Approach for Measuring the Chemistry of Individual Particles in the Size Range Critical for Cloud Formation, *Analytical Chemistry*, *83* (6), 2271-2278.

Appendix 3. Single-particle ultrafine sampling at the Port of Los Angeles

A3.1 Objective

The goal of this analysis was to test the growth-tube ultrafine aerosol time-of-flight mass spectrometer (GT-UF-ATOFMS) approach described in Chapter 2 and Zauscher et al. (2011) by sampling ultrafine particles at the Port of Los Angeles in May, 2011 during the campaign discussed in Chapter 6. The two main questions were: 1) Is there a significant difference in the composition of ambient ultrafine particles sampled compared to those in the 100-200 nm bin sampled without the growth tube? 2) What percent of ultrafine particles at the port were heavy fuel oil particles?

A3.2 Experimental Methods

Measurements were conducted at the Southern California Marine Institute (SCMI) located at the Port of Los Angeles. The size distribution of 11-590 nm particles were sampled with a scanning mobility particle sizer (SMPS, TSI 3936) every five minutes. The UF-ATOFMS measured the size-resolved composition of 100-1300 nm ambient particles. In addition to UF-ATOFMS measurements, ambient particles were sampled with the GT-UF-ATOFMS during three periods. On 5/11/11, the GT-UF-ATOFMS system was used without size selecting particles. In contrast, on 5/10/11 and 5/13/11, a differential mobility analyzer was used upstream of the GT-UF-ATOFMS system in order to size select 70 nm particles for chemical analysis.

All ATOFMS data was analyzed with the YAADA database program within Matlab and clustered into particle types with an adaptive resonance theory 2a (ART-2a) neural network algorithm. The particle types, named based on previously identified types, are the same as in Chapter 6. Ambient 100-200 nm data measured with the UF-

ATOFMS was selected near each GT-UF-ATOFMS sampling period, which lasted ~1 hour, in order to compare the particle types measured with the GT-UF-ATOFMS.

A3.3 Results

For comparison, Figure A1.1 shows the size distribution of particles types

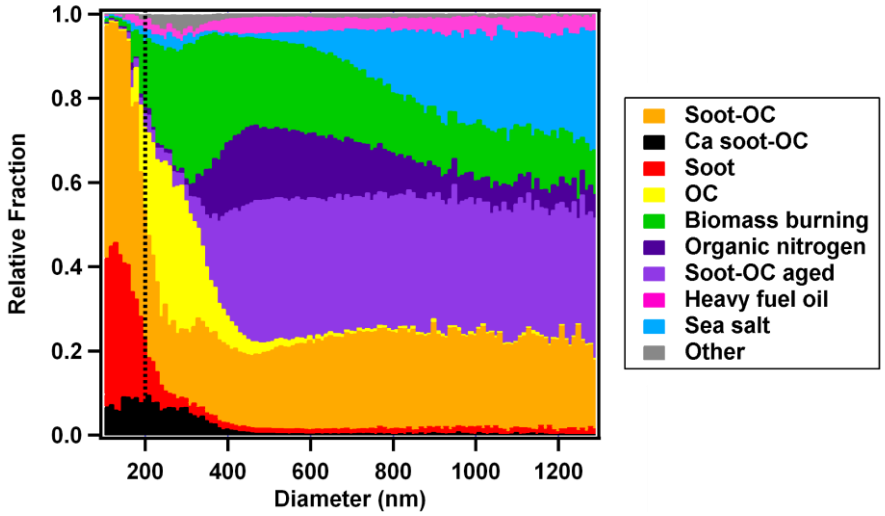

Figure A3.1: Size distribution of all particle types measured with the UF-ATOFMS during whole study. Dashed line separates < 200 nm particles.

measured throughout the whole sampling campaign at SCMI obtained from ambient 100-1300 nm particles sampled with the UF-ATOFMS. 100-200 nm particles types were mainly composed of carbonaceous particles including soot-OC, soot, and Ca soot-OC (diesel), which were different types than those of larger particles. However, there were minor contributions of organic carbon (OC), biomass burning, heavy fuel oil, and soot-OC aged particles in this size range, especially in particles approaching 200 nm. Particles > 200 nm included soot-OC, soot-OC aged, organic nitrogen, biomass burning, OC, heavy fuel oil, and sea salt particles.

A3.3.1 Comparison of UF-ATOFMS and GT-UF-ATOFMS measured particles across all sizes

Figure 3.1 shows the size distribution of particles and the particle types detected during GT-UF-ATOFMS and normal UF-ATOFMS measurements on 5/11/11.On this

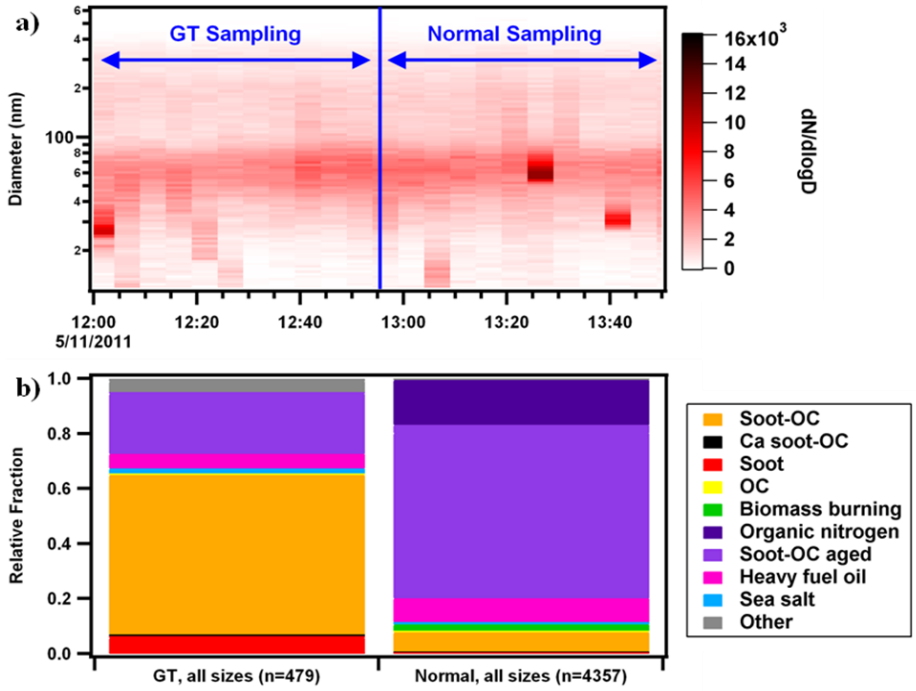

Figure A3.2: Results during May 11, 2011 of a) size distribution of particles during and after the GT-ATOFMS sampling, and b) comparison of 70 nm particle types sampled with the GT-ATOFMS and with only the UF-ATOFMS (normal).

day the GT-UF-ATOFMS analyzed all particle sizes. Similarly, ATOFMS data is shown for all sizes sampled. The ambient particle concentrations were low during this sampling period, with a mode ~ 60 nm. The particle types across all sizes sampled between the GT-UF-ATOFMS and UF-ATOFMS were different. Soot-OC particles were the main type (~50%) measured with the GT-UF-ATOFMS, while soot-OC aged particles were the dominant particle type (~60%) sampled with the UF-ATOFMS. In addition, soot and calcium (Ca) soot-OC (diesel) particles were only observed with the GT-UF-ATOFMS. These differences in particle types can be attributed to differences in particle sizes. Because combustion-generated particles are mainly ultrafine (Lighty et al., 2000), these were not detected with the UF-ATOFMS. However, when the particles were grown with supersaturated water vapor through the GT, these combustion particles

could then be detected by the ATOFMS. Because there were more ultrafine particles during this time than larger particles (Figure 3.1a), these combustion-generated particles overwhelmed the other types once they could be detected. The majority of soot-OC

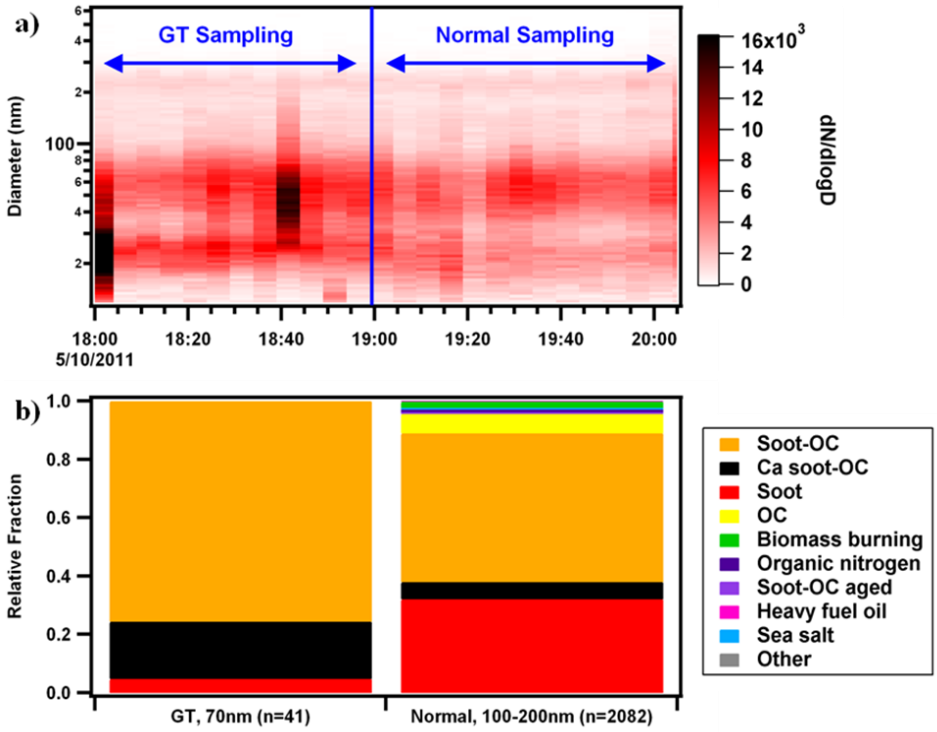

Figure A3.3:Results during May 10, 2011 of a) size distribution of particles during and after the GT-ATOFMS sampling, and b) comparison of 70 nm particle types sampled with the GT-ATOFMS with 100-200 nm particles sampled with the UF-ATOFMS (normal).

aged particles were > 400 nm, as Figure A1.1 shows. Alas, these aged soot-OC particles were still detected by the GT-UF-ATOFMS, but in a smaller fraction. Organic nitrogen particles were detected with the UF-ATOFMS, but not with the GT-UF-ATOFMS. The reason for this is not clear. It should be noted that heavy fuel oil particles were detected with the GT-UF-ATOFMS, although during this sampling period we do not know what size these particles were.

A3.3.2 Comparison of 100-200 nm particles measured with UF-ATOFMS to 70 nm particles detected via GT-UF-ATOFMS

Figure 3.2 and Figure 3.3 show the particle size distributions and comparison between 70 nm and 100-200 nm ambient particle types measured on 5/10/11 and 5/13/11. Almost ten times as many 70 nm particles were sampled on 5/13/11 compared to 5/10/11 (309 versus 41), probably because there were higher ultrafine particle concentrations on 5/13/11 than during 5/10/11. However, the 70 nm particle types were similar during both days, comprising only soot-OC, Ca soot-OC (diesel), and soot particles. The 100-200 nm particles consisted mainly of these same particle types, but with minor contributions of organic carbon (OC), biomass burning, and other types, as observed in Figure A1.1 during the whole study. Therefore, there was no major difference observed between 70 and 100-200 nm particles. Additionally, there were no

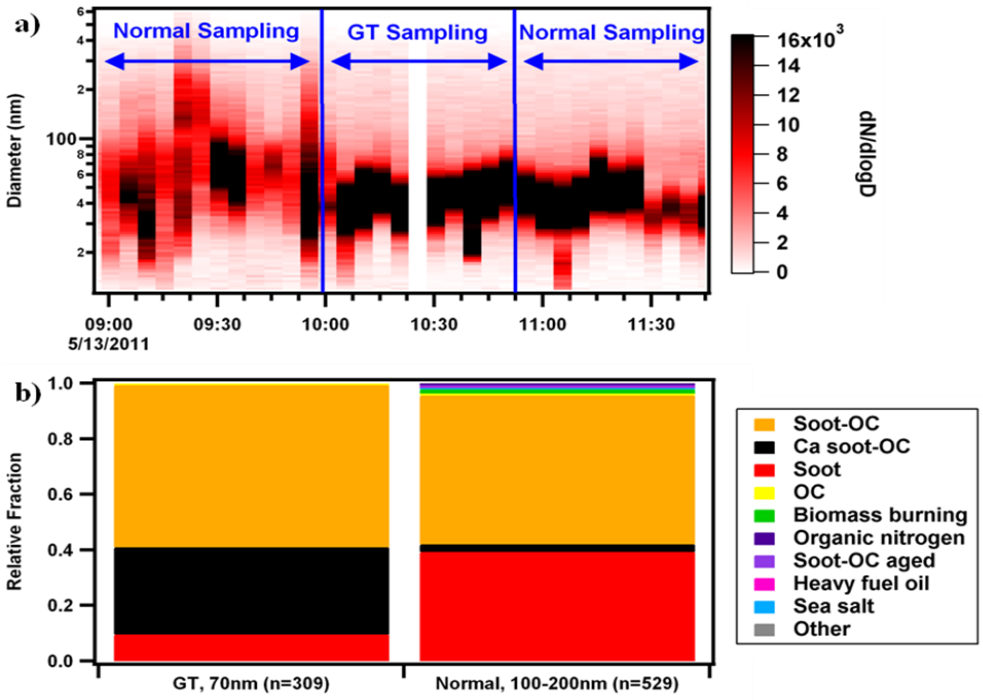

Figure A3.4: Results during May 13, 2011 of a) size distribution of particles before, during, and after the GT-ATOFMS sampling, and b) comparison of 70 nm particle types sampled with the GT-ATOFMS with 100-200 nm particles sampled with the UF-ATOFMS (normal).

ultrafine heavy fuel oil particles detected in this study, which makes sense because ocean-faring ships now must switch from combusting heavy fuel oil to cleaner marine diesel oil 44.5 km from the California coast (Lack et al., 2011). Thus, the heavy fuel oil

particles observed in this study must have been transported to the sampling site allowing time for them to grow through atmospheric processing.

A3.4 Summary

Sampling with the GT-UF-ATOFMS was performed at the Port of Los Angeles and compared with particles sampled without the GT. The 70 nm particles were mainly carbonaceous, similarly to 100-200 nm particles. Additionally, although heavy fuel oil particles were measured with the GT-UF-ATOFMS, these were not detected in ultrafine particles during this study.

A3.5 Acknowledgements

We are grateful to the Southern California Marine Institute for hosting us during this campaign. Susanne Hering and Gregory Lewis, Aerosol Dynamics Inc. are acknowledged for collaborating with us and providing the growth tube used during this study. This work was funded with a grant from the U.S. Environmental Protection Agency PM Center Grant # R832415.

A3.6 References

Lack, D. A., Cappa, C. D., Langridge, J., Bahreini, R., Buffaloe, G., Brock, C., Cerully, K., Coffman, D., Hayden, K., Holloway, J., Lerner, B., Massoli, P., Li, S. M., McLaren, R., Middlebrook, A. M., Moore, R., Nenes, A., Nuaaman, I., Onasch, T. B., Peischl, J., Perring, A., Quinn, P. K., Ryerson, T., Schwartz, J. P., Spackman, R., Wofsy, S. C., Worsnop, D., Xiang, B., and Williams, E. (2011).Impact of Fuel Quality Regulation and Speed Reductions on Shipping Emissions: Implications for Climate and Air Quality, *Environmental Science & Technology*, *45* (20), 9052-9060.

Lighty, J. S., Veranth, J. M., and Sarofim, A. F. (2000).Combustion Aerosols: Factors Governing Their Size and Composition and Implications to Human Health, *Journal of the Air & Waste Management Association*, *50* (9), 1565-1618.

Zauscher, M. D., Moore, M. J. K., Lewis, G. S., Hering, S. V., and Prather, K. A. (2011).Approach for Measuring the Chemistry of Individual Particles in the Size Range Critical for Cloud Formation, *Analytical Chemistry*, *83* (6), 2271-2278.